A comparative study of cationic formulations for the delivery of siRNA and DNA

BY

NGAI PING ALBERT KWOK

UCL INSTITUTE OF CHILD HEALTH

UNIVERSITY COLLEGE LONDON

A thesis submitted for the degree of Doctor of Philosophy

2009

Declaration

I, Ngai Ping Albert Kwok, confirm that the work presented in this thesis is my own. Where information has been derived from other sources, I confirm that this has been indicated in the thesis.

Abstract

RNA interference (RNAi) provides a specific and efficient way to silence gene expression; therefore, it is an attractive tool to be used in basic research on gene function as well as gene therapy. Despite the enormous potential of RNAi, delivering the small interfering RNA (siRNA) to the cells is one of the main hurdles. Previously there have been reports showing effective plasmid DNA delivery to cells and such systems could be used to deliver siRNA to cells due to the similarity of the delivery criteria between plasmid DNA and siRNA. Therefore, I hypothesise that a successful siRNA delivery system will have similar biophysical characteristics as a successful DNA delivery system. The aim of this study is to identify the important criteria to establish a promising siRNA delivery system by comparing the criteria of successful DNA delivery systems such as linear and branched polylysines and linear and branched PEIs.

In order to deliver nucleic acid to a cell, a vector system should be able to bind and form a positively surface-charged nano-sized complex with the nucleic acid for cellular binding and uptake. Inside the cell, the vector should be able to dissociate from the nucleic acid for gene expression or silencing. Therefore, the important parameters to investigate are the binding and dissociation properties of the vector components to the nucleic acid and the size and surface charge of the complex. From the results, generally all the polylysines and PEIs can bind, dissociate and form a positively charged nano-particle with plasmid DNA, which can mediate gene expression. Despite the ability of all the polylysines and PEIs to bind to and dissociate from siRNA, only branched polylysines, linear and branched PEI,

but not linear polylysines can form positively charged nano-particles with siRNA. Indeed, branched PEI behaves similarly towards siRNA and DNA biophysically. Interestingly, only branched PEI and siRNA complexes can mediate cellular uptake and 60% target gene knockdown. Branched polylysines or linear PEI siRNA complexes cannot mediate gene silencing in spite of the formation of positively charged nano-particles. This could be due to poor cellular uptake of these complexes or degradation of siRNA upon uptake. Therefore, to improve the design of the siRNA vector system, there is a need to research the cellular binding and uptake of siRNA complexes in the future.

Table of Contents

Figures

Chapter 1

Figures

Chapter 2

Figures

Chapter 3

Figures

Chapter 4

Figures

Chapter 5

Figures

Tables

Chapter 1

Tables

Chapter 2

Tables

Chapter 4

Tables

Chapter 5

Tables

Chapter 6

Tables

Abbreviations

7 aad	7-amino-actinomycin D
AAV	Adeno-associated virus
ADA	Adenosine deaminase
AGO2	Argonaute 2 protein
AMD	Age-related macular degeneration
ANOVA	Analysis of Variance
ApoB	Apolipoprotein B
ARE	AU-rich element
B-PEI	Branched polyethylenimine
BPG	Bisphosphoglycerate
BSA	Bovine serum albumin
cDNA	Complementary deoxyribonucleic acid
C. elegans	*Caenorhabditis elegans*
CHS	Chalcone synthase
CMV	Cytomegalovirus
DAPI	4,6-diamidino-2-phenylindole
DGCR8	DiGeorge syndrome critical region gene 8
DLS	Dynamic light scattering
DMEM	Dulbecco's Modified Eagle Medium
DMSO	Dimethyl sulfoxide
DNA	Deoxyribonucleic acid

DOPC	Dioleoyl phosphatidyl choline
DOPE	Dioleyl phosphatidylethanolamine
DOTAP	N-[1-(2,3-Dioleoyloxy)propyl]-N,N,N-trimethylammonium methylsulfate
DOTMA	*N*-[1-(2,3-dioleyloxy)propyl]-*N*,*N*,*N*-trimethylammonium chloride
DTS	Dispersion Technology Software
dsRNA	Double stranded ribonucleic acid
EBNA-1	Epstein-Barr nuclear antigen-1
E.coli	*Escherichia coli*
EDTA	Ethylenedinitrilotetraacetic acid
Endo-siRNA	Endogenous siRNA
eGFP	Enhanced green fluorescent protein
FCS	Fetal Calf serum
FGF-4	Fibroblast growth factor 4
G-3-P	Glyceraldehyde-3-phosphate
GAPDH	Glyceraldehyde 3-phosphate dehydrogenase
GFP	Green fluorescent protein
GPI	Glycosyl phosphatidylinositol
HBV	Hepatitis B virus
HIV	Human immunodeficiency
HNA	Hexitol nucleic acids
IL	Interleukin
i.p	Intraperitoneal
irr	Irrelevant small interfering RNA

KSRP	KH-type splicing regulatory protein
L2000	Lipofectamine 2000
LB	Luria Broth
LBGT	Laser beam gene transduction
LCS	Leica Confocal Software
LDA	Laser Doppler Anemometry
LNA	Locked nucleic acids
LMO	LIM domain only 2
L-PEI	Linear Polyethylenimine
Luc	Luciferase
MCS	Multiple cloning sites
mRNA	Messenger RNA
miRNA	MicroRNA
NAD	Nicotinamide adenine dinucleotide
NADH	Reduced nicotinamide adenine dinucleotide
NLS	Nuclear localisation signal
N/P ratio	Nitrogen to phosphate ratio
ORF	Open reading frame
ori	Origin of replication
OTC	Ornithine transcarbamylase
P-body	Processing body
PACT	Protein activator of protein kinase PKR
PBS	Phosphate buffered saline
PCR	Polymerase chain reaction
PEI	Polyethylenimine

PI	Propidium iodide
piRNA	Piwi-interacting RNA
PMT	Photomultiplier tubes
PNA	Peptide nucleic acids
Pol II	Polymerase II
Pre-miRNA	Precursor microRNA
Pri-miRNA	Primary microRNA
qPCR	quantitative PCR
RFU	Relative fluorescence value
RISC	RNA-induced silencing complex
RNA	Ribonucleic acid
RNAi	RNA interference
RLU	Relative luminescence unit
r.p.m	Revolutions per minute
rRNA	Ribosomal RNA
RSV	Respiratory syncytial virus
RT-PCR	Real Time PCR
SCA1	Spinocerebellar ataxia type 1
shRNA	Short hairpin RNA
sieGFP	siRNA targeting eGFP
siLuc	siRNA targeting luciferase
siGAPDH	Small interfering RNA targeting GAPDH
siRNA	Small interfering RNA
SV40	Simian virus 40
TAE buffer	Tris acetate EDTA buffer

TE buffer	Tris EDTA buffer
TK promoter	Thymidine kinase promoter
TRBP	TAR RNA-binding protein
TTP	Tristetrapolin
UPA	Urokinase plasminogen activator
UTR	Untranslated region
UV	Ultraviolet
VEGF	Vascular endothelial growth factor
VEGFR	Vascular endothelial growth factor receptor
v/v	Volume to volume ratio
w/v	Weight to volume ratio
X-SCID	X-linked severe combined immunodeficiency
z-avg	Effective diameter

Units

Kb	Kilobase pair
kDa	Kilodalton
U	Unit
V	Volt
mV	Millivolt
mA	Milliampere
g	Gram
mg	Milligram
µg	Microgram
ng	Nanogram
L	Litre
ml	Millilitre
µl	Microlitre
mmol	Millimole
µmol	Micromole
pmol	Picomole
M	Molarity
mM	Millimolarity
µM	Micromolarity
nM	Nanomolarity
m	Metre
cm	Centimetre
mm	Millimetre

nm	Nanometre
°C	Degree Celsius
g	gravity

Amino acids

Abbreviations		Amino acid	Abbreviations		Amino acid
A	Ala	Alanine	M	Met	Methionine
C	Cys	Cysteine	N	Asn	Asparagine
D	Asp	Aspartate	P	Pro	Proline
E	Glu	Glutamate	Q	Gln	Glutamine
F	Phe	Phenylalanine	R	Arg	Arginine
G	Gly	Glycine	S	Ser	Serine
H	His	Histidine	T	Thr	Threonine
I	Ile	Isoleucine	V	Val	Valine
K	Lys	Lysine	W	Trp	Tryptophan
L	Leu	Leucine	Y	Tyr	Tyrosine

Publications

A. Kwok and S. Hart. *Towards an effective non-viral siRNA delivery system: A comparative study of cationic formulations for DNA and siRNA delivery.* Manuscript In preparation.

A. Kwok and S. Hart. *The molecular structure of non-viral reagents plays an important role in complex formation for nucleic acid delivery.* Manuscript In preparation.

Scott A. Irvine, **Albert Kwok**, Faiza Afzal, Andrew Wu, John B. Wong , Helen C. Hailes, Alethea B. Tabor, Jean R. McEwan, Stephen L. Hart. *Enhancement of Receptor Targeted Nanocomplex (RTN) Vector Mediated Transfection Efficiency by Low Heparin Concentrations.* Manuscript In preparation.

Stephanie M. Grosse, Aris D. Tagalakis, M. Firouz Mohd Mustapa, Martin Elbs, **Albert N. P. Kwok**, Qing-Hai Meng, Tony Brain, Alice Warley, Hannah Armer, Alethea. Tabor, Helen C. Hailes, Stephen L. Hart. *Towards a Viromimetic Vector System for Cancer Gene Therapy by the Incorporation of Chemically Dynamic Linkers into PEG-Shielded Receptor Targeted Nanocomplexes.* Manuscript In preparation.

Published abstracts:

A. N. P. Kwok, A. Takalagis, J. McEwan and S. L. Hart. *A Study of Different Polyethylenimine (PEI) for siRNA Delivery.* RNAi, microRNA and non-coding RNA, Keystone Symposia, Whistler, Canada, March 2008

A. N. P. Kwok, S. A. Irvine, J. McEwan and S. L. Hart. *Development of Lipopolyplex for Efficient siRNA Delivery.* 3rd British Society of Gene Therapy Annual Conference, University of Warwick, March 2007

Acknowledgements

I would like to thank Dr. Stephen Hart for his supervision and for giving me the opportunity to carry out this project. Thanks for his constructive “criticism” in the preparation of the thesis. I would also like to acknowledge Dr. Jean McEwan for her supervision. I would like to show my gratitude to Shahla and Aris for their help and support throughout my project and in the preparation of the thesis. Special thanks also go to Conrad for his help in the thesis preparation. I would also like to acknowledge Michele, Meng, Scott and Stephanie for their kind help at different stages of this project.

Thanks to all the members of the Molecular Immunology Unit at the Institute of Child Health who have provided advice, friendship and technical assistance.

Last but not least, special thanks go to my family for being incredibly helpful, understanding and supportive over the years. This thesis is dedicated to them.

Chapter 1

Introduction

1.1 Gene silencing technology

Gene silencing technology provides an attractive route for disease associated gene identification and treatment. Since the completion of the Human Genome Project, many potential new drug targets await discovery (Hopkins & Groom 2002). However, it is a main hurdle to the translation of genomic information into drug development. To validate gene products which are functionally involved in a disease and the therapeutic effect of silencing these gene products, ribozymes and antisense oligonucleotides have been used to target specific mRNA (Leung & Whittaker 2005). So far, only a single antisense oligonucleotide has been developed to a therapeutic product, Vitravene®, for the treatment of cytomegalovirus-induced retinitis (Winkler 2004). RNA interference (RNAi) is the latest discovery in this field. Since the discovery of double stranded RNA mediated sequence specific gene silencing, RNAi was named as the greatest scientific breakthrough in 2002 by Science magazine (Couzin 2002). The original discovery of this mechanism was awarded with the Nobel Prize in Physiology or Medicine in 2006, reflecting its importance in scientific and medical research. In this section, the background, biology and application of RNAi are discussed. The antisense oligonucleotide and ribozyme technologies are also discussed, and are compared with RNAi.

1.1.1 RNA interference

1.1.1.1 History of the RNA mediated gene silencing discovery

RNA mediated gene silencing was first reported in the early 1990s in a study to improve the colouring of petunia flowers. Researchers introduced mRNA encoding chalcone synthase (CHS), an enzyme for petunia pigmentation, into normal petunia flower to enhance the colouring. Unexpectedly, the petunias became either fully or partially white. It was observed that the mRNA expression of CHS was reduced when both the endogenous and introduced CHS genes were present. The mechanism was unknown and the observation was termed "co-suppression" (Napoli et al. 1990). Further study found that the co-suppression effect was associated with an increased mRNA turnover (van Blokland et al. 1994). Similar phenomena were observed in the fungus *Neurospora crassa* (Romano & Macino 1992) and in Drosophila (Pal-Bhadra et al. 1997).

A similar paradoxical phenomenon was observed in a study on *par*-1 gene function in *Caenorhabditis elegans* (*C. elegans*). In this study, antisense RNA was used to silence the *par*-1 gene expression; interestingly, the sense RNA control produced an identical phenotype as the antisense RNA. The entire mechanism of this silencing remained unknown (Guo & Kemphues 1995).

In 1997, research on viral disease resistance in plants showed a similar gene silencing observation. It was found that plants containing short and non-coding regions of viral RNA

sequences mediated enhanced resistance to viral infection (Covey et al. 1997). In a related study, it was shown that viral gene expression was suppressed in infected plants when viruses were engineered to carry short sequences of plant genes. This phenomenon was termed "virus-induced gene silencing" (Ratcliff et al. 1997). All of the gene silencing observations were named "post transcriptional gene silencing" (Cogoni & Macino 2000; Hammond et al. 2001).

In 1998, the mechanism of the RNA induced gene silencing was discovered in a *C. elegans* model by Craig Mello, Andrew Fire and co-workers. In this study, it was observed that either sense mRNA or antisense mRNA induced modest gene silencing effects; however, double stranded RNA mediated potent gene target silencing (Fire et al. 1998). This phenomenon was termed "RNAi" and this study was awarded the Nobel Prize in Physiology or Medicine in 2006.

1.1.1.2 RNAi mechanism

RNAi is observed to occur in most of the eukaryotic cells, from protists to plants and animals. The RNAi mechanism is a highly evolutionary conserved pathway. This pathway has been identified to play an important in regulating gene expression and defence responses against transposable elements and viruses (Cerutti & Casas-Mollano 2006).

RNAi commences when a double stranded RNA is firstly cleaved into a small interfering RNA (siRNA), a double stranded 21-23 nucleotide product with two-nucleotide 3'

overhangs and 5'-phosphorylated ends, by a Dicer complex in the cytoplasm **(Figure 1.1)** (Bernstein et al. 2001;Vermeulen et al. 2005;Zamore et al. 2000)**.** The siRNA is then incorporated into a mutlicomponent nuclease complex to form the RNA-induced silencing complex (RISC). In RISC, a catalytically active endonuclease called argonaute protein binds to siRNA and degrades one strand of the siRNA, the anti-guide stand or passenger strand, leaving the guide strand intact to direct gene silencing (Gregory et al. 2005). The guide strand tends to have a less stable 5' end than the passenger strand (Preall et al. 2006). The more stable 5' end of the passenger strand may be bound by R2D2 protein, a protein that aids siRNA binding into the RISC, differentiating it from the guide strand (Tomari et al. 2004).

To mediate target mRNA cleavage, it was found that the phosphorylated 5' end of the guide RNA binds to a conserved basic pocket in the PIWI domain of the argonaute protein. The first nucleotide at the 5' end of the guide RNA binds to a conserved tyrosine residue, leaving the successive nucleotides of the guide strand available as a nucleation site for pairing with target mRNA for cleavage (Ma et al. 2005). Target mRNA cleavage then occurs at a position between nucleotides 10 and 11 relative to the 5' end of the guide strand (Rand et al. 2005). The activated RISC complex is then recycled and targets other mRNA (Hutvagner & Zamore 2002).

There is evidence that the target mRNA cleavage initiated by siRNA could occur in a specific region of the cytoplasm called the processing body (P-body) where argonaute proteins and siRNA are located (Jagannath & Wood 2009; Sen & Blau 2005). A high turnover rate of mRNA is observed in P-bodies (Sen & Blau 2005) and disruption of P-

bodies decreases the efficiency of RNAi (Jakymiw et al. 2005), implicating the importance of P-bodies for RNAi.

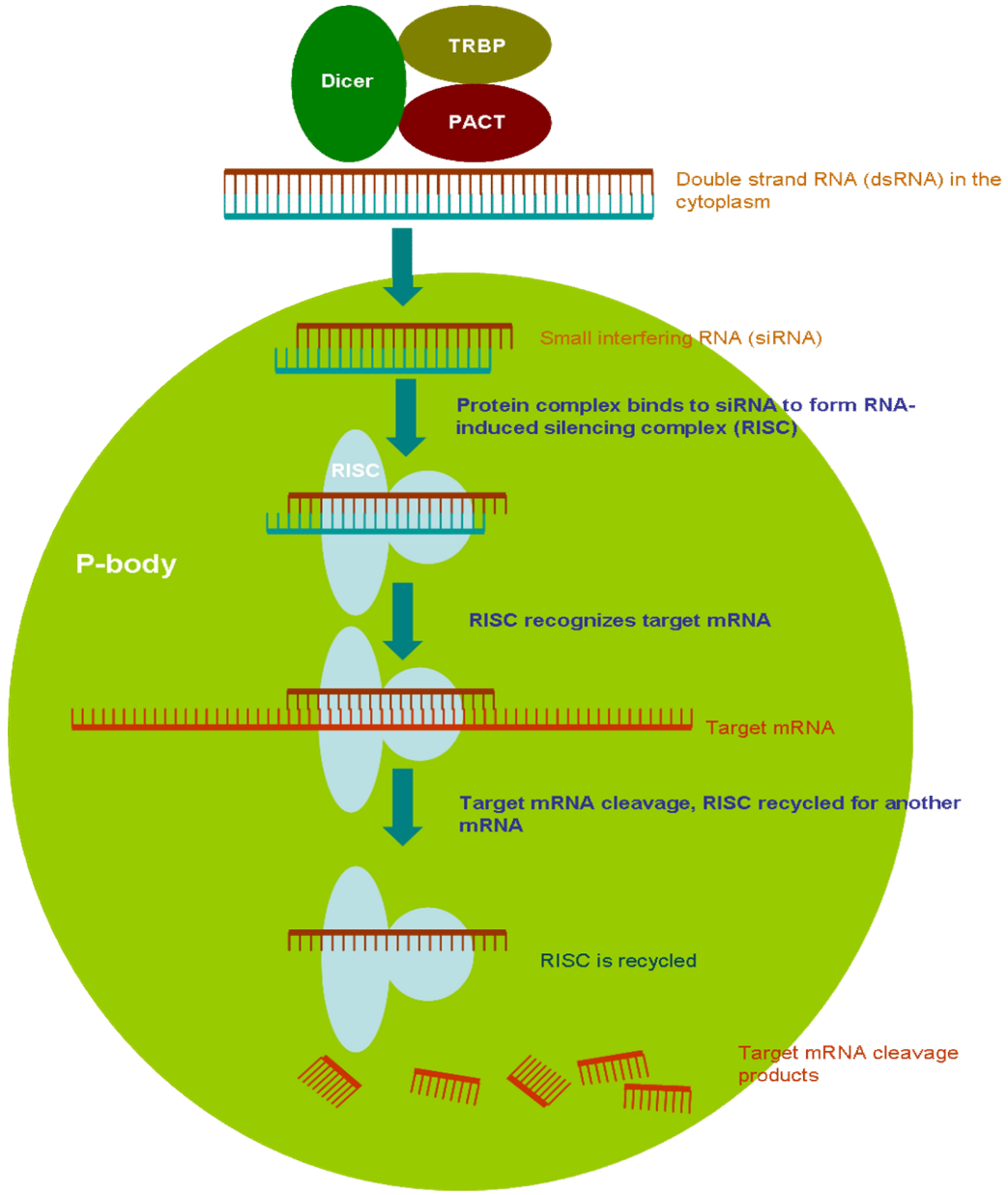

Figure 1.1 RNAi mechanism in mammalian cells. In the cytoplasm, double stranded RNA (dsRNA) is bound and cleaved into siRNA by the Dicer complex consisting of a Dicer, double stranded RNA binding proteins such as the TAR RNA-binding protein (TRBP), and the protein activator of protein kinase PKR (PACT). The siRNA is then bound to the RNA induced silencing complex (RISC). The siRNA guide strand recognises the target site on the target mRNA and cleavage is mediated through the catalytic activated domain of argonaute 2 protein (AGO2).

1.1.1.2.1 mRNA degradation mechanism

The P-body is an important site within the cytoplasm for mRNA degradation after cleavage (Eulalio et al. 2007). Following target mRNA cleavage by the RISC, the mRNA fragments can be degraded through the mRNA degradation mechanism in the P-body **(Figure 1.2)**. During mRNA degradation, the poly(A) tail of the mRNA is removed by poly(A)-specific exoribonucleases. The deadenylated mRNA can then be degraded through two possible pathways. In one pathway, the 5' cap of the deadenylated mRNA is removed by Dcp1 and the Dcp2. Subsequently, the mRNA is degraded by Xrn1 exonuclease from the 5' end to the 3' end of the mRNA (Valencia-Sanchez et al. 2006). In the other pathway, the deadenylated mRNA is degraded from the 3' end to the 5' end of the mRNA by the exosome. The 5' cap is then cleaved by the DcpS (Wilusz & Wilusz 2004).

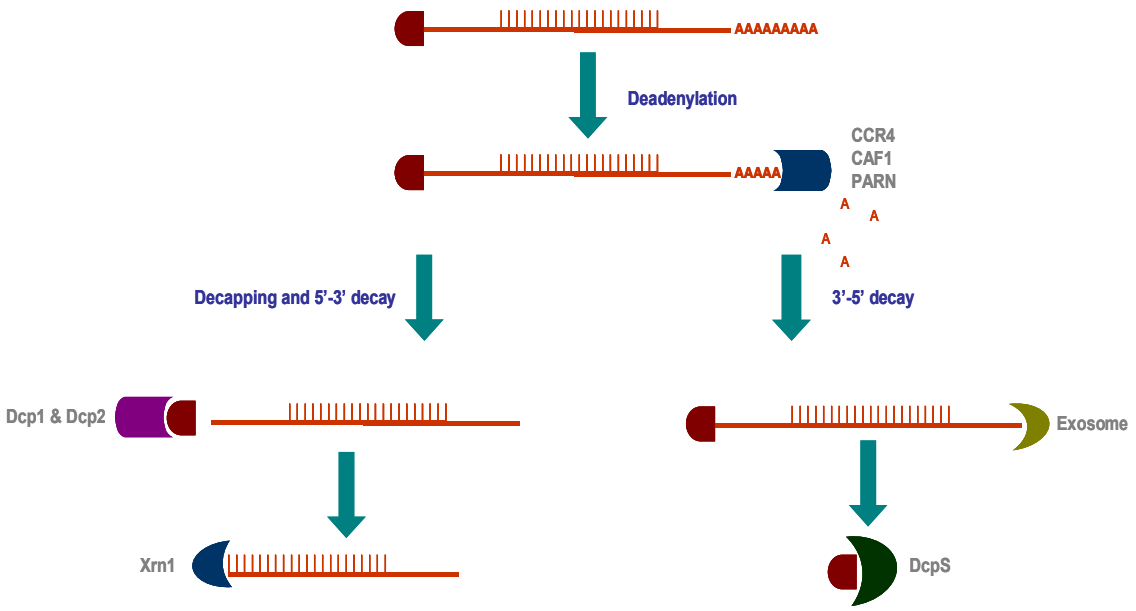

Figure 1.2 General pathway for mRNA degradation. Following deadenylation of the target mRNA by poly(A)-specific exoribonucleases such as CCR4, CAF1 and PARN, the mRNA is decapped by Dcp1 and Dcp2 and degraded from 5' to 3' by Xrn1 (left hand side of the figure). Degradation of the mRNA from 3' end can be mediated by exosome, a large complex of exonucleases. The remaining 5' cap is then broken down by DcpS (right hand side of the figure).

1.1.1.3 Other forms of small molecules for RNAi

Apart from siRNA, there are other classes of RNA molecules such as microRNA (miRNA), short hairpin RNA (shRNA), Piwi-interacting RNA (piRNA) and endogenous siRNA (endo-siRNA) that can induce gene silencing. The biology of these RNA is discussed in this section.

1.1.1.3.1 miRNA

miRNA refers to single stranded RNA of 21-25 nucleotides. It is expressed endogenously in cells and induces RNAi to regulate gene expression. Recent studies have demonstrated that one single miRNA can interact with one hundred targets. miRNA plays an important role in various cellular pathways, particularly vital in controlling developmental and oncogenic processes (Gregory et al. 2006; Winter et al. 2009).

There are several steps for a cell to produce mature miRNA **(Figure 1.3)**. Firstly, a long RNA molecule of around 70 nucleotides is produced in the nucleus of the cell. The RNA is then folded to form a long hairpin structure called "primary miRNA" (pri-miRNA). Most of the pri-miRNA is processed by a multicomponent complex consisting of the RNase III enzyme Drosha and a dsRNA-binding protein Pasha into a 70 nucleotide hairpin structure called "precursor miRNA" (pre-miRNA). However, small potions of pre-miRNAs are generated from introns, referred as mitrons, during transcript splicing rather than the Drosha dependent pathway (Berezikov et al. 2007; Okamura et al. 2007; Ruby et al. 2007).

Pre-miRNA is then exported from the nucleus into the cytoplasm by 5' exportin. The pre-miRNA is then bound and cleaved by a Dicer complex into a 21-25 double strand miRNA. The miRNA binds to RISC and is then guided to the 3' untranslated region of the target mRNA by a seed sequence (2 to 8 nucleotides from the 5' end) to mediate gene silencing mainly by translational repression (Gregory et al. 2006; Pillai et al. 2007). However, mRNA degradation can occur in P-bodies where miRNA activity clusters (Lian et al. 2006).

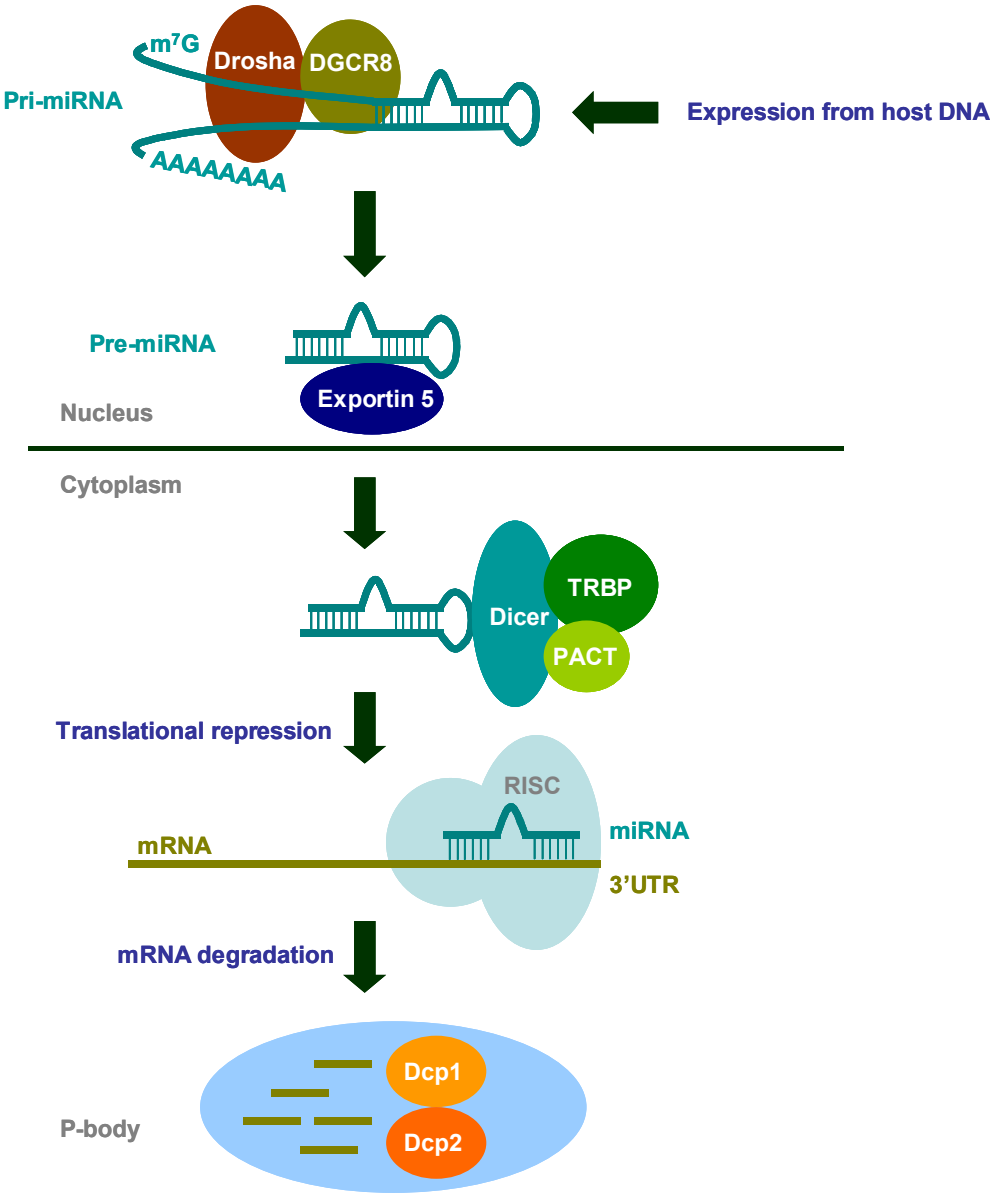

Figure 1.3 miRNA silencing pathway in mammalian cells. In the nucleus, endogenous primary microRNA (pri-miRNA) is transcribed by RNA polymerase II (Pol II). Precursor miRNA (Pre-miRNA) is then generated by Drosha-DGCR8 (DiGeorge syndrome critical region gene 8). Following export from the nucleus to the cytoplasm by 5' exportin, the pre-miRNA is then bound to the Dicer-TRBP-PACT complex which processes the pre-miRNA into miRNA. After associating with RISC, the mature miRNA mediates translational repression by recognising the target mRNA 3' untranslated region (3'UTR). mRNA degradation occurs in the P-body which contains the decapping enzymes DCP1 and DCP2.

1.1.1.3.1.1 Regulation processes for mRNA degradation—AU-rich elements regulation

Apart from the general mRNA degradation pathway **(Section 1.1.1.2.1)**, AU-rich elements (AREs) at the 3'UTR of mRNA can regulate miRNA mediated mRNA cleavage. AREs enhance the mRNA turnover rates by interacting with subunits of the exosome or proteins that interact with the exosome such as KSRP (KH-type splicing regulatory protein) and/or tristetrapolin (TTP). AREs also function with other proteins such as the urokinase plasminogen activator (UPA) associated RNA helicase to manipulate the decapping and deadenylation processes for the mRNA turnover (Wilusz & Wilusz 2004).

A recent study suggested that the miRNA-RISC complex targets ARE sequences in mRNA through interactions with TTP, a sequence specific RNA binding protein. However, downstream mRNA cleavage is not mediated by the exosome as knockdown of the exosome by RNAi does not abrogate the target mRNA degradation, suggesting that the mRNA is degraded through the 5' to 3' end pathway **(Figure 1.2)** or other unknown pathway(s) (Jing et al. 2005)

1.1.1.3.2 Differences in siRNA and miRNA mediated gene silencing

siRNA and miRNA share a similar cellular machinery for their initial processing; however, their gene silencing mechanisms may differ (John et al. 2007). siRNA mediates target mRNA cleavage through perfect base-pairing of the guide strand to the target mRNA while

perfect base-paring is not required in miRNA induced RNAi. It was found that the seed sequence (2 to 8 nucleotides from the 5' end) of miRNA needs an almost perfect pairing to its mRNA target, usually in the 3' untranslated region of the mRNA, while the 3' end of the miRNA can tolerate suboptimal pairing (Pillai et al. 2007). Therefore, a miRNA can silence various genes with similar sequences whereas an siRNA can only mediate cleavage of a specific gene.

1.1.1.3.3 Short hairpin RNA (shRNA)

RNAi can be mediated by plasmid expression of a single stranded RNA able to form a double stranded hairpin structure called shRNA. shRNA are a short double stranded RNA with a stem-loop, often 6-8 nucleotides, on one side. They are exported from the nucleus and processed into siRNA to mediate gene silencing via the RNAi machinery. The silencing effect of shRNA generally lasts longer than the siRNA (Paddison et al. 2002).

1.1.1.3.4 Piwi-interacting RNA (piRNA) and endogenous siRNA (endo-siRNA)

There are other endogenous small RNAs which are found to be able to mediate gene silencing. Such RNAs include Piwi-interacting RNA (piRNA) and endogenous RNA (endo-siRNA). piRNA, which is around 24-31 nucleotide long, is found to be expressed in the germline, implying that it would be important for the germline development. This small RNA does not required Dicer for processing, and some piRNAs involved in silencing

transposon through RNA destabilisation or heterchromatin formation. Endo-siRNAs can be derived from transposing transcripts, sense-antisense transcript pairs and long stem-loop structures. Different to miRNA, endo-siRNAs are dependent on Dicer but not on Drosha. Endo-siRNA (~21 nucleotide long) is shorter than miRNA. Some of the endo-siRNAs have been found to block retrotransposition (Kim et al. 2009; Weinberg & Wood 2009).

	siRNA	miRNA	shRNA
Size	A 19-21 nucleotide double stranded RNA with a 2 nucleotide overhang at the 3' end	A single stranded RNA with 21-25 nucleotides.	A short double stranded RNA with a stem-loop, often 6-8 nucleotides, on one side.
Origin	Introduced exogenously	Endogenously expressed	Introduced exogenously
Processing	siRNA is loaded in the RISC and mediated target cleavage.	Pre-miRNA is generated from the cleavage of pri-miRNA by the Drosha complex or introns during a splicing process. The Pre-miRNA is transported from the nucleus to the cytoplasm through 5' exportin and processed by Dicer to miRNA. miRNA is loaded to RISC for translation repression.	shRNA is expressed from a plasmid and transported from the nucleus to the cytoplasm by 5' exportin. shRNA is cleaved by Dicer to an siRNA and is loaded to RISC for target mRNA cleavage.
Target identification	siRNA mediates target mRNA cleavage through perfect base-pairing of the guide strand to the target mRNA.	Only the seed sequence (2 to 8 nucleotides from the 5' end) of miRNA needs an almost perfect pairing to its mRNA target, usually in the 3' untranslated region of the mRNA.	The siRNA processed from the shRNA mediates target mRNA cleavage through perfect base-pairing of the guide strand to the target mRNA.
Specificity	An siRNA usually designed to mediate cleavage of a specific gene.	A miRNA can silence up to 100 genes with similar sequences.	An shRNA usually designed to mediate cleavage of a specific gene.

Table. 1.1 A summary of siRNA, miRNA and shRNA.

1.1.1.4 Hurdles and improvements of siRNA technology

Although RNAi allows potent and specific gene silencing in cells, there are major hurdles to overcome in order to develop this technology for clinical use. For shRNA, the major hurdle is the side effects caused by overexpressing shRNA within cells. For siRNA, the main hurdles are *in vivo* delivery, stability and specificity of the delivered RNA molecules, and interferon activation induced by siRNA molecules. However, recent improvements in shRNA and siRNA design and modification of siRNA have shed light on the development of RNAi as a therapeutic.

1.1.1.4.1 shRNA design

Grimm and co-workers found that over-expression of shRNA *in vivo* could be fatal to mice. They found that high doses of shRNA and certain shRNA sequences caused mortality by downregulating liver-derived miRNA. Over-expression of shRNA with these sequences resulted in competition of exportin-5' with miRNA, leading to mortality; however, optimising the shRNA dose and sequence can minimise the toxicity effect causing by over-saturating the endogenous small RNA pathway (Grimm et al. 2006).

To address the toxicity effect induced by shRNA, Giering and co-workers demonstrated that an incorporation of a tissue specific polymerase II promoter in a plasmid for shRNA expression minimised the toxicity effect without compromising the gene silencing efficacy (Giering et al. 2008). They showed that a liver-specific apolipoprotein and human α-1-

antitrypsin fusion promoter driven plasmid can yield shRNA silencing the envelope surface antigen of hepatitis B virus (HBV) in mouse liver without major toxicity. McBride and co-workers also showed that modifying the shRNA to an "artificial miRNA", in which it contains a hairpin, mRNA targeting region and a tail region as a substrate for Drosha processing, improved the safety of the shRNA without compromising the gene silencing efficacy (McBride et al. 2008).

1.1.1.4.2 Stability and specificity of siRNA

Unmodified siRNA is susceptible to nuclease mediated degradation. Modifications of the siRNA backbone with boranophosphate (Hall et al. 2004), 2'-fluoro and 2'-O-methyl modified siRNA can increase the half life of siRNA relative to unmodified siRNA (Allerson et al. 2005). Interestingly, these modifications can also improve the gene silencing potency and specificity of the siRNA significantly (Allerson et al. 2005; Hall et al. 2004). In terms of the 2'O-methyl modification, Jackson and co-workers demonstrated that this modification specifically at position 2 on the guide strand further improves siRNA specificity (Jackson et al. 2006). These modifications are believed to improve the siRNA specificity by decreasing the free energy for hybridisation between the guide strand and its non-specific targets. As a result, binding between the guide strand and the non-specific targets becomes suboptimal and therefore target cleavage is not initiated (Jackson et al. 2006).

Off-target or non-specific gene silencing has been observed in some siRNA applications. However, recent studies on a better sequence design may help to improve the specificity of siRNA. It was found that siRNA with characteristics such as low C/G content and low internal stability at the 3'end of the passenger strand are more specific in gene silencing (Reynolds et al. 2004). Absence of inverted repeats or palindromes within the siRNA can also improve gene silencing potency. This may be due to the fact that a guide strand containing an inverted repeat would form an internal fold-back structure which reduces the effective concentration and silencing potential of the siRNA (Reynolds et al. 2004). It was also observed that there is a base preference in certain positions of siRNA for more specific gene silencing. For instance, siRNA with an A at position 3 and 19, U at position 10, the absence of a G at position 13 and the absence of a G or U at position 19 of the sense strand are proven to be more specific in gene silencing (Reynolds et al. 2004). As non-specific gene silencing effects are associated with the perfect pairing of the guide strand from positions 2-7 or 2-8 (the seed sequence) to the 3'UTR of mRNA, but not to the 5'UTR or ORF (Birmingham et al. 2006), siRNA sequences should preferentially be designed not to target the 3'UTR.

1.1.1.4.3 Interferon activation

Interferon activation has been a problem of siRNA mediated gene silencing for *in vivo* or clinical use. It was demonstrated that certain siRNA sequence induced interferon-α (Hornung et al. 2005; Judge et al. 2005). On the other hand, it was shown that 2'O-methyl modifications on uridine or guanosine nucleosides in the passenger strand can prevent

immunostimulation. The exact molecular mechanism is not known; it could be that modification of the GU in the passenger strand sterically hinders the interaction between the siRNA and the toll-like receptor 7 and 8 (Judge et al. 2006), a receptor located in endosomal membrane which recognises the GU content of RNA (Heil et al. 2003; Lee et al. 2003).

1.1.1.4.4 Delivery of siRNA

Delivery efficiency of siRNA *in vivo* is a main problem for the applications of RNAi technology. siRNA is a negatively charged molecules and often require a carrier for cellular delivery. The delivery of siRNA is improved by complex formation of siRNA with polyethyleneimine (PEI) (Urban-Klein et al. 2005) or atelocollagen (Minakuchi et al. 2004), or conjugation of siRNA with cholesterol (Soutschek et al. 2004). Urban-Klein and co-workers were able to deliver siRNA into subcutaneous tumors in mice by systemic (intraperitoneal, i.p.) administration of PEI siRNA complexes targeting the c-erbB2/neu (HER-2) receptor (Urban-Klein et al. 2005). Minakuchi and co-workers showed that atelocollagen siRNA complexes targeting fibroblast growth factor 4 (FGF-4) injected intratesticularly reduced testicular tumour growth in mice (Minakuchi et al. 2004). Soutschek and co-workers demonstrated that siRNA conjugated with cholesterol could silence an endogenous apolipoprotein B (apoB) messenger RNA in liver and jejunum after intravenous injection in mice (Soutschek et al. 2004).

Although these systems improve the efficiency of siRNA delivery, these systems are not cell type specific. Delivery of siRNA to non-disease cells would be harmful (Toub et al. 2006). Therefore, there is a need to further develop a robust, safe and clinically suitable siRNA delivery system (Whitehead et al. 2009). Strategies developed for plasmid delivery could be applicable for the further improvements of siRNA delivery. These strategies are discussed in **Section 1.2.**

1.1.1.5 RNAi based human trials

Despite the delivery hurdle, there are several RNAi-based human trials have been reported, showing the proof of concept of using siRNA or shRNA as a therapeutic. A trial on human immunodeficiency virus (HIV) infection utilised shRNA expressed by a lentiviral vector to target *rev* and *tat* mRNA of HIV-1, alongside a nucleolar-localising TAR RNA decoy and an anti-CCR5 ribozyme to inhibit HIV-1 infection in primary hematopoietic cells (Li et al. 2005; Benitec Limited 2009). This study showed that the primary hematopoietic cells treated with the lentiviral vector had the potential to limit HIV infection. Although this trial also included other silencing technology, it demonstrated the possibility of using shRNA as a medical treatment.

Other trials are conducted for the treatments of diseases in which the disease causing cells such as the epithelial cells can take up naked siRNA. For instance, there was a trial on prevention of respiratory syncytial virus (RSV) infection by intranasal delivery of naked siRNA targeting the P protein, an essential subunit of viral RNA-dependent RNA

polymerase, to inhibit viral gene expression (Alnylam Pharmaceuticals 2008). It was observed that this siRNA was well tolerated in healthy adults and induced significant antiviral efficacy in patients. Two other trials were on the age-related macular degeneration (AMD), an ocular disease which leads to blindness due to excessive blood vessel growth and rupture within the cornea. Naked siRNA targeting vascular endothelial growth factor (VEGF) or its receptor (VEGFR1) was delivered by direct intravitreal injection into the eye to test the safety and efficacy for the AMD treatment (Opko Health 2007; ClinicalTrial.gov 2009). It was reported that the siRNA induced minimal side effects and improved vision in some of the patients initially. However, the phase III trial was terminated because it was deemed that the trial was unlikely to meet its primary end point (Opko Health 2009).

Despite the initial success of some of these trials, the outcomes of the therapeutic values are remained to be seen. Clearly, there is a need to develop a better siRNA delivery system for disease treatments because delivering siRNA to most of the cell types has proven to be a major hurdle to transfer this technology into the clinic (Whitehead et al. 2009). Nevertheless, those trials and pre-clinical studies to date have shown that RNAi can provide an attractive way to target disease causing genes as a therapeutic. Further applications of the siRNA technology will probably require the development of a robust and safe siRNA delivery system for systemic application in the clinic. It is likely that synthetic carriers will play a key role in siRNA delivery in the future.

1.1.2 Other gene silencing technologies

Apart from RNAi, there are other different types of gene silencing techniques including the use of antisense olignucleotides and ribozymes to down-regulate target mRNA. These methods have been used to treat diseases such as cancers and retinitis (Leung & Whittaker 2005).

1.1.2.1 Antisense oligonucleotides

Antisense oligonucleotides can base pair with target mRNA and mediate mRNA degradation by RNase H, which cleaves the RNA in a DNA-RNA duplex (Sazani & Kole, 2003), or by double stranded RNase which degrades double stranded RNA (Lima & Crooke, 1997) **(Figure 1.4A)**. However, some of the oligonucletides do not silence a gene by RNase H, instead they decrease gene expression by translational repression (Sazani & Kole, 2003; Juliano et al. 2008) **(Figure 1.4B)**. Since oligonuclotides are unstable in the biological environment, there are several improvements to increase their stability. For instance, the oligonucleotide backbone can be modified into locked nucleic acids (LNAs), peptide nucleic acids (PNAs) and hexitol nucleic acids (HNAs). However, these modified oligonucleotides are not able to mediate RHase H based mRNA degradation (Manoharan 2002; Kurreck 2003; Crooke 2004). It was found that introduction of several phosphodiester residues within the central parts of these modified oligonuleotides allowed RNase H mediated target mRNA degradation while the stability of the oligonucleotides was still retained (Crooke 2004).

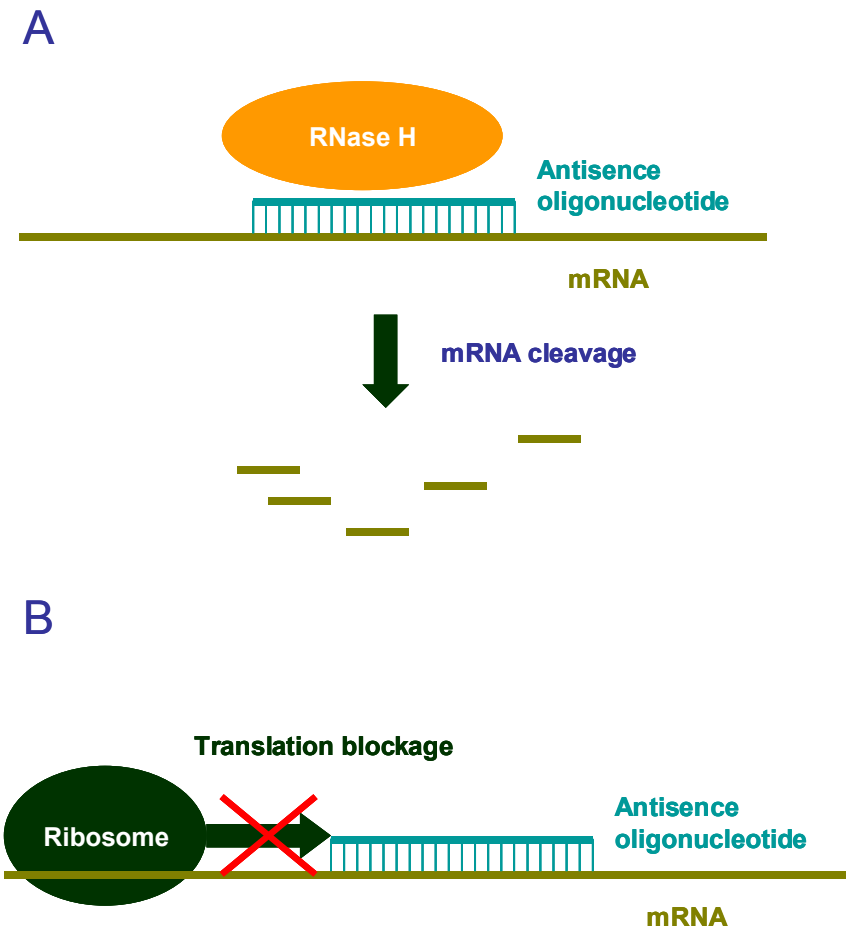

Figure 1.4 A schematic diagram showing the mechanisms of antisense induced gene silencing. **(A)** RNase H cleavage mediated by antisense oligonucleotides. **(B)** Translational suppression of gene expression.

1.1.2.2 Ribozyme

Since the discovery of catalytically active RNA molecules known as ribozyme (Kruger et al. 1982; Guerrier-Takada et al. 1983), there has been much researches on developing these gene silencing molecules for therapeutic uses. Ribozymes are capable of binding in a sequence specific manner to substrate mRNA through base-pairing interactions, and cleaving the bound RNA **(Figure 1.5)**. Ribozymes then release the cleaved RNA and bind to other target RNA to mediate further RNA cleavage. Repeated cleavage cycles lead to target gene silencing (Sullenger & Gilboa 2002).

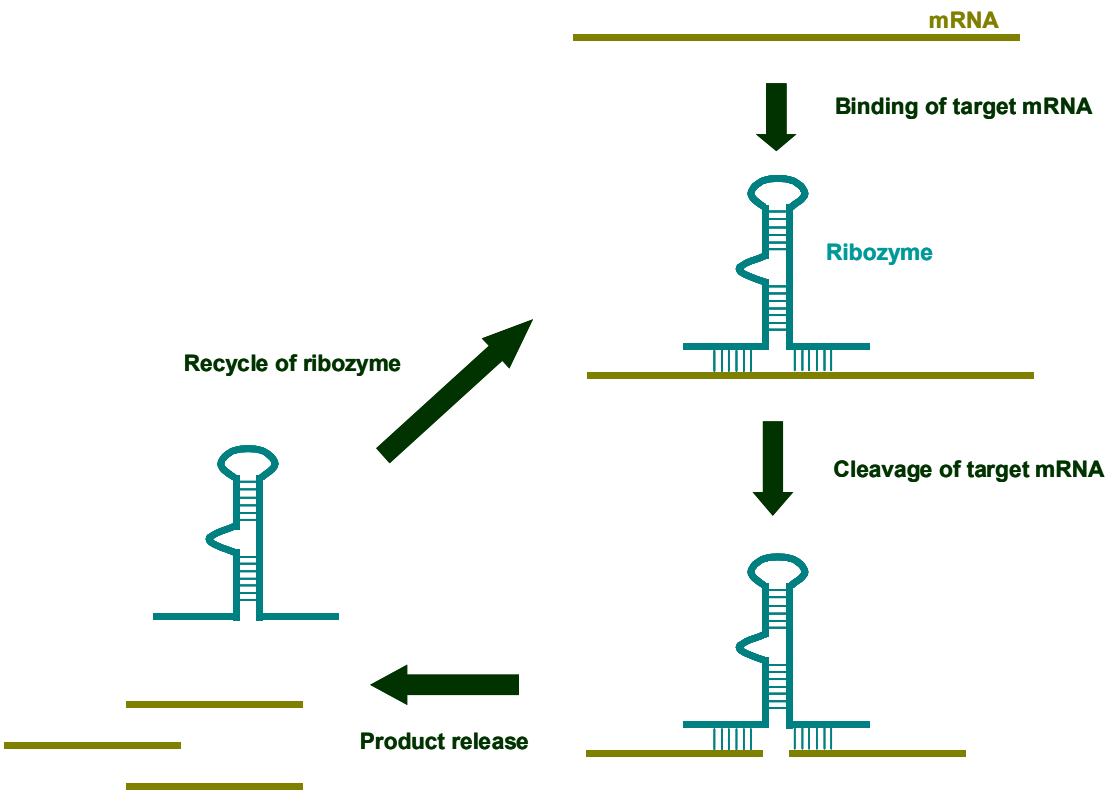

Figure 1.5 A schematic diagram of ribozyme mediated target RNA cleavage. The ribozyme can bind to target RNA through base-pairing interactions. The target RNA is then cleaved and released. The ribozyme is then free to bind to other target RNA.

1.1.3 A comparison of the antisense oligonucleotides, ribozymes and RNAi

The antisense oligonucleotides, ribozymes and RNAi share similar advantages such as target specificity and problems such as poor stability to be used as therapeutics. Some of the problems can be addressed by the improvement of the synthetic technology.

Gene silencing potency: Both of these technologies can be designed to cleave virtually any target mRNA. However, to mediate potent gene silencing, it appears that less amount of siRNA is required whereas relatively high amount of antisense oligonucleotides are needed (Grunweller et al. 2003; Vickers et al. 2003). There are no direct comparisons of the dose effect between siRNA or antisense oligonucleotides and ribozymes (Scherer & Rossi 2003).

Target sequence selection: Although potential target sequences can be estimated by certain design rationales, the antisense oligonucleotide or siRNA sequence still needs to be verified by systemic testing of various potential targets which is proven to be time consuming (Scherer & Rossi 2003). There are also limitations for the design of the ribozyme sequences. For example, ribozymes are required to contain specific sequences such as GUC triplet to mediate target RNA cleavage (Kurreck 2003; Scherer & Rossi 2003). This limits the choices of RNA target site for ribozymes.

Non-specific gene silencing: There is potential that these molecules could mediate non-specific gene silencing. It was shown that antisense oligonucleotides directed RNase H

to mediate non-specific RNA cleavage (Scherer & Rossi 2003). There was also a report about non-specific effect by siRNA (Jackson et al. 2003). However, a better understanding of the sequence selection criteria enables non-specific gene silencing to be minimised (Reynolds et al. 2004; Scherer & Rossi 2003). Ribozymes appear to be very specific for target cleavage; however, they may bind to other proteins in the cells, affecting the functions of the bound proteins and resulting in unwanted side effects (Scherer & Rossi 2003).

Stability: All those molecules are susceptible to nucleases. However, as mentioned in **Section 1.1.1.4.2 and 1.1.2.1**, modifications of the backbone of siRNA or antisense oligonucleotides improve their stability. By contrast, modifications of ribozymes may not be available because these would change the conformation of a ribozyme which affects the gene silencing effect (Kurreck 2003).

Effective gene silencing molecules should be able to mediate specific gene silencing with minimal side effects such as off target silencing. They should be stable enough to exert their effect to achieve gene silencing phenotypes. At the moment, RNAi appears to be more effective than antisense oligonuclotides for potent gene silencing and more stable than ribozymes for achieving the gene silencing phenotypes. The potential of siRNA to mediate non-specific gene silencing and immunostimulation can be minimised by better sequence design and backbone modifications **(Section 1.1.1.4.3)**. A better understanding of the biology of antisense oligonucleotides and ribozymes may lead to improvements in the silencing potency, stability and side effects of these molecules.

Today, RNAi is widely used for basic research, target validation and disease treatments. As previously mentioned, RNAi can be delivered using an siRNA or a plasmid expressing an shRNA. However, RNAi delivery *in vivo* has proven to be challenging, restricting the development of RNAi-based therapies (Li et al. 2006). The next section will discuss *in vivo* plasmid delivery techniques and how these methods can be modified for siRNA delivery.

1.2 Methods used for delivering RNAi

To mediate RNAi, either an shRNA encoding plasmid, an pri-miRNA expressing plasmid, siRNA or other small RNAs need(s) to be delivered to cells. Generally, methods for nucleic acid delivery can be divided into two main types, namely viral and non-viral methods. Each method has its own advantages and disadvantages and these are discussed in this section.

1.2.1 Viral methods

The choice of vectors for a specific therapeutic use should be determined on the basis of its biological properties. In this section, the most commonly used viral vectors such as the adenoviral and retroviral vectors **(Figure 1.6)** and the adeno-associated viral vector which is used for a recent clinical trial for treating blindness and failing eyesight (Bainbridge et al. 2008; Maguire et al. 2008) are discussed.

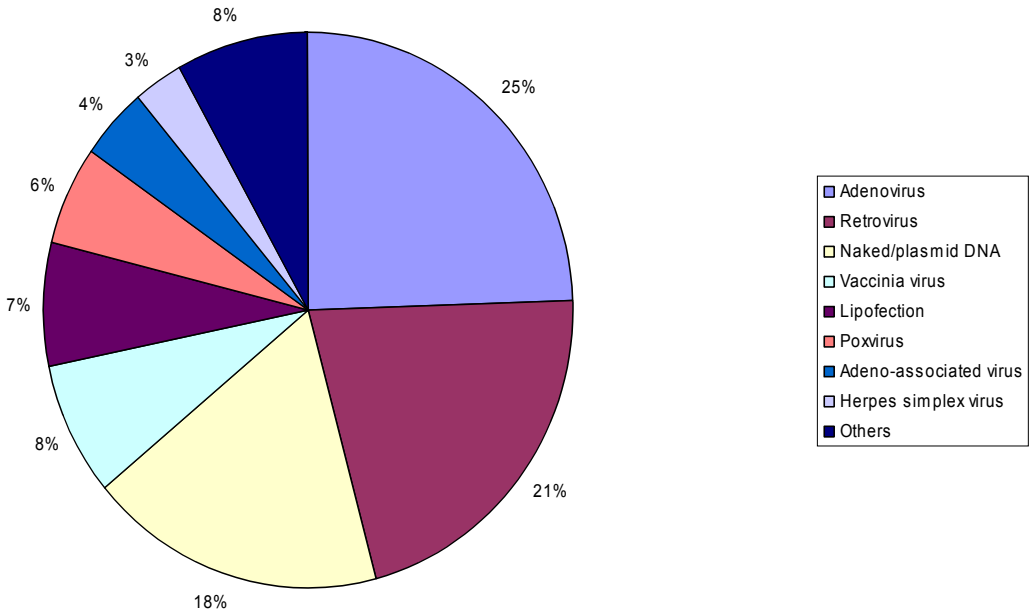

Figure 1.6 A chart showing percentage of different vectors used in gene therapy clinical trials (modified from Edelstein 2008).

1.2.1.1 Adenoviral vector

The adenoviral vector is one of the most efficient vectors for gene delivery (Thomas et al. 2003). Adenovirus is a double stranded DNA virus which infects the human respiratory tract and eyes (El Aneed 2004). It can carry a relatively large transgene compared to other viral vectors due to its large genomic size (36kb), and can infect both dividing and non-dividing cells (Goverdhana et al. 2005). Transduction of tissues including muscle, brain, lung, liver, hematopoietic stem and cancer cells have been demonstrated. This broad tropism gives the adenoviral vectors the potential to treat a wide range of diseases.

Adenoviral vector transgene expression may be transient (5-10 days post-infection) in dividing tissues because it does not integrate the therapeutic gene into the host cell genome (Marshall 2000; Selkirk 2004). The therapeutic gene persists as a non-integrated episome inside the nucleus (Thomas et al. 2003). The non-integrating property means the vector should not pose a risk of insertional mutagenesis (Marshall 2000).

Some studies reported long-term gene expression following adenovirus-mediated transfer. This can be done by injecting vectors into cells of nude mice or mice in which both the vectors and immunosuppressing agents are injected (Verma & Somia 1997). The gene transfer is more efficient in immunodeficient animals (El Aneed 2004), implying that transient expression may also be caused by an immune response.

One of the main drawbacks of adenoviral vectors is that the viral proteins stimulate a strong immune reaction (Marshall 2000). At high doses the vector may induce a lethal inflammatory reaction (El Aneed 2004). The viral gene products can elicit a cytotoxic T-lymphocyte response while the viral caspid can induce humoral virus-neutralising antibody responses and cytokine-mediated inflammatory responses, resulting in inflammation (Thomas et al. 2003). Inflammation caused by a high vector dose is believed to have caused the death of a young patient involved in a clinical trial using an adenoviral vector which was conducted at the University of Pennsylvania in Philadelphia (Ferber 2001; Selkirk 2004).

The immunogenic problem must be solved to make the adenoviral vectors suitable for therapeutic applications. A “gutless” adenoviral vector, which lacks immunogenic factors,

has been generated to serve this purpose (Selkirk 2004). The vector has a lower immunogenicity as all viral genes, except the elements that define the beginning and the end of the genome, and the viral packaging sequence, are deleted (Goverdhana et al. 2005). It has also been observed that adenoviral vectors coated with lipids (Singh et al. 2008) or polymers (Green et al. 2008) show reduced immunogenicity, probably due to masking of the immunogenic adenoviral capsid proteins (Kreppel & Kochanek 2008).

The use of adenoviral vector for shRNA delivery *in vivo* has been reported. Uchida and co-workers demonstrated that silencing of survivin, an antiapoptotic molecule widely overexpressed in malignancies but not detected in terminally differentiated adult tissues, induced apoptosis cancer cells and led to remarkably attenuated tumour growth *in vivo* following intratumuoral injection of the adenoviral vector (Uchida et al. 2004). Recently, Zhang and co-workers silenced Ki-67, a nuclear protein which is associated with cell proliferation, to induce apoptosis of tumour cells and efficiently suppress tumour growth in nude mice following an intratumoural injection of the adenoviral vector (Zhang et al. 2009). These reports showed that adenoviral vectors can be good candidates for shRNA delivery, provided that side effects such as immunogenicity are minimised.

1.2.1.2 Adeno-associated viral vector

The adeno-associated virus (AAV) is a single stranded DNA virus (Verma & Somia 1997) which is non-pathogenic in humans (Check 2003). Vectors derived from AAV have shown low immunogenicity and stable gene expression (Monahan et al. 2002). Most preclinical

and clinical studies show that the vector is non-pathogenic to the human immune system (Marshall 2000; Monahan et al. 2002).

As with adenoviral vectors, AAV vectors are able to transfer genes *in vivo* with high efficiency and infect both dividing and non-dividing cells (Marshall 2000). However, it has a limited gene-carrying capacity due to its small genomic size (5kb) (Goverdhana et al. 2005; Marshall 2000). This restricts the length of therapeutic DNA sequence that it can carry.

One of the drawbacks of the AAV vector is that the viral genome integrates itself into the host genome (Marshall 2000) preferentially at chromosome 19 (Verma & Somia 1997). This poses a risk of insertional mutagenesis (Check 2003). However, more than 90% of the vector genome appears as the episomes (Thomas et al. 2003). Therefore, the chances of mutagenesis are not as high as retroviral vector **(Section 1.2.1.3)**. Despite the low frequency of integration, AAV vector was observed to cause liver tumour in mice in a recent study (Donsante et al. 2007).

There are studies showed some successes using AAV to deliver shRNA *in vivo*. Xia and co-workers delivered shRNA to target ataxin-1 in spinocerebellar ataxia type 1 (SCA1) transgenic mice by injecting the AAV intracerebellarly. Following the shRNA treatment, the authors observed a profound decrease of ataxin-1 expression in the Purkinje cells, neural cells located in the cerebellar cortex. The SCA1 mice showed an improvement in motor coordination and a restoration of cerebellar morphology (Xia et al. 2004). On the other hand, Chen and co-workers demonstrated persistent HBV inhibition up to 22 weeks

in HBV transgenic mice using shRNA targeting the HBV surface antigen delivered by intravenous injection of AAV (Chen et al. 2009). These reports indicated that AAV can be an option for RNAi delivery. However, as AVV poses a risk of insertional mutagenesis, there is a need to study the long term safety of AAV mediated gene silencing.

1.2.1.3 Retroviral vector

The retroviral vector is the most common class of gene transfer vector in clinical studies and was among the first class of viral vectors to be developed for clinical use. It is now the vector of choice for *ex vivo* gene delivery to hematopoietic cells (Thomas et al. 2003).

The vector has a plus strand RNA with a small genomic size (7-10 kb) and only infects dividing cells (Marshall 2000) as the vector genome can only gain access to the cell nucleus when the nuclear envelope breaks down (Thomas et al. 2003). It is efficient in gene transfer and does not produce a strong immune response (Marshall 2000), but it does not express genes in cell stably even though it integrates itself into the host genome as a double stranded DNA provirus as a result of reverse transcription (Marshall 2000). One possible explanation is that large portions of the vectors integrate themselves in the transcriptionally silent heterochromatin, which hinders gene expression. This is called the position effects (Emery et al. 2000). The integration property indeed is unsafe for patients as it poses the risk of insertional mutagenesis. The T cell leukemia development of the X-SCID patients in the clinical trials in France and United Kindgom is due to the insertion of the therapeutic gene near proto-oncogene such as LIM domain only 2 (*LMO2)*, leading to transcription and

expression of the oncogene (Cavazzana-Calvo et al. 2004; Thrasher et al. 2005; Williams & Baum 2003). However, more recently developed self-inactivating retroviral vectors are believed to be less likely to cause such events (Thornhill et al. 2008).

Nevertheless, retroviral vector was among the first viral vectors to infect cells for *in vivo* shRNA expression. In this study, Brummelkamp and co-workers effectively suppressed tumour growth in nude mice by targeting the oncogene K-RASV12 gene, which is essential for tumour viability (Brummelkamp et al. 2002). This demonstrated the specificity of RNAi and highlighted the possibility of using shRNA as therapeutics.

Vector	Viral genome	Cloning capacity	Tropism	Inflammation	Vector genome forms	Main limitations	Main advantages
Adenovirus	dsDNA	36 kb	Broad	High	Episomal	Capsid mediates an inflammatory response; preexisting anti-Ad antibodies in most humans	Highly efficient transduction of most tissues; large cloning capacity; high titer and long-term expression
AAV	ssDNA	<5 kb	Broad	Low	Episomal (>90%), Integrated (<10%)	Small cloning capacity	Broad cell tropism; noninflammatory and non-pathogenic
Retrovirus	RNA	8 kb	Dividing cells only	Low	Integrated	Integration might induce insertional mutagenesis and oncogenesis in some applications	Transduces dividing cells

Table 1.2 A summary of the characteristics of the adenoviral, adeno-associated and retroviral vectors.

1.2.2 Non-viral vector systems

It is generally accepted that non-viral vector delivery systems are less efficient for gene transfer *in vivo* compared to viral vectors. However, they are less immunogenic, low risks of insertional mutagenesis, are flexible in delivering different kinds of nucleic acids such as antisense oligonucleotides, ribozymes and siRNA and are generally easier for mass-production and quality control than the viral vectors; therefore, they are an attractive tool for nucleic acid transfer (Li & Huang 2000). A number of physical and chemical methods for non-viral gene transfer have been developed for nucleic acid delivery to improve the gene transfer efficiency and time period of gene expression.

1.2.2.1 Physical methods

Physical methods for gene delivery include electroporation, hydrodynamic delivery, ultrasound delivery, laser beam gene transduction (LBGT) and ballistic gene delivery. These methods have been shown to mediate effective *in vivo* gene delivery, and these methods are discussed in this section.

1.2.2.1.1 Electroporation

One of the most powerful physical methods is electroporation, which improves gene transfer efficiency by 100-fold relative to naked DNA injection. This method involves the use of electrodes to apply an electric field across the target tissue to facilitate gene delivery.

The mechanism behind this remains unknown, but it is believed that under the influence of an electric field, temporary pores are formed on the cell membrane and this allows DNA to enter the cells (Wells 2004).

Indeed, electroporation has been used recently to deliver siRNA into solid tumours to mediate effective gene silencing (Golzio et al. 2007). Golzio and co-workers generated a mouse tumour model in which the tumour expressed enhanced green fluorescent protein (eGFP) stably. They found that eletroporation following a single injection of the siRNA targeting eGFP into the tumour led to eGFP silencing for three days.

1.2.2.1.2 Hydrodynamic delivery

The hydrodynamic delivery can increase gene transfer efficiency and the duration of gene expression without integration of transgenes into the host genome (Ferber 2001). Experiments on mice showed that the plasmid can persist in liver cells for a year, which is half of a typical mouse lifetime (Stoll et al. 2001).

The procedure of the method involves quickly injecting the tail vein of a mouse with naked DNA in a relatively large volume of saline solution, roughly equal to the entire blood volume of the mouse. A high pressure will be generated in the blood after injection, allowing creation of temporarily pores in the cell membrane of the mouse liver cells. As a result, plasmids can enter the cells and be expressed (Kobayashi et al. 2004; Zhang et al. 2004). Though it is impossible to inject humans with solutions that are half the volume of

human blood, hydrodynamic delivery has been shown to improve gene transfer efficiency in large animal models. For example, DNA was injected into rhesus monkeys via arteries that feed the arm and leg muscles by using a blood-pressure cuff to temporarily increase blood pressure. Gene expression was detected in about 30% of muscle cells, similar to the efficiency of viral delivery (Ferber 2001).

A recent study has shown that hydrodynamic delivery can mediate effective *in vivo* siRNA transfer in various mouse organs such as liver, kidney, pancreas, spleen and bone marrow. The siRNA remained in these organs for at least 24 hours following the hydrodynamic delivery (Larson et al. 2007). Other studies showed that delivering siRNA targeting the surface antigen region of HBV by hydrodynamic injection in mice resulted in 70% - 80% silencing of the antigen, effectively preventing HBV replication (Giladi et al. 2003; Klein et al. 2003).

1.2.2.1.3 Ultrasound gene delivery

Though electroporation and hydrodynamic delivery are effective in gene transfer, they are invasive to tissues. As a result, other less invasive methods have been examined for their ability to transfer DNA and siRNA. One such method is ultrasound, which works by transiently disrupting the cell membrane to increase cell permeability to DNA (Newman & Bettinger 2007). A recent study has shown that delivery of unmodified siRNA to the synovium of the knee joints of rats can be achieved by ultrasound sonication (Saito et al. 2007). In this study, delivery of siRNA targeting luciferase mediated 70% luciferase

knockdown in luciferase expressing synovium in rats. Suzuki and co-workers showed that ultrasound delivery of siRNA targeting luciferase silenced 80% of luciferase expression for 24 weeks in luciferase expressing intervertebral discs in mice. They also demonstrated that ultrasound delivery of siRNA targeting the FasL gene inhibited 53% of endogenous FasL expression in intervertebral discs for 20 weeks (Suzuki et al. 2009).

1.2.2.1.4 Other physical methods

Laser beam gene transduction (LBGT) is one of the methods to transfer genes into cells. It is highly effective and has similar efficiency as electroporation. The mechanism behind the improvement of gene transfer is not clear, but it is believed that the laser beam creates transient holes in the cell membrane to facilitate DNA uptake (Zeira et al. 2003). On the other hand, ballistic gene delivery can also enhance gene transfer by "shooting" plasmids coated in microparticles into cells or tissues by using a machine called gene gun. The machine can increase the velocity of the microparticles so that they can bombard into the target cells or tissues. However, this technique is limited to superficial tissues such as skin (Dileo et al. 2003). To date there are no publications reporting the use of these methods for *in vivo* siRNA delivery, though this may be a possibility of transferring these techniques for siRNA delivery in the future.

1.2.2.1.5 Disadvantages of physical methods

Physical delivery of nucleic acids does not allow targeting to specific cell types; therefore, the uses of these methods are usually limited to local administration to the body such as skin, muscle, lung or tumour (Ferber 2004; Well 2004). To mediate cell targeting nucleic acid delivery, a synthetic vector system containing a cell targeting ligand can be used for nucleic acid transfer.

1.2.2.2 Synthetic vector systems

Generally, synthetic vector systems can be classified into a lipid based (lipoplex), polymer based (polyplex) and lipid polymer hybrid (lipopolyplex) system. These systems are described in this section.

1.2.2.2.1 Lipoplex

DNA delivery using the cationic lipid *N*-[1-(2,3-dioleyloxy)propyl]-*N*,*N*,*N*-trimethylammonium chloride (DOTMA) as a carrier was first reported by Felgner and co-workers (Felgner et al. 1987). Since then, a number of cationic lipids have been investigated for DNA transfer (Bennett et al. 1997; Felgner & Ringold 1989; Gao & Huang 1991; Sternberg et al. 1998). It has been shown that cationic lipid DNA complexes, or lipoplexes, can be efficient for gene delivery for many cell types, and some of the lipoplexes are currently being evaluated in clinical trials **(Figure 1.6)**.

Cationic lipids can bind to and condense DNA through electrostatic interactions (Felgner et al. 1987). As a result, nano-sized lipoplexes are formed which can enter cells by endocytosis (Farhood et al. 1995; McLachlan et al. 1995; Wrobel & Collins 1995). Within the cells, DNA must escape from the endosome and traffick to the nucleus for transcription. To enhance the endosomal escape capability, helper lipids such as dioleyl phosphatidylethanolamine (DOPE), cholesterol or dioleoyl phosphatidyl choline (DOPC) can be added to lipoplexes (Farhood et al. 1995; Zuhorn et al. 2005).

Although lipoplexes can improve gene delivery, they are not cell type specific. To improve cell type specificity, receptor ligands including transferrin (Simoes et al. 1999), monoclonal antibodies (Wang and Huang 1987), or folate receptors (Lee and Huang 1996) can be covalently attached to the vector to allow internalisation of the lipoplexes through receptor-mediated endocytosis.

Cationic lipids have been studied for siRNA delivery. Cardoso and co-workers found that cationic lipids, which were formulated with N-[1-(2,3-Dioleoyloxy)propyl]-N,N,N-trimethylammonium methylsulfate (DOTAP) and cholesterol, associated with transferrin can deliver siRNA (Cardoso et al. 2008). In this study, they observed 40% of *in vivo* luciferase and c-Jun gene silencing without adverse cytotoxic effects. However, a contrary study showed that although DOTAP/cholesterol can be used for siRNA delivery, this complex may induce an immune response (Ma et al. 2005b). Sioud and Soensen also found that liposomes could be used for *in vivo* siRNA delivery, but there may also be an immune response caused by the lipid-siRNA complex (Sioud & Soensen 2003). The difference in the cytotoxicity induced by the siRNA complexes could be due to the different siRNA

molecules that were used in these two studies. It has been shown that the cytotoxic effect of an siRNA complex is dependent on the siRNA sequence (Robbins et al. 2008).

As well as cationic lipids, Landen and co-workers showed that a neutral liposome, DOPC, can be used for *in vivo* siRNA delivery. With the combination of siRNA complexes targeting a tyrosine kinase receptor, EphA2, and a conventional chemotherapeutic drug, paclitaxel, ovarian tumour growth was inhibited (Landen et al. 2005).

Clearly, the understanding of lipid based siRNA delivery systems is evolving. There is still a need to further improve the nucleic acid transfer efficacy and study the cytotoxic effect. More researches into the mechanism of lipid based siRNA delivery may allow the problems of lipoplex delivery to be addressed, helping to develop this system for clinical applications in the future.

1.2.2.2.2 Polyplex

Polyplex refers to a complex using a polymer as a carrier to deliver nucleic acids to a cell. Cationic polymers such as polyethylenimine (PEI) (Gautam et al. 2000; Godbey et al. 1999; Goula et al. 1998), polyarginine (Kim et al. 2007), histidylated polylysine peptides (Read et al. 2005), chitosan (Koping-Hoggard et al. 2001; Lee et al. 1998), polylysine (Dash et al. 1999; Ramsay et al. 2000; Wu & Wu 1987; Zauner et al. 1997) and dendrimers (Bielinska et al. 1999; Kukowska-Latallo et al. 1999) have been widely used to condense plasmid DNA and form nanoparticles. It has been reported that the polyplexes are taken up by cells

through endocytosis (Khalil et al. 2006). To further improve cellular uptake and cell specificity of the polyplexes, the polymers can be conjugated with a ligand or antibody that binds to a cell surface receptor. For example, polylysine linked to an asialoorosomucoid ligand, a liver-specific asialoglycoprotein receptor, has been used to deliver plasmid DNA to the liver *in vivo* (Kwoh et al. 1999; Perales et al. 1997). Other targeting systems including transferrin linked PEI (Kircheis et al. 1999), polylysine conjugated epidermal growth factor (Schaffer & Lauffenburger, 1998; Schaffer et al. 2000; Xu et al. 1998) and polylysine associated with an integrin targeting peptide (Hart et al. 1998; Jenkins et al. 2003) have been shown to improve gene delivery.

One of the main hurdles for effective gene delivery with the majority of polyplexes is degradation of the vectors within cells, usually in the acidic late endosomes **(Section 1.3.1.1)** (Erbacher et al. 1996; Meyer & Wagner 2006). However, it was reported that polymer systems which have a high buffer capacity such as the histidylated polylysine peptides and PEI can mediate endosomal escape by increasing the osmotic pressure of the late endosome, leading to endosomal destabilisation and release of DNA (Kichler et al. 2001; Read et al. 2005). For polyplexes that cannot mediate endosomal escape, the addition of an endosomal destabilising peptide including the influenza virus hemagglutinin HA-2 (Wagner et al. 1992) can enhance transfection efficiency. Also, it has been found that an addition of endosomal buffering agents such as chloroquine can improve endosomal escape by increasing the osmotic pressure in the late endosome, resulting endosomal destabilisation and release of DNA (Erbacher et al. 1996).

Since plasmid DNA must be transcribed in the nucleus, an addition of a nuclear localising signal (NLS) peptide to vector systems can further improve the transfection efficiency. For example, it has been shown that vector systems containing an NLS peptide such as simian virus 40 (SV40) large-T antigen (Kaneda et al. 1989), protamine (Wienhues et al. 1987), histone H2 (Balicki et al. 2002) or melittin-derived peptides (Ogris et al. 2001) showed enhanced transfection efficiency.

A number of polymers have been used to improve the *in vitro* siRNA delivery efficiency such as PEI (Grayson et al. 2006), polyarginine (El-Sayed et al. 2008; Kumar et al. 2007), histidylated polylysine peptides (Leng et al. 2008), chitosan (Katas & Alpar 2006), polylysine (El-Sayed et al. 2008) and dendrimers (Patil et al. 2008). For *in vivo* siRNA delivery, some studies have demonstrated that these polymers can also be used. Ge and co-workers showed that a PEI-siRNA complex could deliver siRNA targeting the influenza viral nucleocapsid protein or a component of influenza virus RNA transcriptase into lung tissue to treat and prevent influenza infections in mice (Ge et al. 2004). On the other hand, Urban-Klein and co-workers demonstrated that a PEI-siRNA complex could silence HER-2 expression in SKOV-3 ovarian cancer xenografts, leading to tumour growth inhibition (Urban-Klein et al. 2005). These early studies demonstrated the principle of using polymers to form nanoparticle with siRNA for *in vivo* siRNA delivery.

Howard and co-workers showed that a chitosan-siRNA complex could reduce eGFP expression by 40% in bronchiole epithelial cells in transgenic eGFP mice (Howard et al. 2006). In another study, Kumar and co-workers showed that oligoarginine peptides conjugated with a ligand targeting the acetylcholine receptor expressed by neuronal cells

could form complexes with siRNA and deliver it to neuronal cells *in vitro*. Moreover, they observed that this siRNA complex could by pass the blood brain barrier and deliver siRNA to the brain *in vivo* (Kumar et al. 2007). Recently, Leng and co-workers demonstrated that histidylated polylysine peptides could carry siRNA to tumour xenografts for tumour growth inhibition. Their strategy was to use siRNA targeting Raf-1 mRNA in tumour cells to induce apoptosis. However, there are concerns related to the cytotoxicity of this polyplex system (Leng et al. 2008).

Although polymer based siRNA delivery systems are still in the early stages of development, some reports have already shown promising siRNA delivery, highlighting the potential of these systems. However, more efforts are still needed to further improve the siRNA delivery efficiency and address the cytotoxicity of polyplexes. A systematic study of the polyplex properties and siRNA delivery efficacy may help address these issues and improve these systems for clinical applications in the future.

1.2.2.2.3 Lipopolyplex

A lipopolyplex is composed of cationic lipids, cationic polymers and nucleic acids. It is a hybrid of the lipoplex and polyplex system. In the lipopolyplex system, cationic polymers condense nucleic acids into nanoparticles by electrostatic interaction. Lipids are added to the system to improve gene delivery efficiency by enhancing endosomal escape of the complex. With the addition of the lipid, lipopolyplexes mediate 100-fold higher gene delivery efficiency than polyplexes (Hart et al. 1998).

To further improve gene delivery efficiency, the polymer in the lipopolyplex can conjugate with a ligand or NLS to enhance cellular uptake and nuclear localisation of the lipopolyplex as described in **Section 1.2.2.2.2.**

Lipopolyplexes have been used to deliver siRNA *in vivo*. Li and co-workers demonstrated that a lipopolyplex system containing DOTAP/cholesterol, polyethylene glycol (PEG)-conjugated anisamide ligand, protamine, calf thymus DNA and siRNA against MDM2, c-myc, and VEGF could mediate specific gene silencing. In this system, calf thymus DNA is believed to act as a carrier to help siRNA condensation with protamine to form a nanoparticle. It was found that this lipopolyplex mediated oncogene silencing and led to tumour growth suppression (Li et al. 2008). Despite this promising result, so far this is the only report using a lipopolyplex containing genomic DNA for siRNA delivery. Therefore, more studies are needed to demonstrate the efficacy and safety of siRNA delivery by this system.

1.3 Barriers to nucleic acid delivery using synthetic vector systems

Although different methods for plasmid DNA or siRNA delivery are available, there is a need to improve the *in vivo* nucleic acid delivery efficiency, especially for siRNA (Li et al. 2006). Several key areas must be addressed, including cellular uptake of the complex, release of nucleic acids within cells and trafficking of nucleic acids to the correct subcellular compartment, to improve nucleic acid delivery.

1.3.1 Cellular internalisation of vector complexes

Synthetic nucleic acid complexes can enter cells through either the endocytic or non-endocytic routes (Khalil et al. 2006). There are two main types of endocytosis including phagocytosis and pinocytosis. Phagocytosis occurs only in specialised cells such as macrophages whereas pinocytosis can be carried out by all mammalian cells. Four main pinocytotic pathways have been characterised, namely clathrin-mediated endocytosis, caveolae-mediated endocytosis, macropinocytosis and clathrin and caveolae independent endocytosis.

1.3.1.1 Clathrin-mediated endocytosis

Upon receptor binding by ligands such as cholesterol or transferrin (Brodsky et al. 2001; Schmid 1997), clathrin is recruited and coated on the inner side of the plasma membrane to form a pit **(Figure 1.7)**. The pit is then budded off the membrane to form a vesicle (Belting,

Sandgren, & Wittrup 2005; Conner & Schmid 2003; Nichols 2003) with a size from 100 to 150 nm in diameter (Takei & Haucke 2001). The clathrin is then depolymerised and recycled, and this results in the formation of an early endosome. The endosome fuses with other pre-existing endosomes, which further fuse with lysosomes (Brodsky et al. 2001).

The pH changes through this endocytic process, from neutral to pH 6 in the lumen of the early endosome. The pH further decreases to 5 during the progression from the late endosome to the lysosome (Maxfield & McGraw 2004). Since the complexes within the lysosome will be degraded (Goldstein et al. 1985; Maxfield & McGraw 2004), it is important for the complexes to escape from the late endosome and release the nucleic acid into the cytoplasm.

Most clathrin-mediated endocytosis occurs through receptor-mediated endocytosis. However, other endocytosis pathways such as caveolae-mediated endocytosis are also capable of mediating receptor-dependent uptake events (Khalil et al. 2006; Parton et al. 1994).

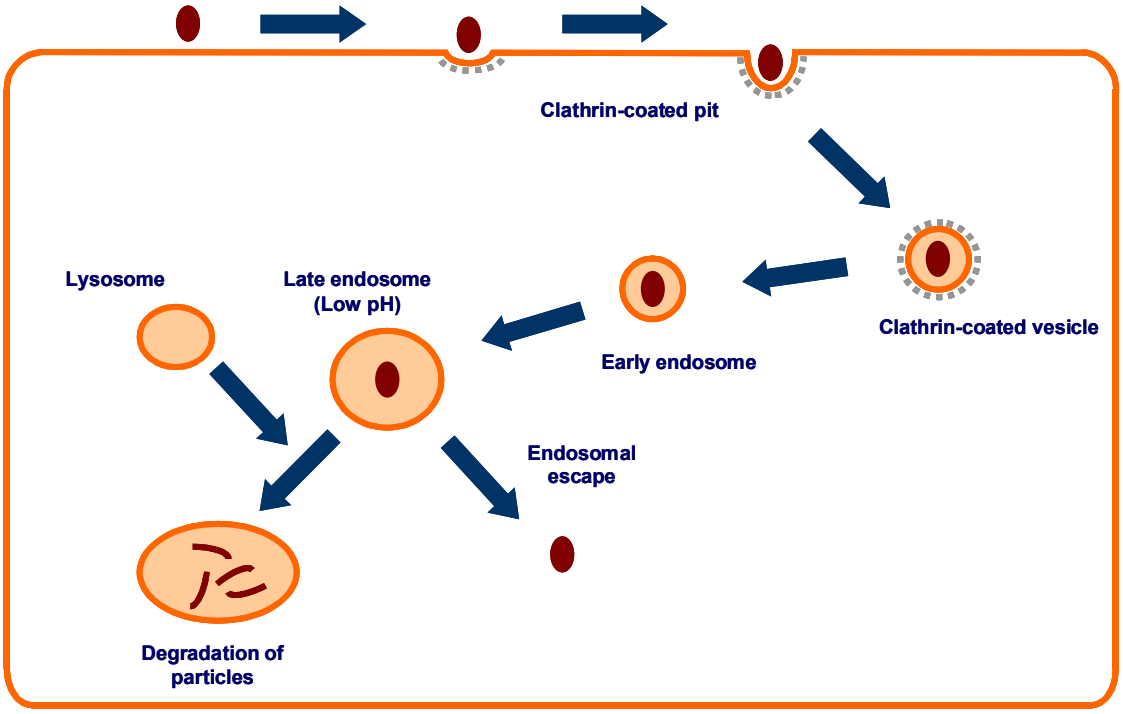

Figure 1.7 Clathrin-mediated endocytosis. Following the ligand binding to a specific cell receptor, a clathrin coated pit is formed around the particle. The pit is then pinched off from the plasma membrane to form an intracellular clathrin-coated vesicle. Depolymerisation of the clathrin leads to the formation of an early endosome. The pH in the early endosome decreases when it progresses to a late endosome. Molecules may escape from the late endosome to the cytoplasm, otherwise the late endosome fuses with a lysosome where the molecules are degraded.

1.3.1.2 Caveolae-mediated endocytosis

Caveolae are lipid rafts that are rich in cholesterol and glycosphingolipids (Harris et al. 2002; Matveev et al. 2001).They can be flaskshaped, flat, tubular, or detached vesiclar invaginations (50–80 nm in diameter) on the cell surface **(Figure 1.8)** (Pelkmans et al.

2001; Smart et al. 1999), and contain a high level of caveolin proteins, which are essential for caveola formations (Harris et al. 2002).

The mechanism of caveolae-mediated endocytosis has been elucidated by the cellular uptake of the SV40 virus. SV40 binds to the cell membrane and becomes trapped in a caveola (~50-60nm). The virus is then taken up into a caveosome and delivered to the endoplasmic reticulum (Conner & Schmid 2003).

A major difference between clathrin-mediated and caveolae-mediated endocytosis is that caveolae-dependent uptake is non-acidic and non-digestive (Ferrari et al. 2003). Since the pH does not decrease in the caveolae, the cargo can be transported directly to the Golgi and/or endoplasmic reticulum, avoiding lysosomal degradation (Khalil et al. 2006). Therefore, caveolae-dependent endocytosis may provide an effective route for nucleic acid complex internalisation.

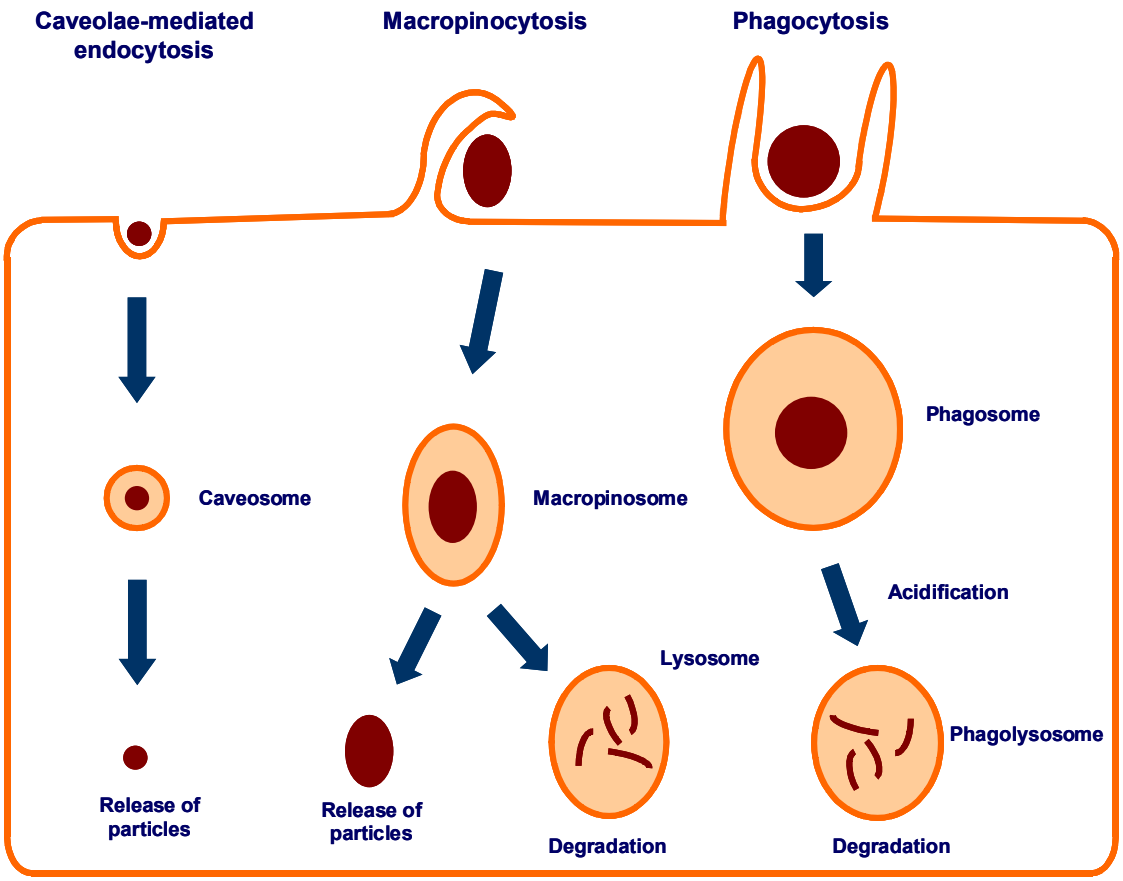

Figure 1.8 Caveolae-mediated endocytosis, macropinocytosis and phagocytosis. Caveolae-mediated endocytosis occurs when molecules associate to the cell membrane. The molecules are then trapped in a caveola and are taken up by the cell via caveosomes. Caveolar uptake is non-acidic and non-digestive.

Macropinocytosis allows internalisation of molecules by actin-mediated cell surface ruffling. The molecules are then trapped in macropinosomes. In some cells such as macrophage, the macropinosomes are fused to lysosomes and the molecules are degraded. In other cells such as A431, the macropinosomes are leaky and the molecules are released into the cytoplasm.

Phagocytosis occurs mainly in specialised cells such as phagocytes. Cell surface extension is formed to engulf the molecules. The molecules are internalised in phagosomes. The phagosomes are then acidified and develop into mature phagolysosomes where the molecules are degraded.

1.3.1.3 Macropinocytosis

Upon stimulation by growth factors or other signals, cell membrane ruffles (Conner & Schmid 2003; Swanson & Watts 1995) due to outward-directed actin polymerisation **(Figure 1.8)**. The ruffle then fuses with the cell membrane to form a macropinosome (Swanson & Watts 1995). Macropinosomes are relatively large, up to 5 μm in diameter. The fate of the macropinosome depends on the cell type (Meier & Greber 2003 Swanson & Watts 1995). For instance, in macrophages, it migrates toward the center of the cell where it becomes acidified and merges with a lysosome (Meier & Greber 2003). In other cell types such as human A431 cells, the macropinosome does not interact with endocytic compartments (Swanson & Watts 1995). It is believed that macropinosomes are relatively "leaky" vesicles compared with other types of endosomes (Wadia et al. 2004), so this pathway could be effective for nucleic acid delivery (Khalil et al. 2006).

1.3.1.4 Phagocytosis

Phagocytosis is carried out to clear large (>0.5 μm) pathogens or debris such as bacteria, yeast, dead cells or arterial fat deposits. In mammals, phagocytosis is performed by specialised cells such as macrophages, monocytes, and neutrophils (Allen & Aderem 1996).

Particle internalisation is mediated by interaction of specific receptors on the phagocyte with ligands on the surface of the particle **(Figure 1.8)**. This interaction leads to the

formation of cell surface extensions which surround the particle. The particle is then internalised and trapped in a phagosome, which matures into a phagolysosome in which the internalised particle is degraded (Allen & Aderem 1996).

Since phagocytosis is primarily conducted by specialised cells, it is not expected to play a significant role in other cells for gene delivery. However, some studies showed that a phagocytosis-like mechanism might take part in the uptake of large cationic lipid-DNA complexes (lipoplexes) and PEI polyplexes (Kopatz et al. 2004; Matsui et al. 1997).

1.3.1.5 Other internalisation pathways

Some molecules such as the interleukin (IL) 2 receptor β subunit glycosyl phosphatidylinositol (GPI)-anchored proteins are internalised through endocytic pathways other than clathrin-, caveolae-dependent and macropincytotic endocytosis. The mechanisms of these pathways are not clearly understood; however, it is found that these pathways involve different components to initiate cellular uptake of molecules (Gong et al. 2008).

It was found that some peptides, such as the TAT, penetratin, and VP22 peptides, may be able to enter cells without endocytosis (Brooks et al. 2005; Gupta et al. 2005; Nakase et al. 2004; Thoren et al. 2003; Vives et al. 1997). It was proposed that the positive charge of the peptides plays a role in the direct penetration of the lipid bilayer (Trehin & Merkle 2004). However, it was shown that the mechanism of internalisation could change to endocytosis when these peptides were linked to other cargo (Khalil et al., 2004; Lundberg et al., 2003;

Richard et al., 2003). Further studies need to be done to confirm whether non-endocytic uptake can be useful for nucleic acid delivery.

1.3.2 Nucleic acid release within cells

Following the cellular uptake of nucleic acid complexes, the nucleic acid needs to be dissociated from the complex within the cytoplasm or nucleus, depending on the type of nucleic acid used, for its respective biological function (Khalil et al. 2006). Since the complexes usually localise to endosomes, escape of the nucleic acid is essential. Strategies to mediate endosomal escape include the addition of a helper lipid DOPE to stabilise the endosomal membrane or the use of a high buffer capacity peptide such as PEI to enhance endosomal escape **(Section 1.2.2.2.2)**.

1.3.3 Nuclear transport

After the release of nucleic acids, plasmid DNA must migrate to the nucleus for transcription whereas siRNA must traffick to the P-body in the cytoplasm. Only molecules with size less than 70kDa or ~10 nm diameter can pass through nuclear envelope pores; therefore, plasmid DNA is too large to enter the nucleus through passive diffusion (Melchior & Gerace 1995). It is generally accepted that plasmid DNA nuclear entry can be achieved during mitosis when the integrity of the nuclear envelope is temporarily lost. For non-dividing cells, plasmid DNA may need assistance from other factors such as an NLS for nuclear entry (Jans & Hubner 1996).

1.4 siRNA versus shRNA encoding plasmid

Compared to delivery of plasmid DNA using a synthetic system, delivering siRNA to cells is theoretically easier since plasmid DNA must be transported into the nucleus while siRNA is only required to be released in the cytoplasm. Therefore, siRNA can be delivered into both dividing and non-dividing cells for gene silencing without a need of a mechanism for nuclear uptake.

The criteria for successful plasmid DNA or siRNA delivery systems are similar; both vector systems need to mediate cellular uptake of the complexes and allow release of the nucleic acids within the cells. However, differences in the structural and chemical composition and biological function between plasmid DNA and siRNA means that the complex formation properties for plasmid DNA delivery may differ from those of siRNA.

1.4.1 A comparison of the properties of plasmid DNA and siRNA

1.4.1.1 Similarity

Plasmid DNA and siRNA share two major similarities. Firstly, they are both double stranded nucleic acids. Secondly, they both have anionic backbones with the same negative charge to nucleotide ratio. Therefore, they are both expected to interact electro-statically with cationic polymers. Despite the similarities, siRNA and plasmid DNA are different in some aspects which may have implications on the interaction to the cationic polymers.

1.4.1.2 Differences

1.4.1.2.1 Differences in size and topology/ geometry attributes

Firstly, plasmid DNA and siRNA have different sizes. While plasmid DNA is usually several kilobase pairs long, siRNA is usually 21-23 base pairs. Secondly, the topology of siRNA is different to that of plasmid DNA. siRNA is believed to form an A-form helix whereas DNA is expected to be in B-form. A-form has a larger diameter and a smaller rise per base pair and displacement of the base pairs from the helix axis; therefore, it is stiffer than B-form. As a result, the persistence length, which refers to the tendency of a chain to persist in a given direction (Hagerman 1997), of the A-form structure is larger than that of a B-form structure (Nelson & Cox 2004).

Geometry attribute	A-form RNA	B-form DNA
Helix sense	Right-handed	Right-handed
Rise/ bp along the axis	0.27 nm	0.332 nm
Diameter	2.6 nm	2 nm
Persistence length	72nm ± 7 nm	40-50 nm

Table 1.3 A comparison of the topology and geometry attributes of RNA and DNA (Nelson & Cox 2004).

1.4.1.2.2 Half life and duration of biological function

The second major structural difference between siRNA and DNA is the composition of the backbone. The backbone of siRNA consists of ribose which has a hydroxyl group in the 2′ position of the pentose ring, while the backbone of DNA consists of deoxyribose which contains a hydrogen atom at the 2' position of the pentose ring. As a result, RNA is more susceptible to hydrolysis by serum nucleases which cleave the phosphodiester backbone of nucleic acids (Banan & Puri 2004).

In terms of the duration of the biological function, plasmid DNA lasts longer than siRNA. Generally plasmid DNA can be expressed transiently for up to 2-3 weeks (Kay et al. 1997) whereas siRNA gene knockdown usually lasts for 3-7 days, dependent on the cell types and the half life of the targeted gene (Bartlett & Davis 2006). However, modifying the structure of the siRNA could result in longer gene silencing effect **(Section 1.1.1.4.2)**.

1.5 Project aims and objectives

RNAi holds enormous potential for treating a wide range of diseases; however, delivery of siRNA to targeted cells is one of the major hurdles to transfer this technology in therapeutic uses. Cationic polymers have been used for gene delivery by condensing plasmid DNA to form a positive surface charged nanoparticle for effective cellular binding, uptake and transfection. Therefore these polymers could possibly be used to condense and deliver siRNA into cells. Despite the fact that there are different types of cationic polymer systems which could be used for siRNA delivery, the discovery of these systems is through trial and

error rather than a systematic development process. Therefore, there is a need to identify the important criteria for siRNA delivery.

It is hypothesised that an efficient DNA or siRNA delivery complex would be a nanoparticle with positive surface charge which facilitates cellular binding and uptake. These complexes would have similar dissociation properties to allow the nucleic acids to detach from the complexes for transcription or gene silencing. Therefore, the aims of this study are:

- to systematically clarify the relationship between the biophysical and transfection properties of effective cationic polymer based plasmid DNA delivery systems.

- to elucidate the requirements of the cationic polymers for successful siRNA complex formation and delivery.

- to compare the biophysical properties between efficient DNA and siRNA delivery systems so as to generate information for further development of an effective siRNA delivery system.

Chapter 2

Materials and methods

2.1 Materials

Unless otherwise stated, all tissue culture reagents were supplied by Gibco BRL (Invitrogen), and all general chemicals were supplied by Sigma.

2.1.1 siRNA

Reagents	Suppliers
Silencer Cy-3 labelled siRNA	Ambion
Anti-Luc siRNA (Appendix I)	Dharmacon
Anti-eGFP siRNA (Appendix I)	Dharmacon
Anti-GAPDH siRNA (Appendix I)	Ambion
Irrelevant siRNA control	Ambion

Table 2.1 The siRNA used in this study.

2.1.2 Transfection reagents

Reagents	Suppliers
Linear PEI	Polyplus transfection
Branched PEI	Sigma
Lipofectin	Invitrogen
Lipofectamine 2000	Invitrogen
siLentfect	Biorad
The linear lysine peptides (K8, K16, K24 and K32) and peptide Y	Synthesised by immunoKontact
The Kbranch peptide	Synthesised by UCL chemistry department
Ultrapure water	Gibco, Invitrogen
5 × reporter lysis buffer	Roche
Luciferase reporter gene assay kits	Promega
Protein assay buffer	Biorad
Bovine serum albumin	Sigma
KDalert GAPDH kits	Ambion
CellTiter 96 AQueous One Solution Assay	Promega

Table 2.2 The transfection reagents used in this study.

2.1.3 Reagents for DNA manipulation

Reagents	Suppliers
Restriction enzymes and buffers	Promega
Ligase and buffers	Promega
Ethidium bromide	Sigma
Plasmid endofree miniprep and endofree maxiprep kits	Qiagen
QIAquick gel extraction kit	Qiagen
DH5α Competent Cells	Invitrogen
Agar	MERCK
Ampicillin	Stratagene
Luria Broth Base (LB)	Invitrogen
Magnesium Chloride	Fisher Scientific

Table 2.3 The reagents for DNA manipulation used in this study.

2.1.4 Reagents for electrophoresis

Reagents	Suppliers
Agarose and low melting point agarose	Invitrogen
Loading dye (10 mM Tris pH 7.5, 50 mM EDTA, 10% Ficol 400, 0.4% Orange G)	Sigma
1 Kb+ ladder	Invitrogen
siRNA ladder	Promega
1× TAE (40 mM Tris-acetate, 5 mM EDTA)	Sigma

Table 2.4 The reagents used for electrophoresis.

2.1.5 Tissue culture reagents

Reagents/apparatus	Suppliers
DMEM, sodium bicarbonate, sodium pyruvate, Optimem, Trypsin/EDTA, PBS, ULTRApure water	Gibco, Invitrogen
Black-walled plates for luciferase assay	Fisher Scientific
Fetal calf serum (FCS), Minimum Essential Medium Eagle	Sigma
DMSO	Sigma
Tissue- culture treated flasks, dishes and plates	Nunc

Table 2.5 The reagents and apparatus used for tissue culture.

2.1.6 Cell lines

Name	Origin
HEK 293T	Human embryonic kidney cell line (ATCC: CRL-11268)
HEK 293T eGFP expressing cell	Kind gift from Dr. Tassos Georgiadis (Institute of Child Health, University College London)
HT1080	Human fibrosarcoma cell line (ATCC: CCL-121)
Neuro 2a	Mouse neuroblastoma cell line (ATCC: CCL-131)
NIH 3T3	Mouse fibroblast (ATCC: CRL-1658)

Table 2.6 The cell line used in this study.

2.1.7 Reagents, apparatus and machines for PicoGreen related, particle sizing and zeta potential assays

Reagents/apparatus/machines	Suppliers
TE buffer	Sigma
PicoGreen	Invitrogen
Heparin	Sigma
Colourless flat bottomed 96 well plate	Greiner bio-one
FLUOstar Optima	BMG labtech
Low volume disposable cuvette	Sarstedt, Germany
Zetasizer folded capillary cell	Malvern
Zetasizer Nano S and the related software (Dispersion technology software v.5.03)	Malvern

Table 2.7 The reagents, apparatus and machines used for the PicoGreen related, particle sizing and complex surface charge assays.

2.1.8 Reagents, apparatus and machines for flow cytometry and confocal imaging

Reagents/apparatus/machines	Suppliers
Vectashield mounting medium for Fluorescence with DAPI	Vector Laboratories
Alexa Fluor 488 phalloidin	Molecular Probe, Invitrogen
1 × PBS	Gibco, Invitrogen
Polylysine slide and cover slip	VWR International Inc.
Formaldehyde	Polysciences, Inc
0.5% triton	Sigma
Mounting varnish	Maxiflex
Immedge pen	Vector Laboratories
Milli-Q water	Milli-Q Biocel System
Cy5 DNA labelling kit	Mirus
Confocal microscope and the related software (LCS Lite version)	Leica
Flow cytometry tube	Nunc
Epics XL flow cytometer and the related softwares (Summit v.4.3 and FlowJo v.8.6.3)	Beckman Coulter
SPECTRAmax plate reader	Molecular Devices

Table 2.8 The reagents, apparatus and machines used for flow cytometry and confocal imaging.

2.1.9 Reagents, apparatus and machine for Real Time PCR

Reagents/apparatus/machine	Suppliers
RNAeasy kit	Qiagen
Taqman primers and probes	Applied Biosystems
Platinum qPCR SuperMix-UDG with ROX	Invitrogen
DNase I and buffer	Invitrogen
Superscript II	Invitrogen
Reagents for cDNA formation	Invitrogen
ABI Prism and the related software	Applied Biosystems

Table 2.9 The reagents, apparatus and machine used for Real Time PCR.

2.1.10 Centrifuges

Centrifuges	Suppliers
Microcentrifuge	Heraeus Biofuge Fresco
Tabletop centrifuge	Sorvall Legend RT
Superspeed centrifuge	Sorvall Evolution RC

Table 2.10 The centrifuges used in this study.

2.2 Methods

2.2.1 Bacterial Manipulation

2.2.1.1 Growth and Maintenance of *Escherichia coli*

Escherichia coli (*E.coli*) were either cultured in liquid LB media at 37 ºC with 250 r.p.m agitation or plated out on solid LB plates containing 1.5 % bacto agar. *E.coli* transformed with plasmids were maintained in the LB media supplemented with ampicillin (100 µg/ml) at the same conditions.

To store the transformed *E.coli*, the bacterial cultures were mixed with glycerol in 20 % volume for volume (v/v) and kept at -80 °C.

2.2.1.2 Transformation of *E.coli* by heat shock method

100 µl of competent DH5α cells were transformed with 100 ng of plasmid DNA by incubating the cells on ice for 40 minutes and then heat-shocking the cells at 42 °C for 90 seconds, followed by a further 2 minutes incubation on ice. The cells were diluted to a final volume of 1 ml in 37 °C pre-warmed LB media and the media/bacterial culture was agitated at 250 r.p.m at 37 °C for 1 hour. Following incubation, 100 µl of the culture was spread on LB agar plates containing 100 µg/ml of ampicillin, and the plates were incubated overnight at 37 °C.

2.2.2 DNA manipulation

2.2.2.1 Restriction Enzyme Digestion

1 µg plasmid DNA (pCEP4 or pCI-Luc) was digested in a final volume of 20 µl with 10 × buffer, bovine serum albumin (BSA) and restriction enzyme (*Not*I *or Hin*dIII) at 37 °C for 3 hours **(Table 2.11)**. Following the digestion, the reaction was stopped by heat inactivation of the endonucleases at 65 °C for 10 minutes. The two digestions with *Not*I *or Hin*dIII were performed sequentially, and DNA digestion was verified by visualisation of DNA fragments following 1 % agarose gel electrophoresis.

Reagents	**Volume**
Milli-Q water	14µl
BSA (10 mg/ml)	2 µl
10× buffer	2 µl
Restriction enzyme (*Not*I *or Hin*dIII)	1 µl
Plasmid DNA (pCEP4 or pCI-Luc) (1 mg/ml)	1 µl
Total volume	20 µl

Table 2.11 The reagents used for restriction digestion of pCEP4 or pCI-Luc.

2.2.2.2 Agarose Gel Electrophoresis

The DNA fragments were separated by electrophoresis using 1 % agarose gels. To prepare the gels, agarose powder was dissolved in 1 × TAE buffer by boiling in a

microwave oven for 1-2 minutes. After cooling the agarose solution, 0.5 μg/ml ethidium bromide was added for visualisation of the DNA samples. The agarose solution was then poured into a gel rack with a comb inserted on one side of the rack. Once the gel had formed, it was put in a gel tank filled with 1 × TAE buffer. DNA samples then were mixed with Orange G loading buffer in a 5 to 1 (v/v) and loaded onto the agarose gels. A "1 Kb plus DNA ladder" was loaded onto the gels for estimation of the DNA fragment sizes. Under a voltage of 50-100 V (up to 150 mA), the DNA fragments were resolved and were visualised by exposure to a ultra-violet lamp using an UVIdoc gel documentation system.

2.2.2.3 Gel Purification of DNA

Following electrophoresis, DNA fragments were excised from 1% agarose gels using a clean scalpel blade under ultra-violet light. The DNA was then extracted from the agarose gel by a silica membrane in high-salt buffer using a QIAquick gel extraction kit following the manufacturer's instructions.

2.2.2.4 Ligation

The DNA fragments were ligated at vector to insert ratios of 1:3, 1:6 or 1:9 (100 ng vector DNA). With a final volume of 10 μl of 10 × T4 DNA ligase buffer (diluted to 1 × with distilled water) containing 1 unit of T4 DNA ligase, the ligation reactions were

performed overnight at 16 °C. The end products of the reactions were either used to transform chemically-competent *E.coli* (2 µl) or stored at -20 °C for later use.

2.2.2.5 Measurement of nucleic acid concentration and purity

Nucleic acid concentration was measured from light absorbance at a wavelength of 260 nm (A_{260}) using a NanoDrop ND-1000 spectrophotometer. The DNA purity was determined by dividing the A_{260} by the absorbance value of protein at 280 nm (A_{280}). Any value equal or higher than 1.8-2.0 indicated that the DNA was acceptably pure for downstream procedures (Dieffenbach & Dveksler 2003).

2.2.2.6 Plasmid DNA preparation

For small scale plasmid DNA preparation, transformed *E.coli* were inoculated in 5 ml of LB medium containing ampicillin (100 µg/ml) overnight (overnight cultures). Plasmid DNA was then prepared from the overnight cultures by alkaline lysis on a resin column and precipitated with isopropanol using Qiagen Mini-prep kits according to the manufacturer's instructions.

For large scale plasmid DNA preparation, 100 µl of a 6-hour starter culture were inoculated in 100 ml of LB medium containing ampicillin (100 µg/ml) overnight at 37 ^{o}C with constant agitation at 250 r.p.m. Plasmid DNA was then prepared using Qiagen Endofree Maxi-Prep kits following the manufacturer's instructions.

2.2.3 Cell Culture

2.2.3.1 Propagation of adherent cell lines

All adherent cell lines were maintained in their respective medium as shown in **Table 2.12**. Cells were grown in 25 cm^2, 80 cm^2 or 175 cm^2 tissue culture flasks or in 10 cm tissue culture dishes in 37 ºC incubators in a 5 % CO_2 atmosphere. Cells were passaged when 80-90 % confluence was reached. To passage the cells, the cells were washed twice with Dulbecco's phosphate buffered saline (1 × PBS). Following removal of the PBS, the cells were incubated with trypsin/EDTA for 5 minutes at 37 °C. The cells were then pelleted by centrifugation at 1200 r.p.m (306 × *g*) for 5 minutes. The supernatant was removed and the pellet was resuspended in full growth medium. One tenth of the cells were split to a new culture flask. Completed medium was added to fill up the flask to its suggested optimum volume.

Cell line	Complete growth medium
293T and 293T eGFP expressing cells	DMEM supplemented with 10% FCS
HT 1080	Minimum Essential Medium Eagle supplemented with 10% FCS, 1% sodium pyruvate and 1% L-Glutamine
Neuro2a and Neuro 2a luciferase expressing cells	DMEM supplemented with 10% FCS, 1% sodium bicarbonate and 1% sodium pyruvate
NIH 3T3	DMEM supplemented with 10% FCS and 2% sodium bicarbonate

Table 2.12 The complete growth media to culture the cell lines used in this study.

2.2.3.2 Long Term Storage of Cell Lines

For long term storage, 2-5 x 10^6 cells or cells of a 90 % confluent monolayer from a 80 cm^2 tissue culture flask were pelleted by centrifugation at 1200 r.p.m (306 × *g*) for 5 minutes. The cells were then resuspended in 1 ml freezing medium (90 % FCS, 10 % dimethylsulfoxide (DMSO)) and transferred to a cryovial. Cells were frozen slowly overnight to -70 °C in an isopropanol freezing box, then transferred to liquid nitrogen.

To revive the frozen cells, an aliquot of cells was thawed in a 37 °C waterbath and transferred quickly to 9 ml complete growth medium. The cells were pelleted at 1200 r.p.m (306 × *g*) to remove the DMSO and then resuspended in 5 ml complete growth medium and transferred to a 25 cm^2 tissue culture flask.

2.2.3.3 Mammalian cell transfection

2.2.3.3.1 Plasmid transfection using polyplex

All the plasmid transfections were performed either with plasmid expressing eGFP (pEGFP-N1) **(Appendix II)** or plasmid expressing luciferase (pCI-Luc) **(Appendix II)**. Cells were seeded 24 hours before transfection in order to reach 70 % confluence/well in either 12 well or 96 well plates. Plasmid transfection complexes were formed by mixing 50 µl lysine based peptides or PEIs with 50 µl plasmid DNA in different Nitrogen to Phosphate (N/P) ratios in Optimem for 30 minutes at room temperature **(Section**

2.2.3.3.1.1 for the calculation of the N/P ratio, and Section 4.1.1 and 4.1.2 for the lysine based peptides and PEIs). Optimem was then added to dilute the complexes so that complexes containing 0.125 to 0.5 µg DNA in 200 µl were used in a well of 96 well plates whereas complexes containing 1 to 2 µg DNA in 1ml were used in a well of 12 well plates. After removing complete media from the cells, polyplexes were added to the plates. Following centrifugation at 1500 r.p.m (478 × *g*) at room temperature for 5 minutes to increase the transfection efficiency, the plates were incubated with the cells for 4 hours at 37 °C, 5% carbon dioxide. The polyplexes were replaced by normal media for 24 hours for luciferase assay or 48 hours to visualise eGFP expression.

2.2.3.3.1.1 Calculation of Nitrogen/Phosphate (N/P) ratio (charge ratio)

To calculate the N/P ratios of the lysine based peptides, firstly the nitrogen (N) value of each peptide was calculated as follows:

N value= (mass / molecular weight) × net charge

	Molecular weight	**Net charge (N)**
K8	1043	+8
K16	2068	+16
K24	3111	+24
K32	4154	+32
Kbranch	3072	+14

Table 2.13 The molecular weight and net charge of the peptides used in this study.

The calculation of the phosphate (P) value of the DNA and siRNA:

P value= (mass / molecular weight) × net charge

	Molecular weight	Net charge (P)
Anti-Luciferase	13278	-42
Anti-eGFP	13323.1	-42
pCI-Luc	3753380	-11386

Table 2.14 The molecular weight and net charge of the nucleic acids used in this study.

The calculation of the N/P ratios of B-PEI and L-PEI were performed as follows:

N/P ratio = (Volume of L-PEI in µl × 50) / mass of the nucleic acids

The B-PEI was diluted to 1 mg/ml in MilliQ water. 6.5 µl B-PEI was diluted in 493.5 µl MilliQ before use. For calculation of N/P ratio of the B-PEI is as follows:

N/P ratio = (Volume of B-PEI in µl × 10) / mass of the nucleic acids

2.2.3.3.2 Plasmid transfection using lipoplex or lipopolyplex

The transfection procedures were as stated in **Section 2.2.3.3.1**, except for transfection complex preparation procedures. For plasmid transfection using lipoplexes, 50 µl lipids were mixed with 50 µl plasmid DNA in desired weight ratios in Optimem for 30 minutes at room temperature. For plasmid transfection using lipopolyplexes, 50 µl Lipofectin, 80 µl epithelial targeting peptide (K16Y) with the sequence K16-GACYGLPHKFCG and 50 µl plasmid DNA were prepared in a 2:4:1 ratio (w/w/w) in Optimem for 30 minutes at room temperature. Optimem was added to dilute the complexes so that complexes containing 0.125 to 0.5 µg DNA in 200 µl were used per well of 96 well plates whereas complexes containing 1 to 2 µg DNA in 1 ml were used per well of 12 well plates.

2.2.3.3.3 siRNA transfection using polyplex

Cells were seeded 24 hours before transfection in order to reach 30-50 % confluence/well in either 12 well or 96 well plates. siRNA transfection complexes were formed by mixing 50 µl of the cationic polymers or peptides with 50 µl of siRNA in different N/P ratios **(Section 2.2.3.3.1.1 for calculation of the N/P ratio)** in Optimem for 30 minutes at room temperature. Optimem was then added to dilute the complexes so that complexes containing 1 to 32 nM siRNA in 200 µl were used per well of 96 well plates whereas complexes containing 5 to 150 nM siRNA in 1 ml were used per well of 12 well plates. After removing complete media from the cells, polyplexes were added to

the plates. Following centrifugation at 1500 r.p.m (478 × *g*) at room temperature to increase the transfection efficiency, the plates were incubated with the cells for 4 hours at 37 °C, 5% carbon dioxide. The polyplexes were then replaced by normal media after the transfection.

2.2.3.3.4 siRNA transfection using Lipofectamine 2000 (L2000)

The transfection procedures were as stated in **Section 2.2.3.3.3** except transfection complex preparation and exposure time of the transfection complexes. For 24 hour transfection in a 96 well plate setting, 0.125-1 µl of L2000 was diluted into 25 µl with Optimem and was mixed with 25 µl siRNA in Optimem for 20 minutes at room temperature. The complexes were then overlaid onto the cells containing 150 µl full growth medium per well. Complexes were replaced with fresh complete medium following transfection. In a 12 well plate setting, 0.5-1 µl of L2000 was dilute into 25 µl with Optimem and was mixed with 25 µl siRNA in Optimem for 20 minutes at room temperature. The complexes were then overlaid onto the cells containing 950µl full growth medium per well.

For 4 hour transfection in 96 well plates, 0.125-0.5 µl of L2000 was diluted into 25 µl with Optimem and was mixed with 25 µl siRNA in Optimem for 20 minutes at room temperature. The complexes were then diluted in Optimem so that complexes containing 1 to 32 nM siRNA in 200 µl were used in 96 well plates. After removing complete media from the cells, the complexes were added to the plates. Following centrifugation

at 1500 r.p.m (478 × *g*) at room temperature to increase the transfection efficiency, the plates were incubated with the cells for 4 hours at 37 °C. The complexes were then replaced by normal media after the transfection. In 12 well plates, 0.5-1 µl of L2000 was diluted into 25 µl with Optimem and was mixed with 25 µl siRNA in Optimem for 20 minutes at room temperature. The complexes were then diluted in Optimem so that complexes containing 5 to 150 nM siRNA in 1 ml were used per well.

2.2.3.3.5 siRNA transfection using siLentfect

The 24 hour transfection procedures were as stated in **Section 2.2.3.3.4** except the transfection complex preparation procedures. 0.1-0.4 µl/well of siLentfect was dilute into 25 µl with Optimem and was mixed with 25 µl siRNA in Optimem for 20 minutes at room temperature. The complexes were then overlaid onto the cells containing 150 µl full growth medium per well in a 96 well plates. Complexes were replaced with fresh full growth medium following transfection.

2.2.4 Construction of stable luciferase expressing Neuro 2a cells

2.2.4.1 Kill curve

Following seeding of 5×10^5 Neuro 2a cells per well of 6 well plates with full growth medium for 24 hours, different concentrations of hygromycin B, ranging from 0-1000 μg/ml, were added to the cells. After washing with PBS, the cells were trypsinised and counted at day 1, day 2 and day 4 following addition of hygromycin B. During cell counting, the cells were treated with trypan blue to distinguish viable cells and were counted using a hematocytometer. The numbers of viable cells from the treatments of different hygromycin B concentrations over the time course were used to plot a kill curve to indicate the optimal hygromycin B concentration for stable cell line generation. 200 μg/ml hygromycin B was deemed to be suitable for generation of stable Neuro2a cells.

2.2.4.2 Transfection

The luciferase reporter gene of pCI-Luc was subcloned into pCEP4, which consists of a hygromycin B resistant gene, to yield pCEP4-Luc for transfection as described previously. Briefly, 10^6 Neuro 2a cells were seeded in a 10 cm tissue culture dish overnight. The cells were transfected with complex composing 2 μg of pCEP4-Luc and 8 μg of lipofectin for 4 hours. Following removal of the transfection complex, full growth medium containing 200 μg/ml hygromycin B was added to the cells.

2.2.4.3 Selection

Fresh full growth medium containing 200 µg/ml hygromycin B was exchanged every 3 days and dead cells gently washed off with PBS during the selection process, which lasted for 4 weeks. After 10 to 14 days of the transfection procedure, single viable cells appeared **(Section 3.2.3.4)**. The single cells were observed until discrete colonies were formed. The colonies were harvested into separate wells of a 96 well flat-bottomed plate and expanded in antibiotic selection medium until cells were confluent in 6 well plates. 10^5 cells were then seeded in 96 well plates to test for luciferase expression. Once luciferase expression was confirmed, the cells were further expanded into a tissue culture flask. Some of the cells were then frozen for long term storage as described previously.

2.2.4.4 *In vivo* tumour formation

Procedures were performed in line with the animal scientific procedure act 1986 home office regulations. 1.5×10^6 Neuro 2a luciferase expressing cells in 100 µl PBS were injected subcutaneously into the right posterior flank of five 6-8 weeks female AJ 3.1 mice. After 10 to 15 days, tumours with a minimum 12mm diameter were harvested and frozen at -80 °C. Following thawing of the tumours on ice, they were homogenized in Reporter Lysis Buffer and the luciferase expression in the lysates were assayed.

2.2.5 Gene expression and cytotoxicity analyses

2.2.5.1 Luciferase expression assay

For a 96 well plate setting, cells were washed twice with 1 × PBS and incubated with 20 µl/well 1 × reporter lysis buffer for 20 minutes at 4 ˚C then -80 ˚C for at least 30 minutes. After the cells were defrosted at room temperature, luciferase assay buffer was prepared as described according to the manufacturer's protocol and 100 µl buffer was added to each well. Luciferase activity in the cells was then measured in terms of Relative Light Unit (RLU) using FLUOstar Optima. Protein content of each cell lysate was estimated by transferring 20 µl lysate to 180 µl 1 × Bio-Rad Protein Assay Reagent. After 10 minutes incubation of the lysate and the reagent, the OD590 of the mixture was recorded and the protein content of each lysate was calculated by comparing the OD590 with a BSA standard curve. RLU per milligram (mg) of protein represented luciferase activity per protein unit (RLU/mg).

For a 12 well plate setting, cells were washed twice with 1 × PBS and incubated with 100 µl/well 1 × reporter lysis buffer for 20 minutes at 4 ˚C then -80 ˚C for at least 30 minutes. After the cells were defrosted at room temperature, 20 µl/well of cell lysate was transferred to a 96 well plate. The downstream procedures were then the same as the 96 well plate luciferase assay as mentioned above.

For gene knockdown assays, the RLU/mg of the cells treated with siRNA was normalised to the untreated luciferase expressing cells to yield percentage of gene knockdown.

2.2.5.2 eGFP expression assay

eGFP expression was detected by FLUOstar Optima using the fluorescent screening detection mode with a 488nm excitation filter and 520 nm emission filter. The eGFP signal was expressed as Relative Fluorescent Unit (RFU). To standardise the RFU signal with cell number, cell titer assay buffer was prepared according to the manufacturer's protocol and 100 µl of the buffer was added per well of the cells. After 2 minutes incubation at room temperature with the cell titer assay buffer, the RLU of the lysates, which indicated the number of cells, were recorded and the RLU of each lysate was compared to the standard curve generated from RLU of different cell numbers to yield the cell number. The eGFP signal per cell was calculated by dividing RFU by the cell number from the same well.

For gene knockdown assays, 293T eGFP expressing cells, a kind gift from Dr. Tassos Georgiadis (Institute of Child Health, University College London), were used. Following siRNA transfection, the reduced level of RFU from the cells treated with siRNA was normalised with the untreated eGFP expressing cells to yield percentage of gene knockdown.

2.2.5.3 GAPDH expression assay

The GAPDH knockdown in the cells was studied two days post siRNA transfection in a 96 well plate setting by measuring the conversion rate of NAD^+ to NADH by GAPDH using KDalert GAPDH assay kit following the manufacturer's instructions. The GAPDH activity was measured using real time kinetic measurements by FLUOstar Optima.

2.2.5.4 Cell toxicity assay

Cell toxicity was assessed using the CellTiter 96 AQueous One Solution Assay which is a colorimetric method for determining the number of viable cells. The assay was performed essentially as described in the manufacturer's protocol. 5×10^4 Neuro 2a cells were transfected with siRNA complexes or B-PEI alone for 4 hours in a 96 well plate as described in **Section 2.2.3.3.3**. Following the transfection, 100µl full growth medium was added to the cells and incubated for 24 hours. 20 µl of CellTiter 96 AQueous One Solution was added to the untreated cells, treated cells and 3 wells containing medium only. The cells were incubated for 3 hours at 37°C, and the absorbance at 490nm was recorded using a SPECTRAmax plate reader. Background 490nm absorbance from the triplicate set of control wells (medium only-"no cell" control) was calculated and the average 490nm absorbance from the "no cell"control wells subtracted from all other absorbance values to yield corrected absorbances.

2.2.6 Methods related to the biophysical studies of the nucleic acid complexes

2.2.6.1 Gel retardation assay

Gel retardation assay is an application of agarose gel electrophoresis. In this assay, lysine based peptides or PEIs were mixed with nucleic acids and loaded onto the gel. Under an electric field, nucleic acids which bind to lysine based peptides or PEIs were retarded from migration due to their increased size and the decreased negative charge of the complexes. When lysine based peptides or PEIs neutralised all charges of the nucleic acids, the complexes did not migrate through the gel, suggesting the formation of stable complexes.

To resolve DNA or siRNA complexes, 0.2µg DNA or siRNA was diluted to 10 µl in distilled water and used to form a complex with 10µl complex reagents in distilled water at different N/P ratios. Following 30 minutes incubation at room temperature, 4 µl loading dye was added to the complexes. DNA complexes were then loaded onto a 1 % agarose gel whereas siRNA complexes were loaded onto a 4 % agarose gel **(Section 2.2.2.2)**. As a control, 0.2 µg naked DNA or siRNA was diluted to 20 µl in distilled water and mixed with 4 µl loading dye prior to addition to the gels. 10 µl DNA or siRNA ladder was also loaded onto the respective gels. Following electrophoresis, the images of the complex migration patterns were recorded by an UVIdoc gel documentation system.

2.2.6.2 PicoGreen fluorescence quenching experiment

The PicoGreen fluorescence quenching assay provides another way to investigate the effectiveness of lysine based peptides or PEI nucleic acid complex formation. The PicoGreen reagent intercalates with double stranded nucleic acids and emits fluorescence when exposed to UV light. Complex formation, however, shields the nucleic acids from exposure to the excitation waves and therefore quenches the fluorescent signal. Thus, a lower fluorescence value indicates increasing binding of nucleic acids to the lysine based peptides or PEIs.

To carry out the assay, PicoGreen was diluted in 1 × TE buffer and added to DNA or siRNA diluted in 1 × TE buffer. PicoGreen was added to DNA or siRNA in 1:150 (v/v) for 10 minutes at room temperature so that every 100 µl of the solution contained 0.2 µg nucleic acid. During the incubation of the DNA or siRNA to the PicoGreen, different amount of peptides or PEIs were diluted in 1 × TE buffer. Following incubation, 100 µl peptides or PEIs were added per well of flat bottomed 96 well plates and 100 µl (0.2 µg) DNA or siRNA containing the PicoGreen was added to the peptides or PEIs. As a control, 100 µl naked DNA or siRNA labelled with PicoGreen was added to 100 µl 1 × TE buffer per well in 96 well plates. Following 30 minutes incubation at room temperature, 100 µl 1 × TE buffer was added to each well. The PicoGreen signals were then detected with a fluorescent plate reader, FLUOstar Optima. The PicoGreen signals from the complexes were normalised with the naked DNA or siRNA control to yield the percentage of the PicoGreen signal detected.

2.2.6.3 Heparin induced complex dissociation assay

Once taken up by the cells, an effective nucleic acid delivery system should allow DNA or siRNA to dissociate from the vector components so that the DNA can traffick to the nucleus for gene expression whereas the siRNA should be retained in the cytoplasm for gene silencing. The abilities of the lysine based peptides or PEIs to dissociate from DNA were studied using heparin sulfate, a competitive binding agent (Sundaram et al. 2005). Heparin is highly negative and can compete with nucleic acids in binding with lysine based peptides or PEIs. Therefore, addition of different amount of heparin to the complexes allows an estimation of the dissociation behaviors of complexes.

To carry out this assay, 100 µl (0.2 µg) DNA or siRNA labelled with PicoGreen was added to 100 µl peptide or PEI per well in 96 well plates. As a control, 100 µl naked DNA or siRNA labelled with PicoGreen was added to 100 µl 1 × TE buffer per well. Following 30 minutes incubation at room temperature, 100 µl heparin diluted in 1 × TE buffer was added to 200 µl complexes or naked DNA or siRNA for 30 minutes. The fluorescent signals from PicoGreen were recorded using the fluorescent plate reader, FLUOstar Optima. siRNA or DNA alone labelled with PicoGreen were used to normalise the PicoGreen signal detected from the complexes.

2.2.6.4 Particle sizing

The sizes of the complexes were measured by a technique called Dynamic Light Scattering (DLS). In this technique, a laser is applied across the complexes in suspension. As a result of the movements of the complexes due to Brownian motion, the intensity of the scattered laser light changes at a rate depending on the sizes of the complexes. Analysis of these intensity fluctuations leads to velocities of the complex motions which can then use to estimate the sizes of the particles (Malvern Instruments Ltd. 2009).

10 µg DNA or siRNA was diluted to 25 µl in Ultrapure water and mixed with 25 µl cationic peptides or PEIs in Ultrapure water at different N/P ratios at room temperature. The complexes were then diluted to 500 µl in Ultrapure water and transferred to a low volume transparent cuvette. The cuvette was then placed into the particle sizing machine, Malvern Nano ZS, for particle size measurement using the DLS technique. The data were then processed using Dispersion Technology Software (DTS) v.5.03.

Two types of data, the Z-average size and the polydispersity index, were generated. The Z-average size refers to the mean hydrodynamic size of the particle whereas the polydispersity index reflects the range of the particle size distribution. The polydispersity index can range between 0 and 1. Particle with polydispersity values less than 0.2, which were deemed to be monodisperse, were presented in this study.

2.2.6.5 Zeta potential

The surface charge of the complex interacts with the surrounding ions, creating a charged layer around the complex. This charged layer is a spatial dimension that is associated to the complex, and the potential in the layer is called the zeta potential (Malvern Instruments Ltd. 2009b) **(Figure 2.1)**.

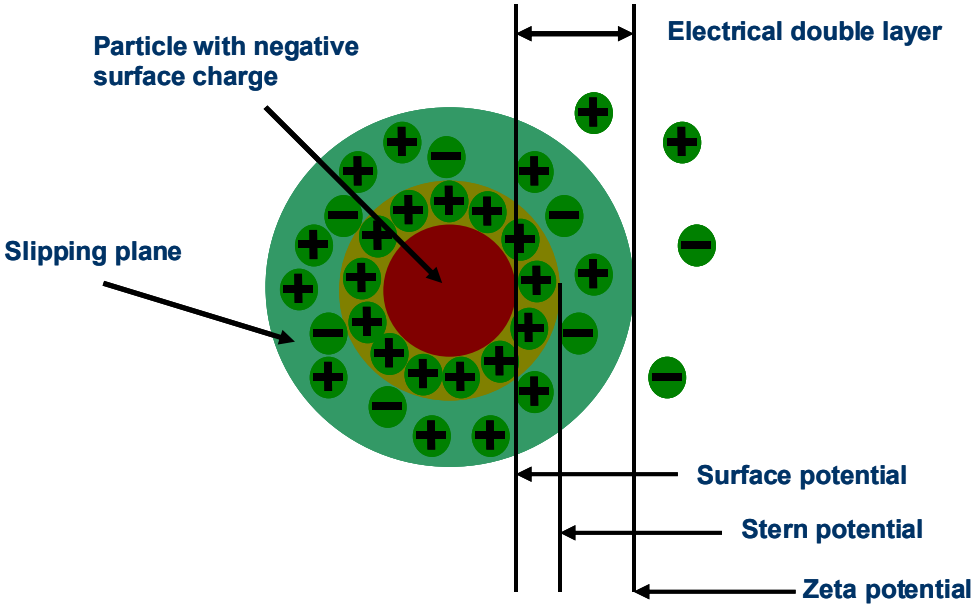

Figure 2.1 A schematic diagram showing the zeta potential of a complex.

In order to measure zeta potential of the complexes, an electric field is applied across the complex suspension. Complexes with a surface charge will migrate toward the oppositely charged electrode with a velocity proportional to the magnitude of the zeta potential (Malvern Instruments Ltd. 2009b).

This velocity is measured using the technique of Laser Doppler Anemometry (LDA). Upon illumination by laser, the movements of the complexes will cause a frequency shift or phase shift of the incident laser. This is measured as the particle mobility which can be converted to the zeta potential (Malvern Instruments Ltd. 2009b).

10 µg DNA or siRNA was diluted to 25 µl in Ultrapure water and mixed with 25 µl cationic peptides or PEIs in Ultrapure water at different N/P ratios in room temperature. The complexes were then diluted to 700 µl in Ultrapure water and transferred to a capillary cell. The capillary cell was then placed into the Malvern Nano ZS for the zeta potential measurement. The data were then processed using DTS v.5.03.

2.2.7 Methods related to flow cytometry analysis

2.2.7.1 Introduction to flow cytometry analysis

A flow cytometry machine can separate, classify and quantify living cells in a suspension on the basis of size and the colour of the fluorescence emitted from a labelled fluorophore associated with a cellular structure. In principle, cell suspensions are passed through a narrow dropping nozzle so that each cell is in a small droplet. One or more laser beams are passed through the cell, causing light to scatter and fluorescent dyes to emit light at various frequencies. Photomultiplier tubes (PMT) receive the scattered light signals and convert them to electrical signals. The electrical signals will then generate into data by a computer connected to the machine (Shapiro 2003).

Three types of data will be generated; data from forward scatter, side scatter and fluorescence. The forward scatter data estimate the approximate cellular size while the side scatter data identify cell complexity and granularity. With these data, the dead cells and debris can be identified. Under the illumination of a laser beam, the fluorophores associated with the cells will fluoresce and such fluorescence will be collected by the PMT (Shapiro 2003).

In this study, the fluorescent dyes propidium iodide (PI) and 7-amino-actinomycin D (7aad) were used as dyes for investigating cell death. Both dyes work by binding to double stranded nucleic acids and emit fluorescence. As the dyes can only penetrate

though the cell membranes of dead or dying cells to intercalate with the genomic DNA, they can be used to distinguish viable cells from dead cells (Shapiro 2003).

2.2.7.2 Fluorescence labelling of plasmid DNA

Plasmid DNA were covalently labelled with Cy5 for flow cytometry and confocal studies using Label IT Tracker Cy 5 kit following the manufacturer's instructions. In principle, the labelling reagent covalently attaches to any reactive heteroatom, any atom that is not carbon or hydrogen, within the plasmid.

2.2.7.3 PI or 7aad staining of the cells

Cells transfected with either Cy5 labelled DNA or Cy3 labelled siRNA were trypsinised from the plates and counted. 2×10^5 to 1×10^6 cells were then transferred to flow cytometry tubes. After pelleting at 1000 r.p.m. ($212 \times g$) at 4^{o}C for 5 minutes, the cells were washed with 500 µl 1 × PBS and were pelleted again at 1000 r.p.m. ($212 \times g$) at 4 ^{o}C for 5 minutes. Following three washes with 1 × PBS, the cells were resuspended in 300 µl 1 × PBS. 3 µl of 100 µg/ml PI were added to each tube containing cells transfected with Cy5 labelled DNA whilst 3 µl of 100 µg/ml 7aad was added to each tube containing cells transfected with Cy3 labelled siRNA. The tubes were then incubated in darkness at 37 ^{o}C for 30 minutes. Afterwards, the cells were analysed by the Epics XL flow cytometer.

2.2.8 Methods related to confocal microscopy

2.2.8.1 Introduction to confocal microscopy

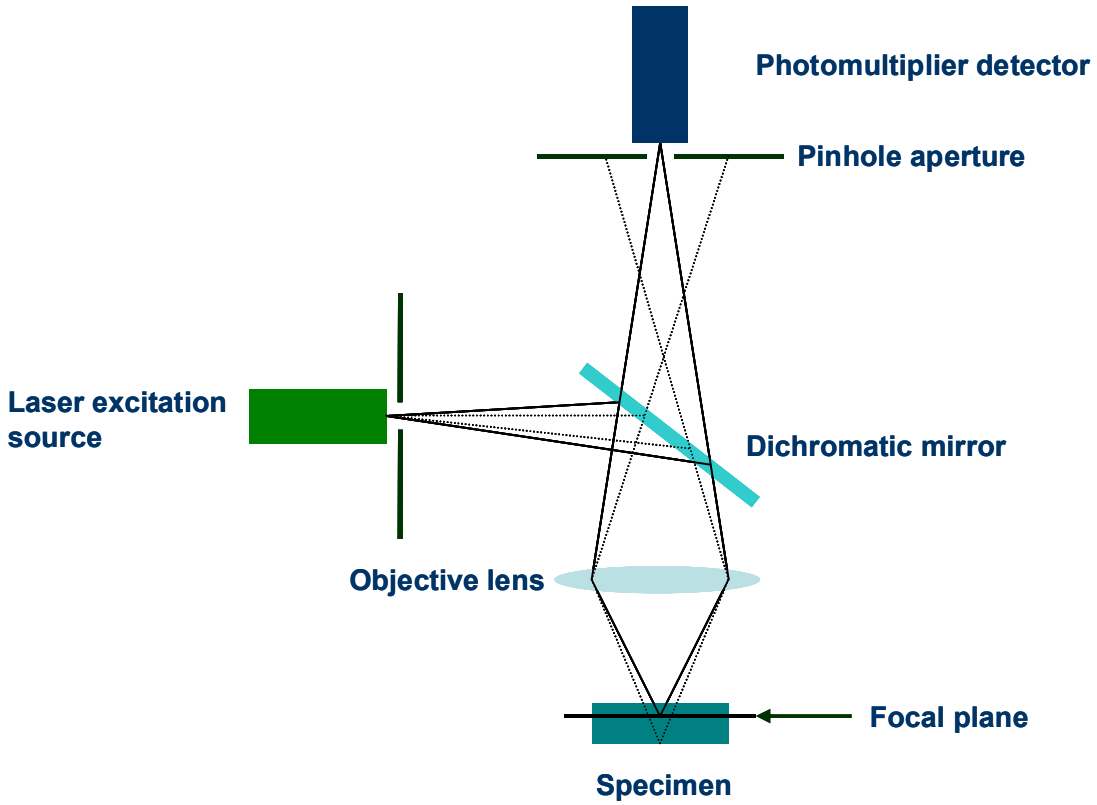

Figure 2.2 A schematic diagram showing the components of the microscope and optical pathway of the beam.

Confocal microscopy allows production of a final image of a specimen at the same plane of focus as the object. A confocal microscope is capable of filtering out the out-of-focus light from above and below the point of focus in the object. For an image from a fluorescence microscope, the signal produced is from the full thickness of the specimen

which does not allow most of it to be in focus to the observer. On the contrary, the confocal microscope is able to eliminate the out-of-focus image by a pinhole located in front of the image plane. This pinhole aperture acts as a filter and allows only the in-focus portion of the light to be imaged. As a result, light from above and below the plane of focus of the object is eliminated from the final image (Murphy 2002).

A major problem of the image from a confocal microscope is that the light from the in-focus image is greatly reduced by the pinhole. To increase the sensitivity for imaging, laser beams, which produce extremely bright light at specific wavelenghts for fluorochrome excitation, are used. Also, photomultiplier-detectors are used to improve the sensitivity of the collected signals from the fluorochrome (Murphy 2002).

2.2.8.2 Fixing cells for confocal miscroscopy

2×10^5 cells were seeded per well of 12 well plates so that 50% confluence was reached overnight. 1 µg of Cy-5 labelled DNA or 100 pmole of Cy-3 labelled siRNA was diluted into 25 µl with Optimem and mixed with 25 µl transfection reagents in Optimem to their respective formations and incubated for 30 minutes at room temperature. After removing the growth medium from the cells, the complexes were added to cells and incubated at 37 °C in humidified atmosphere in 5 % carbon dioxide for 4 hours. Cells were then trypsinised, resuspensed in 100 µl of growth medium and seeded on polylysine slides for 30 minutes at 37 °C in humidified atmosphere in 5 % carbon dioxide. Following washing with 1 × PBS three times, the cells were fixed in 4 % formaldehyde for 20

minutes at room temperature. The cells were washed three times with 1 × PBS and then permeabilised with 0.5 % Triton X-100 in 1 × PBS for 5 minutes at room temperature. In order to distinguish an entire cell, F-actin of the cell was stained using Alexa Fluor 488 phalloidin for 30 minutes at room temperature. Following washing three times with MilliQ water, Vectashield mounting medium for fluorescence with 4'- 6-Diamidino-2-phenylindole (DAPI) were added on top of the cells and cover slips were overlaid on top of the cells. Mounting varnish was used to seal the cover slip.

2.2.8.3 Slide imaging using confocal microscopy

The slides were visualised using Lecia confocal microscopy. The images were captured using sequential mode in order to avoid crosstalk between different channels. Images were taken and analysed using Leica Confocal Software (LCS) Lite version.

2.2.9 Methods related to qPCR

2.2.9.1 Isolation of RNA

Following two washes with 1 × PBS, cells were incubated with trypsin/EDTA for 5 minutes at 37 °C. The cells were then pelleted by centrifugation at 1200 r.p.m (306 × *g*) for 5 minutes. RNA was then purified by selective binding to a silica-based membrane at high salt concentration using the Qiagen RNeasy kit following the manufacturer's instructions.

2.2.9.2 RNA yield and quality determination

The yield and quality of RNA can be determined by spectrophotometry **(Section 2.2.2.5)**.

2.2.9.3 DNase I treatment of RNA

Isolation of total RNA invariably contains trace amounts of genomic DNA which may affect downstream applications such as real time PCR. To eliminate the contaminating genomic DNA, 1 µg of the RNA sample, in a total volume of 16 µl, was incubated with 2 µl DNase I and 2 µl DNase I buffer (10 ×) at room temperature for 15 minutes. Following the reaction, EDTA was added and the sample was incubated at 65 ºC for 5 minutes for inactivation of the DNase I.

2.2.9.4 cDNA synthesis

To prepare cDNA from RNA for subsequent PCR reactions, 1 μg of RNA was incubated with 2 μl of random hexamer primers (100 μg/ml) and Ultrapure water to a final volume equal to 11 μl. The sample was heated at 70 ^{o}C for 10 minutes and then cooled on ice immediately. After a brief spin, 8μl of master mix **(Table 2.15)** was added to the sample. Following incubation at room temperature for 2 minutes, 1 μl of superscript II was added to the mixture. After gentle mixing and incubation at room temperature for a further 10 minutes, the mixture was incubated at 42 ^{o}C for 1 hour. To stop the cDNA reaction the mixture was incubated at 70 ^{o}C. The mixture was then stored at -20 ^{o}C.

Reagents	Volume for one reaction
5 × first strand buffer	4 μl
0.1 DDT	2 μl
10mM dNTP	1 μl
RNasin	1 μl

Table 2.15 The volume of the reagents used to formulate a master mix for a 20μl reaction of cDNA synthesis.

It is important to set up a negative control for each sample to see whether there is still some genomic contamination. A negative control can be set up following the aforementioned processes of cDNA synthesis, except 1 μl Ultrapure water was added in place of 1 μl of superscript II. If DNA amplification is recorded in the negative control

in the subsequent quantitative PCR experiment, this means genomic DNA is present and the sample should be reprocessed.

2.2.9.5 Quantitative Real Time PCR

Quantitative Real Time PCR (qPCR) was carried out to quantify the amount of cDNA synthesised from the mRNA of GAPDH and β-actin in Neuro2a cells from various sets of experiments. Generally, the qPCR technology allows the absolute quantity of mRNA found in a sample to be ascertained by the incorporation of light emitting dyes into the PCR product.

2.2.9.6 Sequence-specific Taqman probes

In the study, the Taqman probe assay system was used. This assay system utilises a sequence specific dual labelled probe, which has a fluorophore dye incorporated to the 5' end of the sequence and a quencher dye at the 3' end. During the extension phase of the PCR, the probe is cleaved and the fluorescent and quenching dyes are separated. This results in the emission of a detectable fluorescent signal that is produced in a proportional manner to the accumulating PCR product.

As the probe system cannot distinguish the product resulting from a cDNA template or a genomic DNA template, it was necessary to ensure that the PCR products were not a result of contamination. Therefore as with all the RT-PCR reactions carried out, cDNA

samples prepared without inclusion of the reverse transcriptase were included in each run to determine if there was any genomic DNA contamination present.

2.2.9.7 qPCR reaction

The reactions were performed in a final volume of 20 µl in thin walled microcentrifuge tubes. 10 µl master mix was added per tube, followed by an addition of 1 µl of the Taqman probe, 8 µl of Ultrapure water and 1 µl of cDNA (1 µg).

The tubes were then placed in a controlled heat block in the qPCR machine, ABI Prism, and subjected to a thermal cycle as shown in **Table 2.16**. The results obtained from the reactions were analysed using ABI Prism 7000 SDS software version 1.1.

Step	Temperature	Duration	Process
1	95^{o}C	15 min	Activating enzyme
2	95^{o}C	30 sec	Denaturing cDNA
3	60^{o}C	30 sec	Annealing cDNA
4	72^{o}C	30 sec	Extending cDNA
5	Plate read		

Table 2.16 The thermal cycling profile required for the Taqman probe assay system.

In order to compare the relative mRNA levels from the gene of interest in different samples, the mRNA levels of a house keeping gene, β-actin, were also measured from

each sample. The mRNA levels of β-actin from different samples could be used to normalise the mRNA values of the gene of interest of the respective samples.

2.2.10 Statistical analysis

Data presented in this study was analysed using a two-tailed, unpaired Student t-test where applicable. Statistical analysis was also performed using Analysis of Variance (ANOVA) followed by Tukey's test as a post-hoc test for multiple mean comparisons. All statistical analyses were performed with the GraphPad Prism version 4 software.

Chapter 3

Establishment of models for DNA transfection and siRNA knockdown assays

3.1 Introduction

To develop nucleic acid delivery systems, it is important to have suitable models to evaluate the nucleic acid delivery efficiency. For plasmid delivery, there are several reporter gene systems such as luciferase and enhanced green fluorescent protein (eGFP) that can be used for vector formulation screening. Likewise, there are different gene silencing models that can be used to evaluate siRNA delivery efficiency. Such systems include co-transfection with a reporter gene plasmid and an siRNA targeting the reporter gene, endogenous gene silencing and stably transfected reporter gene silencing models. In this section, establishment, advantages and disadvantages of different gene expression and gene silencing models will be discussed.

3.1.2 Reporter gene assay models

Reporter genes are useful for the screening of synthetic vector systems for plasmid delivery due to their easily identifiable characteristics, with reporter gene expression usually detected visually or by other simple assays. The commonly used reporter genes include genes that encode green fluorescent protein (GFP) and luciferase.

3.1.2.1 GFP

GFP is a fluorescent protein originally observed in the bioluminescent jellyfish *Aequorea victoria*. It is a 238-residue polypeptide with a typical beta barrel structure containing one

beta-sheet and alpha helix(s) with the fluorophores located inside the centre of the alpha helix (Tsien 1998).

GFP emits green fluorescence with a wavelength of 509 nm when excited by a light wave of wavelength 488 nm. An advantage of GFP is that transfected cells can be visualized in real time under a fluorescence microscope, and by using a plasmid encoding GFP, transfection efficiency can be estimated by the emission of fluorescence (Sambrook & Russell 2001). To further enhance the GFP fluorescence, a point mutation can be introduced into the GFP DNA sequence to yield a mutant called enhanced GFP (eGFP) (Stepanenko et al. 2008).

3.1.2.2 Luciferase

Luciferase is widely used in cell biology to study gene expression. The most commonly used form of luciferase comes from the firefly *Photinus pyralis*. Firefly luciferase is a monomeric 61kDa protein, and it catalyses luciferin oxidation using ATP-Mg^{2+} as a cosubstrate. As a result, light is emitted by converting the chemical energy of luciferin oxidation through an electron transition, forming the product molecule oxyluciferin **(Figure 3.1)** (Wood 1990). By recording the intensity of the light emitted from this reaction, gene expression can be estimated. The main advantage of using luciferase as a reporter gene is that it allows a sensitive quantitative estimation of gene expression.

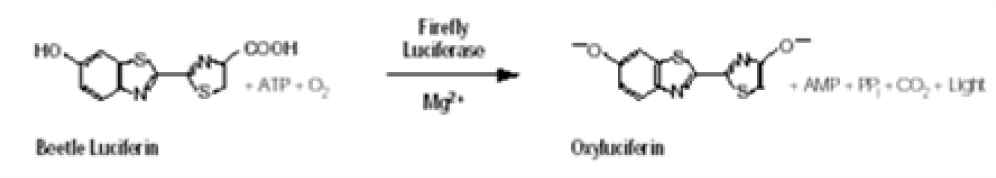

Figure 3.1 The biochemical process of luciferase-catalysed light emission (Adapted from Wood 1990)**.**

3.1.3 Gene silencing models

A variety of models for gene silencing include co-transfection of a plasmid encoding a reporter gene and its siRNA counterpart, silencing of a stably expressed reporter gene in a cell line, and silencing of an endogenous gene in a cell. Such models will be described in this section.

3.1.3.1 Cotransfection model

In the cotransfection model, cells are transfected with plasmid complexes and siRNA complexes together **(Figure 3.2).** The plasmid contains a reporter gene whilst the siRNA targets the reporter gene. By analysing the reporter gene expression following the siRNA transfection, the siRNA delivery efficacy of the complex system can be evaluated.

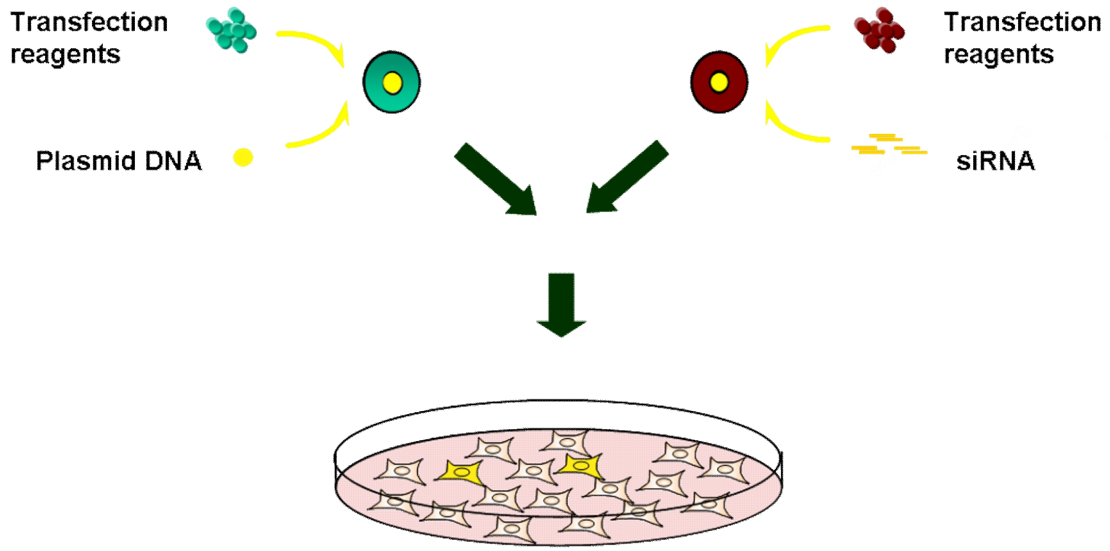

Figure 3.2 A schematic diagram showing the cotransfection model. Cells were seeded 24 hours prior to transfection. Plasmid transfection and siRNA transfection complexes were made separately according to the transfection protocols. These complexes were mixed and added to the cells. The reporter gene silencing was then analysed.

The advantages of this model are that it is relatively easy to set up and cheap to maintain compared to other models. The reagents required in this model consist of a plasmid expressing a reporter gene, siRNA targeting this reporter gene, transfection reagents and a cell line. All of these components are used in routine experiments and are therefore easily prepared and/or purchased. Since the silencing target in the co-transfection model is usually a reporter gene such as GFP, this model is considerably cheaper than an endogenous gene knockdown model which involves other assays to estimate the endogenous gene silencing such as Real Time Polymerase Chain Reaction (RT-PCR) and Western blotting. However, one of the main problems of this model is the potential for the plasmid complexes to

interfere with the siRNA complexes. The plasmid or siRNA complexes are formed by reversible electrostatic interactions between the complex reagent and the plasmid DNA or siRNA. Mixing the plasmid complexes with the siRNA complexes could lead to a rearrangement of the complex reagent within the plasmid or siRNA complexes **(Figure 3.3)**. As a result, some of the complex reagent within the plasmid complexes may dissociate from the plasmid complexes and bind to the siRNA complexes or *vice versa*. Therefore, the gene silencing results obtained may not necessarily reflect the siRNA delivery efficiency of the siRNA complexes in a particular formulation. Also, since *in vivo* plasmid delivery using complexes is already a hurdle, it could be difficult to use this model to evaluate *in vivo* siRNA delivery efficacy.

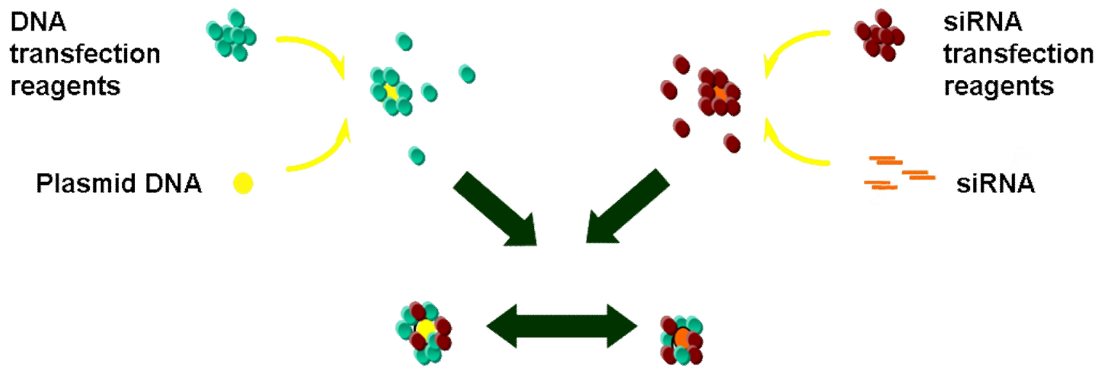

Figure 3.3 A schematic diagram depicting the "cross-talk" of the DNA and siRNA transfection complexes in the cotransfection model. Since both plasmid DNA and siRNA complexes were formed by a reversible electrostatic attraction between the nucleic acids and the reagents, there is a possibility that the complex regents on each complex would be attracted and bind to the other complexes. Also, the free transfection reagents in the complex medium could bind to these complexes.

3.1.3.2 Endogenous gene silencing model

Another way to evaluate siRNA delivery efficiency involves delivering siRNA to target endogenous genes within the cells. In this system, the gene silencing efficiency can be estimated by the remaining expression, relative to unsilenced controls, of target mRNA or protein levels using enzyme assays, RT-PCR or Western blotting. Indeed, there is a functional assay that could be used to study remaining protein level, the glyceraldehyde-3-phosphate dehydrogenase (GAPDH) assay, following transfection using anti-GAPDH siRNA.

GAPDH, which is composed of 36 kD protein subunits, is a tetrameric enzyme. As shown in **Figure 3.4,** it catalyses the oxidative phosphorylation of glyceraldehyde-3-phosphate (G-3-P) to bisphosphoglycerate (BPG).

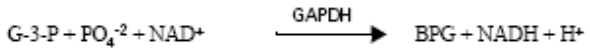

Figure 3.4 The biochemical process of the GAPDH.

In the presence of phosphate and G-3-P, the conversion rate of NAD^+ to NADH is proportional to the concentration of GAPDH. The higher the GAPDH presence, the faster the conversion rate. By measuring the rate of the NAD^+ to NADH conversion, the amount of GAPDH present in the cells can be determined.

The main advantages of this assay are that it can be used on different cell types and can yield gene silencing results within a short period of time compared to methods involving RT-PCR and Western blotting. However, this assay is very expensive, so is therefore often not ideal for use in formulation screening. This model can rather be used to confirm a specific formulation.

3.1.3.3 Stably transfected reporter gene silencing model

To generate this model, a reporter gene must stably integrate into the host cell genome. By transfecting cells with a plasmid encoding both a reporter gene and a selectable marker, the cells with the reporter gene integrated into the genome can be identified. The reporter gene within these stably transfected cells can then be targeted by siRNA delivery and knockdown efficiency can be evaluated.

This model is attractive since the reporter gene silencing can be easily measured by well-established reporter gene assays. Also, reporter gene assays are usually quick and more economical to monitor gene expression compared to monitoring endogenous gene expression involving RT-PCR and Western blotting; therefore it can be an ideal model for formulation screening. However, generating such a model can prove to be very time consuming.

3.1.3.4 Control for siRNA experiment

Since an overdose of siRNA can mediate non-specific gene silencing, irrelevant siRNA are used as a negative control. Irrelevant siRNA is an siRNA which does not target any gene. By comparing the results of the targeted siRNA complexes and the irrelevant siRNA complexes, the specificity of the gene silencing of the targeted siRNA complexes can be evaluated.

3.1.4 Aim

- To establish models suitable for high through-put screening of cationic formulations for gene expression or gene silencing.

3.2 Results

3.2.1 Gene expression model

To evaluate the gene delivery efficiency of different cationic formulations, plasmids containing eGFP or luciferase reporter gene were used. A transfection protocol was developed to deliver the plasmid to Neuro 2a cells in a 96 well plate setting. The cells were seeded 24 hours prior to transfection, and following the removal of full growth medium, the transfection complexes were overlaid onto the cells in serum free medium. The cells were transfected at 50 to 70% confluence so that the cells would not be overgrown at the time of analysis. Overgrowth of cells could be a potential problem because many cell types exhibit growth contact inhibition. The eGFP expression was analysed 48 hours following transfection whereas luciferase expression was evaluated 24 hours post-transfection **(Figure 3.5)**.

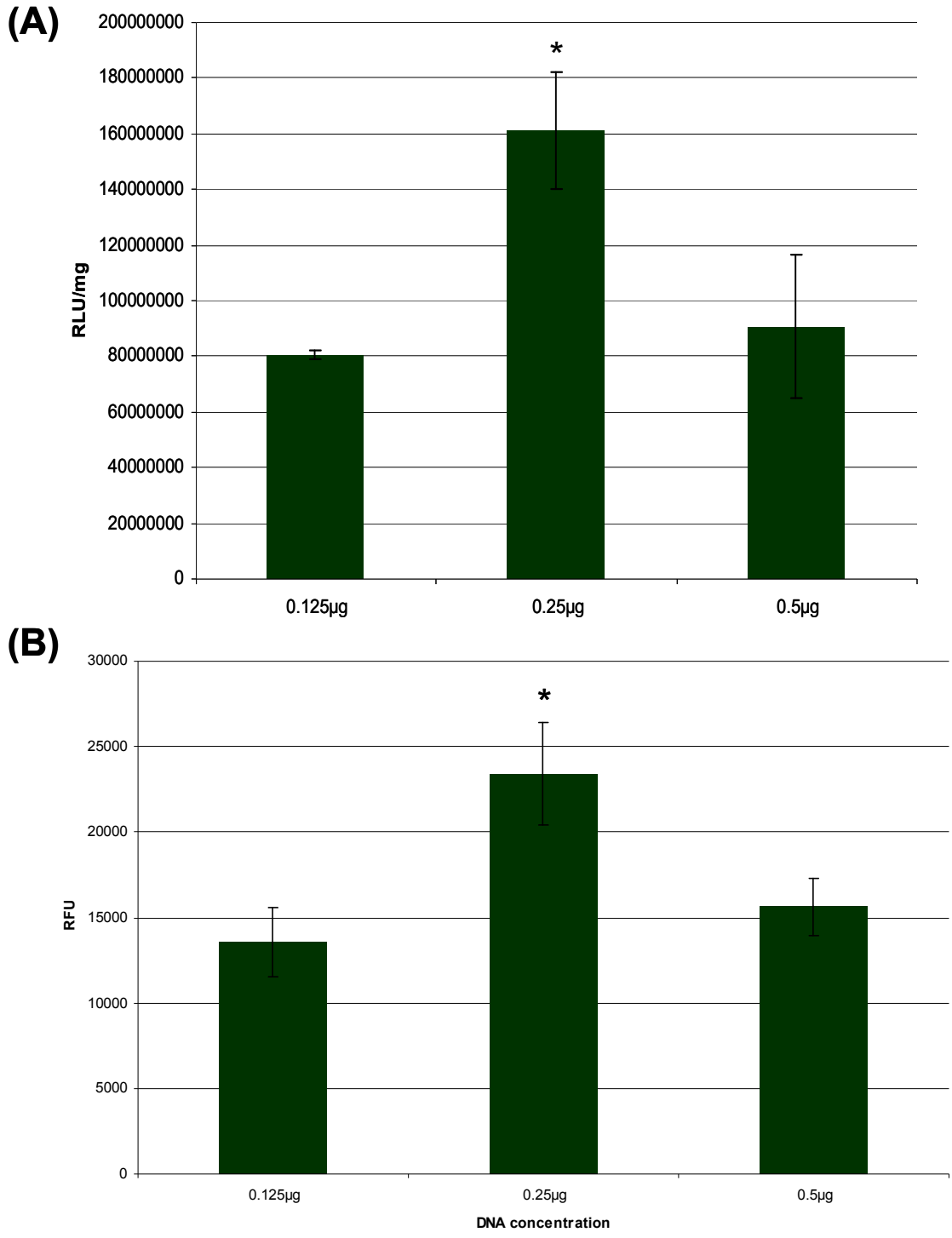

Figure 3.5 Optimisation of the amounts of plasmid DNA for transfection. 5×10^4 Neuro 2a cells were seeded 24 hours prior to transfection (in a 96 well plate). Plasmid transfection complexes were made by mixing a lipid, peptide Y and plasmid DNA together in a 2:4:1 weight ratio for 30

minutes in Optimem **(Section 2.2.3.3.2)**. Following removal of full growth medium, complexes were overlaid onto the cells for 4 hours. After removing the transfection complexes, full growth medium was added to the cells. Luciferase activity in the cells was analysed 24 hours post-transfection as a relative luminescence unit (RLU) **(Section 2.2.5.1)** whereas eGFP expression was analysed 48 hours post-transfection as a relative fluorescence unit (RFU) to estimate the transfection efficiencies of the complexes **(Section 2.2.5.2)**. **(A)** Luciferase activity (RLU/mg) following transfection using different amounts of plasmid DNA. It was shown that 0.25 µg of plasmid DNA in a well of a 96 well plate yielded a significantly higher transfection efficiency ($P < 0.05$) **(B)** eGFP expression (RFU) following transfection using different amounts of plasmid DNA. It was shown that 0.25 µg of plasmid DNA in a well of a 96 well plate yielded a significantly higher transfection efficiency ($P < 0.05$) Statistical analysis was performed using Student t-test. RLU/mg: Relative luminescence unit/ protein content of the samples.

Different amounts of plasmid were used to transfect Neuro 2a cells to investigate the optimal amount of plasmid for gene delivery screening. As shown in **Figure 3.5**, Neuro 2a cells were transfected with eGFP or luciferase plasmid. It was observed that 0.25µg plasmid per well was optimal for plasmid transfection. Both 0.125 µg and 0.5µg plasmid per well yielded a lower gene expression level.

3.2.2 Gene knockdown model

3.2.2.1 GAPDH knockdown model

The GAPDH knockdown model can be used to investigate endogenous gene knockdown. In this model, the cells were seeded 24 hours prior to transfection. Having prepared the siRNA complexes with siRNA targeting GAPDH in Optimem, the cells were transfected

and the GAPDH levels were analysed 48 hours post-transfection. The cells treated with irrelevant siRNA complexes could indicate the non-specific gene silencing although cell toxicity could also decrease GAPDH activity.

Figure 3.6 shows the results of the GAPDH knockdown on Neuro 2a cells. **(Please refer to appendix III for the GAPDH knockdown on NIH 3T3 and HT1080 cells.)** The siRNA transfection complexes were formed using a commercial reagent, siLentfect, and siRNA targeting GAPDH (siGAPDH) or irrelevant siRNA (irr). The amount of the siLentfect and siRNA used per well in the 96 well plate were as indicated.

As shown in **Figure 3.6**, siRNA alone or siRNA formed complexes with 0.1µl siLentfect with 5, 10 or 20 nM siGAPDH did not mediate any gene silencing. Increasing the siLentfect to 0.2 µl allowed 5, 10 or 20 nM siGAPDH to induce 30-40% of GAPDH silencing. In fact, 0.4 µg siLentfect with 5, 10 or 20 nM siGAPDH was able to mediate 70-80% of GAPDH knockdown in the cells.

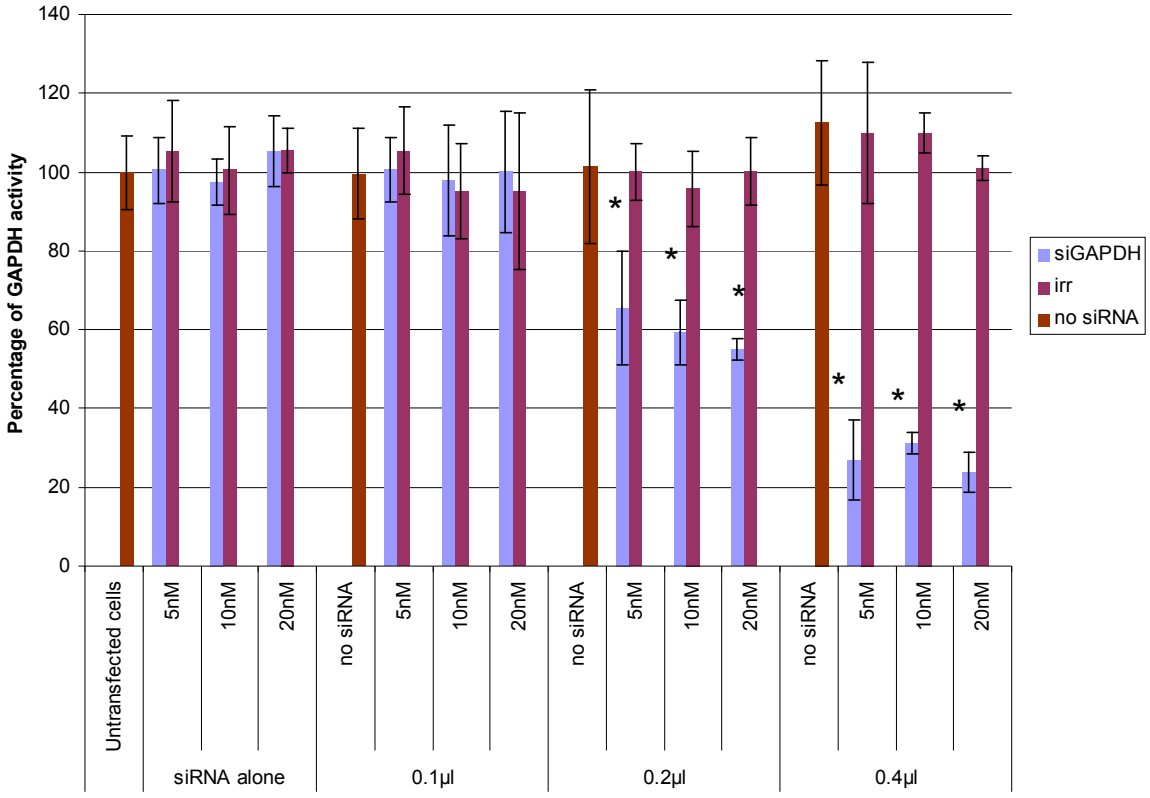

Figure 3.6 The GAPDH knockdown model. 5×10^4 Neuro 2a cells were seeded 24 hours prior to transfection (in a 96 well plate). siRNA transfection complexes were made by mixing siLentfect with siRNA for 30 minutes in Optimem **(Section 2.2.3.3.5)**. The complexes were then overlaid onto the cells for 24 hours. After removing the transfection complexes, full growth medium was added to the cells. Following 2 days post-transfection, the GAPDH activity of each sample was measured as the relative fluorescence unit (RFU) **(Section 2.2.5.3)**. The GAPDH activity of the untransfected cells was used to normalise the GAPDH activity of the treated cells to yield the percentage of GAPDH activity. It was shown that 0.2 µl siLecfect with siGAPDH ($P < 0.05$) or 0.4 µl siLecfect with siGAPDH ($P < 0.05$) mediated a significant decrease of GAPDH activity compared to cells treated with siLecfect irr complexes containing the same amount of siLentfect and siRNA and the untreated cells. Statistical analysis was performed using Student t-test. siGAPDH refers to siRNA targeting GAPDH; irr refers to siRNA not targeting any mRNA in the cells.

3.2.2.2 eGFP knockdown model

A model containing an eGFP stable cell line and siRNA targeting eGFP were used. The transfection procedures used to evaluate siRNA delivery efficiency using this model are very similar to the GAPDH model. 293T eGFP expressing cells **(Section 2.1.6)** were seeded 24 hours prior to transfection. siRNA transfection complexes were made by mixing Lipofectamine 2000 (L2000) and siRNA targeting eGFP (sieGFP) for 30 minutes. Following 24 hours of transfection, the complexes were removed and full growth medium was added to the cells. eGFP silencing was analysed in the subsequent days.

To identify the optimal time point for detecting eGFP silencing, the kinetics of eGFP expression in the cells was studied at different time points using L2000 with different concentrations of siRNA targeting eGFP **(Figure 3.7)**. As shown in the figure, around 45% of eGFP expression was detected immediately after the 24 hour transfection period. The eGFP expression level was around 20% at 24 hours post-transfection. Two days after transfection, the eGFP signal further decreased; however, there is an increase of the eGFP expression 3 days after transfection. Therefore, 2 days after transfection is the optimal time point to detect eGFP silencing.

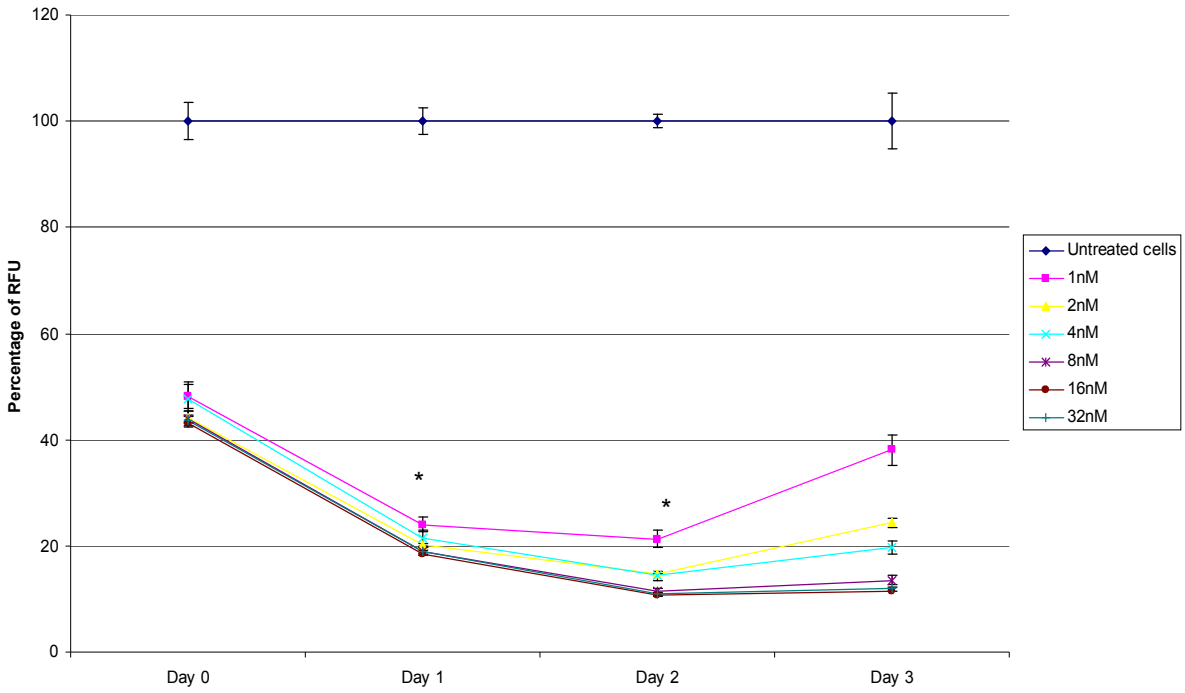

Figure 3.7 The kinetics of the eGFP knockdown model. 5×10^4 293T eGFP expressing cells were seeded 24 hours prior to transfection (in a 96 well plate). siRNA transfection complexes were made by mixing L2000 (0.25ug/well) with different concentrations of siRNA targeting eGFP for 30 minutes. The complexes were then overlaid onto the cells for 24 hours. After removing the transfection complexes, full growth medium was added to the cells. The remaining eGFP expression was analysed at different time points. Day 0 means the eGFP was measured immediately following the 24 hour transfection. Day 1, Day 2 and Day 3 refer to the eGFP measurement made at 24, 48 and 72 hours following transfection respectively **(Section 2.2.3.3.4 and 2.2.5.2)**. The percentage of relative fluorescence unit (RFU) refers to the eGFP signal detected from cells treated to different sieGFP complexes normalised with the untreated eGFP expressing cells. Statistical analysis was performed using ANOVA followed by Tukey's test and it showed that there was a significant decrease of the percentage of RFU of the cells treated with the L2000 sieGFP (from 2 to 32 nM) complexes on day 1 and day 2 compared to day 0 ($P < 0.05$).

Figure 3.8 shows the optimisation of the amounts of L2000 and sieGFP required to mediate eGFP knockdown. The optimal L2000 siRNA complex was used as a positive control in the subsequent cationic formations screening. As shown in the figure, naked siRNA does not mediate any eGFP silencing. At 0.125µg of L2000 per well, siRNA concentrations ranging from 4nM to 32nM in 200 µl induced around 75% of eGFP silencing. When L2000 increased to 0.25µg per well, 80% or more of eGFP knockdown was observed using sieGFP ranging from 4nM to 32nM in 200 µl. For 0.5µg L2000 per well, although sieGFP ranging from 1nM to 32nM in 200 µl mediated more than 80% eGFP silencing, a decrease of eGFP expression of the cells treated with irrelevant siRNA indicated that there was non-specific gene silencing or cell toxicity mediated by this formulation. Therefore, the optimal L2000 siRNA formulation was 0.25µg L2000 with 8nM of siRNA because this is the formulation using less siRNA to mediate more than 80% gene silencing without any non-specific gene knockdown or cell toxicity.

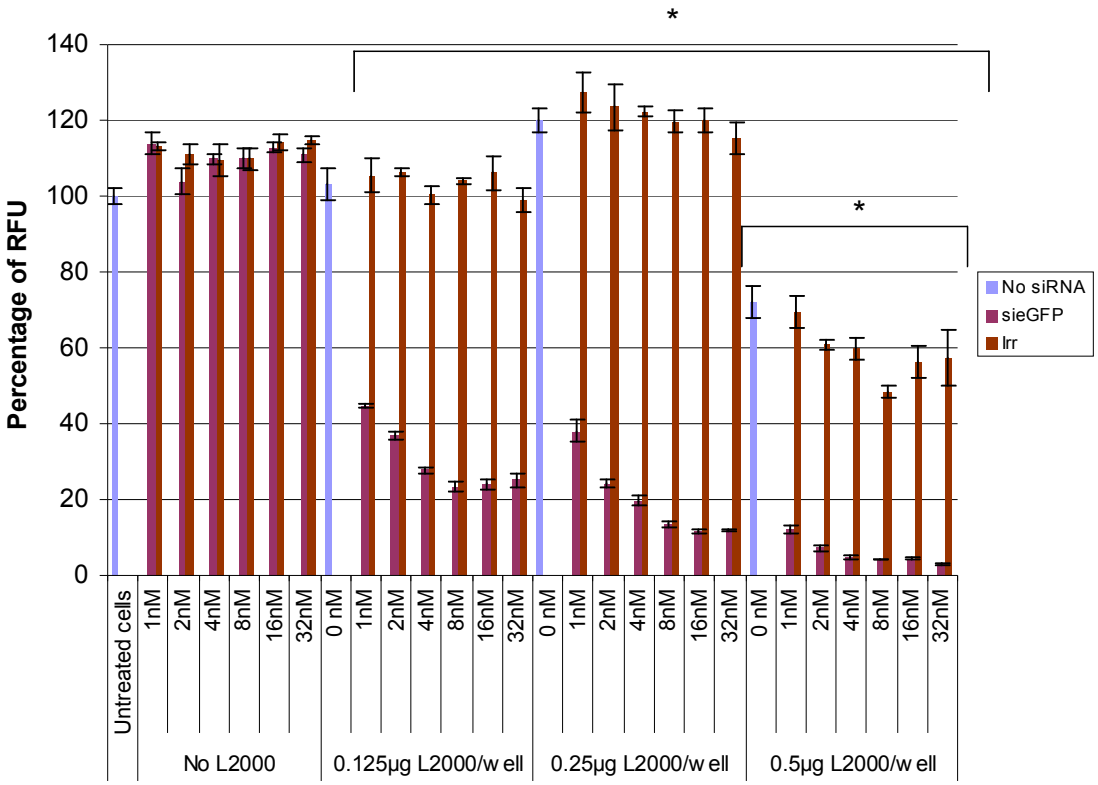

Figure 3.8 eGFP knockdown optimisation. 5×10^4 293T eGFP expressing cells were seeded 24 hours prior to transfection (in a 96 well plate). siRNA transfection complexes were made by mixing L2000 with siRNA for 30 minutes. The complexes were then overlaid onto the cells for 24 hours. After removing the transfection complexes, full growth medium was added to the cells. The remaining eGFP expression were analysed 2 days post-transfection **(Section 2.2.3.3.4 and 2.2.5.2)**. The percentage of relative fluorescence unit (RFU) refers to the eGFP signal detected from cells treated to different sieGFP complexes normalised with the untreated eGFP expressing cells. sieGFP refers to siRNA targeting eGFP; irr refers to siRNA not targeting any mRNA in the cells. Statistical analysis was performed using Student t-test and it showed significant difference between the L2000 sieGFP complexes and the L2000 irr complexes with the same amount of L2000 and siRNA ($P < 0.05$). It also showed that the percentage of RFU of the cells treated with the L2000 irr complexes with 0.5 µg of L2000 decreased significantly compared to the untreated cells and the cells treated with siRNA alone ($P < 0.05$).

Indeed, there were some disadvantages of this model for formulation screening. Firstly, the 293T cells grew quickly and needed to be passaged after 2 days post-transfection, and this complicates the procedures for screening. Also, this cell type is easily detached from the plastic well which was problematic for other transfection methods described in **Section 2.2.3.3**.

Therefore, a better model would be a cell line containing a gene target with a shorter half life which could be used easily for evaluation of siRNA delivery. A mouse neuroblastoma cell line (e.g. Neuro 2a) expressing luciferase could be a good model for *in vitro* and *in vivo* formulation screening. Neuro 2a cells are easy to culture *in vitro* and can be used to generate subcutaneous tumour in a mouse, which acts as an *in vivo* model to evaluate siRNA delivery. On the other hand, luciferase, which has only a 2 hour half life, is easily used for *in vitro* and *in vivo* quantification and imaging (Ignowski & Schaffer 2004). Therefore, Neuro 2a luciferase expressing cell line would be a good model for cationic formulation screening.

3.2.3 Generation of a luciferase knockdown model

3.2.3.1 Generation of luciferase construct for Neuro 2a luciferase expressing cell line

The Neuro 2a cell line stably expressing luciferase was generated by integration of a plasmid containing both the luciferase reporter and selectable marker genes into the

genome of the cells so that both the luciferase reporter and selectable marker genes were expressed endogenously. A selectable marker is a gene that confers a specific trait to the cells for artificial selection (Goldstein et al. 2005). In this study, the hygromycin B resistance gene was used as the selectable marker. Hygromycin B is an antibiotic that kills the cells by inhibiting protein synthesis. The cells expressing a hygromycin B resistance gene will therefore survive in hygromycin B conditions and the cells lacking this gene will not survive (Makridou et al. 2003). Therefore, to make a cell line that expresses luciferase stably, the first step is to generate a plasmid construct containing both luciferase and hygromycin B.

3.2.3.2 Plasmid subcloning for stable cell line construction

Figure 3.9A outlines the plasmids pCEP 4 and pCI-Luc used in the subcloning procedures. The pCEP4 consists of a hygromycin B resistance gene and multiple cloning sites (MCS) downstream of the CMV prometer. Within the MCS, there are sites for restriction enzymes *Hin*dIII and *Not*I. The pCI-Luc contains a firefly luciferase gene flanked by restriction sites *Hin*dIII and *Not*I, therefore the strategy to generate the plasmid for use in stable cell line construction is to excise the luciferase gene from pCI-Luc and insert it into the pCEP4 MCS. **Figure 3.9B** shows the restriction digestion of the pCEP4 and pCI-Luc plasmids. Following digestion with *Hin*dIII and *Not*I, the luciferase gene from pCI-Luc (lane 9) was purified and ligated to the digested pCEP4 (lane 5) to yield pCEP4-Luc **(Figure 3.10A)**. A transfection was performed to confirm that the pCEP4-Luc plasmid was able to express the

luciferase reporter gene **(Figure 3.10B)**. This plasmid was used for the subsequent transfection for stable cell line generation.

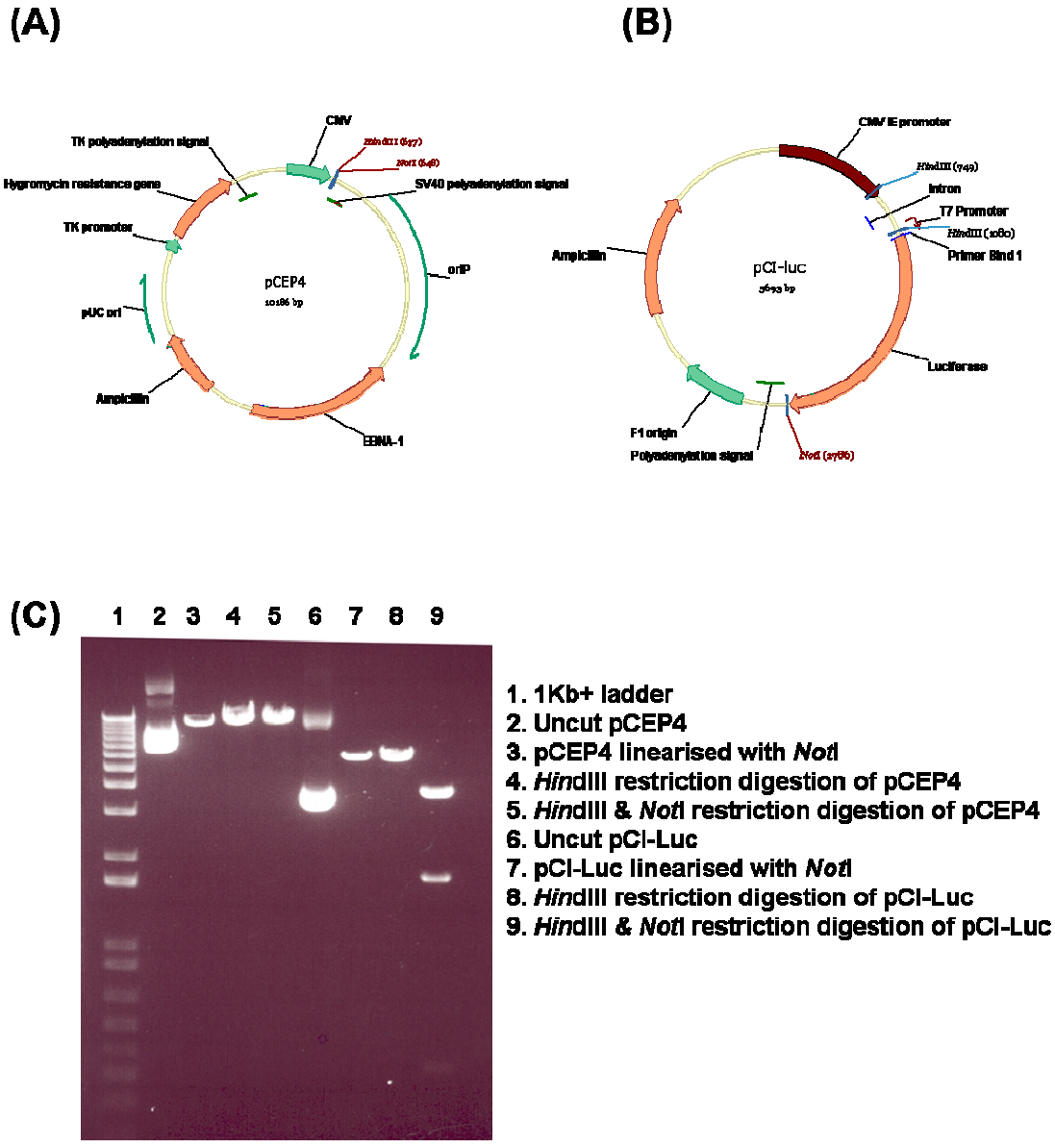

Figure 3.9 Generation of luciferase plasmid for stable cell construction. (A) a schematic diagram of the pCEP4 construct, **(B)** a schematic diagram of the pCI-Luc, **(C)** Restriction digestion of the pCEP4 and the pCI-Luc plasmids. The pCEP4 and pCI-luc were digested with *Hin*dIII and *Not*I for 2 hours at 37°C and resulting fragments separated on a 1% agarose gel **(Section 2.2.2)**.

(A)

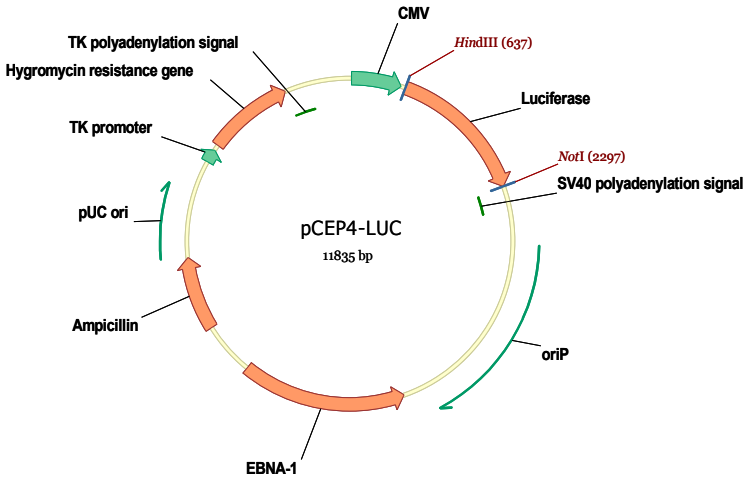

(B)

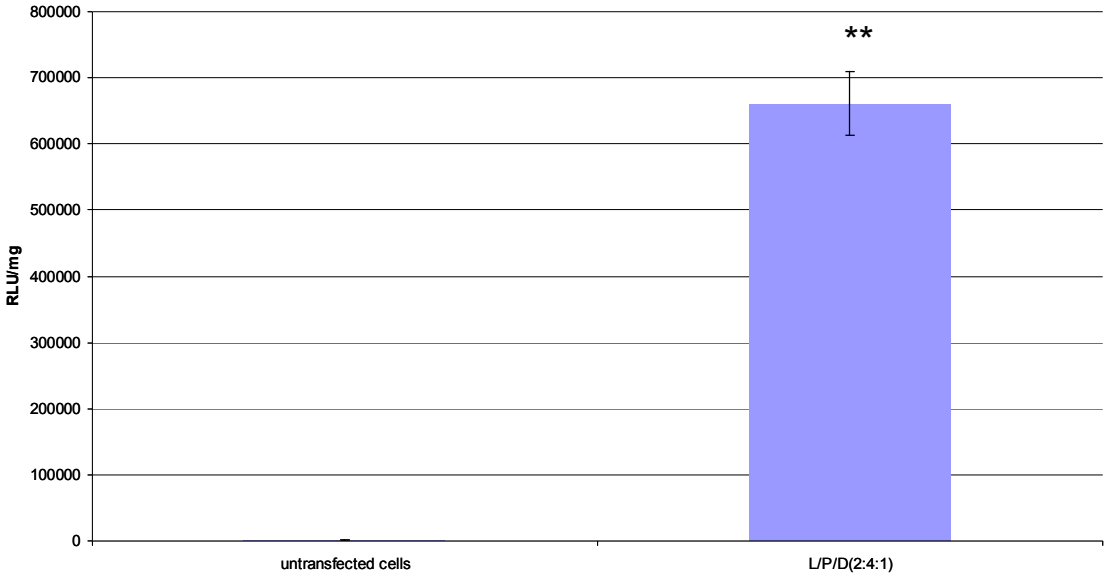

Figure 3.10 Testing of the pCEP4-Luc plasmid for luciferase expression. Neuro 2a cells were seeded 24 hours prior to transfection. Plasmid transfection complexes were made by mixing lipid:peptide:DNA in a 2:4:1 weight ratio for 30 minutes in Optimem **(Section 2.2.3.3.2 and 2.2.5.1)**. The complexes were then overlaid onto the cells for 24 hours. After removing the transfection complexes, full growth medium was added to the cells. Luciferase activity was analysed 24 hours post-transfection. (A) a schematic diagram of the pCEP4-Luc plasmid. (B)

Luciferase activity in Neuro 2a cells transfected with the pCEP4-Luc plasmid compared to the untreated cells. Statistical analysis was performed using Student t-test and it showed a significant difference between the luciferase activity in transfected cells and the untransfected cells ($P < 0.01$).

3.2.3.3 Optimisation for hygromycin B selection

In order to establish the hygromycin B concentration suitable for selection, Neuro 2a cells were incubated with different amounts of hygromycin B for 4 days. As shown in **Figure 3.11**, when no hygromycin B was added, the cells proliferated after 2 days but the cell number decreased after 4 days. The decrease of cell number was due to cell death as a result of overgrowth. Conversely, cell growth was observed from cells treated with 100 and 200µg/ml of hygromycin B after 2 days, suggesting that these amounts of hygromycin B were not enough to kill the cells not expressing the resistance gene. When the hygromycin B concentration increased to 400µg/ml, the cell number decreased after 2 days of treatment, indicating that 400µg/ml of hygromycin B is lethal for the Neuro 2a cells. Further increase of hygromycin B concentration caused a higher cell death rate of the Neuro 2a cells. 400µg/ml of hygromycin B was therefore chosen as the concentration for the selection process as it was the minimum hygromycin B concentration needed to mediate cell death. Therefore, cells expressing a low amount of the hygromycin B resistance gene will survive.

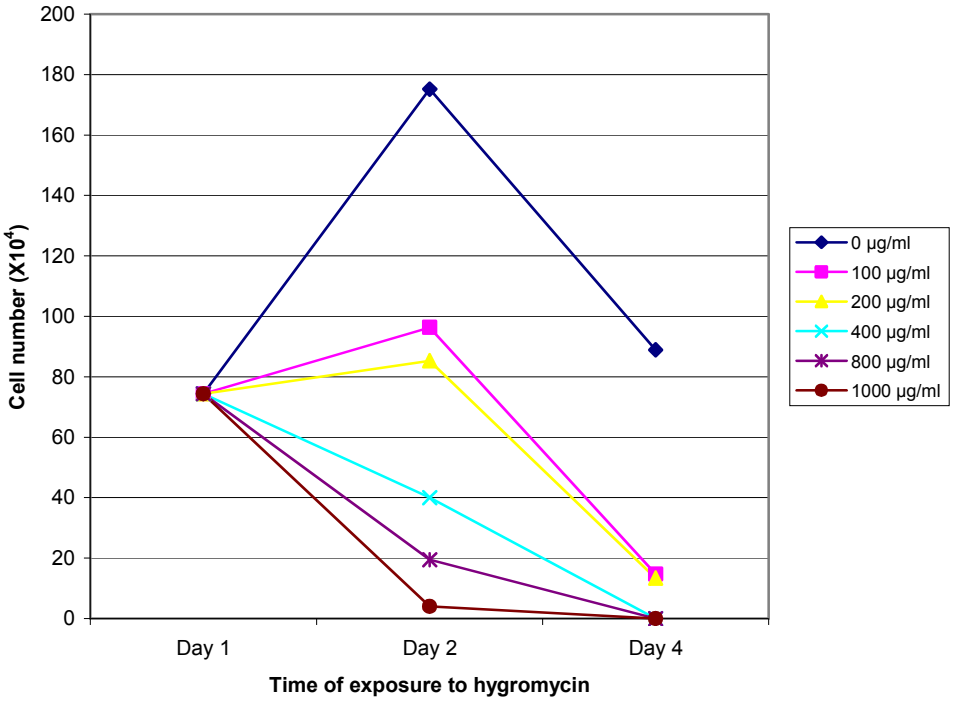

Figure 3.11 Generation of a kill curve for stable cell selection. Neuro 2a cells were treated with different concentrations of hygromycin B for 4 days. The viable cells were counted on day 1, day 2 and day 4 using a trypan blue exclusion assay **(Section 2.2.4.1)** in order to generate the kill curve.

3.2.3.4 Transfection of pCEP4-Luc and selection of hygromycin B resistant cell line

To generate the stable luciferase expressing cell line, Neuro 2a cells were transfected with the pCEP4-luc plasmid and cultured in 400µg/ml of hygromycin B for 2 months. Briefly, the cells were cultured with full growth medium in a 6 cm plate 24 hours prior to transfection. Lipofectin was used to form complexes with a plasmid for 30 minutes. Following removal of the growth medium from the cells, the transfection complexes were

added to the cells for 4 hours. The transfection complexes were then removed and full growth medium with 400µg/ml of hygromycin B was added to the cells for the selection process. This full growth medium with 400µg/ml of hygromycin B was replaced every two days.

Within the first 10 days of this selection process, the majority of cells did not survive. The living cells were scattered in the plate and some wells contained a single surviving cell **(Figure 3.12)**. These single cells were located and observed for the subsequent selection process. For the further 10 to 20 days, some of the single cells grew into colonies. The colonies were then selected, expanded and tested for luciferase expression.

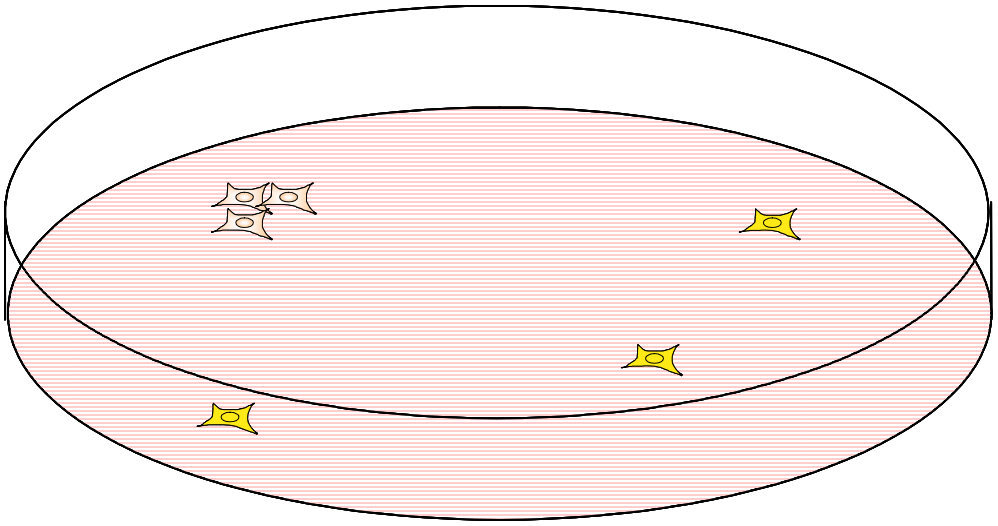

Figure 3.12 A schematic diagram showing the process to identify a single hygromycin B resistance cell. Following transfection using the pCEP-4-Luc plasmid, the cells were treated with hygromycin B. The hygromycin B resistant cells would either survive as a single cell (yellow cell) or in a cluster of cells (pink cells). The single cells were identified and observed to follow colony formation. These single cell colonies were then isolated and expanded.

After expansion of the cells from the colonies, the cells were assayed for level of luciferase expression. As shown in **Figure 3.13A**, some of the cells were luciferase negative while some of the cells were luciferase positive. It is an assumption that the luciferase expressing cells must contain the luciferase and hygromycin B resistance genes integrated within their genome, or else survival within the hygromycin selective conditions would not be possible over the two month period.

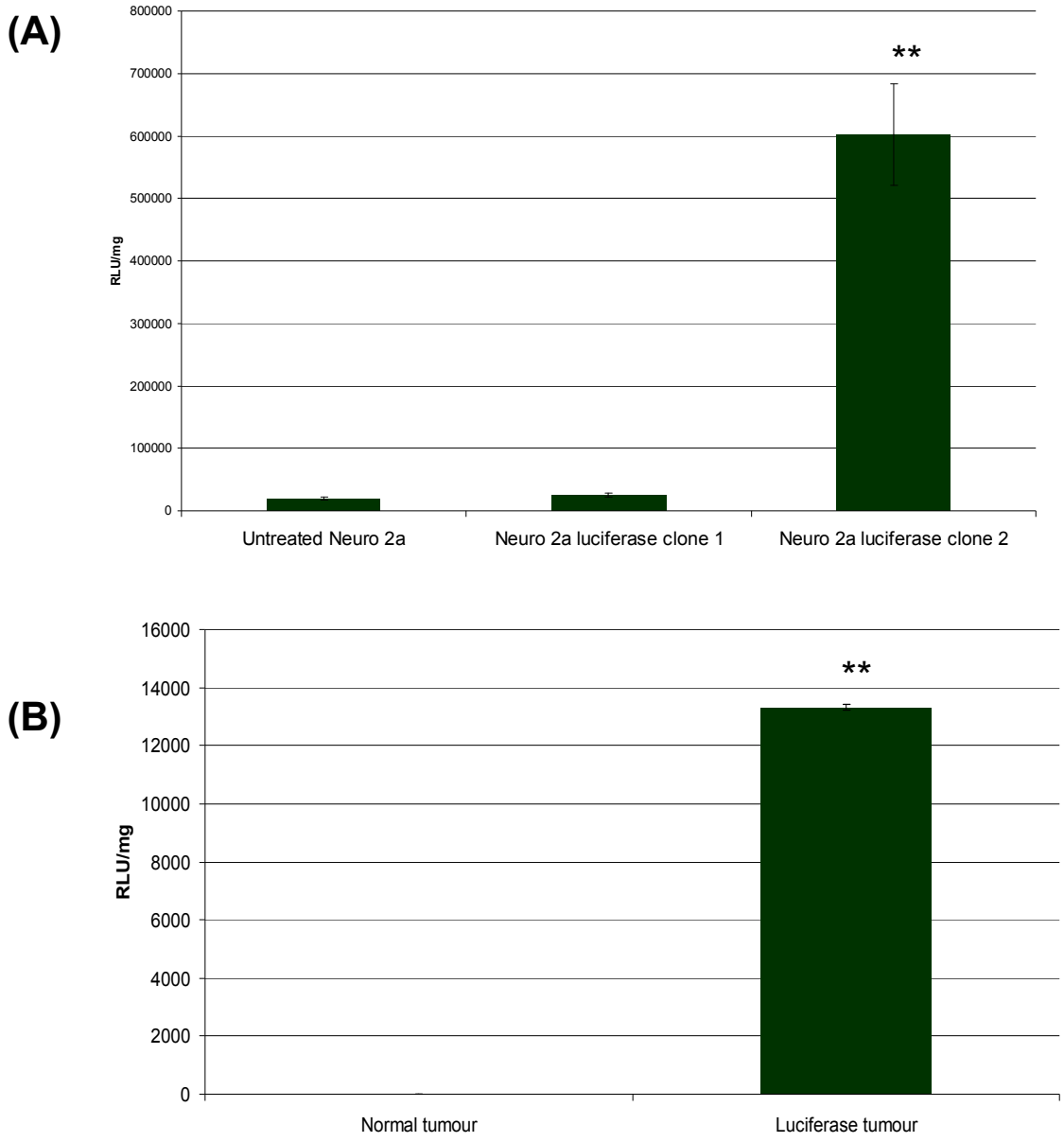

Figure 3.13 Neuro 2a stably expressing luciferase cells for *in vitro* and *in vivo* use. (A) The luciferase activity within the hygromycin B resistant single cell colonies. The luciferase activity of Neuro 2a clone 2 is significantly higher than Neuro 2a clone 1 ($P < 0.01$). **(B)** Luciferase activity from a tumor generated from the Neuro 2a luciferase expressing cells from clone 2 was significantly higher than that of the normal tumour, which refers to a tumour generated from the parental Neuro 2a cells ($P < 0.01$). Statistical analysis was performed using Student t-test.

To test if the Neuro 2a luciferase expressing cells can be used *in vivo* to establish tumours in the same way as the parental Neuro2a cells, the cells were injected into a mouse subcutaneously **(Section 2.2.4.4)**. A tumour was observed 15 days after injection. As shown in **Figure 3.13B**, luciferase expression was observed. Therefore, this Neuro 2a-Luc cell line can be used as a model to evaluate gene silencing *in vitro* and *in vivo*.

3.2.3.5 Optimisation of the Neuro 2a-Luc model

To identify the optimal time point for detecting luciferase silencing in the stably transfected cells, the kinetics of luciferase expression in the Neuro-2a-Luc cells was studied. The cells were transfected with siRNA as described in **Section 3.2.2.2** and the luciferase expression was analysed at different time points. **Figure 3.14** shows the results of the kinetic study. The percentage of relative luminescence units (RLU) is the luciferase signal detected from cells treated with different siLuc complexes normalised to the untreated luciferase expressing cells. As shown in the figure, around 20% of luciferase expression was detected from day 0 to day 2 post-transfection. The luciferase expression level began to increase 3 days following transfection. Therefore, any time less than 2 days post-transfection would be optimal to detect luciferase silencing. Taking consideration of the Neuro 2a cell proliferation rate, the optimal time to detect luciferase silencing would be 24 hours post-transfection.

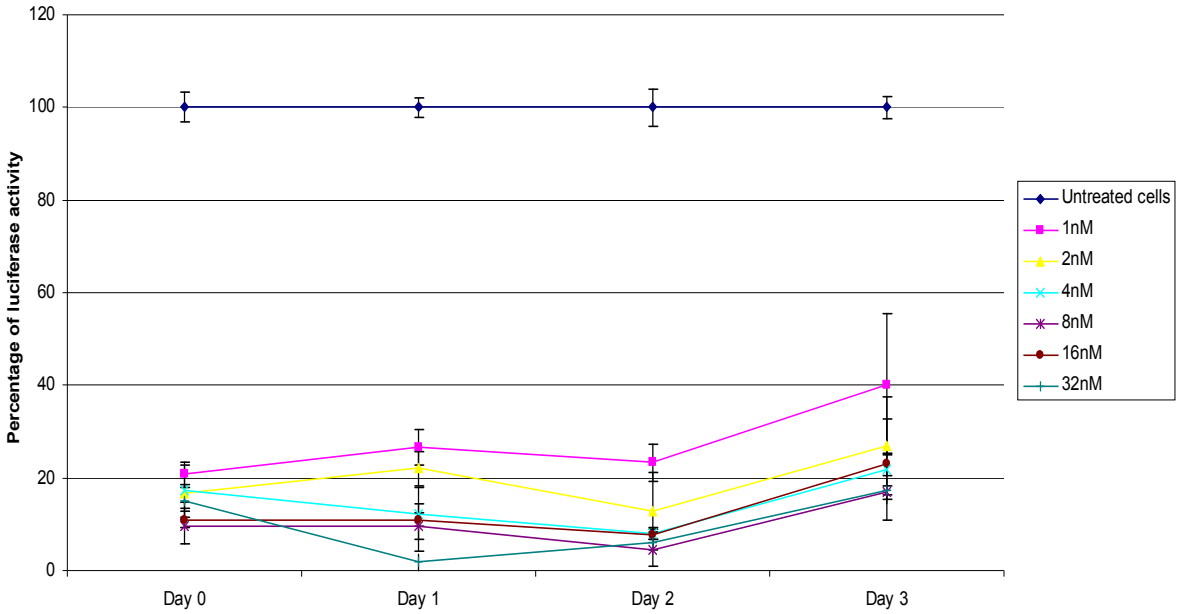

Figure 3.14 The kinetics of the luciferase knockdown model. 5×10^4 Neuro 2a luciferase expressing cells were seeded 24 hours prior to transfection (in a 96 well plate). siRNA transfection complexes were made by mixing L2000 (0.25ug/well) with siRNA targeting luciferase for 30 minutes in Optimem. The complexes were then overlaid onto the cells for 24 hours. After removing the transfection complexes, full growth medium was added to the cells. The remaining luciferase activity were analysed at different time points **(Section 2.2.3.3.4 and 2.2.5.1)**. The percentage of luciferase activity refers to the luciferase activity detected from cells treated with different siLuc complexes normalised to the untreated luciferase expressing cells. Day 0 means the luciferase activity was measured immediately following the 24 hour transfection. Day 1,2 and 3 denote luciferase activity measurement at 24, 48 and 72 hours respectively. Statistical analysis using ANOVA followed by Tukey's test showing the percentage of luciferase activity in the cells treated with the L2000 siRNA (1 to 32 nM) complexes (from day 0 to day 3) were significantly different to the untreated luciferase expressing cells ($P < 0.01$).

Figure 3.15 shows the optimisation of L2000 siLuc complexes needed to induce luciferase knockdown. The optimal L2000 siRNA complex was used as a positive control in the subsequent cationic formation screening. Similar to the eGFP silencing experiment, naked siRNA did not mediate any luciferase silencing. At 0.125µg of L2000 per well, siRNA concentrations ranging from 1nM to 32nM in 200µl could induce around 80% of luciferase silencing. Further increase of L2000 to 0.5µg per well with the same range of siRNA slightly increased the gene silencing efficacy. Importantly, the increase of the L2000 amount did not cause cell toxicity. To conclude, 0.125µg of L2000 with 1nM in 200µl of siRNA was enough to mediate 80% luciferase knockdown in this model.

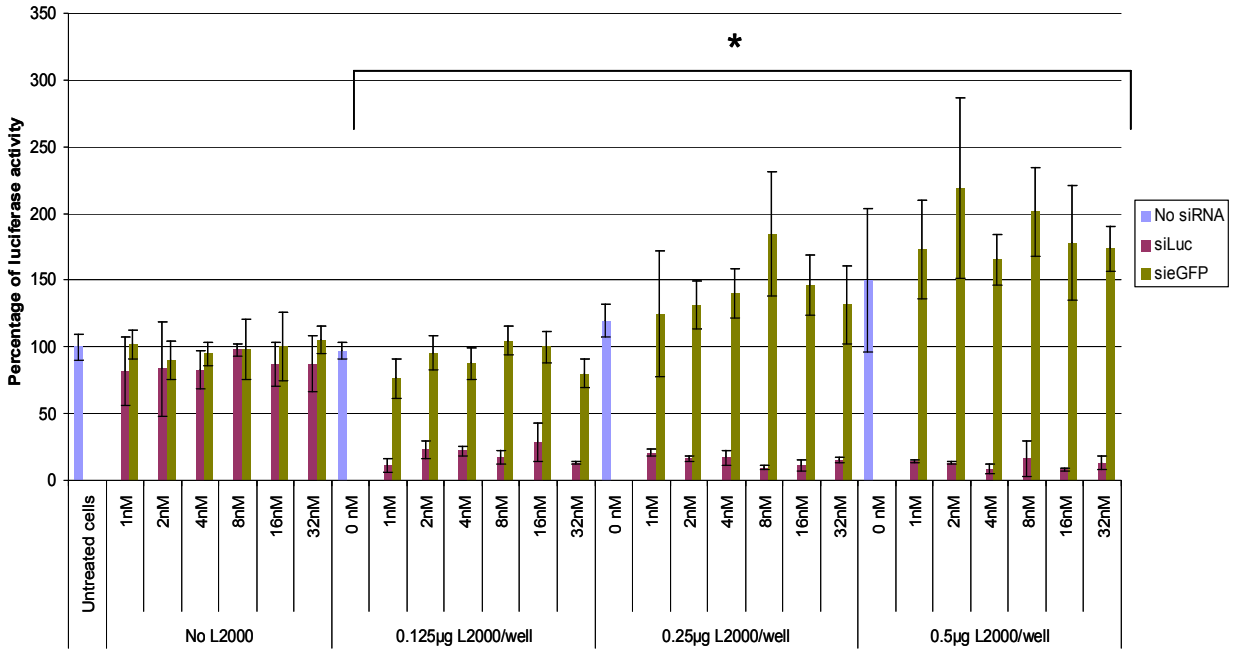

Figure 3.15 Luciferase knockdown optimisation. 5×10^4 Neuro 2a luciferase expressing cells were seeded 24 hours prior to transfection (in a 96 well plate). siRNA transfection complexes were made by mixing L2000 with siRNA for 30 minutes. The complexes were then overlaid onto the cells for 24 hours. After removing the transfection complexes, full growth medium was added to the cells. The remaining luciferase activity was analysed 24 hours post-transfection **(Section 2.2.3.3.4 and 2.2.5.1)**. The percentage of luciferase activity refers to the luciferase activity detected from cells treated with different siLuc complexes normalised to the untreated luciferase expressing cells. Statistical analysis was performed using Student t-test and it showed a significant difference between the L2000 siLuc complexes and the L2000 sieGFP complexes with the same amount of L2000 and siRNA ($P < 0.05$). siLuc refers to siRNA targeting luciferase; sieGFP refers to siRNA targeting eGPF which is a negative control in the experiment.

3.3 Discussion

3.3.1 Gene expression models for high throughput cationic formulation screening

In this study, a model using Neuro 2a cells and eGFP or luciferase expressing plasmid was established for the evaluation of plasmid delivery efficiency. This model was optimised to transfect cells in 96 well plate conditions which allowed high throughput screening of the cationic formulations, and was used to compare the transfection efficiency of different plasmid DNA complexes formed with different cationic polymers in chapter 4.

3.3.2 GAPDH and 293T eGFP expressing cell line models were not ideal for this study

To study gene silencing mediated by different synthetic siRNA delivery systems, a GAPDH silencing model, eGFP and luciferase stable cell line models were established. These models have their own advantages and disadvantages and therefore would be useful in different experimental circumstances. For instance, the GAPDH gene knockdown model can be used on different cell types; however, it is the most expensive model to use in this study. Therefore, this model would be useful for verifying a specific cationic formulation on different cell types rather than high throughput screening. On the other hand, the 293T eGFP model is a better alternative to the GAPDH gene knockdown model for screening purposes because it is very economical. However, due to the long half life of eGFP (48

hours) (Ignowski & Schaffer 2004) and the fast growth rate of the 293T cells (24 hours doubling time), this model requires high maintenance to culture the treated cells which may not be ideal for high throughput screening purposes. Also, since the 293T cells can often be found not very adherent to the plate, washing steps in transfection procedures could easily detach the cells. Therefore, this model is not ideal to be used in evaluating different transfection methods which include several washing steps.

3.3.3 Neuro 2a luciferase expressing cells were more suitable for this study

The Neuro 2a luciferase expressing cell gene knockdown model is more ideal than the GAPDH and eGFP models for formulation screening. Even though Neuro 2a cells grow quickly, the 2 hour half life of the luciferase allows the transfected cells to be analysed 24 hours post-transfection. Another advantage of the Neuro 2a luciferase cells is that they can generate a tumour containing cells which are expressing luciferase *in vivo*. Since luciferase can be easily imaged *in vivo* in a real time fashion (Ignowski & Schaffer 2004), this model allows researchers to use fewer animals to evaluate the kinetics and the efficacy of certain siRNA complexes *in vivo*.

3.3.4 Stable cell line construction

In this study, the Neuro 2a cells stably expressing luciferase were expanded from single cell colonies identified in a 6 cm plate. Other strategies to expand the stable cells could be

seeding the cells in a 96 well plate with one cell per well. This can be done using cell sorting techniques (Shapiro 2003). However, this technique may not be practical because some cells, such as Neuro 2a, do not respond well to such isolation and consequently do not proliferate well in single cell conditions.

3.3.5 L2000 as an siRNA delivery reagent

In this study, L2000 was used as a positive control to deliver siRNA because it is well-known as an effective commercial siRNA delivery reagent. However, it is also known to be toxic to the cells. Fedorov and co-workers showed that treatment of L2000 on cells can alter global gene expression patterns in the cells (Fedorov et al. 2005). Therefore, despite its effectiveness for siRNA delivery, there is still a need to develop better siRNA delivery formulations for clinical use. Also, L2000 does not target to a specific cell type; therefore, it may not be ideal for siRNA delivery in a clinical setting.

3.4 Conclusion

In this section, gene expression and gene silencing models were established for the development of DNA and siRNA delivery systems. The gene expression efficiency was assessed by luciferase or eGFP expression following transfection, whilst gene silencing efficiency was estimated by the remaining luciferase expression level from the luciferase expressing cell model. The gene silencing efficiency can be further confirmed by endogenous knockdown of the GAPDH level within the cells.

Chapter 4

A study on the biophysical and transfection properties of different cationic formulations of DNA complexes

4.1 Introduction

Gene therapy is a powerful tool to treat diseases by delivering nucleic acids to induce expression of missing genes, elevate expression of existing genes and/or silence disease related genes in targeted cells. However, one of the main hurdles in gene therapy is to develop an efficient and safe vector system. Although viral vectors are highly efficient for gene delivery, high toxicity and immunogenicity of these vectors remains a concern. Synthetic or nonviral vectors are attractive alternatives to viral vectors due to their low immunogenicity and low acute toxicity. However, the main disadvantage of nonviral vectors is the low transfection efficiency compared with viral vectors. Therefore, improving the delivery efficiency of the non-viral system could be a way to produce a safe and efficient vector system for DNA delivery.

Two biophysical properties that limit the cellular delivery of DNA are their polyanionic nature and large size. The polyanionic characteristic hinders the interaction between DNA and the cell membrane while the size restricts it from passive diffusion through the cell membrane. To overcome these barriers, cationic molecules have been used to neutralise the negative charge of the DNA and form nano-sized complexes to facilitate cellular uptake (Grayson et al. 2006). The complex must then be able to dissociate from the DNA within cells to allow them to be transcribed (Kichler et al. 2001). Therefore, the abilities of the cationic molecule to bind, dissociate and form nano-sized particles with the DNA are important criteria for a successful DNA delivery system.

To understand the characteristics of efficient DNA delivery systems, lysine based peptides and polyethylenimine (PEI), which are widely used for plasmid DNA delivery, were used to form complexes with plasmid DNA. The subsequent biophysical and transfection properties of those complexes were analysed.

4.1.1 Lysine based peptides

Lysine based peptides have been used to package DNA for gene delivery (Zenke et al. 1990; Erbacher et al. 1996). Lysine, which is the basic unit of these peptides, can be protonated through a nitrogen atom and condense DNA to form complexes, which can subsequently enter cells by endocytosis (Mislick et al. 1995).

In this study, two types of lysine based peptides were used, the linear lysine and the Kbranch peptides.

4.1.1.1 The linear lysine peptides

Four different linear lysine peptides were used in this study. The molecular weight and net charge of the peptides K8, K16, K24 and K32 **(Figure 4.1)** are summarised in **Table 4.1**. Since the linear lysine peptides differ only in their sizes, this may help to elucidate the relationship between peptide size and nucleic acid packaging and delivery efficacy.

K8 KKKKKKKK

K16 KKKKKKKKKKKKKKKK

K24 KKKKKKKKKKKKKKKKKKKKKKKK

K32 KKKKKKKKKKKKKKKKKKKKKKKKKKKKKKKK

Figure 4.1 The structures of the linear lysine peptides.

	Molecular weight	Net charge per peptide
K8	1043	+8
K16	2068	+16
K24	3111	+24
K32	4154	+32

Table 4.1 The molecular weight and the net charge of the K8, K16, K24 and K32 peptides.

4.1.1.2 The Kbranch peptide

The KBranch peptide (3 kDa), which has a charge of +14 per peptide, contains a branched lysine domain to condense DNA **(Figure 4.2).** It also contains an integrin targeting domain to facilitate cellular binding and uptake (Hart et al. 1998; Mustapa et al. 2007).

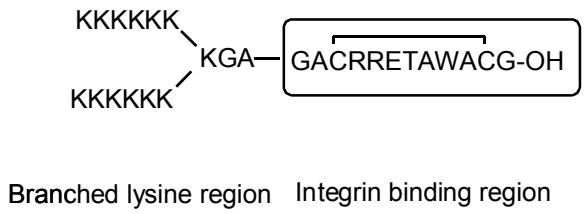

Figure 4.2 The structure of the Kbranch peptide.

The Kbranch peptide is similar in size to the linear lysine peptides; therefore, the nucleic acid packaging properties of the Kbranch peptide can be compared with those of the linear lysines to better understand the effect of molecular structure on nucleic acid packaging.

4.1.2 PEI

PEIs have been used to deliver DNA or other kinds of nucleic acid in various cell types *in vitro* and *in vivo* (Boussif et al. 1996; Goula et al. 1998; Kichler et al. 2001; Grayson et al. 2006; Sundaram et al. 2007; Shim & Kwon 2008). They are made either as a branched or linear form. The branched form is produced by cationic polymerisation from aziridine monomers whereas the linear form is generated from cationic polymerisation from a 2-substituted 2-oxazoline monomer, or at low temperature using aziridine monomers **(Figure 4.3)** (Godbey et al. 1999).

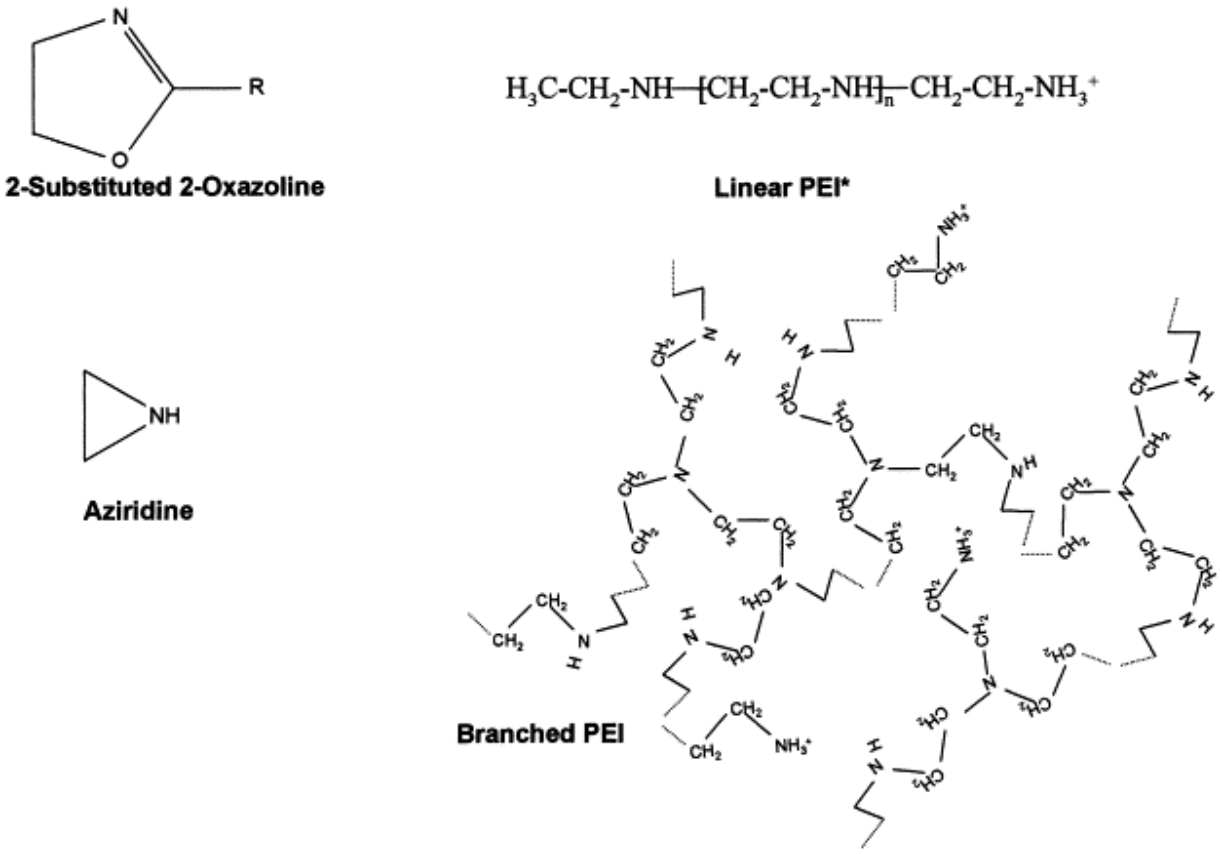

Figure 4.3 The structures of the linear and branched PEI (Adapted from Godbey et al. 1999).

The basic unit of PEI consists of a backbone of two carbons and one nitrogen atom. The nitrogen atom can be protonated and can bind to and condense DNA to form complexes (Godbey et al. 1999). The complexes can be taken up by the cells through endocytosis (Ogris et al. 1998).

In this study, branched and linear PEIs were used. The branched PEI (B-PEI) was 25 kDa whereas the linear PEI (L-PEI) was 22 kDa. Since L-PEI and B-PEI have a similar size, the

relationship between the structure of the complex reagent and nucleic acid complex formation and transfer can be studied. PEIs are larger in size than the lysine based peptides; therefore, comparing the results from the PEI complexes with the lysine based complexes may allow the clarification of the effect of the complex reagent size and chemical composition on the nucleic acid complex formation and transfer.

4.1.3 Aims

- To identify the biophysical properties of different DNA complexes formed by different cationic polymers and DNA.
- To elucidate and evaluate the relationship between the biophysical properties and transfection efficiency.
- To clarify the criteria of a successful DNA delivery system which can be used to develop siRNA delivery systems.

4.2 Results

4.2.1 Binding properties of the lysine based peptides or PEIs to DNA

In order to deliver DNA to the cell, the vector system should firstly bind to the DNA to form a complex and later dissociate within the cell. Therefore, the binding capacity of the vector system to the DNA represents an important criterion for successful DNA delivery. PEIs and the lysine based peptides are both cationic and can therefore bind to anionic DNA. To examine and compare the binding capacity of the lysine based peptides or PEIs to DNAs, gel retardation and PicoGreen quenching assays were performed.

4.2.1.1 Gel retardation assay of the lysine based peptides or PEIs

To perform the gel retardation assay, the lysine based peptides or PEIs were mixed with DNA in distilled water at different nitrogen to phosphate (N/P) ratios for 30 minutes at room temperature. The complexes were then resolved using 1% agarose gel electrophoresis. The gel was visualised under UV.

Generally, increasing charge ratios **(Section 2.2.3.3.1.1 for calculation of an N/P ratio)** of the complexes retarded the complex migrations **(Figure 4.4)**. As shown in **Figure 4.4A and B**, all the linear lysine peptides (K8, K16, K24 and K32) bound to DNA and completely retarded the DNA migration at an N/P ratio of 3:1. The complete retardation indicated packaging of DNA within the complex reagents. The Kbranch peptide bound to

and formed a stable complex with DNA starting from an N/P ratio of 4:1 **(Figure 4.4C)**. Stable DNA complex formation was also observed using B-PEI at an N/P ratio of 5:1 and L-PEI at an N/P ratio of 2.5:1 **(Figure 4.4D).**

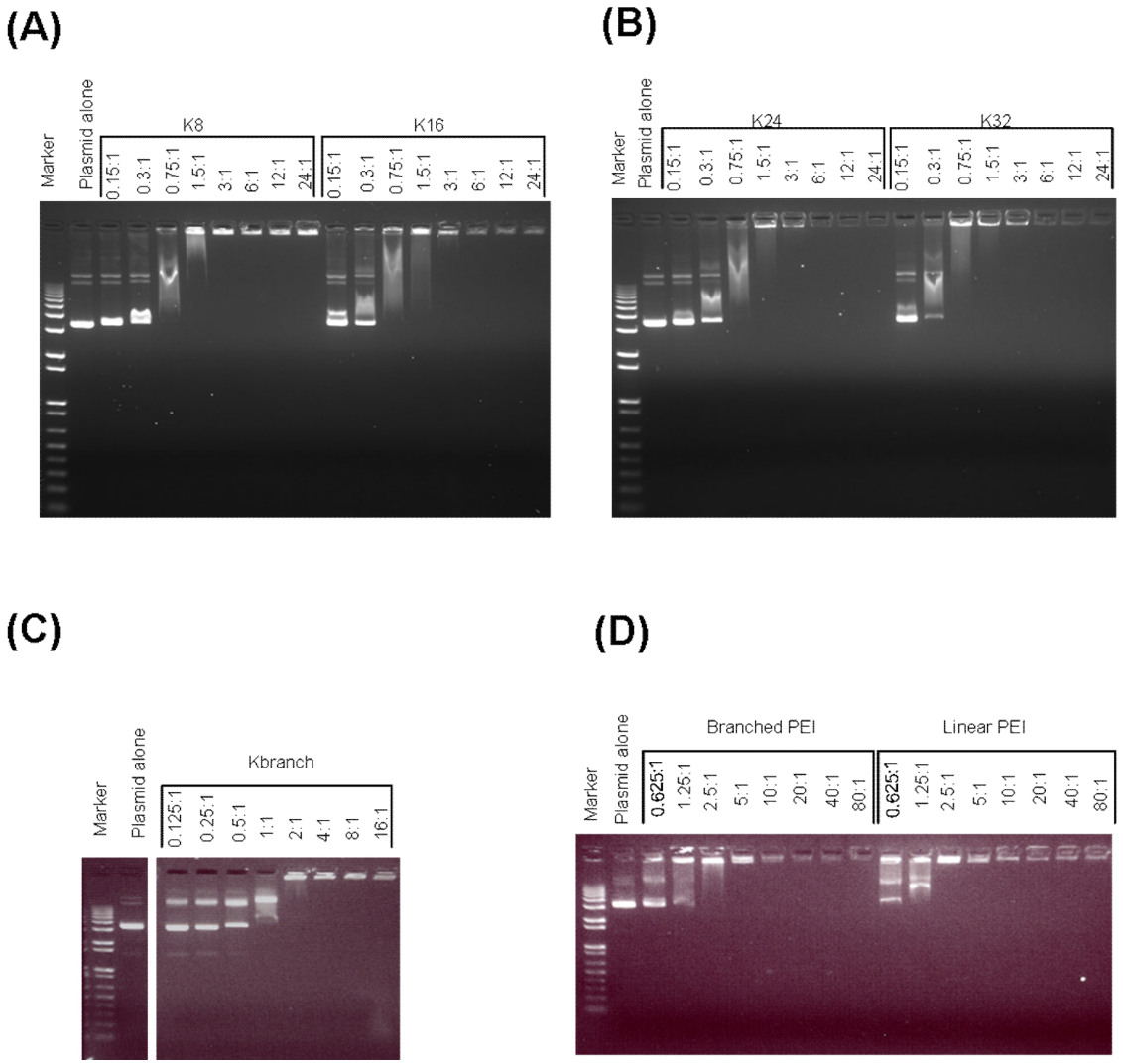

Figure 4.4 The binding properties of peptides or PEIs with plasmid DNA. The lysine based peptides or PEIs were mixed with 5 kb plamsid DNA (pCI-Luc) in distilled water at different N/P ratios for 30 minutes. The complexes were then run on a 1% agarose gel. The gel was visualised using UV **(Section 2.2.6.1)**. **(A)** the K8 DNA and K16 DNA complexes, **(B)** the K24 DNA and K32 DNA complexes, **(C)** the Kbranch DNA complexes, **(D)** the Branched PEI (B-PEI) DNA and Linear PEI (L-PEI) DNA complexes. The formulations of the complexes are expressed as an N/P ratio. K8, K16, K24 and K32 completely retarded the DNA migration at an N/P ratio of 3:1.

Kbranch, B-PEI and L-PEI completely retarded the DNA migration at N/P ratios of 4:1, 2:1, 5:1 and 2.5:1 respectively.

4.2.1.2 PicoGreen fluorescence quenching assay of the lysine based peptides or PEIs

To perform the PicoGreen fluorescence quenching assay, the plasmid DNA was firstly mixed with the PicoGreen reagent in TE buffer for 10 minutes at room temperature, followed by mixing with the lysine based peptides or PEIs in TE buffer at different N/P ratios for 30 minutes at room temperature. The fluorescence emission from each complex was measured using FLUOstar Optima.

The PicoGreen signals from the complexes were normalised with the naked DNA control to yield the percentage of the PicoGreen signal detected. As the PicoGreen signals are directly proportional to the amount of free DNA, lower PicoGreen signals detected suggest better packaging of the DNA within the complexes.

Increasing the lysine based peptides or PEIs to DNA charge ratios, to a certain N/P ratio, led to decreased DNA fluorescence levels **(Figure 4.5 and 4.6)**. All the linear lysine peptides (K8, K16, K24 and K32) bound to DNA and minimised the fluorescence detected at an N/P ratio of 1.5:1 **(Figure 4.5)**. A further increase of the N/P ratio beyond the 1.5:1 N/P ratio of these complexes did not further reduce the fluorescence signal detected. On the other hand, the N/P ratios of the Kbranch peptide, B-PEI and L-PEI necessary to minimise

the fluorescence signals from the PicoGreen labelled DNA were 2:1, 5:1 and 2.5:1 respectively **(Figure 4.6)**. Having reached the N/P ratios that minimise the PicoGreen signals, a further increase of the N/P ratios of these complexes did not further decrease the fluorescence signals detected. The minimum fluorescence signals detected at these N/P ratios suggested that DNA were encapsulated within the complexes.

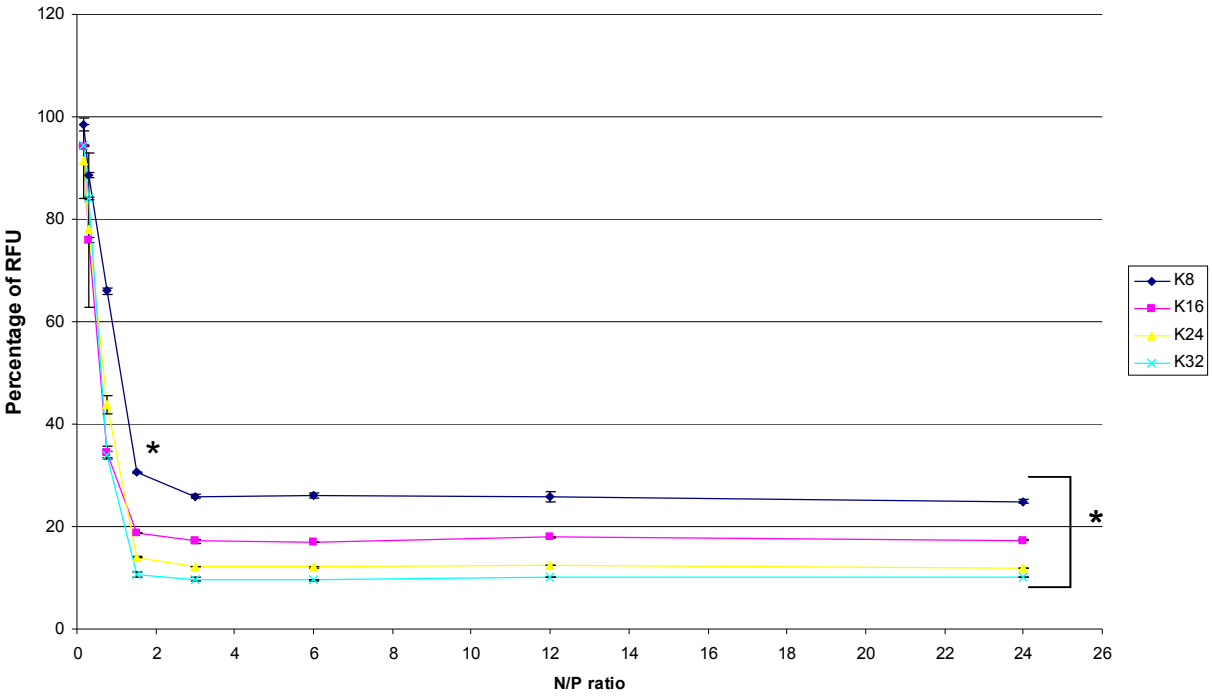

Figure 4.5 The relative binding affinity of linear lysine peptides with plasmid DNA. Linear lysine peptides were mixed with PicoGreen labelled pCI-Luc in TE buffer at different N/P ratios for 30 minutes. The fluorescence intensity of the complexes was then measured using FLUOstar Optima. The PicoGreen signals from the complexes were normalised with the naked DNA control to yield the percentage of relative fluorescence unit (RFU) **(Section 2.2.6.2)**. Statistical analysis was performed using ANOVA followed by Tukey's test and it showed a significant decrease of the percentage of RFU starting from a 1.5:1 N/P ratio for all the complexes ($P < 0.05$). The percentage of RFU of the K8 DNA complexes from an N/P ratio 1.5:1 onwards is significantly different to the K16 DNA, K24 DNA and K32 DNA complexes with the same N/P ratio ($P < 0.05$).

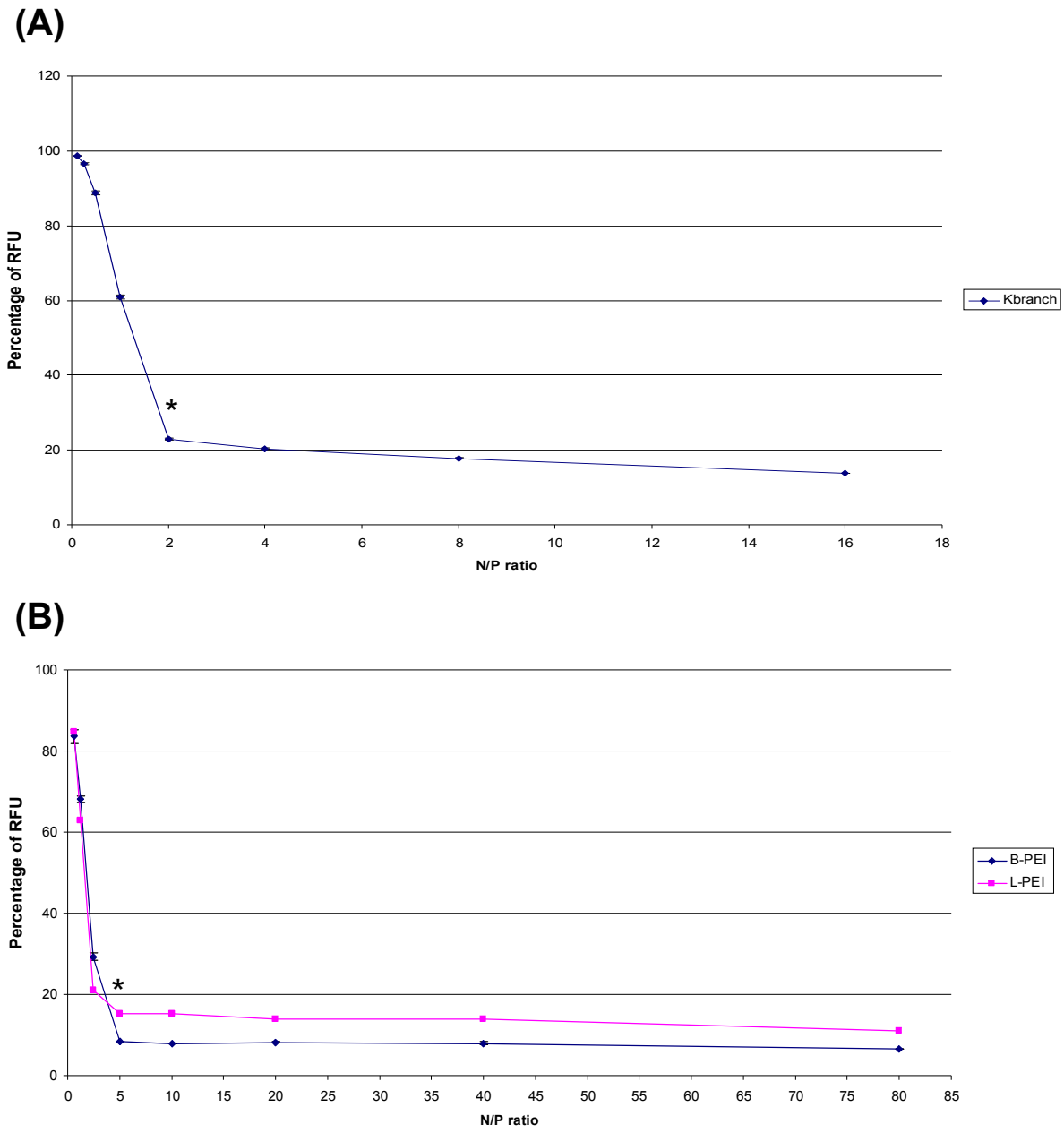

Figure 4.6 The relative binding affinity of Kbranch or PEIs with plasmid DNA. The Kbranch peptide or PEIs were mixed with PicoGreen labelled pCI-Luc in TE buffer at different N/P ratios for 30 minutes. The fluorescence intensity of the complexes was then measured using FLUOstar Optima. The PicoGreen signals from the complexes were normalised with the naked DNA control to yield the percentage of relative fluorescence unit (RFU) **(Section 2.2.6.2)**. **(A)** Kbranch DNA

complexes. Statistical analysis was performed using ANOVA followed by Tukey's test and it showed a significant decrease of the percentage of RFU starting from a 2:1 N/P ratio for all the Kbranch DNA complexes ($P < 0.05$). **(B)** B-PEI DNA and L-PEI DNA complexes. Statistical analysis was performed using ANOVA followed by Tukey's test and it showed a significant decrease of the percentage of RFU starting from a 2.5:1 N/P ratio of the PEI DNA complexes ($P < 0.05$).

The DNA condensation abilities of the polymers, estimated from the gel retardation and PicoGreen fluorescence quenching assays, are summarised in **Table 4.2.** Overall, DNA were packaged by the linear lysine peptides starting from an N/P ratio of 1.5:1 to 3:1. The Kbranch peptide packaged DNA starting from an N/P ratio of 2:1 to 4:1. L-PEI and B-PEI packaged DNA at a 2.5:1 and 5:1 N/P ratio respectively.

	The N/P ratio of the polymer necessary to mediate DNA condensation	
	Gel retardation assay	**PicoGreen fluorescence quenching assay**
K8	3:1	1.5:1
K16	3:1	1.5:1
K24	3:1	1.5:1
K32	3:1	1.5:1
Kbranch	4:1	2:1
B-PEI	5:1	5:1
L-PEI	2.5:1	2.5:1

Table 4.2 The DNA condensation abilities of the complex reagents estimated by different assays.

4.2.2 Dissociation properties of the lysine based peptides or PEIs to DNA

To mediate effective DNA delivery, complex reagents are expected to package DNA into stable complexes for cellular uptake. However, the complex reagents must be able to dissociate from DNA within cells for transcription. To study the stability and dissociation properties of the DNA complexes, a range of different concentrations of heparin sulphate were added to the complexes. Heparin has a highly negative charge and can compete with DNA to bind to the lysine based peptides or PEIs (Sundaram et al. 2005). Therefore, the addition of different amounts of heparin to each complex allows an estimation of the dissociation behaviours of the complexes.

4.2.2.1 Heparin induced complex dissociation assay

To carry out the heparin induced complex dissociation assay, the complexes were first prepared as described in **Section 2.2.6.3**. Different concentrations of heparin were then added and incubated with those complexes in a range of charge ratios for 30 minutes in TE buffer at room temperature. The emissions of the fluorescence from those complexes were then measured using FLUOstar Optima.

A range of five N/P ratios for each complex were chosen according to the binding studies. N/P ratios where the plasmid DNA appeared to be fully condensed were chosen in order to assess the effect on complex stability. Under heparin conditions, when the complexes started to dissociate, the PicoGreen signal would increase due to the release of the labelled

DNA. Since the PicoGreen signals from the complexes were normalised with the naked DNA control to yield the percentage of the PicoGreen signal detected, a complete complex dissociation would lead to a value close to 100% of PicoGreen signal.

4.2.2.2 Dissociation of the linear lysine peptide DNA complexes

In general, increased N/P ratios enhanced the binding between the linear lysine peptides (K8, K16, K24 and K32) and DNA **(Figure 4.7 and 4.8).** The K8 DNA complexes with N/P ratios of 0.75:1, 1.5: and 3:1 dissociated readily under trace amounts of heparin **(Figure 4.7A)**. The 0.75:1 N/P ratio K8 DNA complexes became fully dissociated at a heparin concentration of 0.04 U/ml whereas the 1.5:1 N/P ratio K8 DNA complexes were completely dissociated at 0.08 U/ml of heparin. The K8 DNA complexes with an N/P ratio of 3:1 were fully dissociated at 0.167 U/ml of heparin. On the other hand, the 6:1 and 12:1 N/P ratio K8 DNA complexes began to dissociate at 0.08 and 0.33 U/ml of heparin respectively. The 6:1 charge ratio complexes became fully dissociated at 0.67 U/ml of heparin whereas the 12:1 N/P ratio complexes were completely dissociated at 1.33 U/ml of heparin.

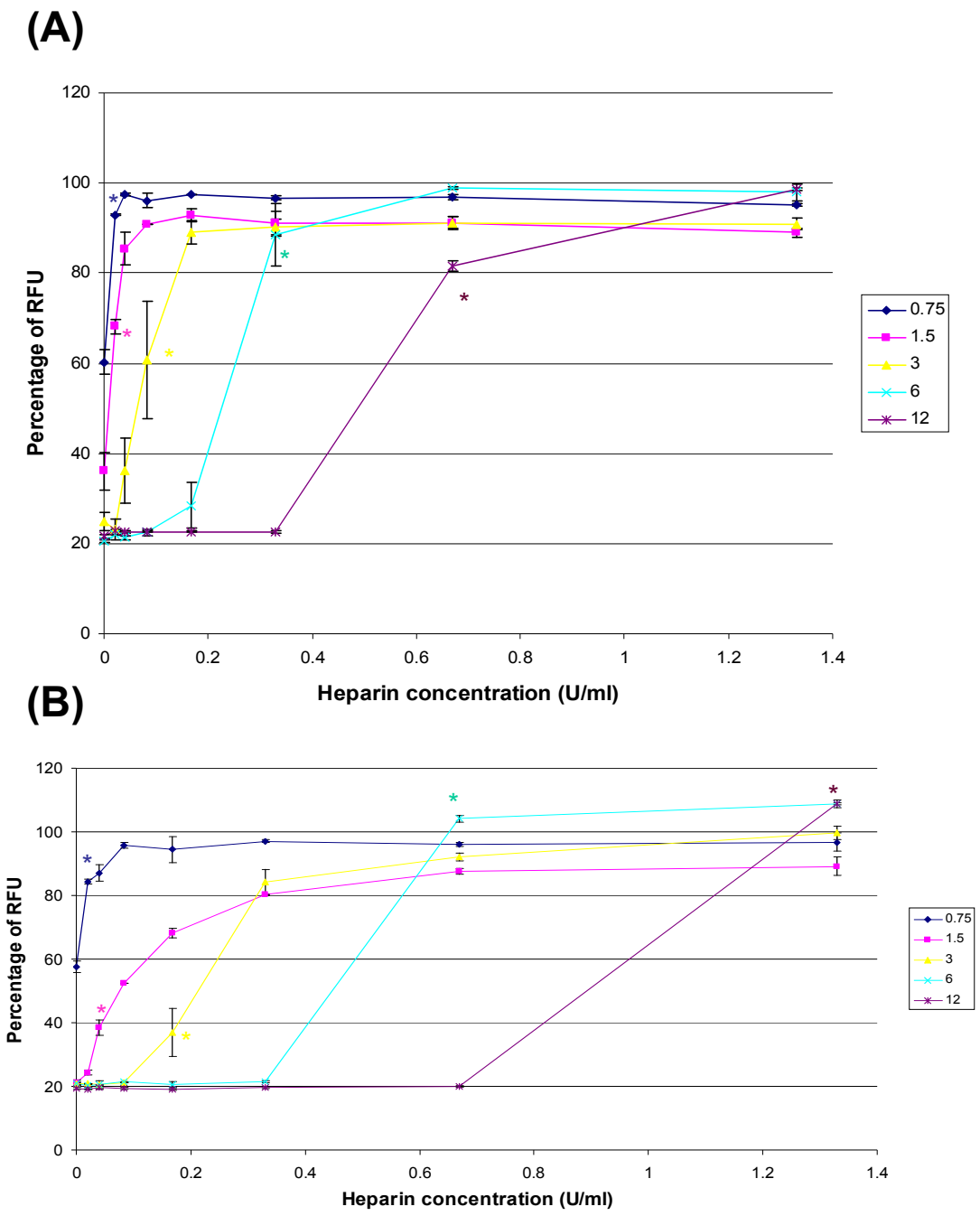

Figure 4.7 The dissociation properties of K8 or K16 with plasmid DNA. K8 or K16 were mixed with PicoGreen labelled pCI-Luc in TE buffer at different N/P ratios for 30 minutes. Different concentrations of heparin were added to the complexes and the fluorescence intensity of the complexes was measured using FLUOstar Optima. The PicoGreen signals from the complexes were

normalised with the naked DNA control to yield the percentage of relative fluorescence unit (RFU) **(Section 2.2.6.3)**. **(A)** K8 DNA complexes. **(B)** K16 DNA complexes. Statistical analysis was performed using ANOVA followed by Tukey's test and it showed a significant increase of the percentage of RFU of the complexes treated with the concentration of heparin marked with * (each * has the same colour as the curve of the N/P ratio of the complexes it corresponds to). In addition, complexes treated with higher heparin concentrations displayed a significant increase of the percentage of RFU compared to that of the untreated complexes ($P < 0.05$).

The 0.75:1 and 1.5:1 charge ratio K16 DNA complexes dissociated readily under trace amounts of heparin and became fully dissociated at 0.08 and 0.167 U/ml of heparin respectively **(Figure 4.7B)**. The K16 DNA complexes with N/P ratios of 3:1 and 6:1 began to dissociate at 0.08 and 0.33 U/ml of heparin respectively, and both of these complexes were completely dissociated at 0.67 U/ml of heparin. With an N/P ratio of 12:1, the K16 DNA complexes remained stable at 0.67 U/ml of heparin and were fully dissociated at 1.33 U/ml of heparin.

As shown in **Figure 4.8A**, the dissociation of the K24 DNA complexes with charge ratios of 0.75:1 and 1.5:1 were initiated under trace amounts of heparin, and these complexes were completely dissociated at 0.167 and 1.3 U/ml of heparin respectively. For the K24 DNA complexes with charge ratios of 3:1 and 6:1, the concentration of heparin required to initiate dissociation were 0.08 and 0.33 U/ml respectively, with both of these complexes becoming fully dissociated at 1.33 U/ml of heparin. With an N/P ratio of 12:1, the K24 DNA complexes remained stable at 0.67 U/ml of heparin and were fully dissociated at 1.33 U/ml of heparin.

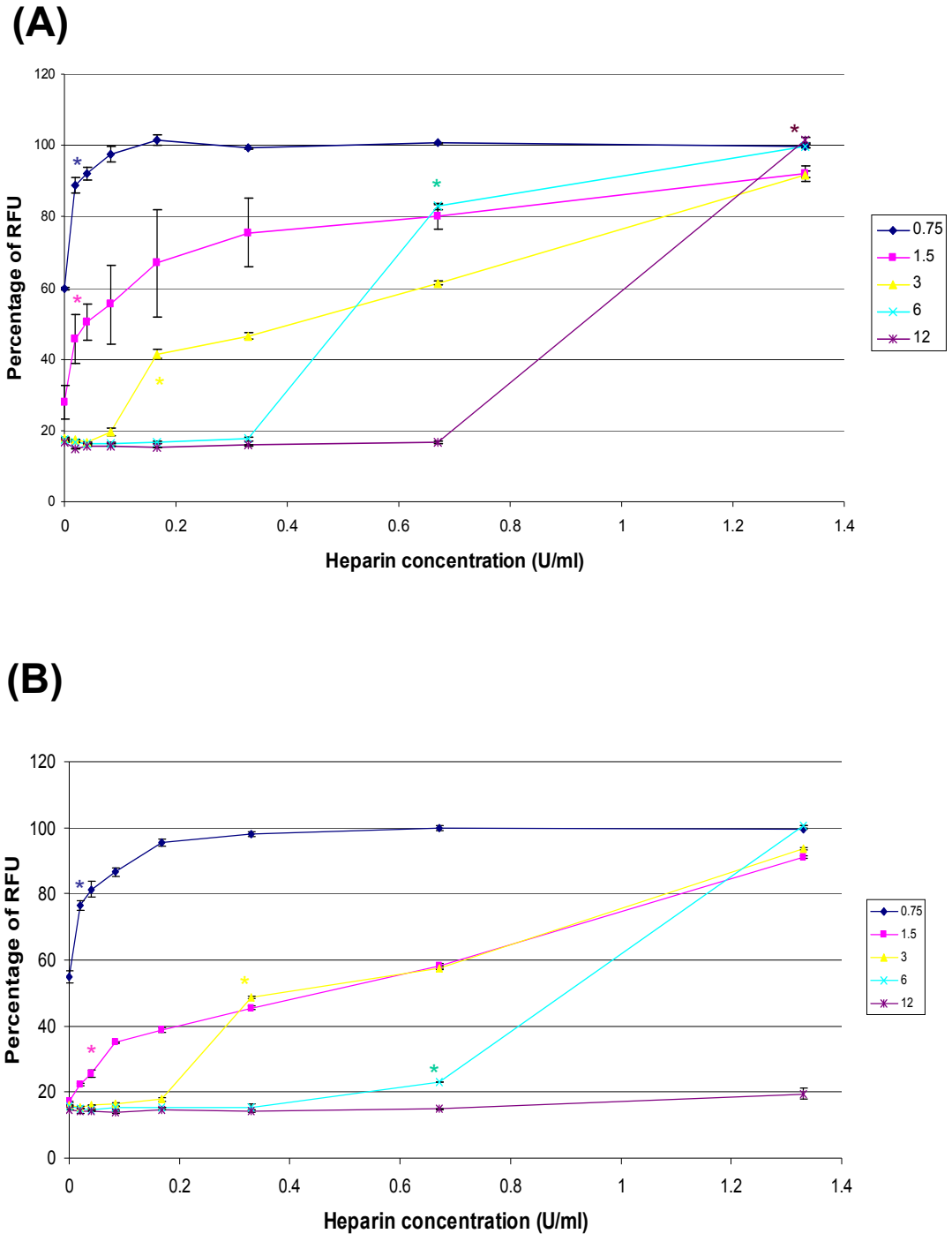

Figure 4.8 The dissociation properties of K24 or K32 with plasmid DNA. K24 or K32 were mixed with PicoGreen labelled pCI-Luc in TE buffer at different N/P ratios for 30 minutes. Different concentrations of heparin were added to the complexes and the fluorescence intensity of

the complexes was measured using FLUOstar Optima. The PicoGreen signals from the complexes were normalised with the naked DNA control to yield the percentage of relative fluorescence unit (RFU) **(Section 2.2.6.3)**. **(A)** K24 DNA complexes, **(B)** K32 DNA complexes. Statistical analysis was performed using ANOVA followed by Tukey's test and it showed a significant increase of the percentage of RFU of the complexes treated with the concentration of heparin marked with * (each * has the same colour as the curve of the N/P ratio of the complexes it corresponds to). In addition, complexes treated with higher heparin concentrations displayed a significant increase of the percentage of RFU compared to that of the untreated complexes ($P < 0.05$).

Figure 4.8B showed that the K32 DNA complexes with N/P ratios of 0.75:1 and 1.5:1 started to dissociate under trace amounts of heparin. These complexes became completely dissociated at 0.33 and 1.33 U/ml of heparin respectively. The K32 DNA complexes with charge ratios of 3:1 and 6:1 began to dissociate at 0.167 and 0.33 U/ml of heparin respectively, and both of these complexes were fully dissociated at 1.33 U/ml of heparin. The K32 DNA complexes with an N/P ratio of 12:1 were not dissociated under 1.33 U/ml of heparin.

The results of the heparin induced nucleic acid dissociation assays of the linear lysine peptide DNA complexes are summarised in **Table 4.3.** Overall, increasing the size of the linear lysine peptides enhanced the binding of the peptides to DNA, which in turns improves the complex stability.

DNA complexes	N/P ratio	Heparin concentration necessary to initiate dissociation (U/ml)	Heparin concentration necessary to allow complete dissociation (U/ml)
K8	0.75:1	0-0.02	0.08
	1.5:1	0.02	0.167
	3:1	0.04	0.167
	6:1	0.08	0.67
	12:1	0.33	1.33
K16	0.75:1	0-0.02	0.08
	1.5:1	0-0.02	0.67
	3:1	0.08	0.67
	6:1	0.33	0.67
	12:1	0.67-1.33	1.33
K24	0.75:1	0-0.02	0.167
	1.5:1	0-0.02	1.33
	3:1	0.08	1.33
	6:1	0.33	1.33
	12:1	0.67-1.33	1.33
K32	0.75:1	0-0.02	0.33
	1.5:1	0-0.02	1.33
	3:1	0.167	1.33
	6:1	0.33	1.33
	12:1	N/A	N/A

Table 4.3 A summary of the heparin induced dissociation of different linear lysine peptide DNA complexes.

4.2.2.3 Dissociation of the Kbranch peptide DNA complexes

The Kbranch DNA complexes, with charge ratios of 1:1 and 2:1, began to dissociate under trace amounts of heparin and were completely dissociated at 0.08 and 0.33 U/ml of heparin **(Figure 4.9)**. With an N/P ratio of 4:1, the Kbranch DNA complexes started to dissociate at a heparin concentration of 0.08 U/ml and became fully dissociated at 0.33 U/ml of heparin. The dissociation of the 8:1 charge ratio Kbranch DNA complexes were initiated at 0.33 U/ml of heparin, and these complexes were completely dissociated at 0.67 U/ml of heparin. With an N/P ratio of 16:1, the Kbranch DNA complexes remained stable at 0.67 U/ml of heparin and were fully dissociated at 1.33 U/ml of heparin.

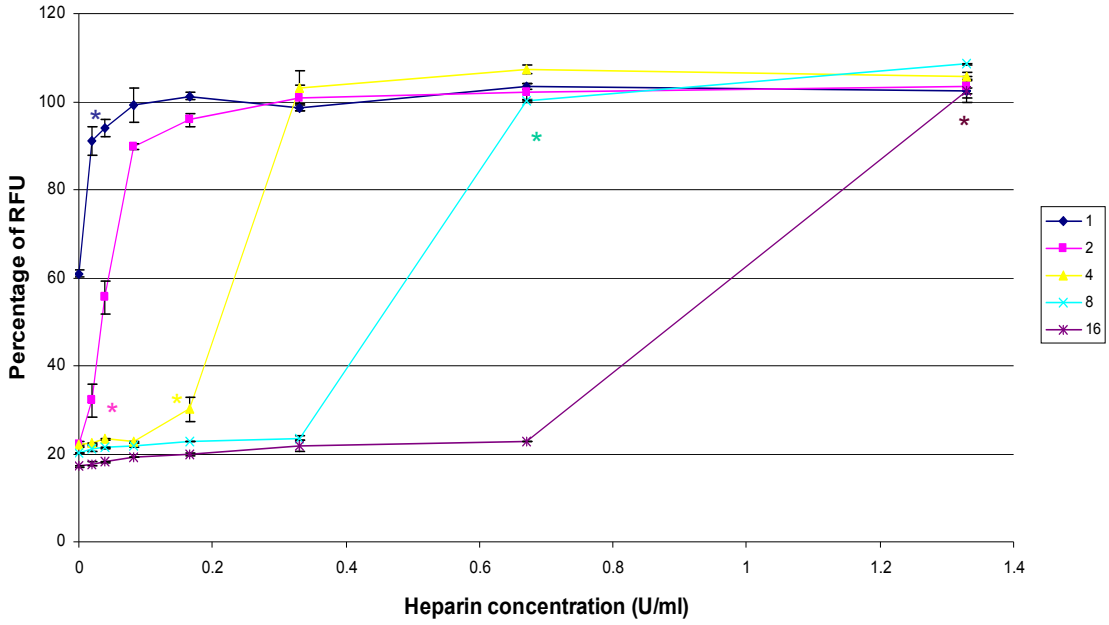

Figure 4.9 The dissociation properties of Kbranch with plasmid DNA. Kbranch were mixed with PicoGreen labelled pCI-Luc in TE buffer at different N/P ratios for 30 minutes. Different concentrations of heparin were added to the complexes and the fluorescence intensity of the complexes was measured using FLUOstar Optima. The PicoGreen signals from the complexes were normalised with the naked DNA control to yield the percentage of relative fluorescence unit (RFU) **(Section 2.2.6.3)**. Statistical analysis was performed using ANOVA followed by Tukey's test and it showed a significant increase of the percentage of RFU of the complexes treated with the concentration of heparin marked with * (each * has the same colour as the curve of the N/P ratio of the complexes it corresponds to). In addition, complexes treated with higher heparin concentrations displayed a significant increase of the percentage of RFU compared to that of the untreated complexes ($P < 0.05$).

4.2.2.4 Dissociation of the PEI DNA complexes

As shown in **Figure 4.10A and B**, the B-PEI DNA complexes with N/P ratios of 2.5:1 and 5:1 began to dissociate under trace amounts of heparin, with these complexes being fully dissociated at 5.3 and 21.3 U/ml of heparin respectively. With charge ratios of 10:1, 20:1 and 40:1, the B-PEI DNA complexes started to dissociate at 0.167, 0.33 and 0.67 U/ml of heparin respectively, and the complexes became fully dissociated at 21.3 U/ml of heparin.

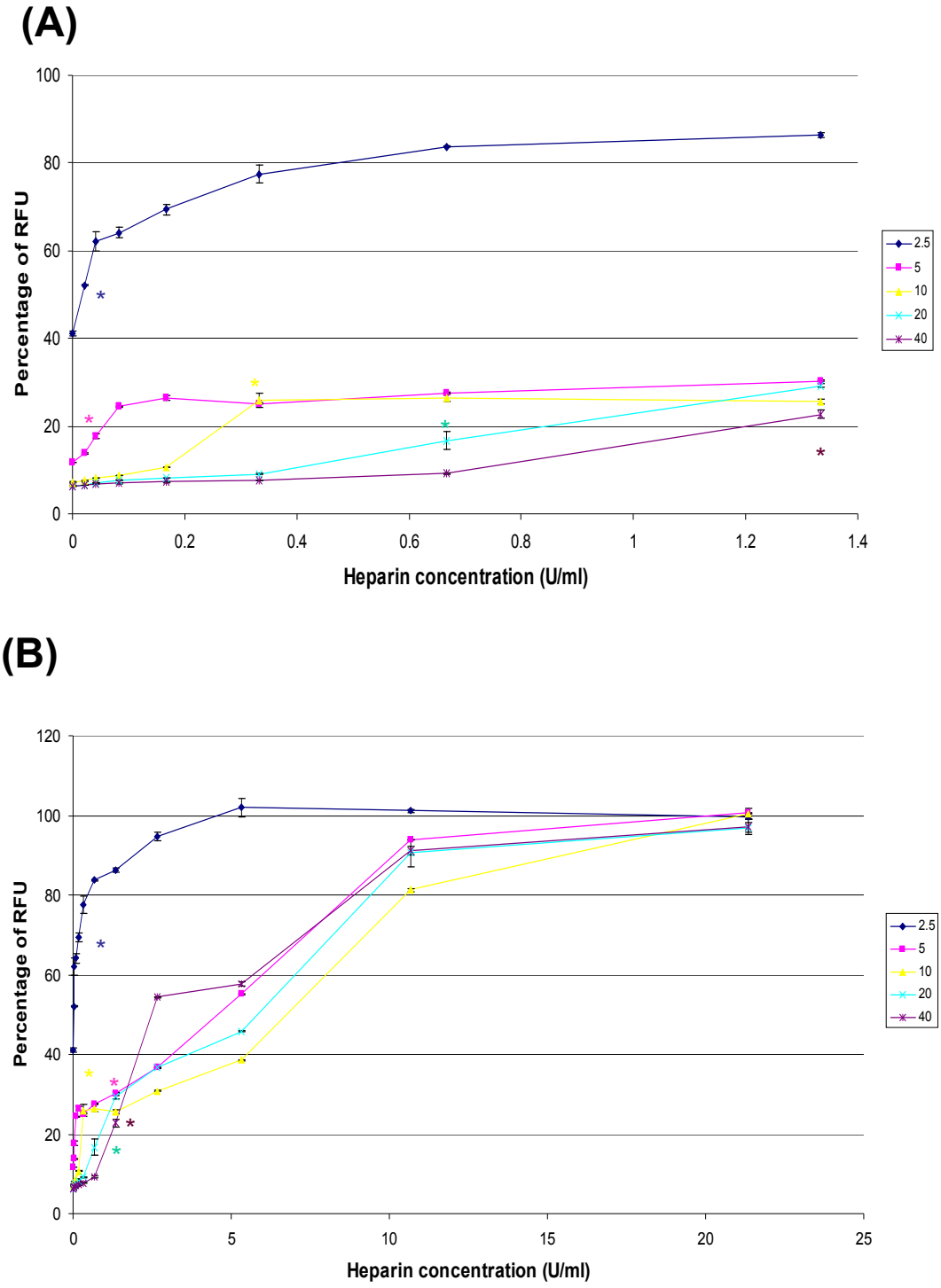

Figure 4.10 The dissociation properties of B-PEI with plasmid DNA. B-PEI were mixed with PicoGreen labelled pCI-Luc in TE buffer at different N/P ratios for 30 minutes. Different

concentrations of heparin were added to the complexes and the fluorescence intensity of the complexes was measured using FLUOstar Optima. The PicoGreen signals from the complexes were normalised with the naked DNA control to yield the percentage of relative fluorescence unit (RFU) **(Section 2.2.6.3)**. **(A)** B-PEI DNA complexes exposed to 0 to 1.33 U/ml of heparin, **(B)** B-PEI DNA complexes exposed to 0 to 21 U/ml of heparin. Statistical analysis was performed using ANOVA followed by Tukey's test and it showed a significant increase of the percentage of RFU of the complexes treated with the concentration of heparin marked with * (each * has the same colour as the curve of the N/P ratio of the complexes it corresponds to). In addition, complexes treated with higher heparin concentrations displayed a significant increase of the percentage of RFU compared to that of the untreated complexes ($P < 0.05$).

The 2.5:1 and 5:1 N/P ratio L-PEI DNA complexes dissociated readily under trace amounts of heparin and were completely dissociated at 2.6 and 5.3 U/ml of heparin respectively **(Figure 4.11A and B)**. The dissociation of the L-PEI DNA complexes with charge ratios of 10:1, 20:1 and 40:1 were initiated at 0.167, 0.67 and 1.33 U/ml of heparin, and all of these complexes were fully dissociated at 5.3 U/ml of heparin.

The results of the heparin induced nucleic acid dissociation assays of the Kbranch DNA, B-PEI DNA and L-PEI DNA complexes are summarised in **Table 4.4.** Overall, B-PEI DNA complexes are more stable than the L-PEI DNA complexes. The L-PEI DNA complexes are more stable than the Kbranch DNA complexes.

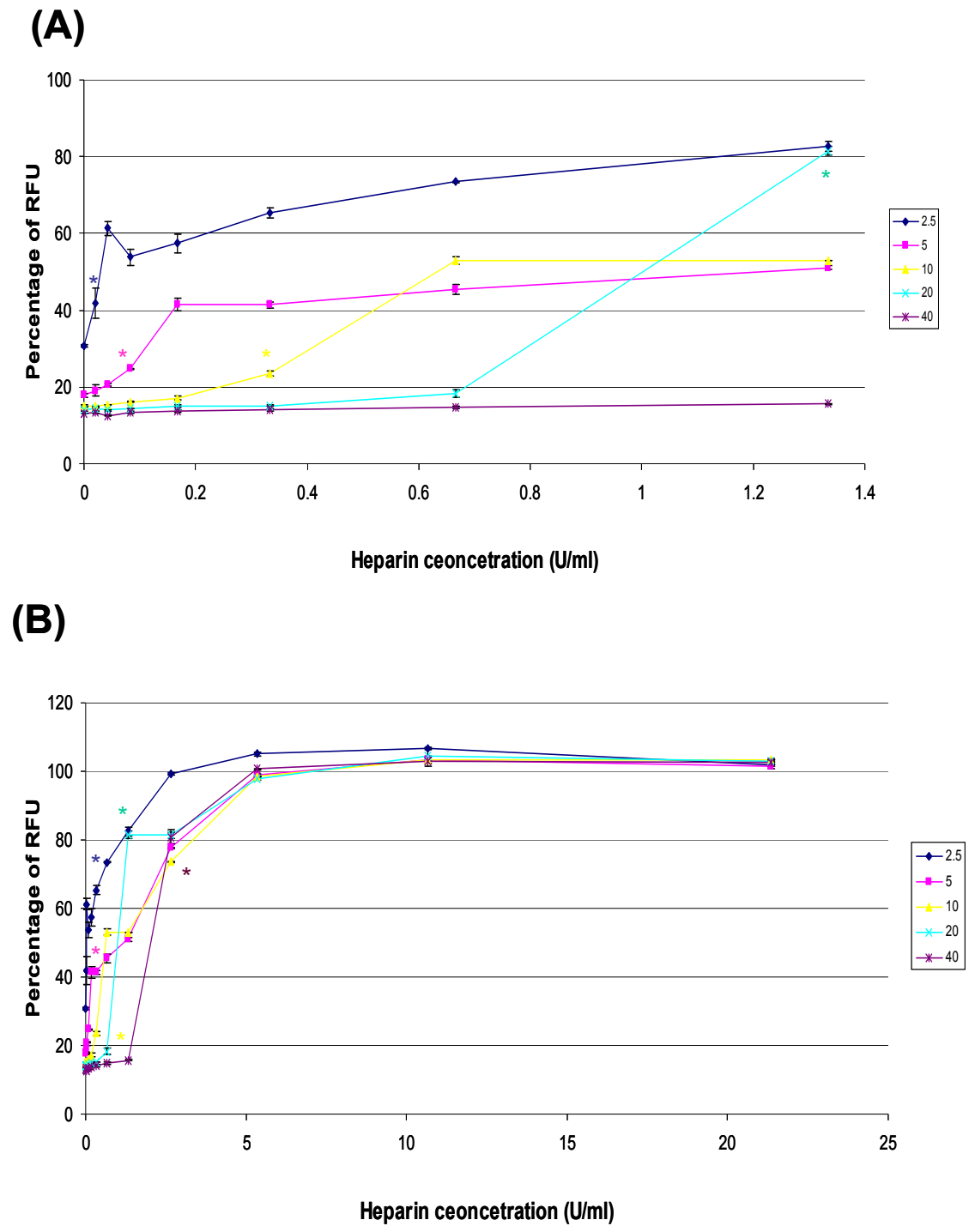

Figure 4.11 The dissociation properties of L-PEI with plasmid DNA. L-PEI were mixed with PicoGreen labelled pCI-Luc in TE buffer at different N/P ratios for 30 minutes. Different concentrations of heparin were added to the complexes and the fluorescence intensity of the

complexes was measured using FLUOstar Optima. The PicoGreen signals from the complexes were normalised with the naked DNA control to yield the percentage of relative fluorescence unit (RFU) **(Section 2.2.6.3)**. **(A)** L-PEI DNA complexes exposed to 0 to 1.33 U/ml of heparin, **(B)** L-PEI DNA complexes exposed to 0 to 21 U/ml of heparin. Statistical analysis was performed using ANOVA followed by Tukey's test and it showed a significant increase of the percentage of RFU of the complexes treated with the concentration of heparin marked with * (each * has the same colour as the curve of the N/P ratio of the complexes it corresponds to). In addition, complexes treated with higher heparin concentrations displayed a significant increase of the percentage of RFU compared to that of the untreated complexes ($P < 0.05$).

DNA complexes	N/P ratio	Heparin concentration required to initiate dissociation (U/ml)	Heparin concentration required to allow complete dissociation (U/ml)
Kbranch	1:1	0-0.02	0.08
	2:1	0-0.02	0.33
	4:1	0.08	0.33
	8:1	0.33	0.67
	16:1	0.67-1.33	1.33
B-PEI	2.5:1	0-0.02	5.3
	5:1	0-0.02	21.3
	10:1	0.167	21.3
	20:1	0.33	21.3
	40:1	0.67	21.3
L-PEI	2.5:1	0-0.02	2.6
	5:1	0-0.02	5.3
	10:1	0.167	5.3
	20:1	0.167	5.3
	40:1	1.33	5.3

Table 4.4 A summary of the heparin induced dissociation of the Kbranch and PEI DNA complexes.

4.2.3 Size and zeta potential of the complexes

The particle size and surface charge are important characteristics of a DNA delivery system for cellular binding and uptake. Positive charged particles with sizes larger than 50 nm are expected to be efficiently taken up by cells (Gao et al. 2005). The particle size can be measured as a mean hydrodynamic size **(Section 2.2.6.4)** using Zetasizer Nano ZS, and the surface charge can be measured as zeta potential **(Section 2.2.6.5)** using Zetasizer Nano ZS.

4.2.3.1 Particle size

To measure the particle size, the lysine based peptides or PEIs were mixed with DNA in distilled water at different N/P ratios for 30 minutes at room temperature. The sizes of the complexes were then measured using Dynamic Light Scattering (DLS).

The measured average hydrodynamic diameters of the complexes formed from DNA and peptides are shown in **Figure 4.12 and 4.13.** With the exception of the K32 DNA complexes at an N/P ratio of 0.75:1, all the linear lysine peptides formed complexes with DNA with mean hydrodynamic sizes ranging from 45 nm to 100 nm. For the Kbranch peptide DNA complexes, the mean complex sizes were between 70 nm and 130 nm. Generally, increasing the N/P ratio of the lysine based peptide DNA complex decreased the complex size.

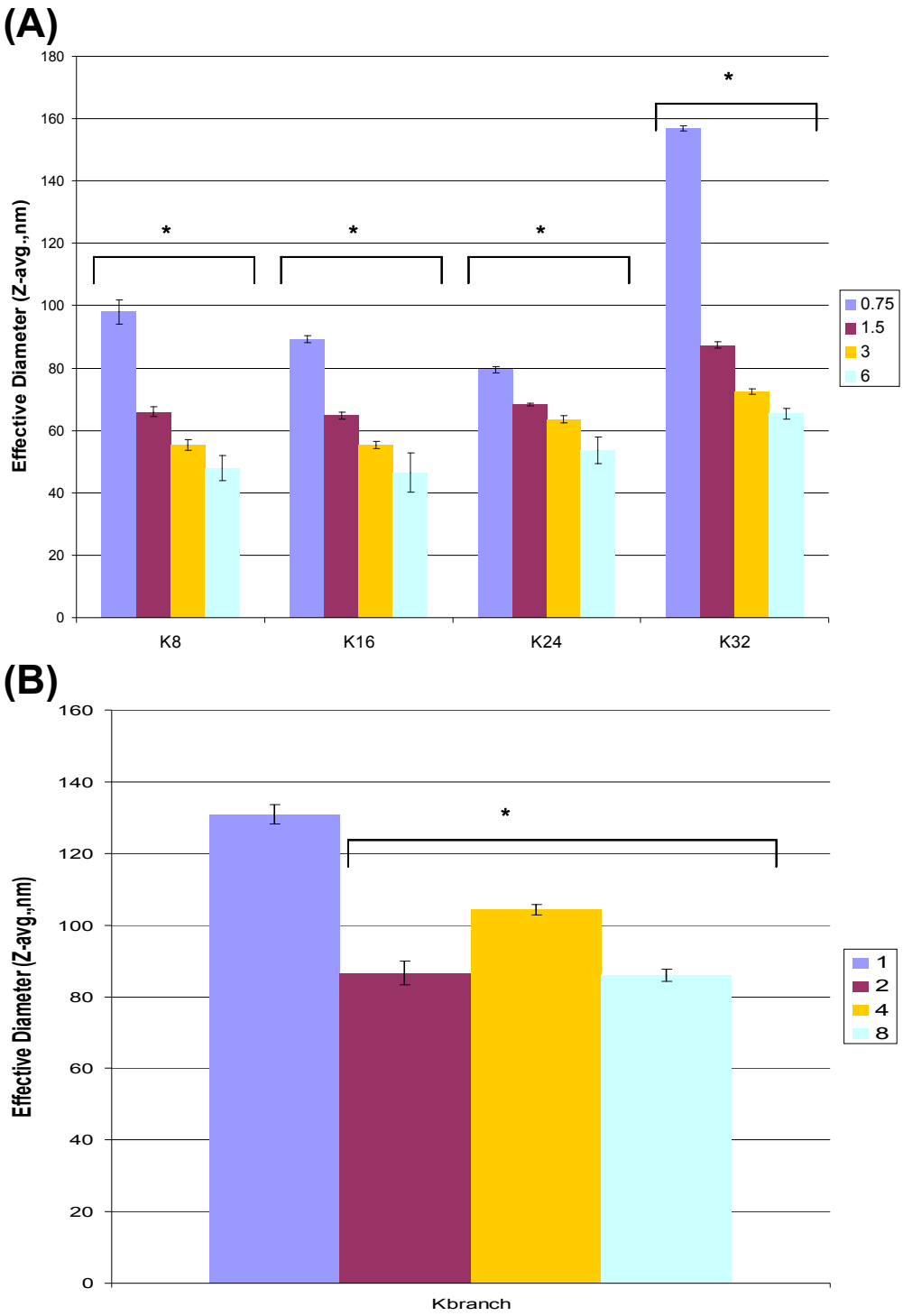

Figure 4.12 The effective diameter of peptide DNA complexes. The peptides were mixed with pCI-Luc in distilled water at different N/P ratios for 30 minutes. The size of each complex was then measured using Zetasizer Nano ZS **(Section 2.2.6.4)**. **(A)** Linear lysine peptide DNA complexes.

Statistical analysis was performed using Student's t-test and it showed a significant decrease of the effective diameters of the complexes from an N/P ratio of 0.75:1 to 6:1 ($P < 0.05$). **(B)** KBranch DNA complexes. Statistical analysis was performed using Student t-test and it showed a significant decrease of the effective diameters of the Kbranch DNA complexes from an N/P ratio of 1:1 to 2:1, 4:1 or 8:1 ($P < 0.05$). The formulations of the complexes are expressed as an N/P ratio.

The mean hydrodynamic sizes of L-PEI DNA complexes ranged from 80 nm to 110 nm **(Figure 4.13)**. However, the mean complex sizes of the B-PEI DNA complexes were distributed across a wider range, from 95 nm to 1000 nm. With N/P ratios of 10:1 and 20:1, the complex sizes of the B-PEI DNA complexes were 150 nm and 95 nm respectively, which are similar to the observation from Tang and Szoka (Tang & Szoka 1997). Decreasing the N/P ratio increased the hydrodynamic sizes of the complexes. For example, at an N/P ratio of 2.5:1, the mean size of the B-PEI DNA complex was 1000 nm. Overall, it was found that an increase of the N/P ratios of the lysine based peptide or PEI DNA complexes decreased the mean complex size.

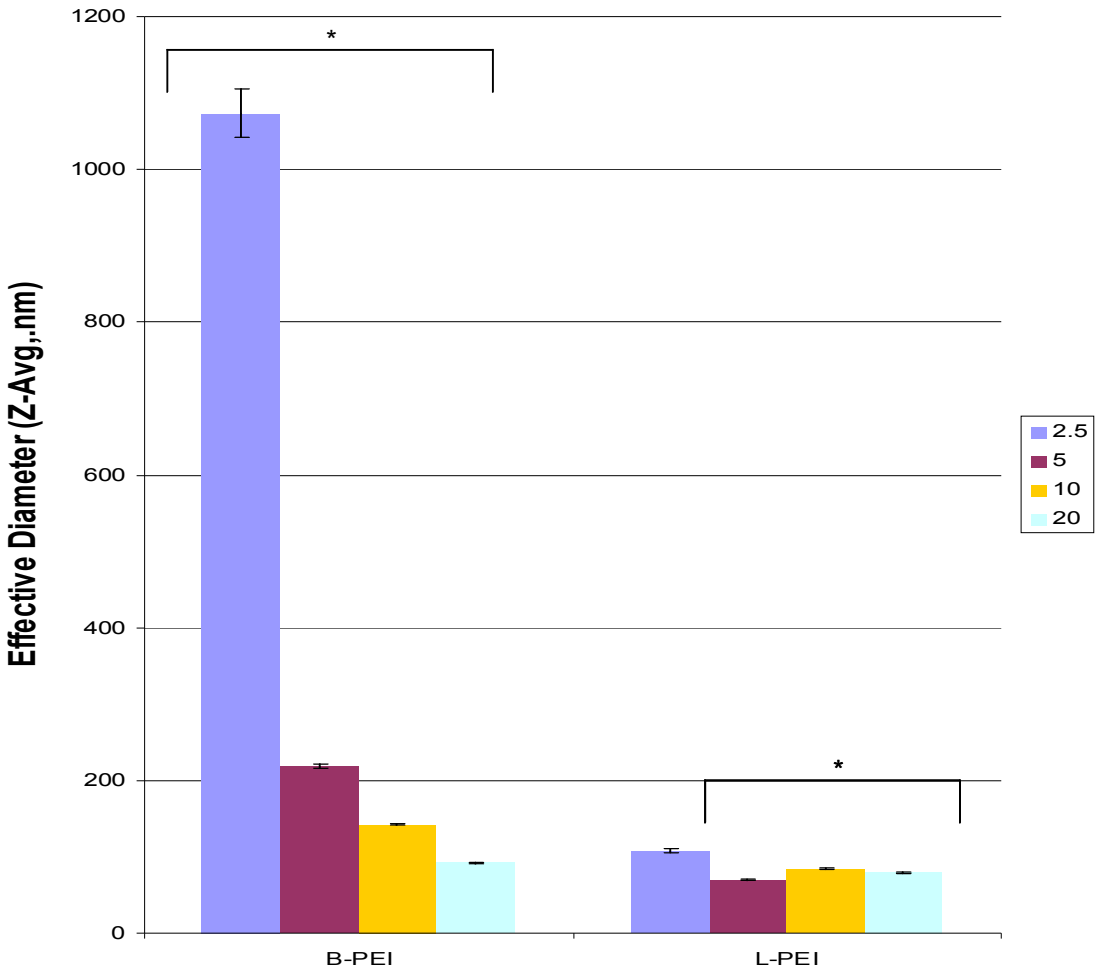

Figure 4.13 The effective diameter of PEI DNA complexes. PEIs were mixed with pCI-Luc in distilled water at different N/P ratios for 30 minutes. The size of each complex was then measured using Zetasizer Nano ZS **(Section 2.2.6.4)**. The formulations of the complexes are expressed as an N/P ratio. Statistical analysis was performed using Student t-test and it showed a significant decrease of the effective diameters of the B-PEI DNA complexes ($P < 0.05$). A significant decrease of the effective diameter of the L-PEI DNA complexes from an N/P ratio of 2.5:1 to 5:1, 10:1 or 20:1 was also observed ($P < 0.05$).

4.2.3.2 Zeta potential

To measure the zeta potential, the lysine based peptides or PEIs were mixed with DNA in distilled water at different N/P ratios for 30 minutes at room temperature. The average zeta potential of the complexes was then measured using Laser Doppler Anemometry.

Generally, the average zeta potential of the linear lysine peptide DNA complexes increased with the N/P ratio **(Figure 4.14)**. With an N/P ratio of 0.75:1, the average zeta potential of the K8 DNA complexes was -17 mV **(Figure 4.14A)**. Increasing the N/P ratio to 1.5:1 increased the mean zeta potential of the K8 DNA complexes to +27 mV. Further increasing the N/P ratio to 3:1 and 6:1 increased the zeta potential of these complexes to +34 and +32 mV respectively.

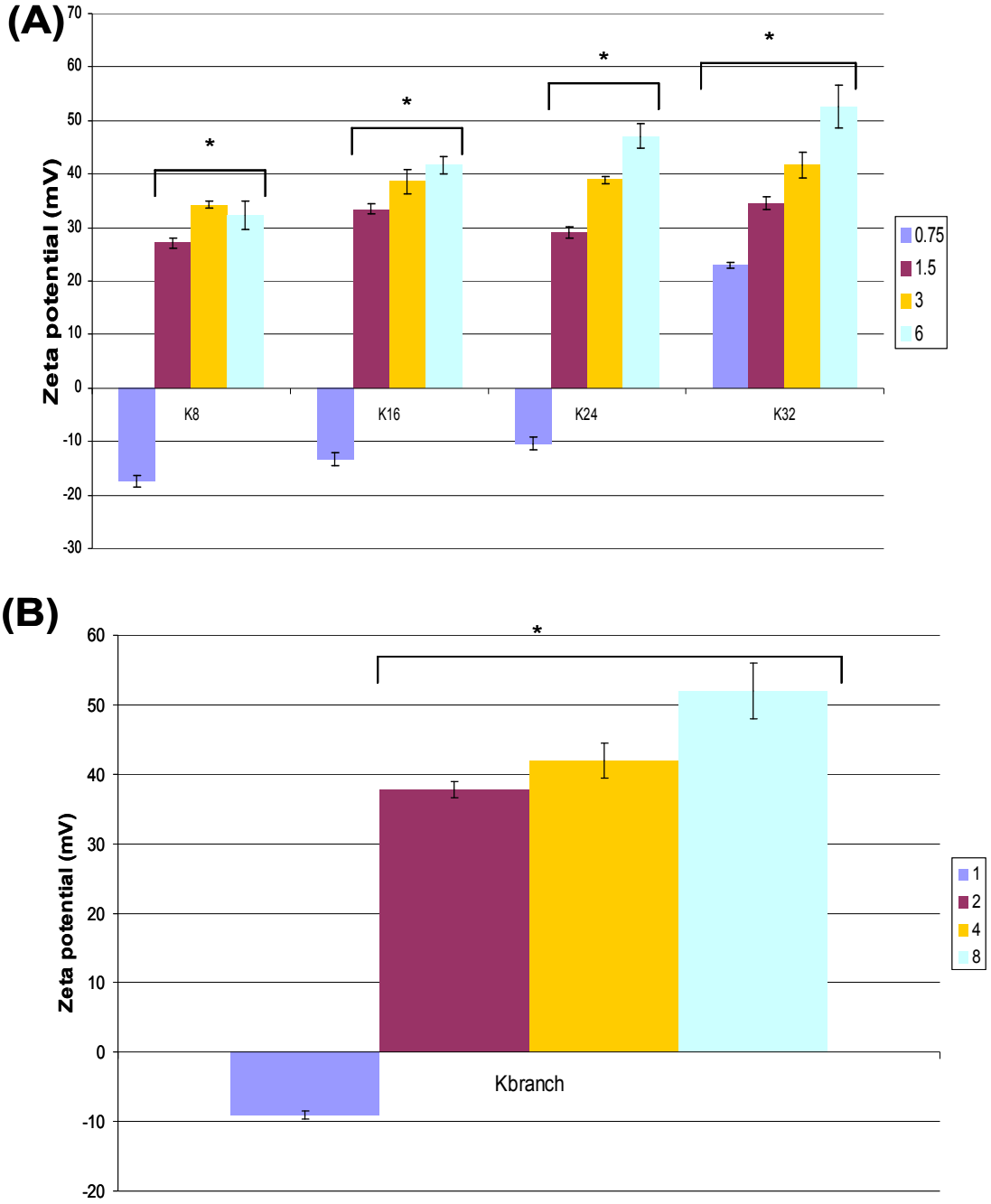

Figure 4.14 The zeta potential of peptide DNA complexes. The peptides were mixed with pCI-Luc in distilled water at different N/P ratios for 30 minutes. The zeta potential of the complexes was then measured using Zetasizer Nano ZS **(Section 2.2.6.5)**. **(A)** Linear lysine peptide DNA complexes. Statistical analysis was performed using Student t-test and it showed a significant

increase of the zeta potential of the linear lysine DNA complexes (For K8 DNA, K16 DNA or K24 DNA complexes, an increase was observed from an N/P ratio of 1.5:1 to 3:1 or 6:1; for K32 DNA complexes, an increase was observed from an N/P ratio of 0.75:1 to 6:1; $P < 0.05$). **(B)** Kbranch DNA complexes. A significant increase of the zeta potential of the Kbranch DNA complexes (from an N/P ratio od 2:1 to 8:1) was also observed ($P < 0.05$). The formulations of the complexes are expressed as an N/P ratio.

The average zeta potential of the K16 DNA complexes with an N/P ratio of 0.75:1 were -13 mV **(Figure 4.14A)**. Increasing the N/P ratio to 1.5:1 increased the zeta potential of the K16 DNA complexes to +34 mV. At N/P ratios of 3:1 and 6:1, the zeta potential of these complexes were +39 and +42 mV respectively.

Similar to the K8 or K16 DNA complexes, the zeta potential of the K24 DNA complexes with an N/P ratio of 0.75:1 were –10 mV**(Figure 4.14A)**. Increasing the N/P ratios to 1.5:1, 3:1 and 6:1 increased the average zeta potential of the K24 DNA complexes to +19, +39 and +49 mV respectively.

As shown in **Figure 4.14A**, the zeta potential of the K32 DNA complexes with N/P ratios of 0.75:1, 1.5:1, 3:1 and 6:1 were +23, +35, +42 and +53 mV respectively.

The average zeta potential of the Kbranch DNA complexes with an N/P ratio of 1:1 was -9 mV **(Figure 4.14B)**. Increasing the N/P ratios to 2:1, 4:1 and 8:1 increased the average potential of the Kbranch complexes to +38, +42 and +52 mV respectively.

For the PEI DNA complexes, generally an increase of the N/P ratio increased the average zeta potential **(Figure 4.15)**. The mean zeta potential of the B-PEI DNA complexes with N/P ratios of 2.5:1, 5:1, 10:1 and 20:1 were +38, +51, +50 and +52 mV whereas that of the L-PEI DNA complexes with the N/P ratios of 2.5:1, 5:1, 10:1 and 20:1 were +36, +40, +38 and +48 mV.

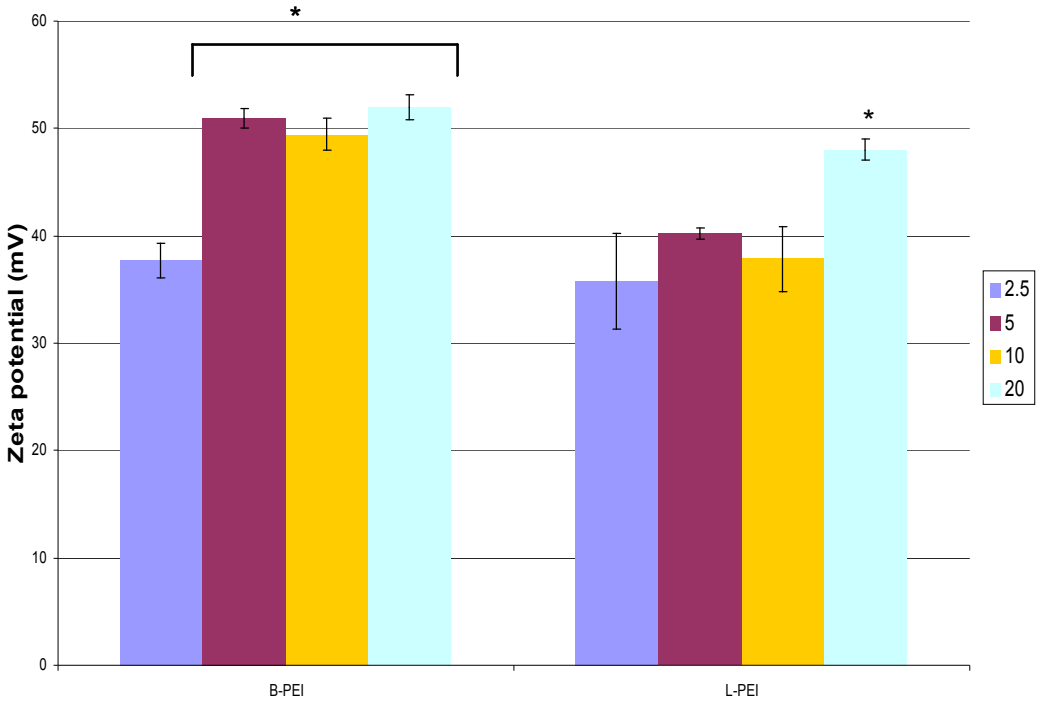

Figure 4.15 The zeta potential of PEI DNA complexes. PEIs were mixed with pCI-Luc in distilled water at different N/P ratios for 30 minutes. The zeta potential of the complexes were then measured Zetasizer Nano ZS **(Section 2.2.6.5)**. Statistical analysis was performed using Student t-test and it showed a significant increase of the zeta potential of the B-PEI DNA complexes from an N/P ratio of 2.5:1 to 5:1, 10:1 or 20:1 ($P < 0.05$). A significant increase of the zeta potential of the L-PEI DNA complexes from an N/P ratio of 10:1 to 20:1 was also observed ($P < 0.05$).

4.2.4 Transfection studies on the lysine based peptides or PEI DNA complexes

To investigate the gene delivery efficiency of different DNA complex formulations, a plasmid containing a luciferase gene was used for complex formation with the lysine peptides or PEIs. The complexes were then added to Neuro 2a cells for 4 hours in serum free Optimem medium. The cells were harvested 24 hours post-transfection for analysis of luciferase expression.

As shown in **Figure 4.16A**, the K8 DNA complexes were not able to deliver DNA to the cells effectively when the N/P ratio was below 12:1; modest gene expression was detected at an N/P ratio of 12:1. The K16 DNA complexes mediated relatively sufficient gene delivery starting from an N/P ratio of 3:1. Increasing the N/P ratio to 6:1 improved the transfection efficiency. However, the transfection efficiency decreased when the N/P ratios were further increased to 24:1.

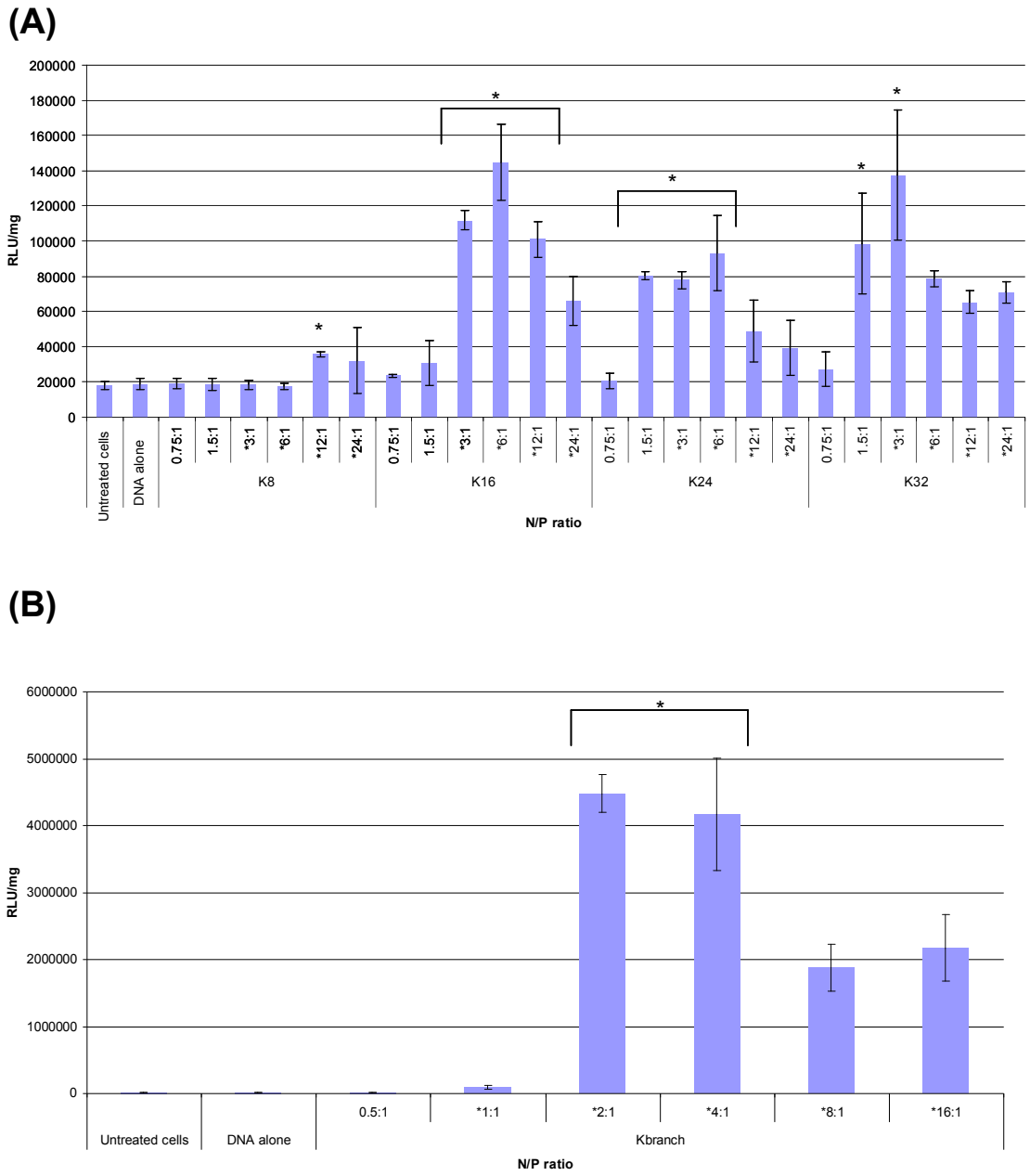

Figure 4.16 Plasmid transfection efficiency mediated by peptides/plasmid (pCI-Luc). 5×10^4 Neuro 2a cells were seeded 24 hours before transfection (in a 96 well plate). The complexes were made by mixing peptides with pCI-Luc in Optimem at different N/P ratios for 30 minutes. Following removal of full growth medium, complexes were overlaid onto the cells for 4 hours. After removing the transfection complexes, full growth medium was added to the cells. Luciferase

activity in the cells was analysed 24 hours post-transfection to estimate the transfection efficiencies of the complexes **(Section 2.2.3.3.1 and 2.2.5.1)**. **(A)** Plasmid transfection using K8, K16, K24 or K32/DNA complexes. Statistical analysis was performed using ANOVA followed by Tukey's test. A significant increase of the luciferase activity in the cells treated with the K8 DNA complexes at an N/P ratio of 12:1 compared to the untreated cells or cells treated with the K8 DNA complexes at all other N/P ratios was observed ($P < 0.05$). A significant increase of luciferase activity in the cells treated with the K16 DNA complexes at N/P ratios of 3:1 to 12:1 compared to the untreated cells or cells treated with the K16 DNA complexes at N/P ratios of 0.75:1, 1.5:1 and 24:1 was observed ($P < 0.05$). A significant increase of luciferase activity in the cells treated with the K24 DNA complexes at N/P ratios of 1.5:1 to 6:1 compared to the untreated cells or cells treated with the K24 DNA complexes at N/P ratios of 0.75:1, 12:1 and 24:1 was observed ($P < 0.05$). It was observed that a significant increase of the luciferase activity in the cells treated with the K32 DNA complexes at N/P ratios of 1.5:1 and 3:1 compared to the untreated cells or cells treated with the K32 DNA complexes at N/P ratios of 0.75:1, 12:1 and 24:1 ($P < 0.05$). **(B)** Plasmid transfection using Kbranch/DNA complexes. Statistical analysis was performed using ANOVA followed by Tukey's test and it showed that there was a significant increase of the luciferase activity in the cells treated with the Kbranch DNA complexes at N/P ratios of 2:1 and 4:1 compared to the untreated cells or cells treated with the Kbranch DNA complexes at N/P ratios of 0.5:1, 1:1, 8:1 and 16:1 ($P < 0.05$). The formulations of the complexes are expressed as N/P ratios.

The K24 DNA complexes transfected the cells adequately starting from a 1.5:1 N/P ratio. The transfection efficiency of these K24 DNA complexes remained similarly effective at N/P ratios of 3:1 and 6:1. Further increasing the N/P ratio of these complexes decreased the transfection efficiency.

Similar to the K24 DNA complexes, the K32 DNA complexes delivered DNA to the cells sufficiently starting from a 1.5:1 N/P ratio. The tranfection efficiency peaked at an N/P ratio of 3:1. Increasing the N/P ratio of this complex from 12:1 onwards decreased the transfection efficiency.

The Kbranch peptide DNA complexes mediated gene delivery starting from an N/P ratio of 2:1 **(Figure 4.16B)**. The best transfection performances of the complexes were at N/P ratios of 2:1 and 4:1. However, further increase of the Kbranch peptide to DNA decreased the transfection efficiency. It is noted that the transfection efficiency of these complexes is 28 fold higher than the most effective transfection complex of the linear lysine peptide DNA complexes (i.e the K16 DNA complexes at an N/P ratio of 6:1 and the K32 DNA complexes at an N/P ratio of 3:1).

Both B-PEI and L-PEI have a similar transfection pattern **(Figure 4.17)**. An increase of the N/P ratio from 2.5:1 gradually increased the transfection efficiency. Similar to Boussif and co-workers' finding, the transfection performance peaked at 10:1 (Boussif et al. 1995), but a further increase of the N/P ratio decreased the transfection performance. Compared to the B-PEI DNA complex at an N/P ratio of 10:1, the L-PEI DNA complex could mediate higher transfection efficiency by 5 fold at the same N/P ratio. Indeed, L-PEI is the most effective transfection reagent in this study; it could mediate transfection 5 fold higher than B-PEI and 130 fold higher than the Kbranch peptide.

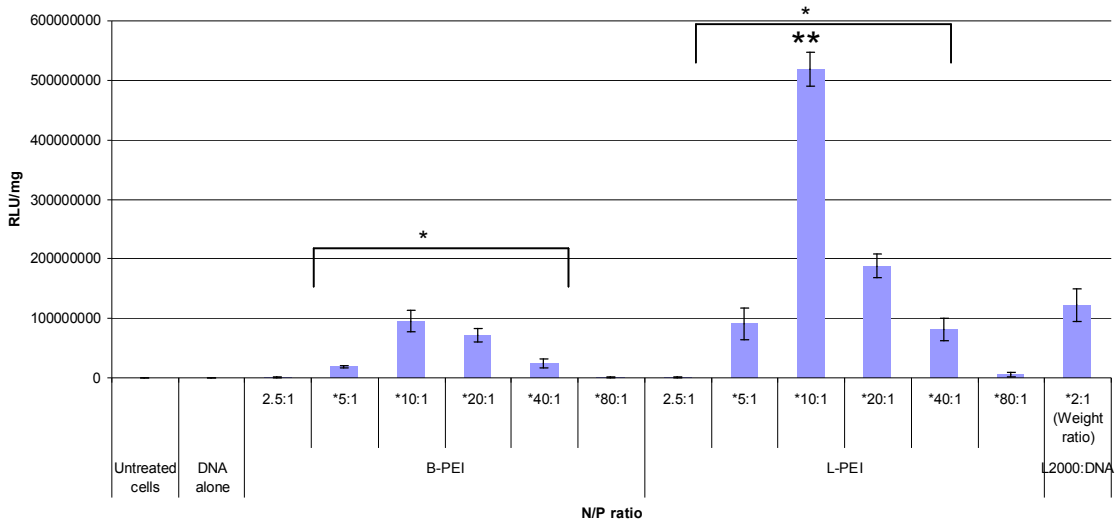

Figure 4.17 Plasmid transfection efficiency mediated by PEIs/plasmid (pCI-Luc). 5×10^4 Neuro 2a cells were seeded 24 hours before transfection (in a 96 plate). The complexes were made by mixing PEIs with pCI-Luc in Optimem at different N/P ratios for 30 minutes. Following removal of full growth medium, complexes were overlaid onto the cells for 4 hours. After removing the transfection complexes, full growth medium was added to the cells. Luciferase activity in the cells was analysed 24 hours post-transfection to estimate the transfection efficiencies of the complexes **(Section 2.2.3.3.1 and 2.2.5.1)**. Statistical analysis was performed using ANOVA followed by Tukey's test and it showed that there was a significant increase of the luciferase activity in the cells treated with the B-PEI DNA complexes at N/P ratios of 5:1 to 40:1 compared to the untreated cells or cells treated with the B-PEI DNA complexes at N/P ratios of 2.5:1 and 80:1 ($P < 0.05$). The cells treated with the B-PEI DNA complexes at N/P ratios of 10:1 and 20:1 were observed to have the highest luciferase activity compared to the cells treated with other B-PEI DNA complexes ($P < 0.05$). Similarly, a significant increase of the luciferase activity in the cells treated with the L-PEI DNA complexes at N/P ratios of 5:1 up to 40:1 compared to the untreated cells or cells treated with the L-PEI DNA complexes at N/P ratios of 2.5:1 and 80:1 was observed ($P < 0.05$). The cells treated with the L-PEI DNA complexes at an N/P ratio of 10:1 was observed to have the highest luciferase

activity compared to the cells treated with other L-PEI DNA complexes ($P < 0.01$). The formulations of the complexes are expressed as N/P ratios.

4.2.5 DNA complexes mediated cellular binding, uptake and cell death

To better understand the relationship between cellular uptake of the DNA complexes and transfection efficiency, Cy5 labelled DNA was used to form complexes with different reagents in Optimem and incubated with the Neuro 2a cells. Following the transfection, flow cytometry was performed to detect the Cy5 signal on the cells. Cy5 signal positive cells indicated cellular binding and uptake of the complexes. To also study the effect of the complexes on cell viability, propidium iodide (PI) was used to stain for dead cells.

As shown in **Figure 4.18**, exposure to naked DNA mediated poor transfection efficiency; only 3% of the cells bound to or took up the plasmid. The K8 DNA complexes were also ineffective; only 5% of the cells were Cy5 positive. Compared to the K8 DNA complexes, it seems that an increase of the lysine length improved cellular binding and/or uptake of the complexes; cellular binding and/or uptake of the K16, K24 or K32 DNA complexes were 35%, 62% and 55% respectively. On the other hand, the L-PEI, B-PEI or the Kbranch peptide DNA complexes were better in cellular binding and/or uptake; the L-PEI DNA complexes induced 64% whereas the Kbranch peptide or B-PEI DNA complexes mediated 72% of complex binding or uptake by the cells.

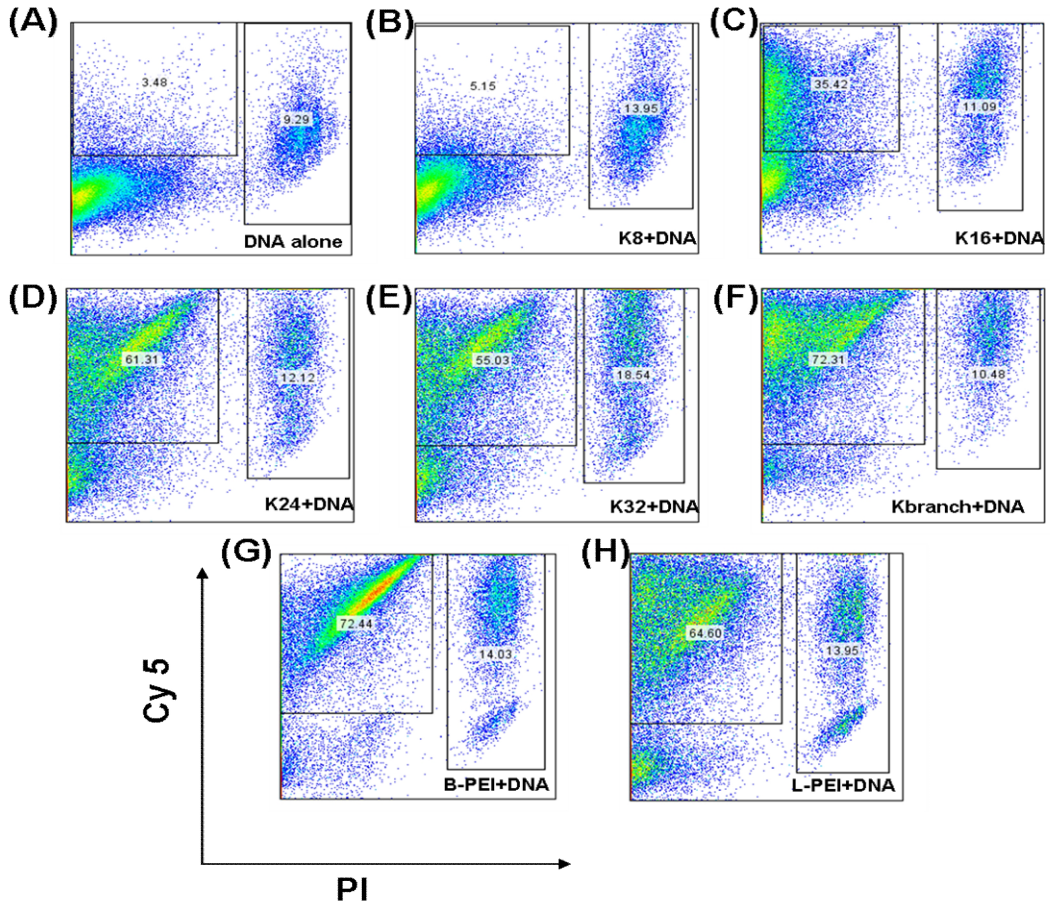

Figure 4.18 Cellular binding and/or uptake efficiencies of peptide or PEI plasmid (pCI-Luc) complexes. Briefly, Neuro 2a cells were seeded 24 hours before transfection. The complexes were made by mixing peptides or PEIs with Cy 5 labelled pCI-Luc in Optimem for 30 minutes **(Section 2.2.3.3.1 and 2.2.7.2)**. Following removal of full growth medium, complexes were overlaid onto the cells for 4 hours. The cells were harvested for analysis after transfection. Propidium iodide (PI) was used to estimate the cell viability following transfection **(Section 2.2.7.3)**. **(A)** Cells exposed to DNA only, **(B)** cells exposed to the K8/DNA complex at a 3:1 N/P ratio, **(C)** cells exposed to the K16/DNA complex at a 3:1 N/P ratio, **(D)** cells exposed to the K24/DNA complex at a 3:1 N/P ratio, **(E)** cells exposed to the K32/DNA complex at a 3:1 N/P ratio, **(F)** cells exposed to the Kbranch/DNA complex at a 4:1 N/P ratio, **(G)** cells exposed to the B-PEI/DNA complex at a 10:1 N/P ratio, **(G)** cells exposed to the L-PEI/DNA complex at a 10:1 N/P ratio.

In terms of cell viability, it is clear that naked plasmid DNA or the DNA complexes were toxic to the cells; around 10% to 18% cell death was observed following the exposure of the naked DNA or complexes.

4.2.6 Internalisation of the DNA complexes

From flow cytometry analysis, it is clear that some of the DNA complexes can mediate cellular binding and/or uptake. To confirm whether the complexes can be taken up following transfection, Neuro 2a cells were transfected with Cy5 labelled DNA for 4 hours in serum free medium. The cells were then harvested and stained with phalloidin for the cell membrane and DAPI for the nucleus.

The results showed that plasmids were inside the cells, mainly clustered in the cytoplasm **(Figure 4.19).** This indicated that the complexes were taken up by the cells within 4 hours.

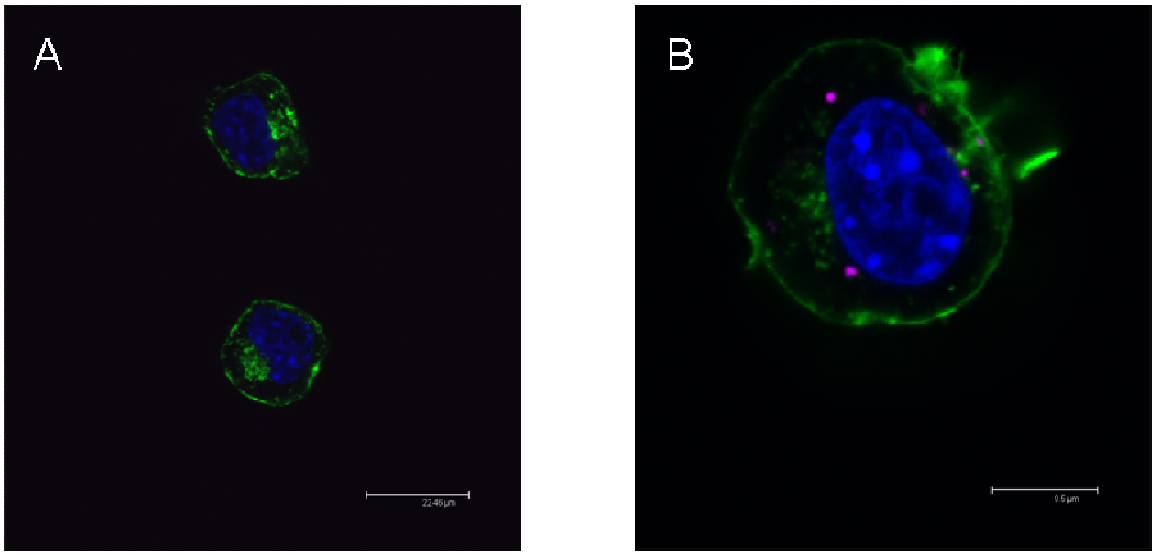

Figure 4.19 Localisation of plasmid following transfection. Briefly, Neuro 2a cells were seeded 24 hours before transfection. The complexes were made by mixing peptides or PEIs with Cy 5 labelled pCI-Luc (Purple) for 30 minutes. Following removal of full growth medium, complexes were overlaid onto the cells for 4 hours **(Section 2.2.3.3.1 and 2.2.7.2)**. The cells were then washed and stained with phalloidin for the F-actin on the cell membrane (Green) and DAPI for the nucleus (Blue) **(Section 2.2.8.2 and 2.2.8.3)**. **(A)** Untreated cells (the untreated cells showed the same result as the cells exposed to naked DNA only or the K8 DNA complexes), **(B)** cells exposed to the Kbranch DNA complexes (the cells incubated with the K16 DNA, K24 DNA, K32 DNA, B-PEI DNA and L-PEI DNA complexes showed a similar results as the cells exposed to the Kbranch DNA complexes).

4.3 Discussion

4.3.1 The hypothesis of a successful cationic polymer based DNA delivery system and the aims of the study

To be successful in gene delivery, a vector system should be able to form a stable DNA complex to (1) encapsulate and protect the DNA from degradation in the extracellular space, (2) mediate cellular binding and uptake, (3) allow DNA dissociating from the carrier for gene expression. Therefore, an ideal DNA delivery system should contain reagent that can bind and condense DNA stably, form a complex with a positive surface charge to facilitate complex-cell membrane interaction and form a nano-sized complex to facilitate endocytosis for effective cellular uptake. Then, the reagent should dissociate from DNA within the cells so that the DNA can traffick to the nucleus for gene expression (Chesnoy et al. 2000; Zhdanov et al. 2002; Niculescu-Duvaz et al. 2003).

In this study, the biophysical and transfection properties of the DNA complexes formed by plasmid DNA and cationic polymers with different sizes and physical structures and chemical composition were investigated. These polymers included the linear lysine peptides (K8, K16, K24 and K32), a branched lysine peptide (the Kbranch peptide), linear and branched PEI. Understanding the relationship between the biophysical and transfection characteristics of the DNA complexes would be useful for the development of other successful nucleic acid delivery systems such as siRNA delivery systems.

4.3.2 The N/P ratio of the complexes, and the size, physical structure and chemical composition of the polymers play a role in complex stability

From both the gel retardation and PicoGreen fluorescence quenching assays, it was found that all the lysine peptides and PEIs can condense and package DNA stably at certain N/P ratios. In general, an increase of the N/P ratios, to a certain point, enhances binding and encapsulation of DNA which could be important for DNA delivery. Having reached the N/P ratios that can completely encapsulate DNA, a further increase of the N/P ratios of the complexes did not improve the DNA packaging. This suggests that a further addition of the polymers to DNA upon the N/P ratios which led to complete DNA condensation would result in free polymers present alongside with the complexes.

In the heparin dissociation assay, it was interesting to find that the molecular sizes of the complex reagents could play a part in term of DNA packaging. Complex reagents with a larger molecular size had a higher affinity to DNA when the N/P ratio of the complexes was the same. For example, K32 (4 kDa) binds more strongly to DNA than K8 (1 kDa) does at the same N/P ratio **(Table 4.5)**. The reason for this observation could be that the larger peptide can improve encapsulation of DNA and therefore it is harder to dissociate the DNA from the complex.

DNA complexes	N/P ratio	Heparin concentration necessary to initiate dissociation (U/ml)	Heparin concentration necessary to allow complete dissociation (U/ml)
K8	3:1	Trace amount	0.167
K32	3:1	0.167	1.33

Table 4.5 A summary of heparin induced dissociation of the K8 DNA and K32 DNA complexes at an N/P ratio of 3:1.

Apart from the size of the reagents, the physical structure and/or chemical composition of the reagents also plays a role in DNA binding. Similar to the finding by Dunlap and co-workers (1997), showing that B-PEI condensed DNA more effectively than L-PEI, it is found that B-PEI (25 kDa) binds 4 times more effectivey to DNA than L-PEI (22 kDa) does at the same N/P ratio **(Table 4.6)**. Intriguingly, the size of B-PEI (25 kDa) is only slightly larger than the size of L-PEI (22kDa). Therefore, the 4-fold difference in binding force between the complexes is probably due to the structural difference (i.e linear and branched) and/or the chemical composition between the PEIs. The branched characteristic of B-PEI may enhance better DNA encapsulation compared to the linear characteristic of the L-PEI. Also, B-PEI consists of the primary, secondary and tertiary amines whereas L-PEI only contains secondary amines for DNA binding. Since the primary amine group has a stronger affinity to DNA than the secondary amine group, this may further enhance the binding between B-PEI and DNA (Brissault et al. 2006).

DNA complexes	N/P ratio	Heparin concentration required to allow complete dissociation (U/ml)
B-PEI	10:1	21.3
	20:1	21.3
	40:1	21.3
L-PEI	10:1	5.3
	20:1	5.3
	40:1	5.3

Table 4.6 A summary of heparin induced dissociation of the B-PEI DNA and L-PEI DNA complexes.

4.3.3 The N/P ratio is inversely related to the size and the zeta potential of the complexes

The average hydrodynamic sizes of the complexes generally were inversely related to the N/P ratios. For example, increasing the N/P ratio of the K24 DNA complexes from 0.75:1 to 6:1 decreased the size from 79 nm to 53 nm. By contrast, the zeta potential of the complexes was directly related to the N/P ratios. For instance, increasing the N/P ratio of the K24 DNA complexes increased the zeta potential from -10 mV to 47 mV. All the reagents used in this study formed positively charged DNA complexes with sizes between 50 nm and 150 nm, therefore it was highly likely that all these complexes could internalise in the cells through either clathrin- or caveolae-mediated endocytosis and possibly mediate gene delivery (Bishop 1997). Among all the complexes, the Kbranch peptide DNA complex was more likely to bind to the cell because this polymer consists of an integrin receptor targeting region while other polymers used in this study do not contain a receptor targeting region (Hart et al. 1998; Mustapa et al. 2007).

4.3.4 The transfection efficiency of the complexes

From the transfection studies, it was found that the transfection efficiency increased with the charge ratio up to an optimal point. A further increase of the charge ratio beyond this actually decreased the transfection efficiency. This observation could be explained by the fact that an initial increase of the charge ratios of the DNA complexes improved the DNA condensation which would be beneficial for gene transfer. However, having reached the optimal charge ratios of the complexes for the DNA condensation, a further increase of the polymers to the complexes would not enhance the DNA packaging. As a result, the excess amounts of polymers would appear as free polymers in the buffer. These free cationic polymers may then bind to the proteoglycans on the cell membrane, and this may decrease the amounts of the available proteoglycans for the binding of the positive charged complexes. As a result, transfection efficiency decreases.

Among the linear lysine based peptides, the K16 DNA, K24 DNA and K32 DNA complexes mediated similar transfection efficiency, which was higher than the K8 DNA complexes. One of the possible reasons for this could be that the K8 peptides were not able to package DNA as well as the K16, K24 and K32 peptides. From the PicoGreen fluorescence quenching assay **(Figure 4.5)**, the K8 peptides could only minimise the DNA signal down to 30% whereas the K16, K24 and K32 peptides could minimise the DNA signal down to 20%. Being less effective in DNA packaging may result in poor cellular uptake of the K8 DNA complexes due to poor complex stability.

Compared to B-PEI, L-PEI was a better transfection reagent, found to mediate 5-fold higher transfection than B-PEI. Since B-PEI binds 4-fold stronger to DNA than L-PEI does **(Table 4.6)**, it could be harder for the B-PEI DNA complexes to dissociate from DNA within the cells for transcription than the L-PEI DNA complexes.

Overall, the transfection efficiency of the reagents is as follows:

L-PEI > B-PEI >> Kbranch > K16, K24, K32 > K8

The finding that the PEI DNA complexes transfected better than the lysine based peptide DNA complexes could be due to the fact that PEIs perform better in endosomal escape. During transfection, PEI DNA complexes are taken up by the cells through endocytosis (Ogris et al. 1998). Inside the cell, H^+ are pumped into the endosome by proton translocating ATPase followed by passively diffused Cl^-. The high buffer capacity of the PEI causes accumulation of large amount of H^+, and this in turn leads to accumulation of Cl^-. Thus the osmotic potential inside the endosome decreases and results in the influx of a large amount of water. This causes the endosome osmotic swelling and subsequent disruption. The PEI DNA complexes then escape from the endosome and traffick to the nucleus for gene expression (Kichler et al. 2001). However, the lysine based peptide DNA complexes are not able to mediate effective endosomal escape, and most of the complexes end up degraded by lysosome (Erbacher et al. 1996).

The Kbranch peptide was more effective in delivering DNA into the cells than the lysine tails as measured by the luciferase reporter gene assay. It was around 28-fold higher than

the most effective transfection complexes of the linear lysine peptide DNA complexes such as the K16 or K32 DNA complexes. This result is expected as the Kbranch peptide contains an integrin targeting peptide which facilitates receptor-mediated endocytosis, therefore this improves cellular uptake of the complexes. However, when compared to the B-PEI, the transfection efficiency of the Kbranch peptide was 130-fold lower. This observation is likely due to the fact that the Kbranch DNA complexes were less efficient in mediating endosomal escape than the B-PEI DNA complexes.

4.3.5 The relationship between the transfection efficiency and cellular binding and uptake of the complexes

From results of the cellular uptake of DNA complexes formed from the linear lysine peptides, it was found that all of the complexes could mediate cellular binding and uptake (35%-60%) except the K8 DNA complexes, which mediated a very low percentage of cellular binding and uptake of the complex (5%). This finding was consistent with the low transfection efficiency of the K8 DNA complexes among the linear lysine based peptide DNA complexes.

It is expected that the Kbranch DNA complexes mediated a relatively effective cellular uptake and binding (72%) since the Kbranch peptide contains an integrin receptor targeting region which can enhance the complex taking up process by the cells through receptor-mediated endocytosis (Hart et al. 1995).

Despite the B-PEI DNA complexes being more effectively bound and taken up by the cells than the L-PEI DNA complexes, the L-PEI DNA complexes were indeed 5 times more efficient in transfecting cells than the B-PEI DNA complexes. This indicates that the L-PEI DNA complexes could be more effective in endosomal escape and/or allowing DNA to traffick to the nucleus for gene expression.

Overall, the cellular binding and uptake efficiencies of the complexes are as follows:

Kbranch, B-PEI > L-PEI > K24 > K32 > K16 >> K8

Although the Kbranch DNA complexes were not as effective as the B-PEI DNA complexes in transfection, their abilities to mediate cellular binding and uptake were similar; 74% of the transfected cells bound to and took up these complexes. It is not surprising to note that the Kbranch DNA complexes were able to mediate cellular binding and uptake effectively because of the targeting domain on the KBranch peptide. However, it is interesting that the B-PEI DNA complexes, which do not have a targeting ligand, can mediate cellular binding and uptake as effective as the Kbranch DNA complexes.

The explanation could be that the B-PEI DNA complexes were more resistant to dissociation than the Kbranch DNA complexes **(Table 4.7)**, therefore the B-PEI DNA complexes were more stable and less susceptible to degradation inside the cells. On the other hand, the Kbranch DNA complexes could have a higher percentage of cellular binding and uptake than the B-PEI DNA complexes initially, but once the Kbranch DNA complexes were taken up, some of them were degraded because these complexes were less

stable. This observation is similar to Ramsay and Gumbleton's (2002) observation that cationic polymer DNA complexes which were more resistant to dissociation could yield higher cellular uptake.

DNA complexes	N/P ratio	Heparin concentration required to initiate dissociation (U/ml)	Heparin concentration required to allow complete dissociation (U/ml)
Kbranch	4:1	0.08	0.33
B-PEI	10:1	0.167	21.3

Table 4.7 A summary of heparin induced dissociation of the Kbranch DNA and B-PEI DNA complexes.

The percentage of cells binding to and taking up the L-PEI DNA complexes (64.6%) was similar to that of the K24 DNA complexes (61.3%); however, the L-PEI DNA complexes were 130-fold better in transfection than the K24 DNA complexes. This observation was probably due to the fact that the K24 DNA complexes were less effective in endosomal escape and/or allowing DNA to traffick to the nucleus for gene expression compared to the L-PEI DNA complexes (Read et al. 2006).

The results of the confocal microscopy confirmed that the complexes that were shown to mediate cellular binding and uptake from the flow cytometry experiment were able to internalise within the cells following transfection.

As expected, no DNA was detected in the nucleus. This is because the nuclear membrane blocks the DNA from transporting to the nucleus. The DNA could enter the nucleus during cell division when the nuclear envelope breaks down (Brunner et al. 2000).

4.3.6 The relationship between the biophysical properties and the transfection efficiency of the complexes

The transfection efficiency and the biophysical properties of the complexes were summarised as **Table 4.8.** The table showed the N/P ratios of the each complex which yielded comparative high transfection efficiency in the respective complex.

Best transfection reagents	N/P ratio	Condensation of DNA	Amount of heparin to initiate complex dissociation (U/ml)	Heparin concentration to allow complete dissociation (U/ml)	Average hydrodynamic size (nm)	Zeta potential (mV)
K16	**3:1**	Complete	0.083	0.67	54	+39
	6:1	Complete	0.33	0.67	47	+42
	12:1	Complete	0.67	1.33	N/A	N/A
K24	**1.5:1**	Complete	Very closed to 0	1.33	68	+29
	3:1	Complete	0.083	1.33	64	+39
	6:1	Complete	0.33	1.33	54	+47
K32	**1.5:1**	Complete	Very closed to 0	1.33	87	+35
	3:1	Complete	0.167	1.33	72	+42
	6:1	Complete	0.33	1.33	65	+53
Kbranch	**2:1**	Complete	Very closed to 0	0.33	87	+37
	4:1	Complete	0.083	0.33	104	+42
B-PEI	**10:1**	Complete	0.167	21.3	83	+49
	20:1	Complete	0.33	21.3	92	+52
L-PEI	**10:1**	Complete	0.167	5.3	142	+37
	20:1	Complete	0.33	5.3	79	+48

Table 4.8 A summary of the biophysical properties of the effective transfection complexes.

In general, these complexes had a positive zeta potential and average hydrodynamic size 50 nm – 150 nm. Also, DNA was completely condensed inside the complexes. These complexes began to dissociate from DNA under heparin concentrations of 0 to 0.33U/ml,

and became fully dissociated under heparin concentrations of 0.33U/ml onwards. Therefore, these biophysical characteristics could be important parameters to investigate when designing other kinds of DNA delivery system.

4.4 Conclusion

In conclusion, the biophysical properties such as the binding and dissociation properties of the complex reagents and DNA, the size and the surface charge of the complexes are important parameters, which are influenced by the size and structure of the cationic polymer used, governing the transfection efficiency. Therefore, these parameters are important to consider for the development of siRNA delivery systems.

Chapter 5

A study on the biophysical and transfection properties of different cationic formulations of siRNA complexes

5.1 Introduction

The criteria for delivering DNA to cells are similar to those of delivering siRNA. Both DNA and siRNA are negatively charged and therefore need a vector system to transport them through the hydrophobic cell membrane into a cell (Grayson et al. 2006). As with DNA delivery, a vector system for siRNA delivery is expected to allow the formation of stable positively charged particles with a size larger than 50 nm for endocytosis (Gao et al. 2005). Once within the cells, the siRNA needs to dissociate from the vector and traffick to the P-body in the cytoplasm for gene silencing (Jagannath & Wood 2009). In Chapter Four, the important criteria of a DNA complex for effective gene delivery were identified and discussed. These criteria require consideration for the establishment of an siRNA delivery system.

Despite plasmid DNA and siRNA being negatively charged double stranded nucleic acids, the structural and compositional differences between plasmid DNA and siRNA could result in different complex formation properties. siRNA is considerably smaller than plasmid DNA; siRNA is usually 21 base pairs whereas plasmid DNA can range from 1 kb to greater than 10 kb. As a ribonucleic acid, the strand pitch and diameter and the geometrical form of siRNA are different to plasmid DNA (Nelson & Cox 2004). Also, siRNA is more susceptible to hydrolysis by nucleases than plasmid DNA (Banan & Puri 2004). Therefore, these size and compositional differences between siRNA and DNA could lead to differences in nucleic acid packaging and thus complex formation.

In this chapter, the lysine based peptides and PEIs were used to form complexes with the siRNA. The biophysical and transfection properties were then studied. The results

from this study can be compared to the results in Chapter Four, the DNA complex study, in order to generate useful information for the establishment of an effective siRNA delivery system.

5.1.2 Aims

- To measure the biophysical properties of different siRNA complex formulations.
- To elucidate and evaluate the relationship between the biophysical properties and transfection efficiency.
- To clarify the criteria of a successful siRNA delivery system.

5.2 Results

5.2.1 Binding properties of lysine based peptides or PEIs to siRNA

The binding capacity of the vector system to the siRNA represents an important criterion for successful siRNA delivery. PEIs and the lysine based peptides are both cationic and can therefore bind to anionic siRNA. To examine and compare the binding capacity of the lysine based peptides or PEIs to siRNA, gel retardation and PicoGreen quenching assays were performed.

5.2.1.1 Gel retardation assay on lysine based peptides or PEIs

To study the binding characteristics of the cationic polymers and siRNA, the polymers were mixed in distilled water with siRNA at different N/P ratios and incubated for 30 minutes at room temperature. The complexes were then resolved using 4% agarose gel electrophoresis. The gel was visualised under UV.

As shown in **Figure 5.1A,** the smear pattern in the gel of the K8 and K16 siRNA complexes indicate that these lysine peptides could bind to and form complexes with siRNA; however, most of the complexes were found to be negatively charged and so migrated towards the positive electrode. The K8 and K16 peptides could not completely retard siRNA migration even up to an N/P ratio of 128:1, suggesting that siRNA cannot be packaged by these peptides. From **Figure 5.1B**, the smear pattern shows that the K24 and K32 peptides bound to siRNA. With the N/P ratio below 16:1, these complexes migrated towards the positive electrode. Intriguingly, with N/P ratios higher than 16:1,

the complexes migrated in the opposite direction, towards the negative electrode. Overall, these results showed that the interactions between siRNA and the K24 and K32 peptides were similar, which were different to the interaction between siRNA and the K8 and K16 peptides.

The Kbranch peptide was able to bind to siRNA and completely retard the siRNA from migration, starting from a N/P ratio of 60:1 **(Figure 5.1C)**. siRNA packaging was achieved using B-PEI at an N/P ratio of 5:1 and L-PEI at an N/P ratio of 10:1 **(Figure 5.1D).**

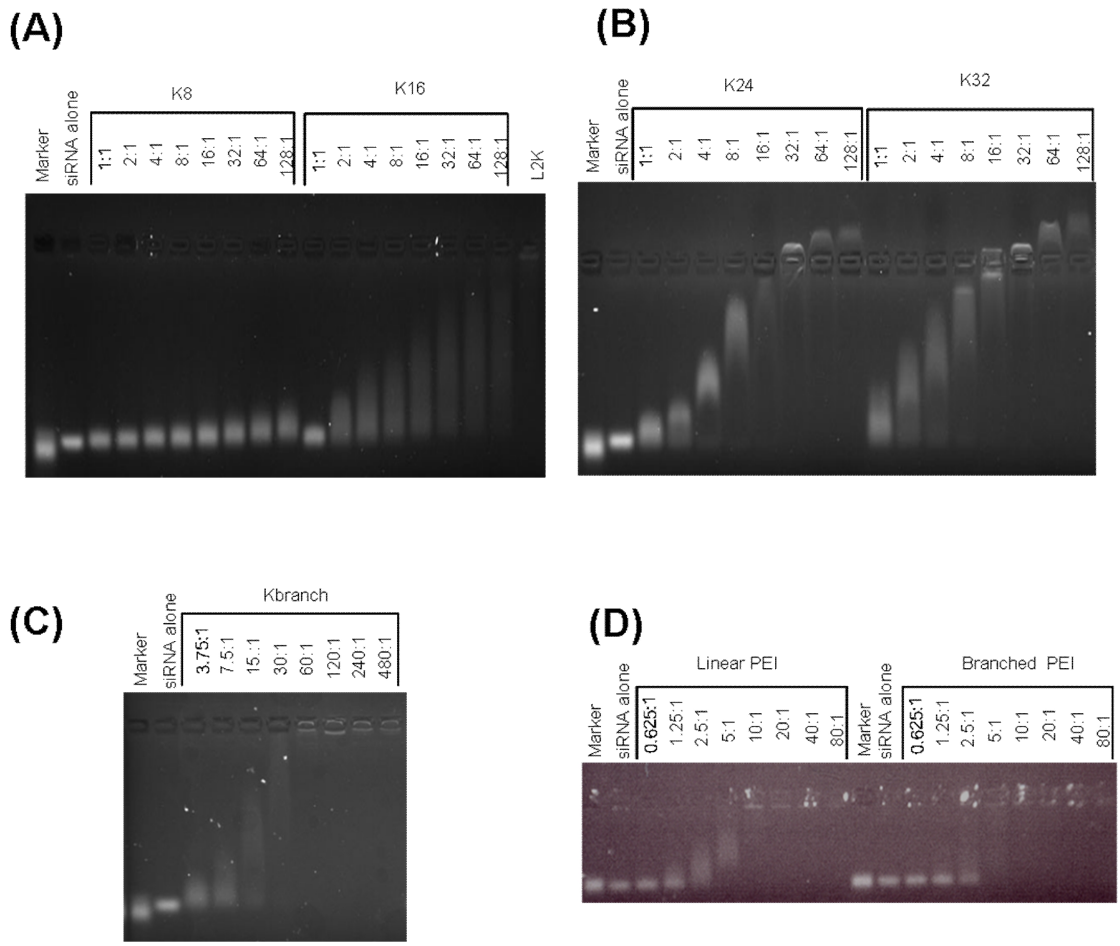

Figure 5.1 The binding properties of peptides or PEIs with siRNA. Peptides or PEIs were mixed with siRNA in distilled water at different N/P ratios for 30 minutes. The complexes were then run on a 4% agarose gel. The gel was visualised using UV **(Section 2.2.6.1)**. **(A)** the K8 siRNA and K16 siRNA complexes, **(B)** the K24 siRNA and K32 siRNA complexes, **(C)** the Kbranch siRNA complexes, **(D)** the B-PEI siRNA and L-PEI siRNA complexes. The formulations of the complexes are expressed as an N/P ratio. K8 and K16 were not able to retard siRNA from migrating through the gel. K24 and K32 were able to retard the siRNA migration. With the N/P ratio above 16:1, these K24 siRNA and K32 siRNA complexes migrated towards the positive electrode. Kbranch, B-PEI and L-PEI completely retarded the siRNA migration at N/P ratios of 60:1, 5:1 and 10:1 respectively.

5.2.1.2 PicoGreen fluorescence quenching assay on lysine based peptides or PEIs

To perform the PicoGreen fluorescence quenching assay, complexes were prepared by mixing the complex reagents with PicoGreen labelled siRNA in TE buffer at different N/P ratios. Following incubation at room temperature for 30 minutes, the complexes were assayed for remaining PicoGreen signals using FLUOstar Optima. As the PicoGreen signals are directly proportional to the free siRNA, lower PicoGreen signals detected suggest better packaging of siRNA within the complexes.

In general, increasing the lysine based peptide to siRNA charge ratios decreased the fluorescence level to a minimum beyond which a further increase in peptide had no effect **(Figure 5.2)**. Indeed, all the linear lysine peptides bound to siRNA and minimised the fluorescence signal starting from an N/P ratio of 2:1. The Kbranch peptide bound to siRNA and the minimal fluorescence signal was detected at a 3:1 N/P ratio and above **(Figure 5.3A)**. PEIs bound to siRNA and minimised the fluorescence signal starting from an N/P ratio of 5:1 **(Figure 5.3B)**.

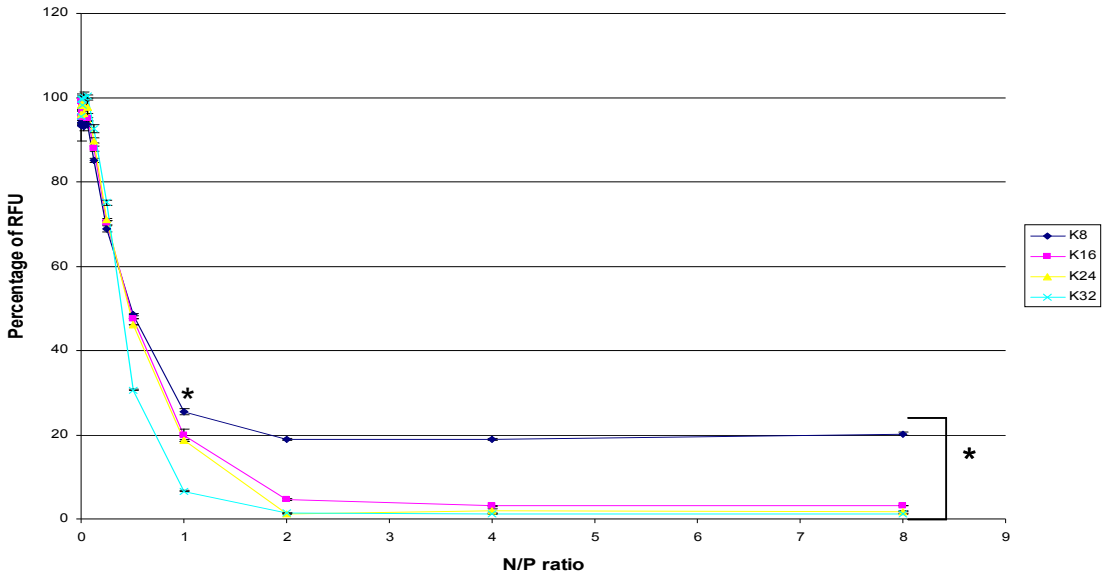

Figure 5.2 The binding of the linear lysine peptides to siRNA. The linear lysine peptides were mixed with PicoGreen labelled siRNA TE buffer at different N/P ratios for 30 minutes. The fluorescence intensity of the complexes was then measured using FLUOstar Optima. The formulations of the complexes are expressed as an N/P ratio. The PicoGreen signals from the complexes were normalised with the naked DNA control to yield the percentage of relative fluorescence unit (RFU) **(Section 2.2.6.2)**. Statistical analysis was performed using ANOVA followed by Tukey's test and it showed a significant decrease of the percentage of RFU starting from a 2:1 N/P ratio of all the complexes ($P < 0.05$). The percentage of RFU of the K8 siRNA complexes from an N/P ratio 2:1 and onwards is significantly different to the other siRNA complexes with the same N/P ratio in the figure ($P < 0.05$).

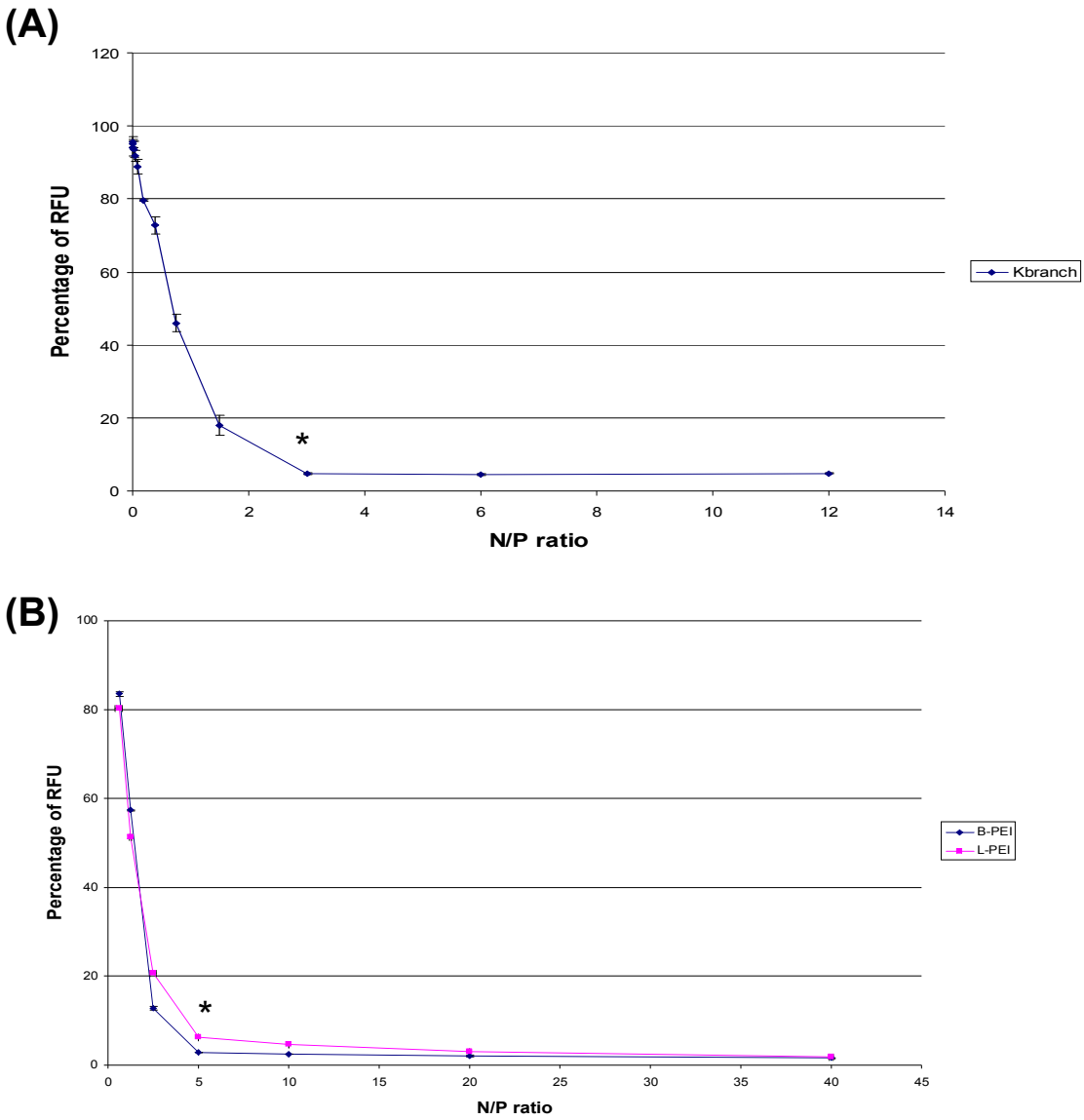

Figure 5.3 The binding of the Kbranch peptide or PEIs to siRNA. The Kbranch peptide or PEIs were mixed with PicoGreen labelled siRNA TE buffer at different N/P ratios for 30 minutes. The fluorescence intensity of the complexes was then measured using FLUOstar Optima. The PicoGreen signals from the complexes were normalised with the naked DNA control to yield the percentage of relative fluorescence unit (RFU) **(Section 2.2.6.2)**. **(A)** the Kbranch siRNA complexes. Statistical analysis was performed using ANOVA followed by Tukey's test and it showed a significant decrease of the RFU starting from a 3:1 N/P ratio of all the Kbranch siRNA complexes ($P < 0.05$). **(B)** the B-PEI or L-PEI siRNA complexes. Statistical analysis was performed using ANOVA followed by Tukey's test and it showed a significant

decrease of the percentage of RFU starting from a 5:1 N/P ratio of the PEI DNA complexes ($P < 0.05$). The formulations of the complexes are expressed as an N/P ratio.

The siRNA packaging abilities of the polymers, estimated from the gel retardation and PicoGreen fluorescence quenching assays, are summarised in **Table 5.1.** Overall, these results suggested that all the complex reagents can bind to siRNA, but only the Kbranch peptide, L-PEI and B-PEI can package siRNA into a complex.

	The N/P ratio of the polymer necessary to mediate siRNA packaging	
	Gel retardation assay	**PicoGreen fluorescence quenching assay**
K8	Not applicable	2:1
K16	Not applicable	2:1
K24	Not applicable	2:1
K32	Not applicable	2:1
KBranch	60:1	3:1
B-PEI	5:1	5:1
L-PEI	5:1	5:1

Table 5.1 The siRNA packaging abilities of the complex reagents estimated by different assays.

5.2.2 Dissociation properties of the lysine based peptides or PEIs to siRNA

To study the stability of the siRNA complexes, a range of different concentrations of heparin sulphate were added to the complexes. The addition of different amounts of heparin to each complex allows an estimation of the dissociation behaviours of the complexes.

5.2.2.1 Heparin induced complex dissociation assay

To carry out the heparin induced complex dissociation assay, complexes were made using the complex reagents and PicoGreen labelled siRNA as described in the PicoGreen fluorescence quenching assay **(Section 2.2.6.3).** Following the incubation of the complexes, different concentrations of heparin were added to the complexes. The PicoGreen signals from the complexes were then measured using FLUOstar Optima. An increase of the PicoGreen signals indicates siRNA dissociation from the complexes.

5.2.2.1.1 Dissociation of the linear lysine peptide siRNA complexes

Increased N/P ratios enhanced the binding between the linear lysine based peptides and siRNA **(Figure 5.4-5.5)**. Compared to other linear lysine peptide siRNA complexes, the K8 siRNA complexes dissociated readily when exposed to heparin. As shown in **Figure 5.4A**, all four K8 siRNA complexes formulated at N/P ratios of 1:1, 2:1, 4:1 and 8:1 dissociated after exposure to trace amounts of heparin. The K8 siRNA complexes with

N/P ratios of 1:1 and 2:1 became fully dissociated at a heparin concentration of 0.67 U/ml whereas the K8 siRNA complexes with an N/P ratio of 4:1 fully dissociated at a heparin concentration of 1.33 U/ml. Only around 60% of the K8 siRNA complexes with an N/P ratio of 8:1 dissociated at a heparin concentration of 1.33 U/ml.

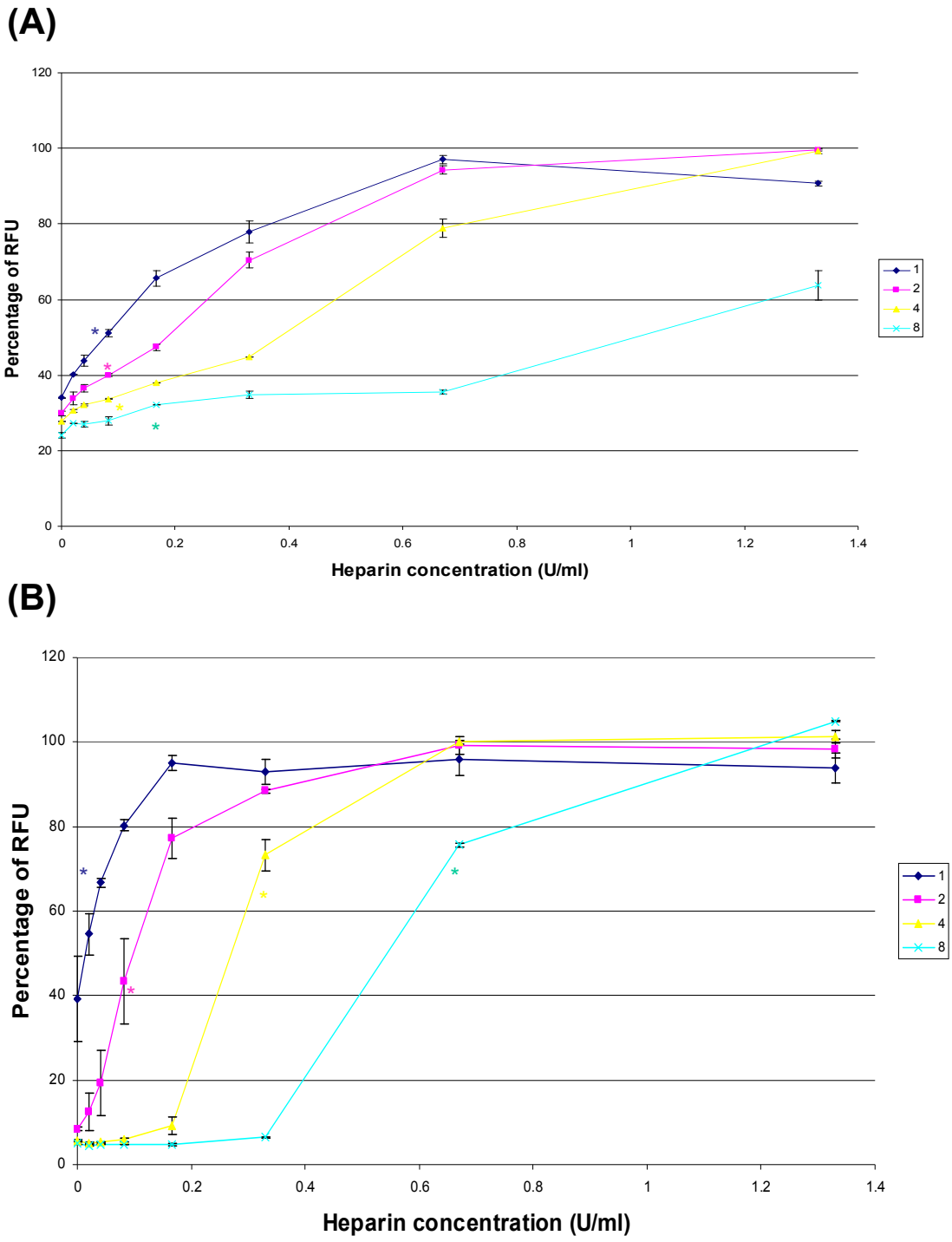

Figure 5.4 The dissociation properties of K8 or K16 siRNA complexes. K8 or K16 were mixed with PicoGreen labelled siRNA in TE buffer at different N/P ratios for 30 minutes. Different concentrations of heparin were added to the complexes and the fluorescence intensity of the complexes was measured using FLUOstar Optima. The PicoGreen signals from the complexes were normalised with the naked DNA control to yield the percentage of relative

fluorescence unit (RFU) **(Section 2.2.6.3)**. **(A)** the K8 siRNA complexes, **(B)** the K16 siRNA complexes. Statistical analysis was performed using ANOVA followed by Tukey's test and it showed a significant increase of the percentage of RFU of the complexes treated with the concentration of heparin marked with * (each * has the same colour as the curve of the N/P ratio of the complexes it corresponds to). In addition, complexes treated with higher heparin concentrations displayed a significant increase of the percentage of RFU compared to that of the untreated complexes ($P < 0.05$). The formulations of the complexes are expressed as an N/P ratio.

The K16 siRNA complexes with N/P ratios of 1:1 and 2:1 dissociated readily in trace amounts of heparin and became fully dissociated at 0.167 and 0.67 U/ml of heparin respectively **(Figure 5.4B)**. With an N/P ratio of 4:1, the K16 siRNA complexes dissociated starting from 0.08 and 0.167 U/ml of heparin and became fully dissociated at 0.67 U/ml of heparin. The K16 siRNA complexes with an N/P ratio of 8:1 started to dissociate at 0.33 U/ml of heparin and were fully dissociated at 1.33 U/ml of heparin.

As shown in **Figure 5.5C**, the K24 siRNA complexes with N/P ratios of 1:1 and 2:1 dissociated readily and became fully dissociated at 0.33 and 0.67 U/ml respectively. The 4:1 N/P ratio K24 siRNA complexes started to dissociate at 0.167 U/ml of heparin and became fully dissociated at 0.67 U/ml of heparin. With an N/P ratio of 8:1, the K24 siRNA complexes dissociated starting from 0.67 U/ml of heparin and were fully dissociated at 1.33 U/ml of heparin.

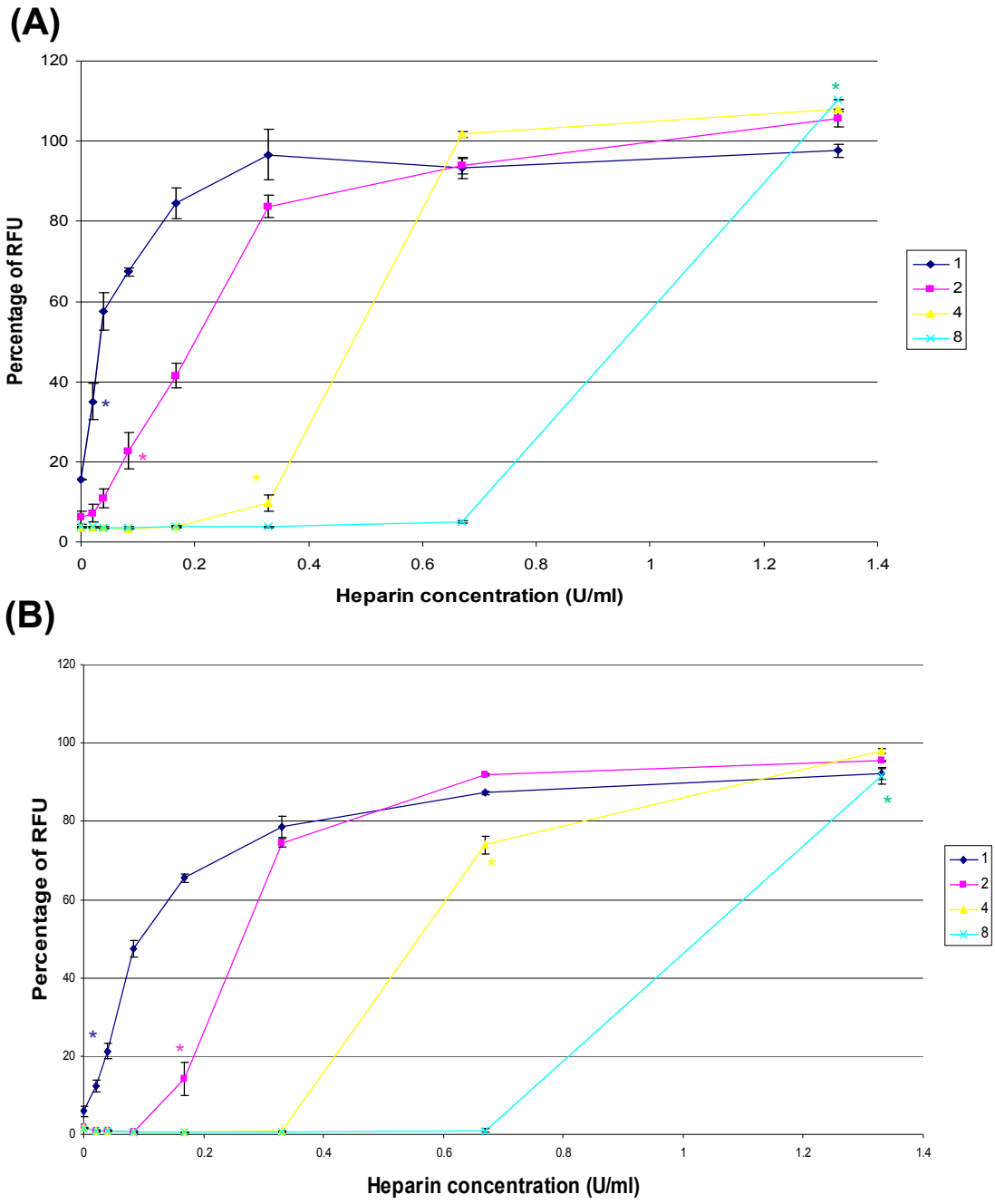

Figure 5.5 The dissociation properties of K24 or K32 siRNA complexes. K24 or K32 were mixed with PicoGreen labelled siRNA in TE buffer at different N/P ratios for 30 minutes. Different concentrations of heparin were added to the complexes and the fluorescence intensity of the complexes was measured using FLUOstar Optima. The PicoGreen signals from the complexes were normalised with the naked DNA control to yield the percentage of relative fluorescence unit (RFU) **(Section 2.2.6.3)**. **(A)** the K24 siRNA complexes, **(B)** the K32 siRNA complexes. Statistical analysis was performed using ANOVA followed by Tukey's test and it

showed a significant increase of the percentage of RFU of the complexes treated with the concentration of heparin marked with * (each * has the same colour as the curve of the N/P ratio of the complexes it corresponds to). In addition, complexes treated with higher heparin concentrations displayed a significant increase of the percentage of RFU compared to that of the untreated complexes ($P < 0.05$). The formulations of the complexes are expressed as N/P an ratio.

Similar to other linear lysine peptide siRNA complexes, the K32 siRNA complexes with an N/P ratio of 1:1 dissociated readily when exposed to trace amounts of heparin **(Figure 5.5D)**. These complexes became fully dissociated at a heparin concentration of 0.67 U/ml. For the K32 siRNA complexes with N/P ratios of 2:1 and 4:1, they started to dissociate at 0.08 and 0.167 U/ml of heparin respectively, and these complexes became fully dissociated at 0.67 U/ml of heparin. The 8:1 N/P ratio K32 siRNA complexes began to dissociate at 0.67 U/ml of heparin and became fully dissociated at 1.33 U/ml of heparin.

The results of the heparin induced complex dissociation assay of the linear lysine peptide siRNA complexes are summarised in **Table 5.2.** Overall, increasing the N/P ratio enhanced the binding between the linear lysine peptides and siRNA.

siRNA complexes	N/P ratio	Heparin concentration required to initiate dissociation (U/ml)	Heparin concentration required to allow complete dissociation (U/ml)
K8	1:1	0-0.02	0.67
	2:1	0-0.02	0.67
	4:1	0-0.02	1.33
	8:1	0-0.02	More than 1.33
K16	1:1	0-0.02	0.167
	2:1	0-0.02	0.67
	4:1	0.08-0.167	0.67
	8:1	0.33	1.33
K24	1:1	0-0.02	0.33
	2:1	0-0.02	0.67
	4:1	0.167	0.67
	8:1	0.67	1.33
K32	1:1	0-0.02	0.67
	2:1	0.08	0.67
	4:1	0.167	0.67
	8:1	0.67	1.33

Table 5.2 A summary of the heparin induced dissociation of different linear lysine peptide siRNA complexes.

5.2.2.1.2 Dissociation of the KBranch siRNA complexes

Increased N/P ratios enhanced the binding between the KBranch peptides and siRNA. **Figure 5.6** demonstrates that increasing the Kbranch peptide enhanced the binding between the Kbranch peptides and siRNA. At N/P ratios of 1.5:1 and 3:1, the Kbranch siRNA complexes dissociated under trace amounts of heparin and were fully dissociated at 0.167 and 0.33 U/ml of heparin respectively. The Kbranch siRNA complexes at an N/P ratio of 6:1 started to dissociate around 0.08 and 0.167 U/ml of heparin. These complexes were fully dissociated at 0.67 U/ml of heparin. When the N/P ratio increased to 12:1, the Kbranch siRNA complexes began to dissociate at 0.33 U/ml of heparin and became fully dissociated at 1.33 U/ml of heparin.

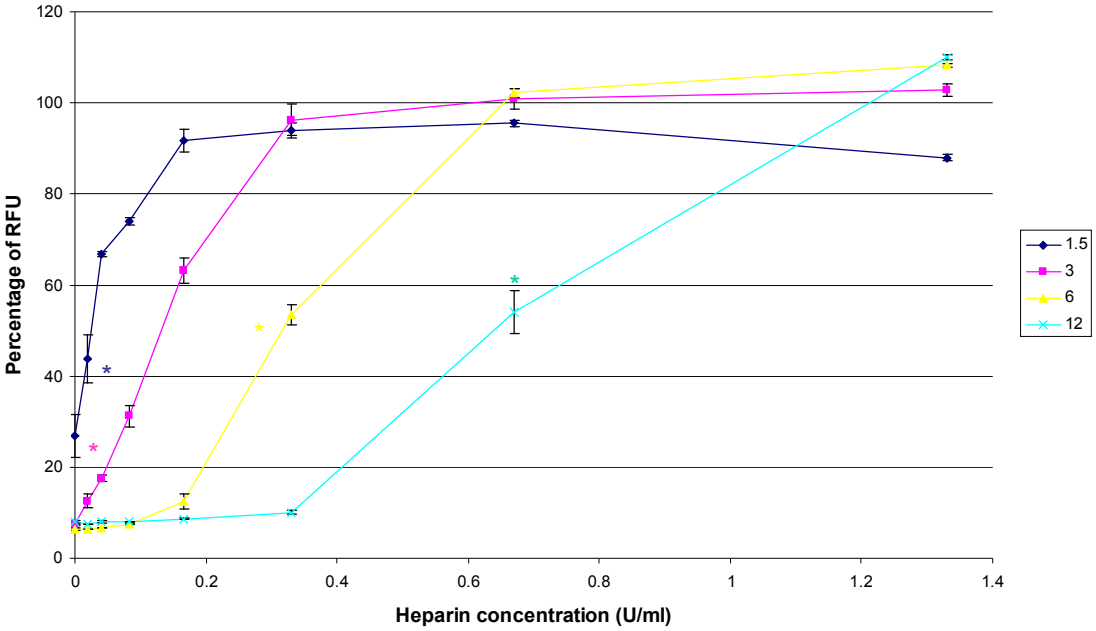

Figure 5.6 The dissociation properties of the Kbranch siRNA complexes. The Kbranch peptide was mixed with PicoGreen labelled siRNA in TE buffer at different N/P ratios for 30 minutes. Different concentrations of heparin were added to the complexes and the fluorescence intensity of the complexes was measured using FLUOstar Optima. The formulations of the complexes are expressed as an N/P ratio. The PicoGreen signals from the complexes were normalised with the naked DNA control to yield the percentage of relative fluorescence unit (RFU) **(Section 2.2.6.3)**. Statistical analysis was performed using ANOVA followed by Tukey's test and it showed a significant increase of the percentage of RFU of the complexes treated with the concentration of heparin marked with * (each * has the same colour as the curve of the N/P ratio of the complexes it corresponds to). In addition, complexes treated with higher heparin concentrations displayed a significant increase of the percentage of RFU compared to that of the untreated complexes ($P < 0.05$).

5.2.2.1.3 Dissociation of the PEI siRNA complexes

Increasing PEIs increased the binding to siRNA **(Figure 5.7 and 5.8)**. As shown in **Figure 5.7A,** the B-PEI siRNA complexes at N/P ratios of 1.25:1 and 2.5:1 dissociated readily under trace amounts of heparin. The 1.25:1 N/P ratio complexes were fully dissociated at 1.33 U/ml of heparin while the 2.5:1 N/P ratio complexes became fully dissociated at 5.3 U/ml of heparin **(Figure 5.7B)**. With N/P ratios of 5:1, the B-PEI siRNA complexes started to dissociate around 0.02 and 0.04 U/ml of heparin **(Figure 5.7A)** and became fully dissociated at 5.3 U/ml of heparin **(Figure 5.7B)**. The B-PEI siRNA complexes with N/P ratios of 10:1 and 20:1 began to dissociate at 0.167 and 0.33 U/ml of heparin respectively, **(Figure 5.7A)** and became fully dissociated at 5.3 U/ml of heparin **(Figure 5.7B)**.

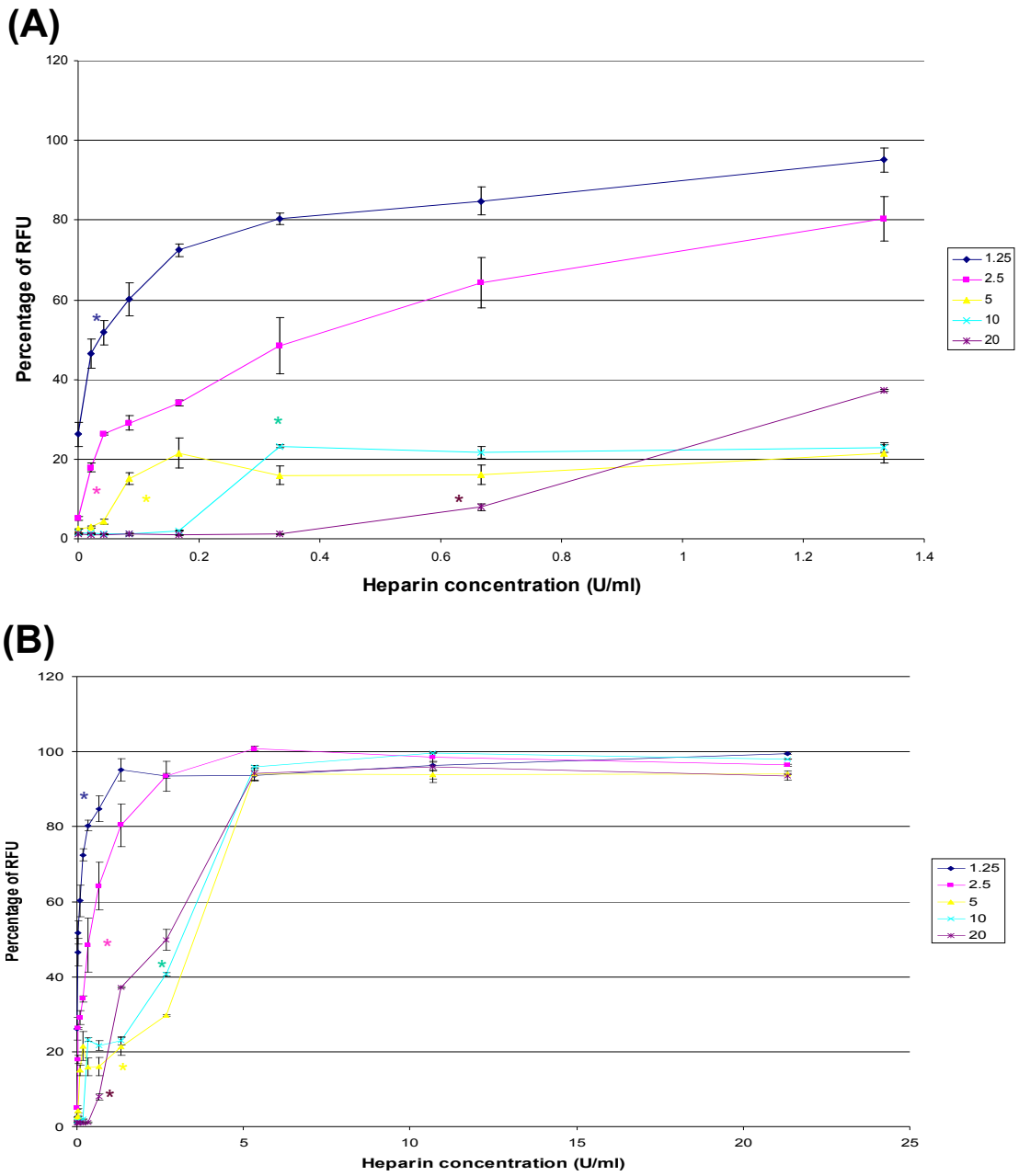

Figure 5.7 The dissociation properties of the B-PEI siRNA complexes. B-PEI was mixed with PicoGreen labelled siRNA in TE buffer at different N/P ratios for 30 minutes. Different concentrations of heparin were added to the complexes and the fluorescence intensity of the complexes was measured using FLUOstar Optima. The PicoGreen signals from the complexes were normalised with the naked DNA control to yield the percentage of relative fluorescence unit (RFU) **(Section 2.2.6.3)**. (A) the B-PEI siRNA complexes exposed to 0 to 1.33 U/ml of heparin , (B) the B-PEI siRNA complexes exposed to 0 to 21.3 U/ml of heparin. Statistical analysis was performed using ANOVA followed by Tukey's test and it showed a significant

increase of the percentage of RFU of the complexes treated with the concentration of heparin marked with * (each * has the same colour as the curve of the N/P ratio of the complexes it corresponds to). In addition, complexes treated with higher heparin concentrations displayed a significant increase of the percentage of RFU compared to that of the untreated complexes ($P < 0.05$). The formulations of the complexes are expressed as an N/P ratio.

Figure 5.8 shows that the L-PEI siRNA complexes with N/P ratios of 1.25:1 and 2.5:1 dissociated readily under trace amounts of heparin. Both of these complexes were completely dissociated at 0.33 U/ml of heparin. With 5:1 and 10:1 N/P ratios, the L-PEI siRNA complexes started to dissociate at 0.08 and 0.167 U/ml of heparin respectively, and these complexes were fully dissociated at 0.67 U/ml of heparin. The 20:1 N/P ratio L-PEI siRNA complexes began to dissociate at a heparin concentration of 0.67 U/ml and became completely dissociated at 1.33 U/ml of heparin.

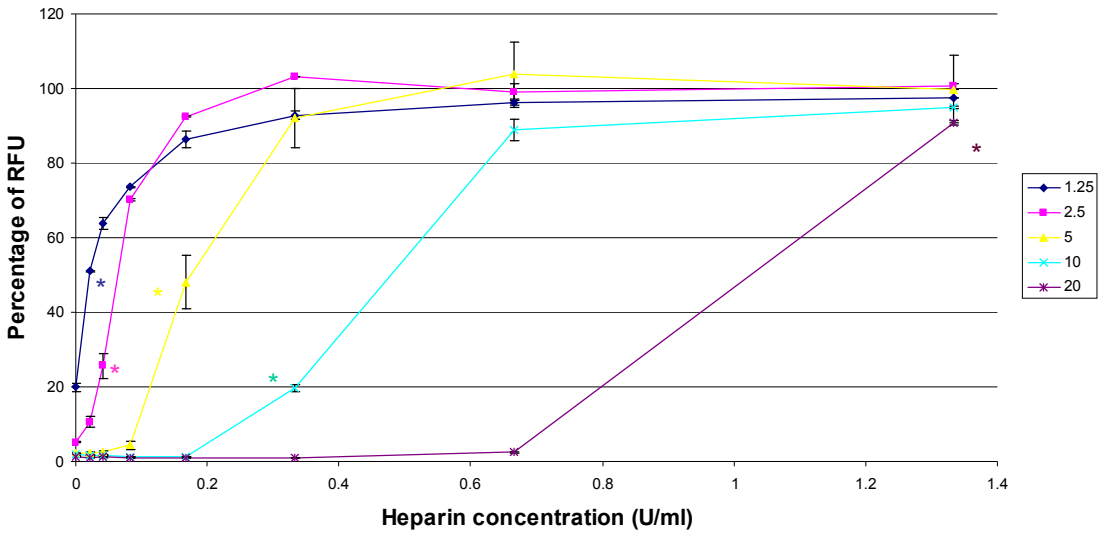

Figure 5.8 The dissociation properties of the L-PEI siRNA complexes. Briefly, L-PEI were mixed with PicoGreen labelled siRNA in TE buffer at different N/P ratios for 30 minutes. Different concentrations of heparin were added to the complexes and the fluorescence intensity of the complexes was measured using FLUOstar Optima. The formulations of the complexes are expressed as an N/P ratio. The PicoGreen signals from the complexes were normalised with the naked DNA control to yield the percentage of relative fluorescence unit (RFU) **(Section 2.2.6.3)**. Statistical analysis was performed using ANOVA followed by Tukey's test and it showed a significant increase of the percentage of RFU of the complexes treated with the concentration of heparin marked with * (each * has the same colour as the curve of the N/P ratio of the complexes it corresponds to). In addition, complexes treated with higher heparin concentrations displayed a significant increase of the percentage of RFU compared to that of the untreated complexes ($P < 0.05$).

The results of the heparin induced complex dissociation assay of the Kbranch siRNA, B-PEI siRNA and L-PEI siRNA complexes are summarised in **Table 5.3.** Overall, increasing the N/P ratio enhanced the binding between the Kbranch peptide, B-PEI or L-PEI and siRNA. It appears that B-PEI binds more strongly to siRNA than L-PEI does. In other words, the B-PEI siRNA complexes are more stable than the L-PEI siRNA complexes.

siRNA complexes	N/P ratio	Heparin concentration necessary to initiate dissociation (U/ml)	Heparin concentration necessary to allow complete dissociation (U/ml)
KBranch	1.5:1	0-0.02	0.167
	3:1	0-0.02	0.33
	6:1	0.08-0.167	0.67
	12:1	0.33	1.33
B-PEI	1.25:1	0-0.02	1.33
	2.5:1	0-0.02	5.3
	5:1	0.02-0.04	5.3
	10:1	0.167	5.3
	20:1	0.33	5.3
L-PEI	1.25:1	0-0.02	0.33
	2.5:1	0-0.02	0.33
	5:1	0.08	0.67
	10:1	0.167	0.67
	20:1	0.67	1.33

Table 5.3 A summary of the heparin induced dissociation of the Kbranch and PEI DNA complexes.

5.2.3 Size and zeta potential of the complexes

The particle size and surface charge are important characteristics of an siRNA delivery system for cellular binding and uptake. Positive charged particles with sizes larger than 50 nm are expected to be efficiently taken up by cells (Gao et al. 2005). The particle size can be measured as a mean hydrodynamic size **(Section 2.2.6.4)** using Zetasizer Nano ZS, and the surface charge can be measured as zeta potential **(Section 2.2.6.5)** using Zetasizer Nano ZS.

5.2.3.1 Size of the complexes

To study the hydrodynamic sizes of the siRNA complexes, complex reagents were mixed with siRNA in distilled water and incubated at room temperature for 30 minutes. The complex sizes were then estimated by the DLS technique.

The mean hydrodynamic sizes of complexes formed from all the linear lysine peptides and siRNA could not be determined due to the highly polydisperse nature of the complexes. This suggests that the linear lysine peptides formed highly irregular complexes or a wide range of different sized complexes with siRNA. Therefore, these complexes are expected to be ineffective for siRNA delivery.

The Kbranch peptide formed complexes with siRNA at an N/P ratio of 1:1 with a size of 144 nm **(Figure 5.9A)**. Gradually increasing the N/P ratio decreased the complex size, and the size of the Kbranch siRNA complexes at an N/P ratio of 6:1 was 92 nm. However, increasing the N/P ratio from 6:1 to 12:1 increased the heterogeneity of these

complexes. At an N/P ratio of 12:1, the average hydrodynamic size of the Kbranch siRNA complexes was 464 nm with a large standard deviation. This indicates that a further increase of the N/P ratio of the Kbranch peptide siRNA complex may cause aggregation or instability of the complex which will result in heterogeneous sized complexes.

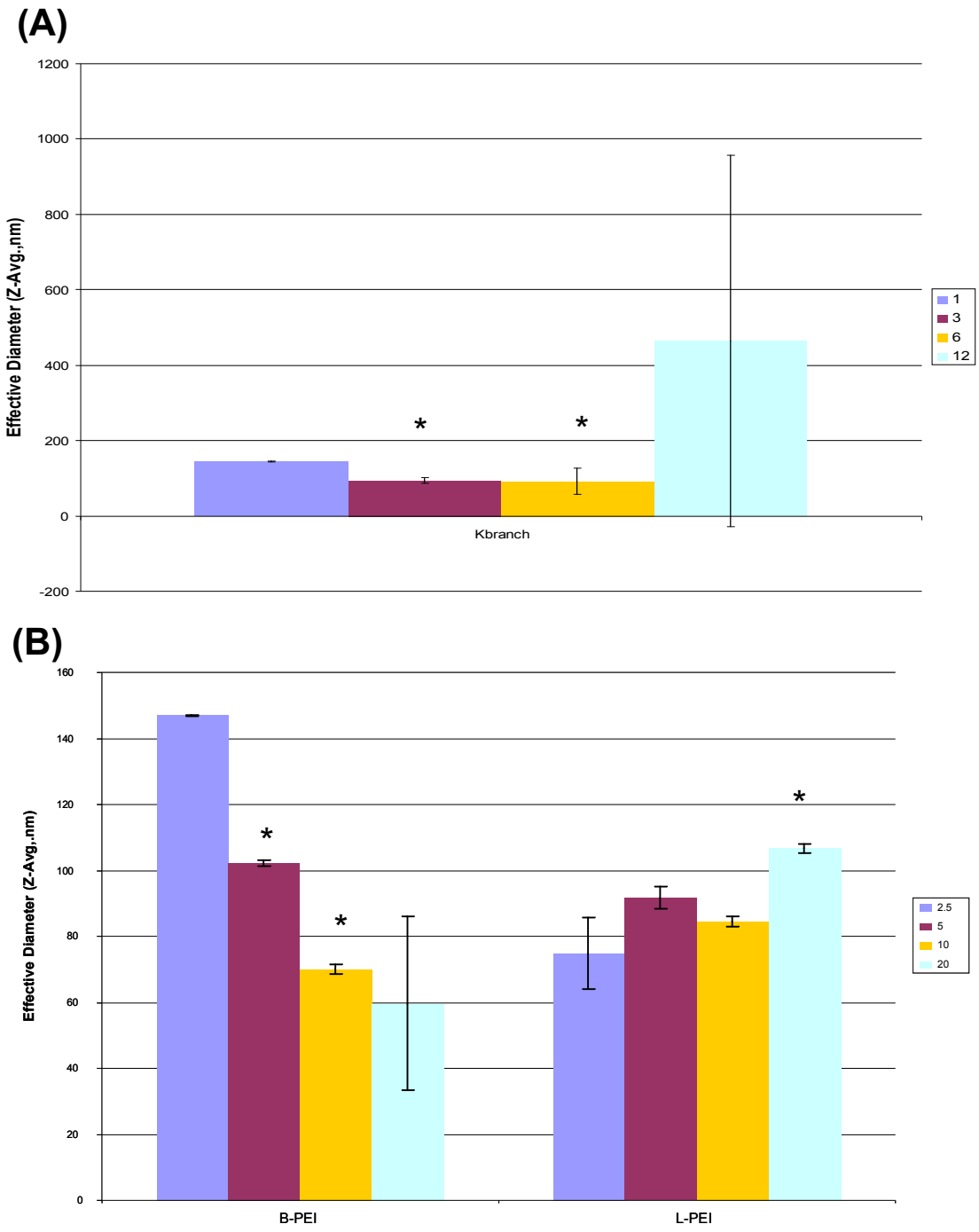

Figure 5.9 The effective diameter of the KBranch or PEIs siRNA complexes. The Kbranch peptide or PEIs were mixed with siRNA in distilled water at different N/P ratios for 30 minutes. The size of the complexes was then measured using Zetasizer Nano ZS **(Section 2.2.6.4)**. **(A)** the mean hydrodynamic size of the Kbranch siRNA complexes. Statistical analysis was performed using Student t-test and it showed a significant decrease of the effective diameters of the Kbranch siRNA complexes from an N/P ratio of 1:1 to 3:1 or 6:1 ($P < 0.05$). **(B)** the mean

hydrodynamic size of the B-PEI or L-PEI siRNA complexes. Statistical analysis was performed using Student t-test and it showed a significant decrease of the effective diameters of the B-PEI siRNA complexes from an N/P ratio of 2.5:1 to 10:1 ($P < 0.05$). A significant increase of the effective diameter of the L-PEI siRNA complexes from an N/P ratio of 2.5:1, 5:1 or 10:1 to 20:1 was also observed ($P < 0.05$). The formulations of the complexes are expressed as an N/P ratio.

Increasing the N/P ratios decreased the size of the B-PEI siRNA complexes **(Figure 5.9B)**. Aside from the B-PEI siRNA complexes at an N/P ratio of 2.5:1, the B-PEI siRNA complexes with N/P ratios of 5:1, 10:1 and 20:1 ranged from 60 nm to 100 nm. On the other hand, all the L-PEI siRNA complexes, which had N/P ratios between 2.5:1 and 20:1, ranged from 70 nm to 110 nm. Conversely, an increase of the N/P ratios of the L-PEI siRNA complexes did not increase the complexes size.

5.2.3.2 Zeta potential of the complexes

To measure the zeta potential, the lysine based peptides or PEIs were mixed with siRNA in distilled water at different N/P ratios for 30 minutes at room temperature. The average zeta potential of the complexes was then measured using LDA.

The zeta potential of the linear lysine peptide siRNA complexes could not be measured due to their high polydispersity. On the other hand, the average zeta potential of the Kbranch peptide siRNA complex at an N/P ratio of 1.5:1 was -27.2 mV **(Figure 5.10A)**. Increasing the N/P ratio to 3:1 increased the average zeta potential to +31 mV. However, a further increase of the N/P ratio did not increase the zeta potential.

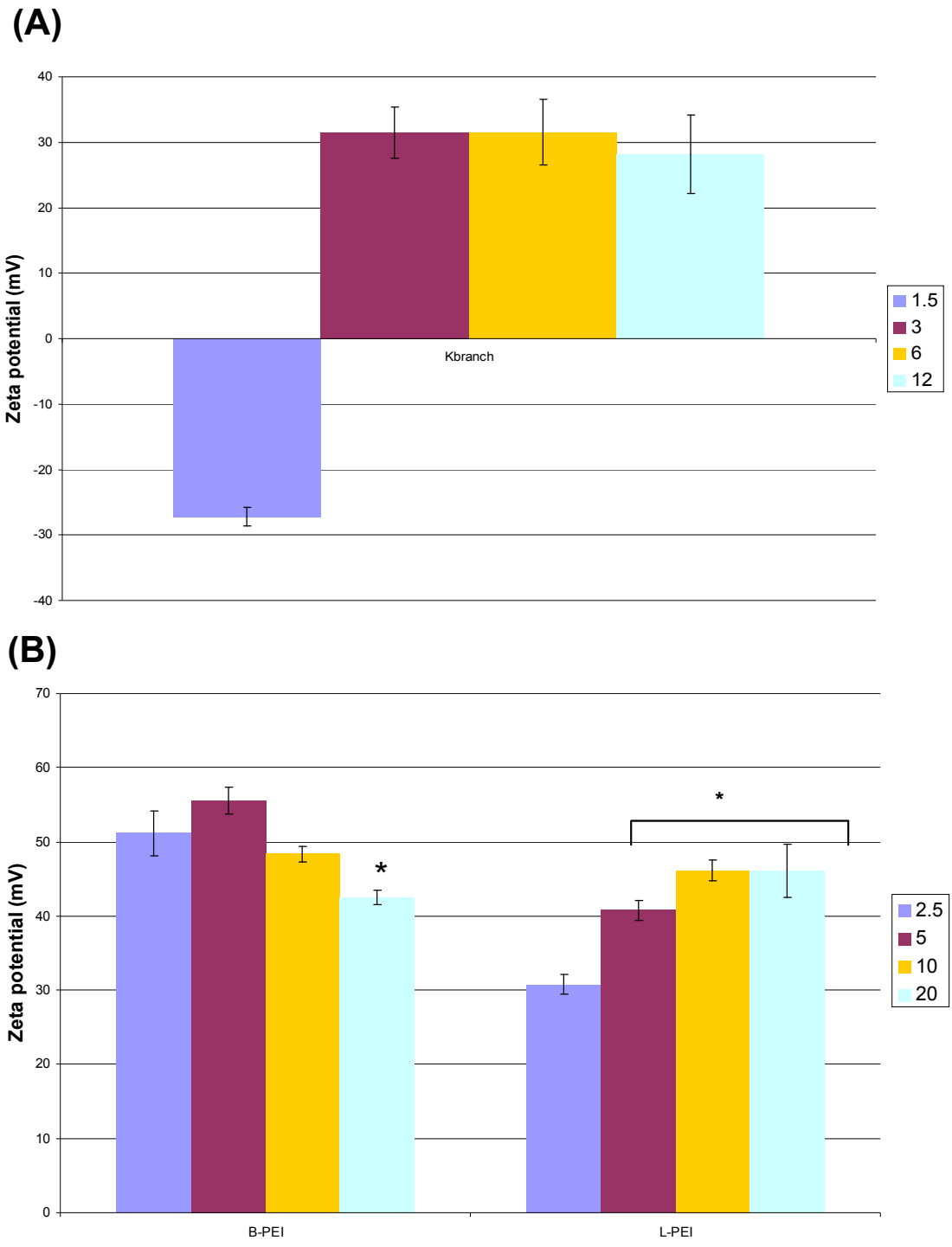

Figure 5.10 The zeta potential of the Kbranch or PEIs siRNA complexes. The cationic polymers were mixed with siRNA in distilled water at different N/P ratios for 30 minutes. The zeta potential of the complexes was then measured using Zetasizer Nano ZS **(Section 2.2.6.5)**. **(A)** the average zeta potential of the Kbranch siRNA complexes. Statistical analysis was performed using Student t-test. There are no significant different between the Kbranch siRNA

complexes with N/P ratios of 3:1, 6:1 or 12:1. **(B)** the average zeta potential of the B-PEI or L-PEI siRNA complexes. Statistical analysis was performed using Student t-test and it showed a significant decrease of the zeta potential of the B-PEI siRNA complexes from an N/P ratio of 2.5:1, 5:1 or 10:1 to 20:1 ($P < 0.05$). A significant increase of the zeta potential of the L-PEI siRNA complexes from an N/P ratio of 2.5:1 to 5:1, 10:1 or 20:1 was also observed ($P < 0.05$). The formulations of the complexes are expressed as an N/P ratio.

Both the B-PEI and L-PEI siRNA complexes with N/P ratios between 2.5:1 and 20:1 have a positive average zeta potential **(Figure 5.10B)**. The average zeta potential of the B-PEI siRNA complex was between +45 mV and +55mV whereas that of the L-PEI siRNA complex was between +30 mV and +45 mV. An increase of the N/P ratio of the L-PEI siRNA complex gradually increased the average zeta potential; however, increasing the N/P ratio of the B-PEI siRNA complex did not increase the average zeta potential.

5.2.4 Transfection studies on the lysine based peptide or PEI siRNA complexes

To investigate the siRNA delivery efficiency of the complexes, siRNA transfection was carried out using Neuro 2a cells stably expressing luciferase as described in **Section 2.2.3.3.3 and 2.2.3.3.4**. By using siRNA targeting luciferase (siLuc), the gene knockdown efficacy was determined by the remaining luciferase activity. To ensure the luciferase knockdown was due to specificity of the anti-luciferase siRNA, an siRNA targeting eGFP (sieGFP) was used as a control. As a positive control, complexes formed with commercially available Lipofectamine 2000 (L2000) and siRNA were used to transfect the cells.

As shown in **Figure 5.11**, no significant luciferase knockdown was observed from the siRNA complexes composed of the linear lysine or Kbranch peptides whereas L2000 siRNA complexes induced 80% gene knockdown. It was perhaps not surprising to note that no gene knockdown was observed for the linear lysine peptides since these peptides cannot form homogenously sized and charged complexes for cellular uptake. However, it was unexpected that the Kbranch peptide siRNA complexes, which can form positively charged stable siRNA nanoparticles, cannot mediate gene silencing.

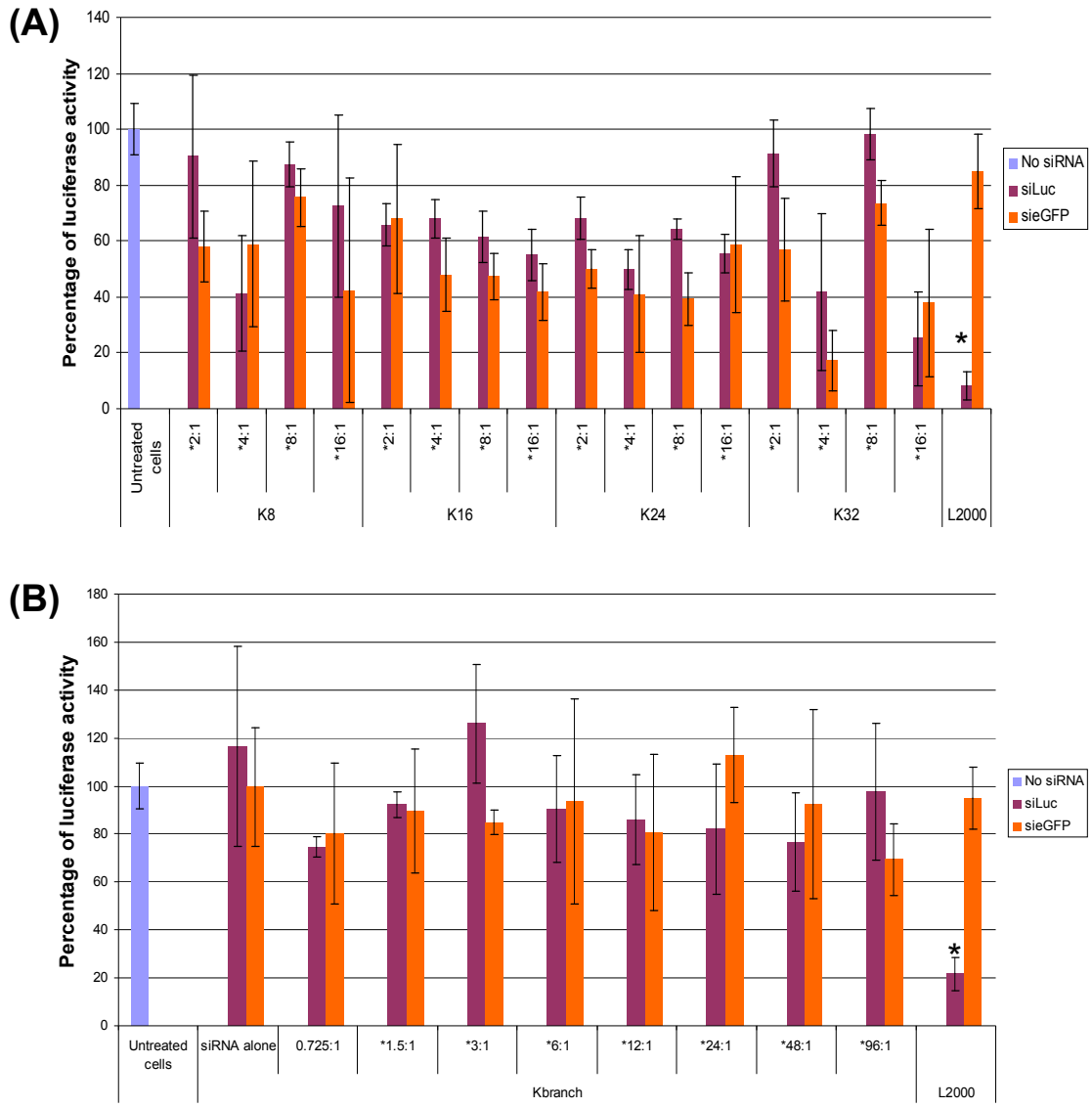

Figure 5.11 siRNA transfection efficiency mediated by the lysine based peptide siRNA complexes. 5 × 10^4 Neuro 2a luciferase expressing cells were seeded 24 hours before transfection (in a 96 well plate). The complexes were made by mixing the linear lysine or Kbranch peptides with siRNA targeting luciferase (siLuc) at different N/P ratios for 30 minutes. Complexes with siRNA targeting eGFP (sieGFP) were used as a control to assess non-specific gene silencing mediated by the complexes. Following removal of full growth medium, complexes were overlaid onto the cells for 4 hours. After removing the transfection complexes, full growth medium was added to the cells **(Section 2.2.3.3.3 and 2.2.3.3.4)**. Luciferase activity in the cells was analysed 24 hours post-transfection to estimate the transfection efficiencies of the complexes **(Section 2.2.5.1)**. The luciferase activity of the untreated cells was used to normalise the luciferase activity of the treated cells to yield the percentage of luciferase activity. **(A)** siRNA transfection using the K8, K16, K24 or K32 siRNA complexes. Statistical analysis was performed using Student t-test and it showed that there was a significant decrease of the

luciferase activity in the cells treated with the L2000 siLuc complexes compared to the cells treated with the L2000 sieGFP complexes ($P < 0.05$) while there was no significant luciferase activity decrease of the cells treated with the linear peptide (K8, K16, K24 and K32) siLuc complexes compared to the cells treated with the linear peptide sieGFP complexes. **(B)** siRNA transfection using the Kbranch siRNA complexes. Statistical analysis was performed using Student t-test and it showed that there was a significant decrease of the luciferase activity in the cells treated with the L2000 siLuc complexes compared to the cells treated with the L2000 sieGFP complexes ($P < 0.05$) while there was no significant luciferase activity decrease of the cells treated with the Kbranch siLuc complexes compared to the cells treated with the Kbranch sieGFP complexes. The formulations of the complexes are expressed as an N/P ratio.

The L-PEI siRNA complexes, which were formulated from an N/P ratio of 2.5:1 to an N/P ratio of 20:1, did not mediate gene silencing **(Figure 5.12A)**. On the other hand, the B-PEI siRNA complexes at an N/P ratio of 20:1 mediated 60% luciferase knockdown **(Figure 5.12B)**. A further increase of the N/P ratio of the B-PEI siRNA complex to 40:1 resulted in a decreased luciferase signal when both siLuc and sieGFP complexes were used. This suggested that complexes at this N/P ratio were either toxic to the cells or delivering excessive amount of siRNA to cells which results in non-specific gene silencing.

To determine whether the decreased luciferase signal caused by the N/P ratio 40:1 B-PEI siRNA complex was due to toxicity, the viability of the cells from the same experiment setting presented in **Figure 5.12B** was analysed. As shown in **Figure 5.13**, the percentage of viable cells treated with the N/P ratio 40:1 B-PEI siRNA complex was around 60% compared to cells treated with siRNA alone, suggesting that it was the cell toxicity rather than non-specific gene silencing caused the decrease of luciferase signal in **Figure 5.12B**. By contrast, both the L2000 siRNA and N/P ratio 20:1 B-PEI siRNA complexes were less toxic to the cells, causing around 20% loss of viable cells.

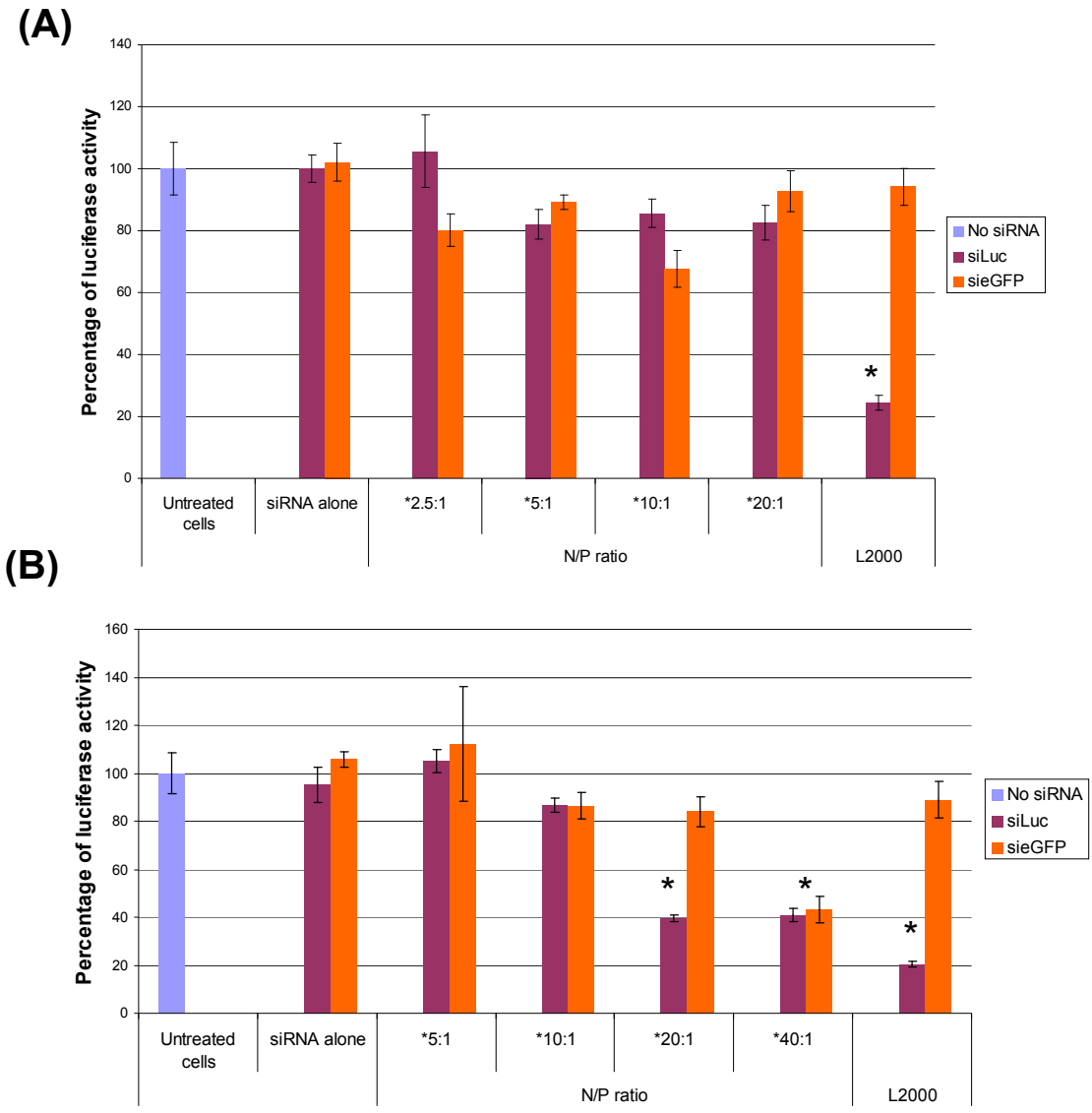

Figure 5.12 siRNA transfection efficiency mediated by the B-PEI siRNA and L-PEI siRNA complexes. 5 × 10^4 Neuro 2a luciferase expressing cells were seeded 24 hours before transfection (in a 96 well plate). The complexes were made by mixing B-PEI or L-PEI with siLuc at different N/P ratios for 30 minutes. Complexes with sieGFP were used as a control to assess non-specific gene silencing mediated by the complexes. Following removal of full growth medium, complexes were overlaid onto the cells for 4 hours. After removing the transfection complexes, the full growth medium was added to the cells **(Section 2.2.3.3.3 and 2.2.3.3.4)**. Luciferase activity within the cells was analysed 24 hours post-transfection to estimate the transfection efficiencies of the complexes **(Section 2.2.5.1)**. The luciferase activity of the untreated control was used to normalise against the luciferase activity of cells treated with

siRNA or the complexes to yield the percentage of luciferase activity. **(A)** siRNA transfection using the L-PEI siRNA complexes. Statistical analysis was performed using Student t-test and it showed that there was a significant decrease of the luciferase activity in the cells treated with the L2000 siLuc complexes compared to the cells treated with the L2000 sieGFP complexes ($P < 0.05$) while there was no significant luciferase activity decrease of the cells treated with the L-PEI siLuc complexes compared to the cells treated with the L-PEI sieGFP complexes. **(B)** siRNA transfection using the B-PEI siRNA complexes. Statistical analysis was performed using Student t-test and it showed that there was a significant decrease of the luciferase activity in the cells treated with the L2000 siLuc complexes compared to the cells treated with the L2000 sieGFP complexes ($P < 0.05$). A significant luciferase activity decrease of the cells treated with the B-PEI siLuc complexes compared to the cells treated with the B-PEI sieGFP complexes ($P < 0.05$). The cells treated with the B-PEI siLuc complexes or the B-PEI sieGFP complexes at an N/P ratio of 40:1 showed a significant decrease of the luciferase activity compared to the cells treated with the siRNA alone or the untreated cells ($P < 0.05$). The formulations of the complexes are expressed as an N/P ratio.

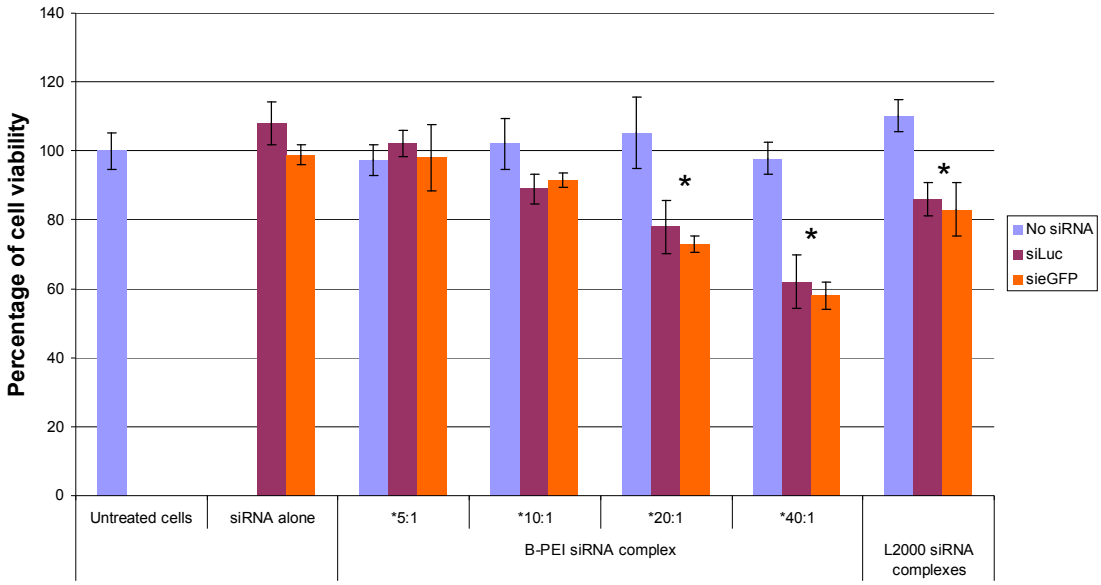

Figure 5.13 Cellular toxicity mediated by B-PEI siRNA complexes. 5×10^4 Neuro 2a luciferase expressing cells were seeded 24 hours before transfection (in a 96 well plate). The complexes were made by mixing B-PEI with siLuc or sieGFP at different N/P ratios for 30 minutes. Following removal of full growth medium, complexes were overlaid onto the cells for 4 hours. After removing the transfection complexes, the full growth medium was added to the cells **(Section 2.2.3.3.3 and 2.2.3.3.4)**. The cell viability was analysed 24 hours post-transfection by a CellTiter 96 AQueous One Solution Assay to estimate the cytotoxicity effect of the complexes on the cells **(Section 2.2.5.4)**. The absorbance of the untreated cells was used to normalise against the absorbance of the cells treated with siRNA alone or the siRNA complexes to yield the percentage of cell viability. Statistical analysis was performed using Student t-test and it showed that there was a significant decrease of viability of the cells treated with the B-PEI siRNA complexes at N/P ratios of 20:1 and 40:1 and the L2000 siRNA complexes compared to the cells treated with siRNA or B-PEI or L2000 only ($P < 0.05$). The formulations of the complexes are expressed as an N/P ratio. The cell viability of the treated cells was normalised with the untreated control to yield percentage of cell viability.

In order to further confirm that the luciferase knockdown mediated by the B-PEI siRNA complexes at a 20:1 N/P ratio was due to a specific siRNA effect, B-PEI was used to form a complex with an siRNA targeting an endogenous gene glyceraldehyde-3-phosphate dehydrogenase (siGAPDH) at the same N/P ratio. The complex was then used to transfect the Neuro 2a cells and the GAPDH knockdown was recorded **(Figure 5.14)**. As a control for gene knockdown specificity, an sieGFP was used to form a complex with B-PEI and the complex was used for cell transfection.

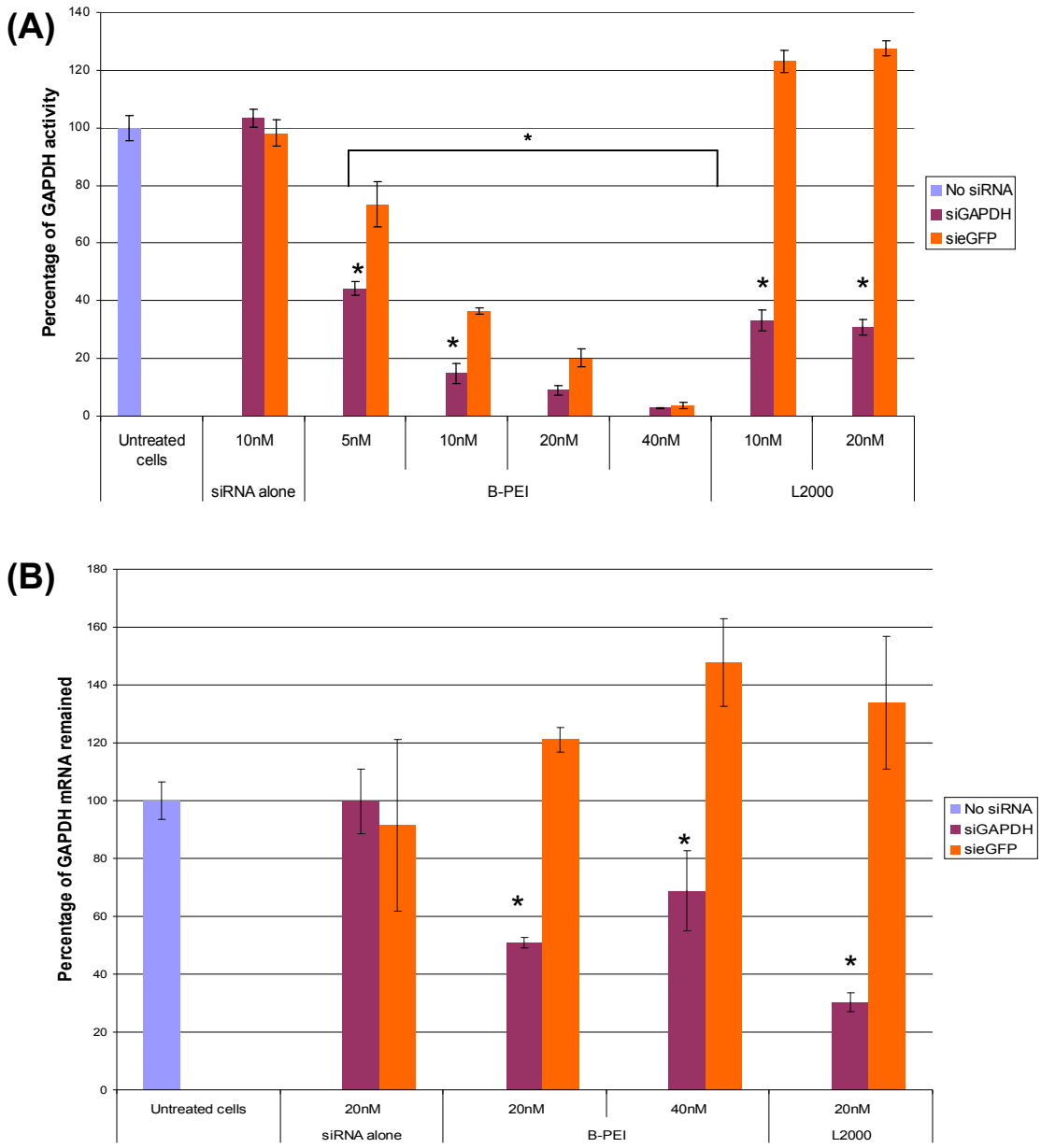

Figure 5.14 GAPDH gene knockdown mediated by the B-PEI siRNA complexes. 5×10^4 Neuro 2a cells were seeded 24 hours before transfection (in a 96 well plate). The complexes were made by mixing B-PEI with different concentration of siGAPDH at an N/P ratio of 20:1 for 30 minutes. Complexes with sieGFP were used as a control to assess non-specific gene silencing mediated by the complexes. Following removal of full growth medium, complexes were overlaid onto the cells for 4 hours. After removing the transfection complexes, full growth medium was added to the cells **(Section 2.2.3.3.3 and 2.2.3.3.4)**. GAPDH mRNA levels **(Section 2.2.9)** and activities **(Section 2.2.5.3)** in the cells were analysed 48 hours post-transfection to estimate the transfection efficiencies of the complexes. **(A)** GAPDH activities. The GAPDH activity of the untreated cells was used to normalise the GAPDH activity of the treated cells to yield the percentage of GAPDH activity. Statistical analysis was performed

using Student t-test and it showed that there was a significant decrease of GAPDH activity in the cells treated with the B-PEI siLuc complexes with 5 to 20 nM compared to the cells treated with the B-PEI sieGFP complexes at the same siRNA concentrations ($P < 0.05$). When compared to the cells treated with siRNA only, a significant decrease of the GAPDH activity of the cells treated with the B-PEI sieGFP (5 to 20 nM) complexes was observed ($P < 0.05$). The L2000 siLuc complexes mediated a significant GAPDH activity decrease in the cells compared to the cells treated with the L2000 sieGFP complexes ($P < 0.05$). **(B)** GAPDH mRNA levels assayed by real time PCR. The mRNA level of the untreated cells was used to normalise against the treated cells to yield the percentage of mRNA level. Statistical analysis was performed using Student t-test and it showed that there was a significant decrease of GAPDH activity in the cells treated with the B-PEI siLuc complexes with 20 and 40 nM or the L2000 siLuc complexes compared to the cells treated with the B-PEI sieGFP complexes or the L2000 sieGFP complexes at the same siRNA concentrations respectively ($P < 0.05$).

As shown in **Figure 5.14A**, the B-PEI siGAPDH complex, with an N/P ratio of 20:1 and 5 nM of the siRNA, mediated 50% GAPDH knockdown. However, the B-PEI sieGFP complex also induced a decrease of the GAPDH expression by 20%. Increasing the amount of the siGAPDH from 10 nM to 40 nM enhanced the GAPDH knockdown, although at the same time the B-PEI sieGFP complex resulted in a further decrease of the GAPDH expression. The decrease of the GAPDH in the cells treated by the B-PEI sieGFP complexes suggested that these complexes either induced non-specific gene silencing or cellular toxicity.

Compared to the B-PEI siGAPDH complexes with 10 and 20 nM of siRNA, the L2000 siGAPDH complex could mediate more than 60% of GAPDH knockdown whereas the L2000 sieGFP complex did not lead to a decrease of GAPDH expression **(Figure 5.14A)**. Also, it was shown that siRNA alone could not mediate gene silencing.

To find out if the decrease of the GAPDH levels in the cells treated with the B-PEI sieGFP complexes was due to toxicity or non-specific gene silencing, the mRNA levels of the GAPDH in the cells exposed to the B-PEI siRNA complexes were analysed. As shown in **Figure 5.14B**, the B-PEI siGAPDH complexes with 20 and 40 nM siRNA induced GAPDH knockdown whereas the B-PEI sieGFP complexes with 20 and 40 nM of siRNA did not. This indicated that increasing the siRNA amounts within the B-PEI siRNA complexes causes cellular toxicity.

5.2.5 siRNA complexes mediated cellular binding, uptake and cell death

From the siRNA transfection study, it is noted that no specific gene knockdown was mediated by the linear lysine peptide siRNA complexes. This was perhaps not surprising since the linear lysine peptides could not form monodisperse nanoparticles with siRNA. Unexpectedly, the Kbranch peptide or L-PEI siRNA complexes did not mediate gene silencing even though they can form positively charged nanoparticles. These results could be due to no cellular uptake of the complexes or the complexes being destroyed following entry into the cells by the endosome (Khalil 2006).

In order to examine the relationship between cellular uptake of the siRNA complexes and transfection efficiencies, Cy 3 labelled siRNA was used to form complexes with the different cationic polymers used in this study. Following 4 hours of transfection, the Neuro 2a cells were harvested. Cellular binding and uptake of the complexes were assayed using flow cytometry **(Figure 5.15)**. Cy3 signal positive cells indicated cellular

binding and uptake of the complexes. To also estimate the cellular toxicity induced by the complexes, 7-amino-actinomycin D (7aad) was used to stain for dead cells.

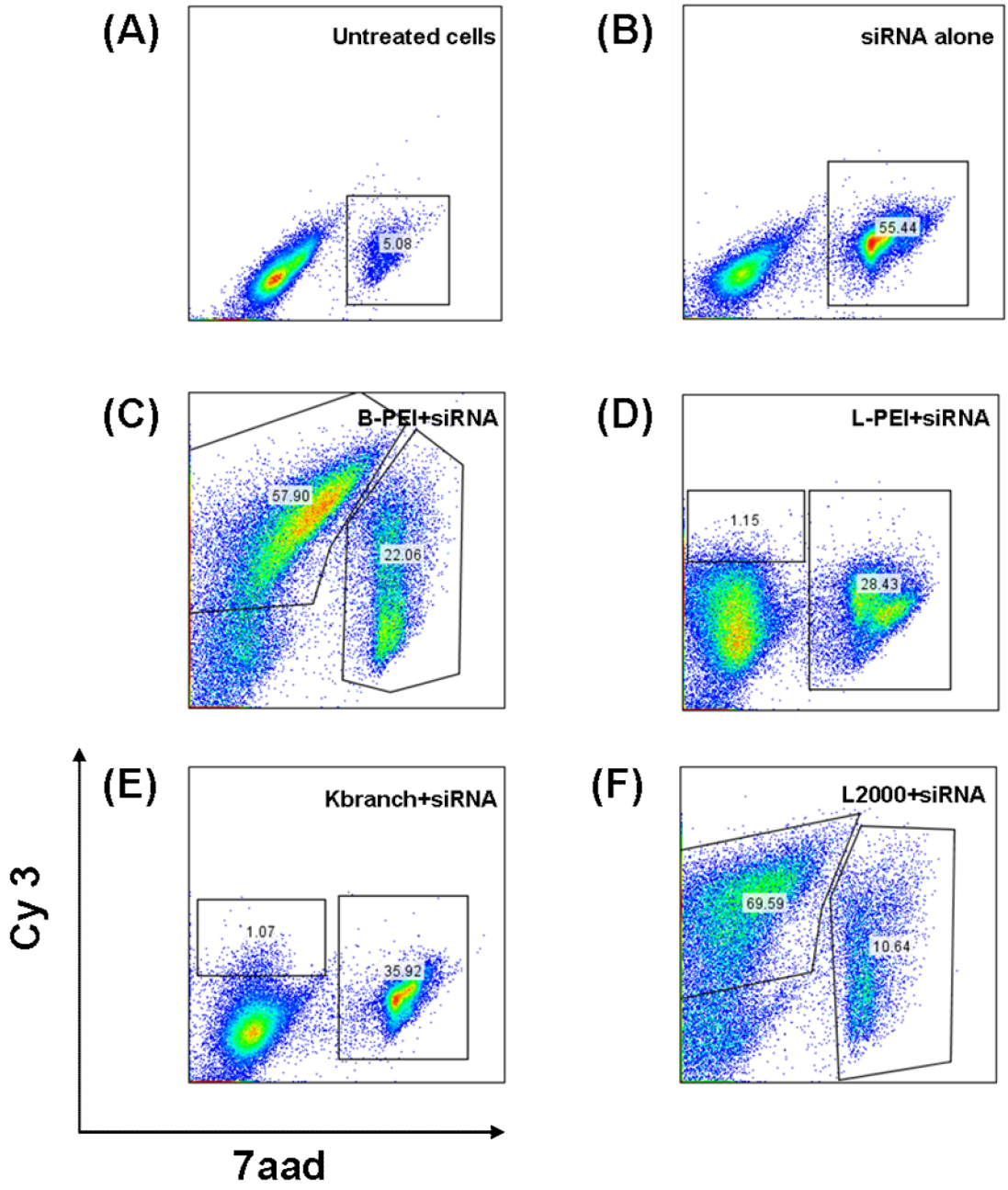

Figure 5.15 Cellular binding and uptake efficiencies of the cationic polymer siRNA complexes. Briefly, Neuro 2a cells were seeded 24 hours before transfection. The complexes were made by mixing the cationic polymers with Cy 3 labelled siRNA for 30 minutes. Following removal of full growth medium, complexes were overlaid onto the cells for 4 hours. The cells were harvested for analysis after transfection **(Section 2.2.3.3.3 and 2.2.3.3.4)**. Cells stained with 7aad were to estimate the cell viability following transfection **(Section 2.2.7.3)**. **(A)** untreated cells, **(B)** cells exposed to naked siRNA only, **(C)** cells exposed to the B-PEI/siRNA complex at 20:1 N/P ratio, **(D)** cells exposed to the L-PEI/siRNA complex at 20:1 N/P ratio, **(E)** cells exposed to the Kbranch/siRNA complex at 6:1 N/P ratio, **(F)** cells exposed to the L2000/siRNA complex.

As shown in **Figure 5.15**, the Cy3 signals were detected from the cells transfected with the B-PEI **(Figure 5.15C)** or L2000 **(Figure 5.15F)** siRNA complexes. The Cy 3 signals were detected from ~70% of the cells transfected with L2000 siRNA complexes and ~60% of the cells treated with B-PEI siRNA complexes. On the other hand, only a very low Cy3 signal could be detected from the cells exposed to the L-PEI **(Figure 5.15D)** or the Kbranch peptide **(Figure 5.15E)** siRNA complexes.

As shown in **Figure 5.15**, 55% of cells exposed to naked siRNA were dead. The percentage of cell death of cells exposed to the B-PEI or L-PEI siRNA complexes were 26% and 28% respectively. The Kbranch siRNA complexes mediated 36% cell toxicity while the L2000 siRNA complexes induced 11% cell toxicity. These findings suggested that cell death and siRNA delivery efficiency could form a reversely correlated relationship.

5.2.6 Internalisation of the siRNA complexes

To confirm the findings from the flow cytometry (i.e. siRNA uptake), Neuro 2a cells were transfected with Cy 3 labelled siRNA complexes in different formulations for 4 hours in serum free medium. The cells were then harvested and stained with phalloidin for the cell membrane and DAPI for the nucleus. The cells were then assessed by confocal microscopy.

The results showed that no siRNA signal was detected from the cells transfected with either the Kbranch peptide or L-PEI siRNA complexes which were consistent to the findings from the flow cytometry **(Figure 5.16)**. siRNA was detected in the cells

exposed to the L2000 or B-PEI siRNA complexes. In particular, siRNA predominantly clustered in the cytoplasm for the cells transfected with the L2000 siRNA complexes. On the other hand, for the cells treated with B-PEI siRNA complexes, siRNA localised predominantly in the nucleus and comparatively less in the cytoplasm.

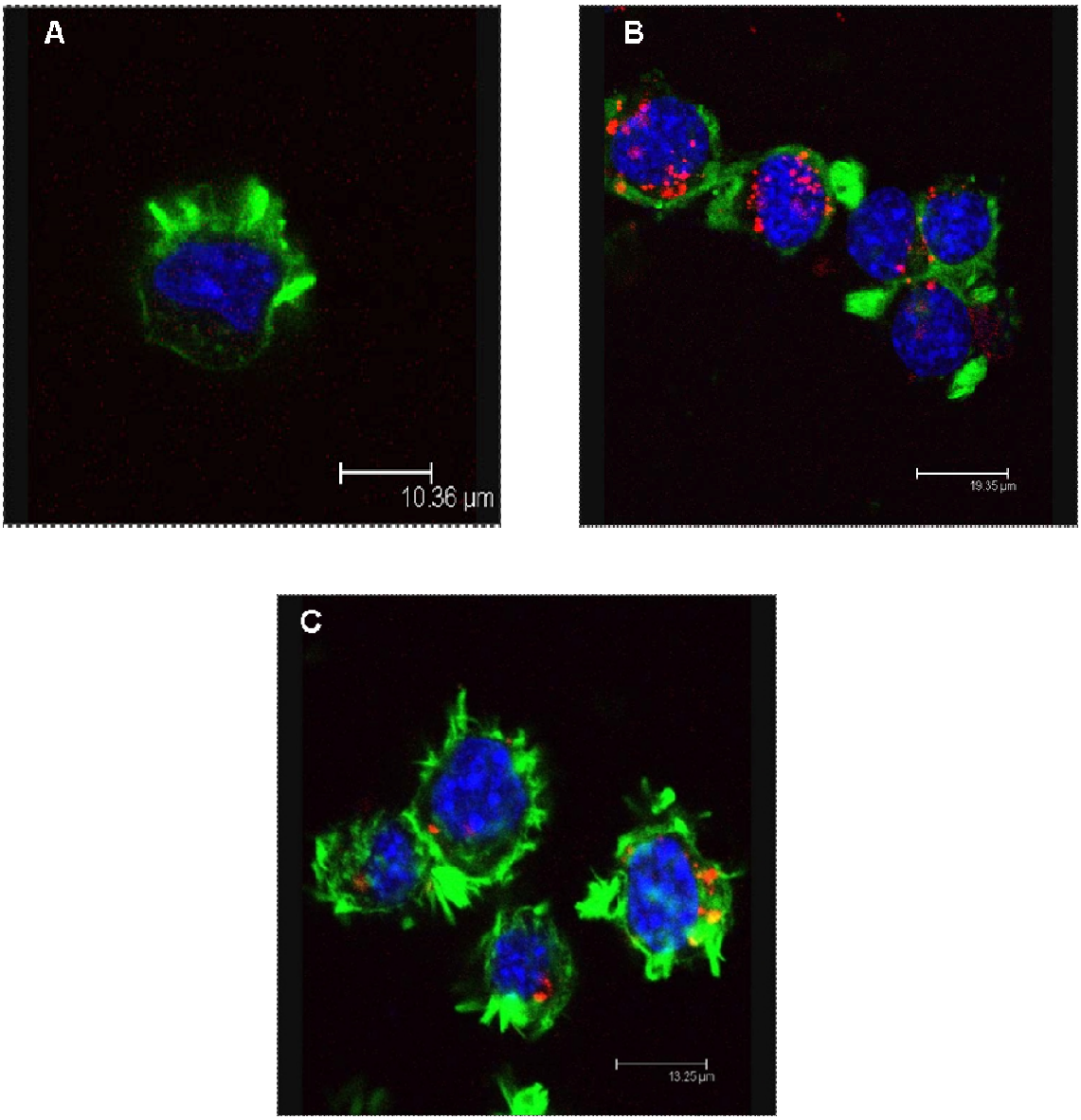

Figure 5.16 Localisation of siRNA following transfection. Briefly, Neuro 2a cells were seeded 24 hours before transfection. The complexes were made by mixing the cationic polymers with Cy 3 labelled siRNA (Red) for 30 minutes. Following removal of full growth medium, complexes were overlaid onto the cells for 4 hours **(Section 2.2.3.3.3 and 2.2.3.3.4)**. The cells were then washed and stained with phalloidin for the F-actin on the cell membrane (Green) and DAPI for the nucleus (Blue) **(Section 2.2.8.2 and 2.2.8.3)**. **(A)** cells exposed to the Kbranch/siRNA complexes (untreated cells, cells exposed to the naked siRNA or the L-PEI/siRNA complexes showed the same result as the cells exposed to the Kbranch/siRNA complexes) **(B)** cells exposed to the B-PEI/siRNA complex, **(C)** cells exposed to the L2000/siRNA complex.

5.3 Discussion

The criteria to deliver DNA and siRNA to the cells are believed to be similar. For instance, both the nucleic acids need to be packaged inside the vectors to form stable nanoparticles with a positive surface charge for cellular entry (Grayson et al. 2006). Once inside the cells, both nucleic acids must be dissociated from the vector systems to their respective compartments for gene expression or silencing. Therefore, it is expected that a successful siRNA delivery system would demonstrate similar biophysical properties to a successful DNA delivery system. However, the differences in the size and the chemical composition of siRNA and DNA could lead to different biophysical characteristics of siRNA complexes compared to that of DNA complexes. These differences in biophysical properties could result in a different nucleic acid delivery behaviour of the siRNA complexes compared to the DNA complexes.

In this chapter, the biophysical and transfection properties of the siRNA complexes were investigated. This information can be compared to the biophysical and transfection properties of the DNA complexes using the same vector reagents. The comparative study could allow the generation of ideas for the development of an effective siRNA delivery system.

5.3.1 The importance of the physical and chemical structure and the size of the complex reagents for siRNA packaging

From the results of the gel retardation assay, it was observed that a linear complex reagent structure may not be as effective as a branched structure to package siRNA. For

instance, the linear lysine peptides were not able to completely retard and encapsulate siRNA whereas the branched lysine peptide, the Kbranch peptide, was able to do so. Also, B-PEI, which completely retarded the siRNA migration at a 5:1 N/P ratio, was more effective in packaging siRNA than L-PEI, which completely encapsulated the siRNA at an N/P ratio of 10:1.

The chemical composition of the complex reagents plays a role in the siRNA packaging. For example, PEIs, which are denser in charge than the lysine peptides, packaged siRNA more effectively than the lysine peptides. The L-PEI and B-PEI completely retarded the siRNA migration at an N/P ratio of 10:1 and 5:1 respectively, whereas the Kbranch peptides completely ceased the siRNA migration at a 60:1 N/P ratio. This suggests that complex reagent with a higher charge density would be more effective for siRNA encapsulation.

Another important parameter for effective siRNA packaging could be the size of the complex reagent. The effective B-PEI and L-PEI siRNA packaging reagents were 25 and 22 kDa respectively; these polymers were 5-6 times larger than the lysine based peptides, which were 1-4 kDa in size. This indicated that larger complex reagent could be more efficient for siRNA packaging.

B-PEI can package siRNA more efficiently than L-PEI. Similarly, the Kbranch peptide is more effective in encapsulating siRNA than the linear lysine peptides. This may suggest that the branched structure of the complex reagents could be more beneficial for siRNA packaging than the linear structure.

5.3.2 A different observation between the PicoGreen fluorescence quenching assay and the gel retardation assay

From the gel retardation assay, it is clear that the linear lysine peptides were not effective in packaging siRNA; only the Kbranch peptide, B-PEI and L-PEI were able to package siRNA. However, the results of the PicoGreen fluorescence quenching assay showed that all the complex reagents used in this study were able to bind to siRNA effectively. There were discrepancies between the results from the gel retardation and PicoGreen fluorescence quenching assays and these are summarised in **Table 5.1**. The difference in the results could be due to the fact that in the gel retardation assay, an electric field is applied across the complexes and therefore the migration patterns of the complexes are influenced by the overall charge of the complexes and the binding strength between cationic peptides and siRNA. There is not this kind of force in the PicoGreen fluorescence quenching assay, therefore, the results in this assay may differ.

In fact, the results of the B-PEI or L-PEI siRNA complexes were similar in both experiments, suggesting that the PEI siRNA complexes were very stable. Conversely, the lysine peptide siRNA complexes were not very stable.

5.3.3 Dissociation patterns of the siRNA complexes

From the heparin induced complex dissociation assay, it was found that an increased N/P ratio enhanced the binding between the complex reagents and siRNA. For the lysine based peptides, it was observed that peptides with a larger size bound more

strongly to siRNA. The affinity of siRNA to the lysine peptides is summarised as follows:

K32, K24 > K16 > Kbranch (consists of 13 lysines)

The K8 peptide was not included in this comparison because the overall dissociation pattern of the K8 siRNA complexes in different N/P ratios were different to that of the other linear lysine siRNA complexes. The K8 siRNA complexes dissociated more gradually than the other linear lysine siRNA complexes. The K8 siRNA complexes started to dissociate more readily in low heparin concentration compared to other lysine peptide siRNA complexes; however, different to the other lysine peptide siRNA complexes, the dissociation rate of the K8 siRNA complexes decreased when the heparin increased. The reason for this could be that the K8 peptides were not strongly bound to either the siRNA or the heparin, therefore the K8 peptides which were dissociated from siRNA by heparin could be reversibly bound back to siRNA.

Nevertheless, the results showed that the different molecular sizes of the peptides gave rise to different binding properties to siRNA, with larger peptides interacting more strongly with siRNA.

Compared to L-PEI, B-PEI had a higher affinity to siRNA. This could be due to the fact that B-PEI (25kDa) is larger than L-PEI (22kDa). On the other hand, B-PEI contains primary, secondary and tertiary amine groups whereas L-PEI mainly consists of secondary amine group (von Harpe et al. 2000). It was shown that the primary amine group had more affinity than the secondary amine group to nucleic acids such as DNA.

Therefore, this may explain the reason why the B-PEI siRNA complexes were more difficult to dissociate than the L-PEI siRNA complexes.

5.3.4 The size and zeta potential of the complexes

The mean hydrodynamic size and zeta potential of the linear lysine peptide siRNA complexes could not be determined due to high polydispersity. In other words, the complexes formed from the linear lysine peptides and siRNA were either too heterogeneous in size or shape. By contrast, the Kbranch peptides could form uniquely sized complexes (monodisperse) with siRNA, showing that the branched lysine peptide was more effective in packaging siRNA than the linear lysine peptides.

Both B-PEI and L-PEI could form monodisperse complexes with siRNA. An increase in the N/P ratio of the B-PEI siRNA complexes was generally found to decrease the mean hydrodynamic size and zeta potential. By contrast, increasing the N/P ratio of the L-PEI siRNA complexes was found to generally increase the mean hydrodynamic size and zeta potential. This observation clearly suggested that B-PEI packaging siRNA in a different way to L-PEI. This difference could be due to the physical branched structure of the B-PEI or higher affinity of the B-PEI to siRNA.

5.3.5 The siRNA delivery efficiency of the complexes

From the siRNA transfection study using the Neuro 2a luciferase expressing model, it was found that only the B-PEI siRNA complexes could transfect the cells at a N/P ratio of 20:1. Other complex reagents used in the study such as the linear lysine, Kbranch

peptides and L-PEI were not able to do so. Indeed, it was not surprising that the linear lysine peptide siRNA complexes were not able to deliver siRNA to the cells since these complexes were not monodisperse nanoparticles. Therefore, it was predicted that those complexes would not be effective in delivering siRNA to the cells.

Unexpectedly, the Kbranch siRNA and L-PEI siRNA complexes, which formed positively charged monodisperse complexes with sizes around 100 nm, were not able to transfect the cells. The reason for this could be due to either no cellular uptake of the complexes, the siRNA failing to be released in the cytoplasm or the complexes being destroyed in the cells following endocytosis.

B-PEI was found to form positively charged monodisperse complexes with siRNA and mediated siRNA delivery. However, only the 20:1 N/P ratio of the complexes was effective in luciferase gene silencing. Further increasing the N/P ratio of these complexes to 40:1 resulted in a decrease of luciferase activity in the cells treated with both the B-PEI siLuc and B-PEI sieGFP complexes due to cell toxicity.

Compared to complexes formed by other polymers and siRNA with similar N/P ratios, the 20:1 N/P ratio B-PEI siRNA complexes required the highest amount of heparin to mediate complex dissociation. In order words, the B-PEI siRNA complexes with an N/P ratio of 20:1 were the most stable complexes in this study. Therefore, stability of the complex could be an important criterion for successful siRNA delivery. However, further increasing the N/P ratio of the B-PEI siRNA complexes to 40:1, which would improve the stability of the complexes, led to non-specific gene silencing and/or toxicity

(Grayson et al. 2006), showing that the balance between complex stability and the resulting cellular toxicity and/or non-specificity is important.

The results of the GAPDH gene silencing assay showed that the B-PEI siRNA complexes with a 20:1 N/P ratio could mediate specific gene silencing on other targeted genes. However, it was found that increasing the amount of siRNA within the complexes could induce cellular toxicity and/or non-specific gene silencing. The real time PCR results indicated that an increase of the amount of the siRNA within the complexes did not induce a non-specific gene silencing effect. This suggests that transfection with a large amount of the B-PEI siRNA complexes is toxic to the cells.

5.3.6 The relationship between the transfection efficiency and cellular binding and uptake of the complexes

Flow cytometry to measure the complex uptake showed that only B-PEI siRNA complexes and the positive control L2000 siRNA complexes could mediate cellular binding and uptake of the complexes. In particular, the L2000 siRNA complexes were more effective in mediating gene silencing.

The results of the confocal microscopy appeared to show that a large percentage of the siRNA delivered by the B-PEI siRNA complexes was localised in the nucleus whereas the siRNA delivered by L2000 siRNA complexes was mainly accumulated in the cytoplasm 30 minutes after transfection. This observation was consistent with the finding that the L2000 siRNA complexes mediated higher gene silencing efficacy than the B-PEI siRNA complexes. Interestingly, the possible reason that the siRNA delivered

by the B-PEI siRNA complexes localised in the nucleus could be due to the nuclear localisation ability of the B-PEI itself (Godbey et al. 1999).

The cell viability assay showed that the naked siRNA and other siRNA complexes used in the study were toxic to the cells. The toxicity of the naked siRNA or the complexes is summarised as follows:

Naked siRNA > KBranch+siRNA > L-PEI+siRNA > B-PEI+siRNA > L2000+siRNA

Interestingly, the naked siRNA, the Kbranch siRNA and L-PEI siRNA complexes, which were not able to mediate gene silencing, were relatively toxic to the cells. The L2000 siRNA complexes, which were more effective in siRNA delivery than the B-PEI siRNA complexes, were less toxic to the cells. These results indicated that improved siRNA delivery may decrease the siRNA induced toxicity to the cells.

5.3.7 The relationship between the biophysical properties and the transfection efficiency of the complexes

In this study, only the 20:1 N/P B-PEI siRNA complexes mediated gene silencing. **Table 5.4** summarises the biophysical properties of these complexes. As an effective siRNA delivery reagent, the B-PEI could encapsulate siRNA into a stable monodisperse particle with a size less than 100 nm, and a positively charged complex.

Best transfection reagent	N/P ratio	Condensation of DNA	Amount of heparin necessary to initiate complex dissociation (U/ml)	Heparin concentration necessary to allow complete dissociation (U/ml)	Average hydrodynamic size (nm)	Zeta potential (mV)
B-PEI	**20:1**	Complete	0.33	5.3	60	+42

Table 5.4 A summary of the biophysical properties of the B-PEI siRNA complexes at an N/P ratio of 20:1.

Other complex reagents such as the Kbranch peptide and L-PEI formed positively charged nano-sized particles with siRNA. However, the main difference between the B-PEI siRNA complexes and the Kbranch siRNA and L-PEI siRNA complexes was that B-PEI had a higher affinity to siRNA than the other complex reagents. In other words, the B-PEI siRNA complexes were the most stable complexes in this study.

5.3.8 Prediction of an ideal complex reagent for effective siRNA delivery

From this study, it was observed that three parameters were important for a successful siRNA delivery reagent; the physical structure and chemical composition of the reagent and the cellular toxicity mediated by the reagents. In terms of the physical structure, it appeared that a branched structure was probably more effective than a linear structure for siRNA packaging. For instance, the Kbranch peptides were similar to the linear

lysine peptides in terms of size; however, the Kbranch peptides packaged siRNA whereas the linear lysine peptides could not.

Larger molecular sizes could also be beneficial for siRNA packaging. Despite L-PEI (22kDa) and the linear lysine peptides (1-4 kDa) being linear in structure, L-PEI was more effective in packaging siRNA. Since siRNA are a rigid rod like structure (Gary et al. 2007), they are not flexible in folding to other conformations. Therefore, larger sized reagents with a branched structure may be more efficient in packaging siRNA because they may provide the flexibility required for siRNA packaging (Grayson & Godbey 2008).

This study showed that PEIs are more effective in packaging siRNA than the lysine peptides. This could also be due to the difference in the chemical composition between the PEI and the lysine peptides. PEIs are denser in amine groups than the lysine peptides per repeating unit. The high density of the amine groups enhances the electrostatic binding between the PEI and siRNA and increases the buffering capacity of PEI to improve endosomal escape of the siRNA complexes (Gary et al. 2007).

The siRNA delivery reagent should be non-toxic; otherwise, it will not be useful for basic research or clinical applications. In this study, it was found that B-PEI was the most effective siRNA delivery reagent apart from the L2000. However, B-PEI was toxic to the cells. To minimise PEI mediated toxicity, van Vliet and co-workers demonstrated that modifying the repeating unit of the PEI with varying proportions of methyl, benzyl, and n-dodecyl groups reduced the cellular toxicity (van Vliet et al. 2008).

Overall, these results suggest that an ideal siRNA complex reagent should be branched and large in molecular size to provide flexibility for siRNA packaging. Also, the complex reagent should have a high charge density to enhance siRNA binding, cellular uptake and endosomal escape. Moreover, the complex reagent should not be toxic to the cells.

5.4 Conclusion

The linear lysine peptides, namely K8, K16, K24 and K32, are not able to encapsulate siRNA and mediate siRNA delivery. Despite the observation that the Kbranch peptide and L-PEI can package siRNA and form a nanoparticle with a positive surface charge, these complexes are not able to mediate siRNA transfer. Only B-PEI can be used to package siRNA into a positively charged nanoparticle and mediate gene silencing. These results suggest that the size and chemical composition of the cationic polymers play an important role in mediating effective siRNA delivery.

Chapter 6

General discussion

6.1 Introduction

Since successful delivery of nucleic acids such as plasmid DNA or siRNA to specific cells is a powerful tool to treat diseases, there have been studies exploiting different polymer systems to deliver nucleic acids to the cells. Examples of these polymer systems include PEI (Grayson et al. 2006), polyarginine, polylysine (El-Sayed et al. 2008; Kumar et al. 2007), histidylated polylysine peptides (Leng et al. 2008), chitosan (Katas & Alpar 2006) and dendrimers (Patil et al. 2008). Despite many reports showing that these polymers can deliver nucleic acids to the cells, systematic studies on the requirements for a good polymer based nucleic acid delivery system have been limited. Therefore, this study aimed to clarify the requirements of a successful nucleic acid delivery system. This information could be useful for the development of new kinds of nucleic acid delivery system and/or further improvement of the existing systems.

There are two main cellular parameters limiting the efficiency of nucleic acid complex delivery mediated by polymers. Firstly, the complexes need to be able to bind and be taken up by the cells. Secondly, the complexes need to mediate endosomal escape and release the nucleic acids within the cells following cellular uptake. Complexes with positive charges and sizes on a nanometre scale would facilitate the cellular uptake processes. Positively charged complexes can interact with the negatively charged cell membrane. This interaction is believed to enhance cellular binding of the complex to the cell membrane which is rich in negatively charged molecules such as heparan sulfate proteoglycans and integrins (Gao et al. 2005; Grayson et al. 2006). Likewise, the size of the complex is crucial

for cellular uptake. Complexes with sizes larger than 50 nm could effectively be taken up by the cells through endocytosis (Gao et al. 2005). Once the complexes are taken up by the cells, they need to dissociate to release the plasmid DNA or siRNA from the vector system for their respective functions (Gary et al. 2007). The relative ability of DNA or siRNA unloading can be estimated through the dissociation properties of the complex system. Hence, it was hypothesised that a successful nucleic acid delivery system would demonstrate biophysical properties that include condensation and dissociation of nucleic acids and formation of a positively charged monodisperse nanoparticle.

In this study, the relationships between the biophysical and transfection properties of some well known polylysine and PEI based DNA delivery systems were investigated. The relationships between the biophysical and transfection properties of siRNA complexes formed from these complex reagents were then studied and compared with the results of the respective DNA complexes. Through this comparative study, the outcome could be useful for developing nucleic acid delivery systems to effectively deliver other kinds of nucleic acids such as siRNA.

As mentioned, polylysine and PEI were used in this study. The polylysine used included the linear lysine K8, K16, K24 and K32 and the Kbranch peptides. The linear lysine peptides used only differ in their sizes so this may help determine the relationship between the size and nucleic acid packaging and delivery efficacy. The Kbranch peptide has a similar size as the linear lysine peptides; therefore, the nucleic acid packaging properties of the Kbranch peptide can be used to compare with that of the linear lysines to find out the effect of different structure on the nucleic acid packaging. L-PEI and B-PEI were also used

in this study since they have a similar size, allowing the relationship between the structure of the complex reagent and nucleic acid complex formation and transfer to be studied. PEIs are larger in size than the lysine based peptides; therefore, comparing the results from the PEI complexes with the lysine based complexes may allow clarification of the effect of the complex reagent size and chemical composition on the nucleic acid complex formation and transfer.

6.2 Overall summary of the relationship between the biophysical properties and the transfection efficacy of the DNA complexes

All the complex reagents except the K8 peptide were able to form complexes with DNA which enabled them to transfect the cells with different efficiencies. Those complexes shared similar biophysical characteristics as expected. For instance, DNA was effectively packaged by the complex reagents to form monodisperse nanoparticles (> 50 nm) with positive surface charges. Moreover, all the complexes formed stable complexes which could withstand the challenge of different concentrations of heparin.

Despite the similarity of the biophysical properties, there are differences in the transfection efficacies which could be due to the abilities of the complexes to mediate cellular uptake and/or endosomal escape. In this study, PEIs were better transfection reagents than the Kbranch DNA complexes, and the Kbranch peptide was more effective than the linear lysine peptides.

In terms of cellular uptake, the Kbranch DNA and PEI DNA complexes were effectively taken up by the cells whereas the linear lysine DNA complexes were comparatively less effective in mediating cellular uptake. The Kbranch DNA complexes were expected to be more effective in cellular uptake than the linear lysine DNA complexes since the integrin targeting peptide on the Kbranch peptide could enhance the cellular binding and uptake of the complexes (Hart et al. 1995). Although the PEI DNA complexes behaved similarly in DNA condensation and nanoparticle formation as the linear lysine DNA complexes, they were more stable than the linear lysine DNA complexes as shown from the heparin induced complex dissociation assay. Gumbleton and Ramsay (2002) showed that complexes with higher stability resulted in higher cellular binding and uptake; the higher stability of the PEI DNA complexes could therefore improve cellular binding and uptake.

In term of endosomal escape, PEI DNA complexes were more effective than peptide DNA complexes in escaping from the endosome via the proton sponge effect (Boussif et al. 1995) whereas there are no such effective endosomal escape mechanisms for the lysine peptides (Read et al. 2005). As the PEI DNA complexes were more superior in mediating cellular uptake and endosomal escape than the linear lysine DNA complexes, they were more effective in transfection. Although the Kbranch DNA complexes mediated effective cellular uptake, the lack of an endosomal escape capacity may have led to less efficient transfection than the PEI DNA complexes.

L-PEI is more effective in transfection than B-PEI. The main difference observed between these complexes was the dissociation properties. This improved transfection capability

could be due to the fact that DNA is more easily dissociated from the L-PEI DNA complex than from the B-PEI DNA complex.

Overall, the most important characteristics of complexes for effective delivery of DNA to the cells would be the stability, size and surface charge of the complexes. The DNA should be stably condensed inside the complexes. The complexes needed to be able to withstand the heparin challenge to a certain level. With the hydrodynamic size larger than 50 nm and with a positive surface charge, the complexes would be able to mediate cellular uptake. It is expected that a successful siRNA delivery system would demonstrate these characteristics.

6.3 Overall summary of the relationship between the biophysical properties and the transfection efficacy of the siRNA complexes

The linear lysine and Kbranch peptides and PEI were used to form complexes with siRNA, and the biophysical properties of these complexes were examined. In the studies on the binding between the complex reagents and siRNA, it was found that the linear lysine peptides could not package and form monodisperse complexes with siRNA. On the other hand, the Kbranch peptide could package siRNA in a positively charged nanoparticle. Since the Kbranch and the linear lysine peptides were similar in size, this suggested that the branched rather than the linear structure of the peptide could enhance the condensation of siRNA.

Despite complex reagents with a linear structure being less effective in packaging siRNA, L-PEI was efficient in forming complexes with siRNA. The main differences between L-PEI and the linear lysine peptides are the size and chemical composition. L-PEI (22 kDa) is larger than the linear lysine peptides (1-4 kDa). With one nitrogen atom in every three atoms in a repeating unit (von Harpe et al. 2000), the charge density of L-PEI is higher than that of the linear lysine peptides. Therefore, complex reagents with a large size and high charge density are more effective in siRNA complex formation. Being branched, large and high charge density, B-PEI was an effective reagent to form complexes with siRNA.

From the heparin induced complex dissociation assay, it was observed that the binding between L-PEI and siRNA was similar to that between the Kbranch peptide and siRNA at similar N/P ratios. On the contrary, it was found that the binding between B-PEI and siRNA was stronger than that between L-PEI and siRNA at the same N/P ratio. This means that the L-PEI siRNA complexes and the Kbranch siRNA complexes were less stable than the B-PEI siRNA complexes. Compared to the L-PEI, which is linear and contains mainly secondary amine group, B-PEI is branched and consists of primary, secondary and tertiary amine groups. The branched structure and the primary amine group could enhance the binding between B-PEI and siRNA (Brissault et al 2006). The B-PEI siRNA complexes were the most heparin-resistant nanoparticle, and were in fact the most stable siRNA complexes compared in this study.

Indeed, the B-PEI siRNA complexes were the only complexes that induced gene silencing in transfection studies apart from the positive control L2000 siRNA complexes. Although the Kbranch peptides and L-PEI could encapsulate siRNA in a positively charged

monodisperse nanoparticle, these siRNA complexes did not mediate gene silencing. As mentioned, more stable complexes mediate better cellular binding and uptake of the complexes (Glumbleton and Ramsay 2002), which might explain the reason why the B-PEI siRNA complexes were more effective in mediating cellular uptake and siRNA delivery.

A study on the cellular uptake of the siRNA complexes using flow cytometry analysis showed that the Kbranch siRNA and L–PEI siRNA complexes did not mediate cellular uptake in the cells. Interestingly, it was found that the Kbranch siRNA and L-PEI siRNA complexes were also more toxic than the B-PEI siRNA and L2000 siRNA complexes which were able to mediate cellular uptake. This observation could suggest that the poor siRNA transfection efficacies of the Kbranch siRNA and L-PEI siRNA complexes might be related to the toxicity of these complexes.

Taken together, it was found that the physical structure and chemical composition of the complex reagents play an important role in forming complexes with siRNA. Large and branched structures with higher charge densities could allow the formation of stable monodisperse complexes for effective siRNA delivery. The large and branched structures could provide flexibility to encapsulate the small and rigid siRNA, which were inflexible in folding (Grayson & Godbey 2008). Higher charge density could enhance the binding to siRNA and improve the complex stability.

6.4 The biophysical properties of the best DNA transfection complexes were similar to those of the most effective siRNA transfection complexes

The best DNA transfection complexes, the L-PEI DNA complexes at N/P ratios of 10:1 and 20:1, shared similar biophysical properties with the most effective siRNA delivery complexes, the B-PEI siRNA complexes with a 20:1 N/P ratio. **Table 6.1** summarised their biophysical properties.

Best transfection performance	N/P ratio	Condensation of DNA or siRNA	Amount of heparin to initiate complex dissociation (U/ml)	Heparin concentration to allow complete dissociation (U/ml)	Average hydrodynamic size (nm)	Zeta potential (mV)
L-PEI + DNA	**10:1**	Complete	0.167	5.3	142	+37
L-PEI + DNA	**20:1**	Complete	0.33	5.3	79	+48
B-PEI + siRNA	**20:1**	Complete	0.33	5.3	60	+42

Table 6.1 A summary of the biophysical properties of the most effective DNA transfection and siRNA transfecion complexes.

The L-PEI DNA and B-PEI siRNA complexes performed similarly in the formation of nanoparticles with positive surface charges. Moreover, these complexes behaved similarly under the heparin challenge, indicating that they had a similar complex stability. This observation supported the notion that a successful nucleic acid delivery system shares similarity in biophysical properties which are important for cellular uptake and endosomal escape. To take it further, this indicated that other kinds of successful self-assembly

polymer-based nucleic acid delivery systems would demonstrate biophysical characteristics similar to these properties.

6.5 Different packaging requirements of DNA and siRNA because of the differences in their sizes and chemical compositions

siRNA is small in size, usually 21 base pair long. As a ribonucleotide, the persistence length, which represents the tendency of a chain to persist in a given conformation and is directly proportional to the helix rigidity, of a double stranded RNA is around 70 nm (Kebbekus et al. 1995); therefore, siRNA, which is less than 30 nm in length, are a very rigid structure and are not flexible in folding. Comparatively, the plasmid DNA used in the study is around 5 kb. Since the persistence length of deoxyribonucleic acids is around 50 nm (Hagerman 1997), this infers that the plasmid DNA is more flexible in folding and easier to condense. As a result, it is easier to form complexes with DNA. Since the siRNA is more rigid, the complex reagents used may need to be (1) more flexible in folding and (2) denser in charge to compromise the inflexibility of the siRNA.

(1) Flexibility of the complex reagents

In terms of flexibility of the complex reagents, linear structures have less rotational freedom in folding than branched structures. Also, smaller sized complex reagents are more rigid than larger complex reagents (Grayson & Godbey 2008). Therefore, the flexibility of the complex reagents used in this study in an ascending order is as follows:

Linear lysine peptides < Kbranch < L-PEI < B-PEI

In this study, it was shown that all the complex reagents can package and form nanoparticles with plasmid DNA but not siRNA. As discussed previously, the reasons for this could be due to the fact that plasmid DNA is more flexible in folding and condensing within a complex. On the other hand, to form a nanoparticle with siRNA, it seems that a more flexible complex reagent is needed.

The results shown in Chapter Five suggested that complex reagents with a larger size could be useful to package siRNA. For example, although both linear lysine peptides and L-PEI are linear in structure, L-PEI is able to encapsulate siRNA but not the linear lysine peptides, suggesting that the size of the reagents plays a role in siRNA packaging.

The structure of the complex reagents such as a linear or branched formation is also important for siRNA complex formation. For instance, Kbranch, but not linear lysine peptides, can package siRNA. Although both L-PEI and B-PEI can encapsulate siRNA, only the B-PEI siRNA complex mediated gene silencing. This again indicates that the branched structure is superior for siRNA complex formation. As shown from an image from atomic force microscopy **(Appendix III**), it seems that a L-PEI siRNA complex is in a rod shape whereas a B-PEI siRNA complex is in a spherical shape. This indicates that different structures would lead to different ways of siRNA complex formation, which in turn affects the efficacy for siRNA delivery.

Other studies have shown that large and branched polymers such as dendrimers, branched histidylated polylysine peptides, chitosan, which is a large branched structure, are all useful for siRNA delivery. Howard and co-workers found that although high molecular weight chitosan can mediate siRNA delivery, low molecular weight chistosan cannot do so (Howard et al. 2006). This again indicates that a flexible structure is needed to package siRNA. Similar to the findings in this study, Grayson and co-workers demonstrated that L-PEI was not able to deliver siRNA *in vitro* whereas B-PEI was able to form complexes with siRNA and mediate gene silencing (Grayson et al. 2006). All in all, polymers with large and branched structures seem to be important features for siRNA packaging and delivery.

(2) High charge density

Other than the size and structure of the complex reagent, the charge density of the repeating unit within the complex reagent may play an important role in complex formation. One example is that the L-PEI, which has a higher charge density within a repeating unit than that of the lysine based peptides, package siRNA better. Another example was shown by Kumar and co-workers and in this study **(Appendix IV)** that a short arginine peptide (R9), which consists of 9 arginines in a row, can package siRNA and form a nanoparticle (Kumar et al. 2007). Indeed, the structure and size of the R9 peptide is similar to that of the K8 peptide, except that the R9 peptide is denser in charge.

In term of the gene silencing ability of the R9 siRNA complexes, however, unlike the finding from Kumar and co-workers which used a similar arginine based peptide and showed gene silencing efficacy, the results from this study showed that these siRNA

arginine based peptide complexes were not able to mediate gene silencing **(Appendix IV)**. Nevertheless, it seemed that a higher charge density would facilitate siRNA complex formation.

6.6 Conclusion and future work

This study showed that complex reagents need to have different properties for efficient DNA or siRNA delivery. For DNA delivery, the complex reagents need to form a positive surface charge complex with DNA to mediate cellular binding and uptake. Within the cells, the complex reagents need to mediate endosomal escape to allow the plasmid DNA to traffick to the nucleus for transcription. On the other hand, siRNA delivery has proven to be more challenging. It was found that even though some of the complex regents can form siRNA nanoparticles with positive surface charges, not all of them can mediate cellular uptake. The data presented in this study suggested that a large and branched structure of a complex reagent is an important feature for siRNA complex formation and delivery.

In the future, further studies could be done to establish the effect of different branched structures on siRNA packaging and the effect of modifying the backbone of the polymer to improve the siRNA delivery efficiency and decrease toxicity. To enhance cellular uptake of the complex, a ligand or antibody could be conjugated with the polymer.

References

Allen, L. A. & Aderem, A. 1996, "Mechanisms of phagocytosis", *Curr.Opin.Immunol.*, vol. 8, no. 1, pp. 36-40.

Allerson, C. R., Sioufi, N., Jarres, R., Prakash, T. P., Naik, N., Berdeja, A., Wanders, L., Griffey, R. H., Swayze, E. E., & Bhat, B. 2005, "Fully 2'-modified oligonucleotide duplexes with improved in vitro potency and stability compared to unmodified small interfering RNA", *J.Med.Chem.*, vol. 48, no. 4, pp. 901-904.

Alnylam Pharmaceuticals., 2008, "Alnylam Achieves First Human Proof of Concept for an RNAi Therapeutic with GEMINI study", *Alnylam Pharmaceuticals web site* [online] <http://phx.corporate-ir.net/phoenix.zhtml?c=148005&p=irol-newsArticle2&ID=1113937&highlight=>

Bainbridge, J. W., Smith, A. J., Barker, S. S., Robbie, S., Henderson, R., Balaggan, K., Viswanathan, A., Holder, G. E., Stockman, A., Tyler, N., Petersen-Jones, S., Bhattacharya, S. S., Thrasher, A. J., Fitzke, F. W., Carter, B. J., Rubin, G. S., Moore, A. T., & Ali, R. R. 2008, "Effect of gene therapy on visual function in Leber's congenital amaurosis", *N.Engl.J.Med.*, vol. 358, no. 21, pp. 2231-2239.

Balicki, D., Putnam, C. D., Scaria, P. V., & Beutler, E. 2002, "Structure and function correlation in histone H2A peptide-mediated gene transfer", *Proc.Natl.Acad.Sci.U.S.A*, vol. 99, no. 11, pp. 7467-7471.

Banan, M. & Puri, N. 2004, "The ins and outs of RNAi in mammalian cells", *Curr.Pharm.Biotechnol.*, vol. 5, no. 5, pp. 441-450.

Bartlett, D. W. & Davis, M. E. 2006, "Insights into the kinetics of siRNA-mediated gene silencing from live-cell and live-animal bioluminescent imaging", *Nucleic Acids Res.*, vol. 34, no. 1, pp. 322-333.

Belting, M., Sandgren, S., & Wittrup, A. 2005, "Nuclear delivery of macromolecules: barriers and carriers", *Adv.Drug Deliv.Rev.*, vol. 57, no. 4, pp. 505-527.

Benitec Limited., 2009, "Benitec and City of Hope human trial update", *Benitec Limited web site* [online] <http://www.benitec.com/documents/pr_BLTCoHupdate_06may09.pdf and http://www.abnnewswire.net/media/en/docs/60084-ASX-BLT-538981.pdf>

Bennett, M. J., Aberle, A. M., Balasubramaniam, R. P., Malone, J. G., Malone, R. W., & Nantz, M. H. 1997, "Cationic lipid-mediated gene delivery to murine lung: correlation of lipid hydration with in vivo transfection activity", *J.Med.Chem.*, vol. 40, no. 25, pp. 4069-4078.

Berezikov, E., Chung, W. J., Willis, J., Cuppen, E. & Lai, E. C., 2007, “Mammalian mirtron genes”, *Mol. Cell.,* vol. 28, pp. 328-36.

Bernstein, E., Caudy, A. A., Hammond, S. M., & Hannon, G. J. 2001, "Role for a bidentate ribonuclease in the initiation step of RNA interference", *Nature*, vol. 409, no. 6818, pp. 363-366.

Bielinska, A. U., Chen, C., Johnson, J., & Baker, J. R., Jr. 1999, "DNA complexing with polyamidoamine dendrimers: implications for transfection", *Bioconjug.Chem.*, vol. 10, no. 5, pp. 843-850.

Birmingham, A., Anderson, E. M., Reynolds, A., Ilsley-Tyree, D., Leake, D., Fedorov, Y., Baskerville, S., Maksimova, E., Robinson, K., Karpilow, J., Marshall, W. S., & Khvorova, A. 2006, "3' UTR seed matches, but not overall identity, are associated with RNAi off-targets", *Nat.Methods*, vol. 3, no. 3, pp. 199-204.

Bishop, N. E. 1997, "An Update on Non-clathrin-coated Endocytosis", *Rev.Med.Virol.*, vol. 7, no. 4, pp. 199-209.

Bitko, V., Musiyenko, A., Shulyayeva, O., & Barik, S. 2005, "Inhibition of respiratory viruses by nasally administered siRNA", *Nat Med*, vol. 11, no. 1, pp. 50-55.

Blaese, R. M., Culver, K. W., Miller, A. D., Carter, C. S., Fleisher, T., Clerici, M., Shearer, G., Chang, L., Chiang, Y., Tolstoshev, P., Greenblatt, J. J., Rosenberg, S. A., Klein, H., Berger, M., Mullen, C. A., Ramsey, W. J., Muul, L., Morgan, R. A., & Anderson, W. F. 1995, "T lymphocyte-directed gene therapy for ADA- SCID: initial trial results after 4 years", *Science*, vol. 270, no. 5235, pp. 475-480.

Boussif, O., Lezoualc'h, F., Zanta, M. A., Mergny, M. D., Scherman, D., Demeneix, B., & Behr, J. P. 1995, "A versatile vector for gene and oligonucleotide transfer into cells in culture and in vivo: polyethylenimine", *Proc.Natl.Acad.Sci.U.S.A*, vol. 92, no. 16, pp. 7297-7301.

Boussif, O., Zanta, M. A., & Behr, J. P. 1996, "Optimized galenics improve in vitro gene transfer with cationic molecules up to 1000-fold", *Gene Ther.*, vol. 3, no. 12, pp. 1074-1080.

Brissault, B., Leborgne, C., Guis, C., Danos, O., Cheradame, H., & Kichler, A. 2006, "Linear topology confers in vivo gene transfer activity to polyethylenimines", *Bioconjug.Chem.*, vol. 17, no. 3, pp. 759-765.

Brodsky, F. M., Chen, C. Y., Knuehl, C., Towler, M. C., & Wakeham, D. E. 2001, "Biological basket weaving: formation and function of clathrin-coated vesicles", *Annu.Rev.Cell Dev.Biol.*, vol. 17, pp. 517-568.

Brooks, H., Lebleu, B., & Vives, E. 2005, "Tat peptide-mediated cellular delivery: back to basics", *Adv.Drug Deliv.Rev.*, vol. 57, no. 4, pp. 559-577.

Brummelkamp, T. R., Bernards, R., & Agami, R. 2002, "Stable suppression of tumorigenicity by virus-mediated RNA interference", *Cancer Cell*, vol. 2, no. 3, pp. 243-247.

Brunner, S., Sauer, T., Carotta, S., Cotten, M., Saltik, M., & Wagner, E. 2000, "Cell cycle dependence of gene transfer by lipoplex, polyplex and recombinant adenovirus", *Gene Ther.*, vol. 7, no. 5, pp. 401-407.

Cardoso, A. L., Simoes, S., de Almeida, L. P., Plesnila, N., Pedroso de Lima, M. C., Wagner, E., & Culmsee, C. 2008, "Tf-lipoplexes for neuronal siRNA delivery: a promising system to mediate gene silencing in the CNS", *J.Control Release*, vol. 132, no. 2, pp. 113-123.

Cavazzana-Calvo, M., Thrasher, A., & Mavilio, F. 2004, "The future of gene therapy", *Nature*, vol. 427, no. 6977, pp. 779-781.

Cerutti, H. & J. A. Casas-Mollano 2006, "On the origin and functions of RNA-mediated silencing: from protists to man." *Curr Genet.,* vol. 50, no.2, pp. 81-99.

Check, E. 2002, "A tragic setback", *Nature*, vol. 420, pp. 116-118.

Check, E. 2003, "Harmful potential of viral vectors fuels doubts over gene therapy", *Nature*, vol. 423, no. 6940, pp. 573-574.

Chen, C. C., Sun, C. P., Ma, H. I., Fang, C. C., Wu, P. Y., Xiao, X., & Tao, M. H. 2009, "Comparative study of anti-hepatitis B virus RNA interference by double-stranded adeno-associated virus serotypes 7, 8, and 9", *Mol.Ther.*, vol. 17, no. 2, pp. 352-359.

Chesnoy, S. & Huang, L. 2000, "Structure and function of lipid-DNA complexes for gene delivery", *Annu.Rev.Biophys.Biomol.Struct.*, vol. 29, pp. 27-47.

Choi, I., Cho, B. R., Kim, D., Miyagawa, S., Kubo, T., Kim, J. Y., Park, C. G., Hwang, W. S., Lee, J. S., & Ahn, C. 2005, "Choice of the adequate detection time for the accurate evaluation of the efficiency of siRNA-induced gene silencing", *J.Biotechnol.*, vol. 120, no. 3, pp. 251-261.

ClinicalTrial.gov., 2009, "A Dose Escalation Trial of an Intravitreal Injection of Sirna-027 in Patients With Subfoveal Choroidal Neovascularization (CNV) Secondary to Age-Related Macular Degeneration (AMD)", *ClinicalTrial.gov web site* [online] <http://clinicaltrials.gov/ct2/show/NCT00363714>

Cogoni, C. & Macino, G. 2000, "Post-transcriptional gene silencing across kingdoms", *Curr.Opin.Genet.Dev.*, vol. 10, no. 6, pp. 638-643.

Colin, M., Maurice, M., Trugnan, G., Kornprobst, M., Harbottle, R. P., Knight, A., Cooper, R. G., Miller, A. D., Capeau, J., Coutelle, C., & Brahimi-Horn, M. C. 2000, "Cell delivery, intracellular trafficking and expression of an integrin-mediated gene transfer

vector in tracheal epithelial cells", *Gene Ther.*, vol. 7, no. 2, pp. 139-152.

Conner, S. D. & Schmid, S. L. 2003, "Regulated portals of entry into the cell", *Nature*, vol. 422, no. 6927, pp. 37-44.

Couzin, J. 2002, "Breakthrough of the year. Small RNAs make big splash", *Science*, vol. 298, no. 5602, pp. 2296-2297.

Crooke, S. T. 2004, "Antisense strategies", *Curr.Mol.Med.*, vol. 4, no. 5, pp. 465-487.

Dash, P. R., Read, M. L., Barrett, L. B., Wolfert, M. A., & Seymour, L. W. 1999, "Factors affecting blood clearance and in vivo distribution of polyelectrolyte complexes for gene delivery", *Gene Ther.*, vol. 6, no. 4, pp. 643-650.

Dieffenbach, C. W. & Dveksler, G. S. 2003, *PCR primer,* Cold Spring Habor Laboratory Press, Cold Spring Harbor, New York.

Dileo, J., Miller, T. E., Jr., Chesnoy, S., & Huang, L. 2003, "Gene transfer to subdermal tissues via a new gene gun design", *Hum.Gene Ther.*, vol. 14, no. 1, pp. 79-87.

Donsante, A., Miller, D. G., Li, Y., Vogler, C., Brunt, E. M., Russell, D. W., & Sands, M. S. 2007, "AAV vector integration sites in mouse hepatocellular carcinoma", *Science*, vol. 317, no. 5837, p. 477.

Dunlap, D. D., Maggi, A., Soria, M. R., & Monaco, L. 1997, "Nanoscopic structure of DNA condensed for gene delivery", *Nucleic Acids Res.*, vol. 25, no. 15, pp. 3095-3101.

Edelstein, M. 2008, *Gene Therapy Trials Worldwide*, The Journal of Gene Medicine, John Wiley and Sons Inc. Available from: <http://www.wiley.co.uk/genmed/clinical/>

El Aneed, A. 2004, "An overview of current delivery systems in cancer gene therapy", *J.Control Release*, vol. 94, no. 1, pp. 1-14.

El Sayed, A., Khalil, I. A., Kogure, K., Futaki, S., & Harashima, H. 2008, "Octaarginine- and octalysine-modified nanoparticles have different modes of endosomal escape", *J.Biol.Chem.*, vol. 283, no. 34, pp. 23450-23461.

Emery, D. W., Yannaki, E., Tubb, J., & Stamatoyannopoulos, G. 2000, "A chromatin insulator protects retrovirus vectors from chromosomal position effects", *Proc.Natl.Acad.Sci.U.S.A*, vol. 97, no. 16, pp. 9150-9155.

Erbacher, P., Roche, A. C., Monsigny, M., & Midoux, P. 1996, "Putative role of chloroquine in gene transfer into a human hepatoma cell line by DNA/lactosylated polylysine complexes", *Exp.Cell Res.*, vol. 225, no. 1, pp. 186-194.

Eulalio, A., Behm-Ansmant, I., Schweizer, D., & Izaurralde, E. 2007, "P-body formation

is a consequence, not the cause, of RNA-mediated gene silencing", *Mol.Cell Biol.*, vol. 27, no. 11, pp. 3970-3981.

Faneca, H., Simoes, S., & de Lima, M. C. 2002, "Evaluation of lipid-based reagents to mediate intracellular gene delivery", *Biochim.Biophys.Acta*, vol. 1567, no. 1-2, pp. 23-33.

Farhood, H., Serbina, N., & Huang, L. 1995, "The role of dioleoyl phosphatidylethanolamine in cationic liposome mediated gene transfer", *Biochim.Biophys.Acta*, vol. 1235, no. 2, pp. 289-295.

Fedorov, Y., King, A., Anderson, E., Karpilow, J., Ilsley, D., Marshall, W., & Khvorova, A. 2005, "Different delivery methods-different expression profiles", *Nat.Methods*, vol. 2, no. 4, p. 241.

Felgner, P. L., Gadek, T. R., Holm, M., Roman, R., Chan, H. W., Wenz, M., Northrop, J. P., Ringold, G. M., & Danielsen, M. 1987, "Lipofection: a highly efficient, lipid-mediated DNA-transfection procedure", *Proc.Natl.Acad.Sci.U.S.A*, vol. 84, no. 21, pp. 7413-7417.

Felgner, P. L. & Ringold, G. M. 1989, "Cationic liposome-mediated transfection", *Nature*, vol. 337, no. 6205, pp. 387-388.

Ferber, D. 2001, "Gene therapy. Safer and virus-free?", *Science*, vol. 294, no. 5547, pp. 1638-1642.

Ferrari, A., Pellegrini, V., Arcangeli, C., Fittipaldi, A., Giacca, M., & Beltram, F. 2003, "Caveolae-mediated internalization of extracellular HIV-1 tat fusion proteins visualized in real time", *Mol.Ther.*, vol. 8, no. 2, pp. 284-294.

Fire, A., Xu, S., Montgomery, M. K., Kostas, S. A., Driver, S. E., & Mello, C. C. 1998, "Potent and specific genetic interference by double-stranded RNA in Caenorhabditis elegans", *Nature*, vol. 391, no. 6669, pp. 806-811.

Flotte, T. R. 2004, "Gene therapy progress and prospects: recombinant adeno-associated virus (rAAV) vectors", *Gene Ther.*, vol. 11, no. 10, pp. 805-810.

Gao, H., Shi, W., & Freund, L. B. 2005, "Mechanics of receptor-mediated endocytosis", *Proc.Natl.Acad.Sci.U.S.A*, vol. 102, no. 27, pp. 9469-9474.

Gao, X. & Huang, L. 1991, "A novel cationic liposome reagent for efficient transfection of mammalian cells", *Biochem.Biophys.Res.Commun.*, vol. 179, no. 1, pp. 280-285.

Gary, D. J., Puri, N., & Won, Y. Y. 2007, "Polymer-based siRNA delivery: perspectives on the fundamental and phenomenological distinctions from polymer-based DNA delivery", *J.Control Release*, vol. 121, no. 1-2, pp. 64-73.

Gaspar, H. B., Bjorkegren, E., Parsley, K., Gilmour, K. C., King, D., Sinclair, J., Zhang, F., Giannakopoulos, A., Adams, S., Fairbanks, L. D., Gaspar, J., Henderson, L., Xu-Bayford, J. H., Davies, E. G., Veys, P. A., Kinnon, C., & Thrasher, A. J. 2006, "Successful

reconstitution of immunity in ADA-SCID by stem cell gene therapy following cessation of PEG-ADA and use of mild preconditioning", *Mol.Ther.*, vol. 14, no. 4, pp. 505-513.

Gautam, A., Densmore, C. L., Xu, B., & Waldrep, J. C. 2000, "Enhanced gene expression in mouse lung after PEI-DNA aerosol delivery", *Mol.Ther.*, vol. 2, no. 1, pp. 63-70.

Ge, Q., Filip, L., Bai, A., Nguyen, T., Eisen, H. N., & Chen, J. 2004, "Inhibition of influenza virus production in virus-infected mice by RNA interference", *Proc.Natl.Acad.Sci.U.S.A*, vol. 101, no. 23, pp. 8676-8681.

Giering, J. C., Grimm, D., Storm, T. A., & Kay, M. A. 2008, "Expression of shRNA from a tissue-specific pol II promoter is an effective and safe RNAi therapeutic", *Mol.Ther.*, vol. 16, no. 9, pp. 1630-1636.

Giladi, H., Ketzinel-Gilad, M., Rivkin, L., Felig, Y., Nussbaum, O., & Galun, E. 2003, "Small interfering RNA inhibits hepatitis B virus replication in mice", *Mol.Ther.*, vol. 8, no. 5, pp. 769-776.

Godbey, W. T., Wu, K. K., & Mikos, A. G. 1999, "Poly(ethylenimine) and its role in gene delivery", *J.Control Release*, vol. 60, no. 2-3, pp. 149-160.

Goldstein, D. A., Tinland, B., Gilbertson, L. A., Staub, J. M., Bannon, G. A., Goodman, R. E., McCoy, R. L., & Silvanovich, A. 2005, "Human safety and genetically modified plants: a review of antibiotic resistance markers and future transformation selection technologies", *J.Appl.Microbiol.*, vol. 99, no. 1, pp. 7-23.

Goldstein, J. L., Brown, M. S., Anderson, R. G., Russell, D. W., & Schneider, W. J. 1985, "Receptor-mediated endocytosis: concepts emerging from the LDL receptor system", *Annu.Rev.Cell Biol.*, vol. 1, pp. 1-39.

Golzio, M., Mazzolini, L., Ledoux, A., Paganin, A., Izard, M., Hellaudais, L., Bieth, A., Pillaire, M. J., Cazaux, C., Hoffmann, J. S., Couderc, B., & Teissie, J. 2007, "In vivo gene silencing in solid tumors by targeted electrically mediated siRNA delivery", *Gene Ther.*, vol. 14, no. 9, pp. 752-759.

Gong, Q., Huntsman, C., & Ma, D. 2008, "Clathrin-independent internalization and recycling", *J.Cell Mol.Med.*, vol. 12, no. 1, pp. 126-144.

Gorman, C. M., Howard, B. H., & Reeves, R. 1983, "Expression of recombinant plasmids in mammalian cells is enhanced by sodium butyrate", *Nucleic Acids Res.*, vol. 11, no. 21, pp. 7631-7648.

Goula, D., Remy, J. S., Erbacher, P., Wasowicz, M., Levi, G., Abdallah, B., & Demeneix, B. A. 1998, "Size, diffusibility and transfection performance of linear PEI/DNA complexes in the mouse central nervous system", *Gene Ther.*, vol. 5, no. 5, pp. 712-717.

Goverdhana, S., Puntel, M., Xiong, W., Zirger, J. M., Barcia, C., Curtin, J. F., Soffer, E. B., Mondkar, S., King, G. D., Hu, J., Sciascia, S. A., Candolfi, M., Greengold, D. S.,

Lowenstein, P. R., & Castro, M. G. 2005, "Regulatable gene expression systems for gene therapy applications: progress and future challenges", *Mol.Ther.*, vol. 12, no. 2, pp. 189-211.

Grayson, A. C., Doody, A. M., & Putnam, D. 2006, "Biophysical and structural characterization of polyethylenimine-mediated siRNA delivery in vitro", *Pharm.Res.*, vol. 23, no. 8, pp. 1868-1876.

Grayson, S. M. & Godbey, W. T. 2008, "The role of macromolecular architecture in passively targeted polymeric carriers for drug and gene delivery", *J.Drug Target*, vol. 16, no. 5, pp. 329-356.

Green, N. K., Morrison, J., Hale, S., Briggs, S. S., Stevenson, M., Subr, V., Ulbrich, K., Chandler, L., Mautner, V., Seymour, L. W., & Fisher, K. D. 2008, "Retargeting polymer-coated adenovirus to the FGF receptor allows productive infection and mediates efficacy in a peritoneal model of human ovarian cancer", *J.Gene Med.*, vol. 10, no. 3, pp. 280-289.

Gregory, R. I., Chendrimada, T. P., Cooch, N., & Shiekhattar, R. 2005, "Human RISC couples microRNA biogenesis and posttranscriptional gene silencing", *Cell*, vol. 123, no. 4, pp. 631-640.

Gregory, R. I., Chendrimada, T. P., & Shiekhattar, R. 2006, "MicroRNA biogenesis: isolation and characterization of the microprocessor complex", *Methods Mol.Biol.*, vol. 342, pp. 33-47.

Griesenbach, U., Geddes, D. M., & Alton, E. W. 2004, "Gene therapy for cystic fibrosis: an example for lung gene therapy", *Gene Ther.*, vol. 11 Suppl 1, p. S43-S50.

Grimm, D., Streetz, K. L., Jopling, C. L., Storm, T. A., Pandey, K., Davis, C. R., Marion, P., Salazar, F., & Kay, M. A. 2006, "Fatality in mice due to oversaturation of cellular microRNA/short hairpin RNA pathways", *Nature*, vol. 441, no. 7092, pp. 537-541.

Grunweller, A., Wyszko, E., Bieber, B., Jahnel, R., Erdmann, V. A., & Kurreck, J. 2003, "Comparison of different antisense strategies in mammalian cells using locked nucleic acids, 2'-O-methyl RNA, phosphorothioates and small interfering RNA", *Nucleic Acids Res.*, vol. 31, no. 12, pp. 3185-3193.

Guerrier-Takada, C., Gardiner, K., Marsh, T., Pace, N., & Altman, S. 1983, "The RNA moiety of ribonuclease P is the catalytic subunit of the enzyme", *Cell*, vol. 35, no. 3 Pt 2, pp. 849-857.

Guo, S. & Kemphues, K. J. 1995, "par-1, a gene required for establishing polarity in C. elegans embryos, encodes a putative Ser/Thr kinase that is asymmetrically distributed", *Cell*, vol. 81, no. 4, pp. 611-620.

Gupta, B., Levchenko, T. S., & Torchilin, V. P. 2005, "Intracellular delivery of large molecules and small particles by cell-penetrating proteins and peptides", *Adv.Drug Deliv.Rev.*, vol. 57, no. 4, pp. 637-651.

Hagerman, P. J. 1997, "Flexibility of RNA", *Annu.Rev.Biophys.Biomol.Struct.*, vol. 26, pp. 139-156.

Hall, A. H., Wan, J., Shaughnessy, E. E., Ramsay, S. B., & Alexander, K. A. 2004, "RNA interference using boranophosphate siRNAs: structure-activity relationships", *Nucleic Acids Res.*, vol. 32, no. 20, pp. 5991-6000.

Hammond, S. M., Caudy, A. A., & Hannon, G. J. 2001, "Post-transcriptional gene silencing by double-stranded RNA", *Nat.Rev.Genet.*, vol. 2, no. 2, pp. 110-119.

Harris, J., Werling, D., Hope, J. C., Taylor, G., & Howard, C. J. 2002, "Caveolae and caveolin in immune cells: distribution and functions", *Trends Immunol.*, vol. 23, no. 3, pp. 158-164.

Hart, S. L. 2005, "Lipid carriers for gene therapy", *Curr.Drug Deliv.*, vol. 2, no. 4, pp. 423-428.

Hart, S. L., Arancibia-Carcamo, C. V., Wolfert, M. A., Mailhos, C., O'Reilly, N. J., Ali, R. R., Coutelle, C., George, A. J., Harbottle, R. P., Knight, A. M., Larkin, D. F., Levinsky, R. J., Seymour, L. W., Thrasher, A. J., & Kinnon, C. 1998, "Lipid-mediated enhancement of transfection by a nonviral integrin-targeting vector", *Hum.Gene Ther.*, vol. 9, no. 4, pp. 575-585.

Hart, S. L., Harbottle, R. P., Cooper, R., Miller, A., Williamson, R., & Coutelle, C. 1995, "Gene delivery and expression mediated by an integrin-binding peptide", *Gene Ther.*, vol. 2, no. 8, pp. 552-554.

Hart, S. L., Knight, A. M., Harbottle, R. P., Mistry, A., Hunger, H. D., Cutler, D. F., Williamson, R., & Coutelle, C. 1994, "Cell binding and internalization by filamentous phage displaying a cyclic Arg-Gly-Asp-containing peptide", *J.Biol.Chem.*, vol. 269, no. 17, pp. 12468-12474.

Heil, F., Ahmad-Nejad, P., Hemmi, H., Hochrein, H., Ampenberger, F., Gellert, T., Dietrich, H., Lipford, G., Takeda, K., Akira, S., Wagner, H., & Bauer, S. 2003, "The Toll-like receptor 7 (TLR7)-specific stimulus loxoribine uncovers a strong relationship within the TLR7, 8 and 9 subfamily", *Eur.J.Immunol.*, vol. 33, no. 11, pp. 2987-2997.

Hopkins, A. L. & Groom, C. R. 2002, "The druggable genome", *Nat.Rev.Drug Discov.*, vol. 1, no. 9, pp. 727-730.

Hornung, V., Guenthner-Biller, M., Bourquin, C., Ablasser, A., Schlee, M., Uematsu, S., Noronha, A., Manoharan, M., Akira, S., de Fougerolles, A., Endres, S., & Hartmann, G. 2005, "Sequence-specific potent induction of IFN-alpha by short interfering RNA in plasmacytoid dendritic cells through TLR7", *Nat.Med.*, vol. 11, no. 3, pp. 263-270.

Howard, K. A., Rahbek, U. L., Liu, X., Damgaard, C. K., Glud, S. Z., Andersen, M. O., Hovgaard, M. B., Schmitz, A., Nyengaard, J. R., Besenbacher, F., & Kjems, J. 2006, "RNA interference in vitro and in vivo using a novel chitosan/siRNA nanoparticle

system", *Mol.Ther.*, vol. 14, no. 4, pp. 476-484.

Hunt, K. K. & Vorburger, S. A. 2002, "Hurdles and Hopes for Cancer Treatment" *Science*, vol. 297, pp. 415-416.

Hutvagner, G. & Zamore, P. D. 2002, "A microRNA in a multiple-turnover RNAi enzyme complex", *Science*, vol. 297, no. 5589, pp. 2056-2060.

Ignowski, J. M. & Schaffer, D. V. 2004, "Kinetic analysis and modeling of firefly luciferase as a quantitative reporter gene in live mammalian cells", *Biotechnol.Bioeng.*, vol. 86, no. 7, pp. 827-834.

Jackson, A. L., Bartz, S. R., Schelter, J., Kobayashi, S. V., Burchard, J., Mao, M., Li, B., Cavet, G., & Linsley, P. S. 2003, "Expression profiling reveals off-target gene regulation by RNAi", *Nat.Biotechnol.*, vol. 21, no. 6, pp. 635-637.

Jackson, A. L., Burchard, J., Leake, D., Reynolds, A., Schelter, J., Guo, J., Johnson, J. M., Lim, L., Karpilow, J., Nichols, K., Marshall, W., Khvorova, A., & Linsley, P. S. 2006, "Position-specific chemical modification of siRNAs reduces "off-target" transcript silencing", *RNA.*, vol. 12, no. 7, pp. 1197-1205.

Jagannath, A. & Wood, M. J. 2009, "Localization of double-stranded small interfering RNA to cytoplasmic processing bodies is Ago2 dependent and results in up-regulation of GW182 and Argonaute-2", *Mol.Biol.Cell*, vol. 20, no. 1, pp. 521-529.

Jakymiw, A., Lian, S., Eystathioy, T., Li, S., Satoh, M., Hamel, J. C., Fritzler, M. J., & Chan, E. K. 2005, "Disruption of GW bodies impairs mammalian RNA interference", *Nat.Cell Biol.*, vol. 7, no. 12, pp. 1267-1274.

Jans, D. A. & Hubner, S. 1996, "Regulation of protein transport to the nucleus: central role of phosphorylation", *Physiol Rev.*, vol. 76, no. 3, pp. 651-685.

Jenkins, R. G., Meng, Q. H., Hodges, R. J., Lee, L. K., Bottoms, S. E., Laurent, G. J., Willis, D., Ayazi, S. P., McAnulty, R. J., & Hart, S. L. 2003, "Formation of LID vector complexes in water alters physicochemical properties and enhances pulmonary gene expression in vivo", *Gene Ther.*, vol. 10, no. 12, pp. 1026-1034.

Jing, Q., Huang, S., Guth, S., Zarubin, T., Motoyama, A., Chen, J., Di Padova, F., Lin, S. C., Gram, H., & Han, J. 2005, "Involvement of microRNA in AU-rich element-mediated mRNA instability", *Cell*, vol. 120, no. 5, pp. 623-634.

John, M., Constien, R., Akinc, A., Goldberg, M., Moon, Y. A., Spranger, M., Hadwiger, P., Soutschek, J., Vornlocher, H. P., Manoharan, M., Stoffel, M., Langer, R., Anderson, D. G., Horton, J. D., Koteliansky, V., & Bumcrot, D. 2007, "Effective RNAi-mediated gene silencing without interruption of the endogenous microRNA pathway", *Nature*, vol. 449, no. 7163, pp. 745-747.

Judge, A. D., Bola, G., Lee, A. C., & MacLachlan, I. 2006, "Design of noninflammatory synthetic siRNA mediating potent gene silencing in vivo", *Mol.Ther.*, vol. 13, no. 3, pp. 494-505.

Judge, A. D., Sood, V., Shaw, J. R., Fang, D., McClintock, K., & MacLachlan, I. 2005, "Sequence-dependent stimulation of the mammalian innate immune response by synthetic siRNA", *Nat.Biotechnol.*, vol. 23, no. 4, pp. 457-462.

Juliano, R., Alam, M. R., Dixit, V., & Kang, H. 2008, "Mechanisms and strategies for effective delivery of antisense and siRNA oligonucleotides", *Nucleic Acids Res.*, vol. 36, no. 12, pp. 4158-4171.

Kaiser, J. 2004, "Gene therapy. Side effects sideline hemophilia trial", *Science*, vol. 304, no. 5676, pp. 1423-1425.

Kaneda, Y., Iwai, K., & Uchida, T. 1989, "Increased expression of DNA cointroduced with nuclear protein in adult rat liver", *Science*, vol. 243, no. 4889, pp. 375-378.

Katas, H. & Alpar, H. O. 2006, "Development and characterisation of chitosan nanoparticles for siRNA delivery", *J.Control Release*, vol. 115, no. 2, pp. 216-225.

Kay, M. A., Liu, D., & Hoogerbrugge, P. M. 1997, "Gene therapy", *Proc.Natl.Acad.Sci.U.S.A*, vol. 94, no. 24, pp. 12744-12746.

Kay, M. A. & Nakai, H. 2003, "Looking into the safety of AAV vectors", *Nature*, vol. 424, no. 6946, p. 251.

Kebbekus, P., Draper, D. E., & Hagerman, P. 1995, "Persistence length of RNA", *Biochemistry*, vol. 34, no. 13, pp. 4354-4357.

Khalil, I. A., Futaki, S., Niwa, M., Baba, Y., Kaji, N., Kamiya, H., & Harashima, H. 2004, "Mechanism of improved gene transfer by the N-terminal stearylation of octaarginine: enhanced cellular association by hydrophobic core formation", *Gene Ther.*, vol. 11, no. 7, pp. 636-644.

Khalil, I. A., Kogure, K., Akita, H., & Harashima, H. 2006, "Uptake pathways and subsequent intracellular trafficking in nonviral gene delivery", *Pharmacol.Rev.*, vol. 58, no. 1, pp. 32-45.

Kichler, A., Leborgne, C., Coeytaux, E., & Danos, O. 2001, "Polyethylenimine-mediated gene delivery: a mechanistic study", *J.Gene Med.*, vol. 3, no. 2, pp. 135-144.

Kim, D. H. & Rossi, J. J. 2007, "Strategies for silencing human disease using RNA interference", *Nat.Rev.Genet.*, vol. 8, no. 3, pp. 173-184.

Kim, H. H., Choi, H. S., Yang, J. M., & Shin, S. 2007, "Characterization of gene delivery in vitro and in vivo by the arginine peptide system", *Int.J.Pharm.*, vol. 335, no. 1-2, pp. 70-78.

Kim, V. N., Han, J. & Siomi, M. C., 2009, "Biogenesis of small RNAs in animals", *Nat. Rev. Mol. Cell. Biol.,*vol. 10, pp. 126-39.

Kircheis, R., Schuller, S., Brunner, S., Ogris, M., Heider, K. H., Zauner, W., & Wagner, E. 1999, "Polycation-based DNA complexes for tumor-targeted gene delivery in vivo", *J.Gene Med.*, vol. 1, no. 2, pp. 111-120.

Klein, C., Bock, C. T., Wedemeyer, H., Wustefeld, T., Locarnini, S., Dienes, H. P., Kubicka, S., Manns, M. P., & Trautwein, C. 2003, "Inhibition of hepatitis B virus replication in vivo by nucleoside analogues and siRNA", *Gastroenterology*, vol. 125, no. 1, pp. 9-18.

Kobayashi, N., Nishikawa, M., Hirata, K., & Takakura, Y. 2004, "Hydrodynamics-based procedure involves transient hyperpermeability in the hepatic cellular membrane: implication of a nonspecific process in efficient intracellular gene delivery", *J.Gene Med.*, vol. 6, no. 5, pp. 584-592.

Koltover, I., Salditt, T., Radler, J. O., & Safinya, C. R. 1998, "An inverted hexagonal phase of cationic liposome-DNA complexes related to DNA release and delivery", *Science*, vol. 281, no. 5373, pp. 78-81.

Kopatz, I., Remy, J. S., & Behr, J. P. 2004, "A model for non-viral gene delivery: through syndecan adhesion molecules and powered by actin", *J.Gene Med.*, vol. 6, no. 7, pp. 769-776.

Koping-Hoggard, M., Tubulekas, I., Guan, H., Edwards, K., Nilsson, M., Varum, K. M., & Artursson, P. 2001, "Chitosan as a nonviral gene delivery system. Structure-property relationships and characteristics compared with polyethylenimine in vitro and after lung administration in vivo", *Gene Ther.*, vol. 8, no. 14, pp. 1108-1121.

Kreppel, F. & Kochanek, S. 2008, "Modification of adenovirus gene transfer vectors with synthetic polymers: a scientific review and technical guide", *Mol.Ther.*, vol. 16, no. 1, pp. 16-29.

Kruger, K., Grabowski, P. J., Zaug, A. J., Sands, J., Gottschling, D. E., & Cech, T. R. 1982, "Self-splicing RNA: autoexcision and autocyclization of the ribosomal RNA intervening sequence of Tetrahymena", *Cell*, vol. 31, no. 1, pp. 147-157.

Kukowska-Latallo, J. F., Chen, C., Eichman, J., Bielinska, A. U., & Baker, J. R., Jr. 1999, "Enhancement of dendrimer-mediated transfection using synthetic lung surfactant exosurf neonatal in vitro", *Biochem.Biophys.Res.Commun.*, vol. 264, no. 1, pp. 253-261.

Kumar, P., Wu, H., McBride, J. L., Jung, K. E., Kim, M. H., Davidson, B. L., Lee, S. K., Shankar, P., & Manjunath, N. 2007, "Transvascular delivery of small interfering RNA to the central nervous system", *Nature*, vol. 448, no. 7149, pp. 39-43.

Kurreck, J. 2003, "Antisense technologies. Improvement through novel chemical

modifications", *Eur.J.Biochem.*, vol. 270, no. 8, pp. 1628-1644.

Kwoh, D. Y., Coffin, C. C., Lollo, C. P., Jovenal, J., Banaszczyk, M. G., Mullen, P., Phillips, A., Amini, A., Fabrycki, J., Bartholomew, R. M., Brostoff, S. W., & Carlo, D. J. 1999, "Stabilization of poly-L-lysine/DNA polyplexes for in vivo gene delivery to the liver", *Biochim.Biophys.Acta*, vol. 1444, no. 2, pp. 171-190.

Landen, C. N., Jr., Chavez-Reyes, A., Bucana, C., Schmandt, R., Deavers, M. T., Lopez-Berestein, G., & Sood, A. K. 2005, "Therapeutic EphA2 gene targeting in vivo using neutral liposomal small interfering RNA delivery", *Cancer Res.*, vol. 65, no. 15, pp. 6910-6918.

Larson, S. D., Jackson, L. N., Chen, L. A., Rychahou, P. G., & Evers, B. M. 2007, "Effectiveness of siRNA uptake in target tissues by various delivery methods", *Surgery*, vol. 142, no. 2, pp. 262-269.

Lee, J., Chuang, T. H., Redecke, V., She, L., Pitha, P. M., Carson, D. A., Raz, E., & Cottam, H. B. 2003, "Molecular basis for the immunostimulatory activity of guanine nucleoside analogs: activation of Toll-like receptor 7", *Proc.Natl.Acad.Sci.U.S.A*, vol. 100, no. 11, pp. 6646-6651.

Lee, K. Y., Kwon, I. C., Kim, Y. H., Jo, W. H., & Jeong, S. Y. 1998, "Preparation of chitosan self-aggregates as a gene delivery system", *J.Control Release*, vol. 51, no. 2-3, pp. 213-220.

Lee, R. J. & Huang, L. 1996, "Folate-targeted, anionic liposome-entrapped polylysine-condensed DNA for tumor cell-specific gene transfer", *J.Biol.Chem.*, vol. 271, no. 14, pp. 8481-8487.

Leng, Q., Scaria, P., Lu, P., Woodle, M. C., & Mixson, A. J. 2008, "Systemic delivery of HK Raf-1 siRNA polyplexes inhibits MDA-MB-435 xenografts", *Cancer Gene Ther.*, vol. 15, no. 8, pp. 485-495.

Leung, R. K. & Whittaker, P. A. 2005, "RNA interference: from gene silencing to gene-specific therapeutics", *Pharmacol.Ther.*, vol. 107, no. 2, pp. 222-239.

Lewis, D. L. & Wolff, J. A. 2007, "Systemic siRNA delivery via hydrodynamic intravascular injection", *Adv.Drug Deliv.Rev.*, vol. 59, no. 2-3, pp. 115-123.

Li, C. X., Parker, A., Menocal, E., Xiang, S., Borodyansky, L., & Fruehauf, J. H. 2006, "Delivery of RNA interference", *Cell Cycle*, vol. 5, no. 18, pp. 2103-2109.

Li, M. J., Kim, J., Li, S., Zaia, J., Yee, J.K., Anderson, J., Akkina, R., Rossi, J. J., 2005, "Long-term inhibition of HIV-1 infection in primary hematopoietic cells by lentiviral vector delivery of a triple combination of anti-HIV shRNA, anti-CCR5 ribozyme, and a nucleolar-localizing TAR decoy." *Mol. Ther.*, vol. 12, no. 5, pp. 900-9.

Li, S. D., Chono, S., & Huang, L. 2008, "Efficient oncogene silencing and metastasis inhibition via systemic delivery of siRNA", *Mol.Ther.*, vol. 16, no. 5, pp. 942-946.

Li, S. & Huang, L. 2000 Nonviral gene therapy: promises and challenges. *Gene Ther,* vol 7**,** pp. 31-4.

Li, S. D. & Huang, L. 2006, "Gene therapy progress and prospects: non-viral gene therapy by systemic delivery", *Gene Ther.*, vol. 13, no. 18, pp. 1313-1319.

Lima, W. F. & Crooke, S. T. 1997, "Cleavage of single strand RNA adjacent to RNA-DNA duplex regions by Escherichia coli RNase H1", *J.Biol.Chem.*, vol. 272, no. 44, pp. 27513-27516.

Liu, F., Nishikawa, M., Clemens, P. R., & Huang, L. 2001, "Transfer of full-length Dmd to the diaphragm muscle of Dmd(mdx/mdx) mice through systemic administration of plasmid DNA", *Mol.Ther.*, vol. 4, no. 1, pp. 45-51.

Lundberg, M., Wikstrom, S., & Johansson, M. 2003, "Cell surface adherence and endocytosis of protein transduction domains", *Mol.Ther.*, vol. 8, no. 1, pp. 143-150.

Ma, J. B., Yuan, Y. R., Meister, G., Pei, Y., Tuschl, T., & Patel, D. J. 2005a, "Structural basis for 5'-end-specific recognition of guide RNA by the A. fulgidus Piwi protein", *Nature*, vol. 434, no. 7033, pp. 666-670.

Ma, Z., Li, J., He, F., Wilson, A., Pitt, B., & Li, S. 2005b, "Cationic lipids enhance siRNA-mediated interferon response in mice", *Biochem.Biophys.Res.Commun.*, vol. 330, no. 3, pp. 755-759.

Maguire, A. M., Simonelli, F., Pierce, E. A., Pugh, E. N., Jr., Mingozzi, F., Bennicelli, J., Banfi, S., Marshall, K. A., Testa, F., Surace, E. M., Rossi, S., Lyubarsky, A., Arruda, V. R., Konkle, B., Stone, E., Sun, J., Jacobs, J., Dell'Osso, L., Hertle, R., Ma, J. X., Redmond, T. M., Zhu, X., Hauck, B., Zelenaia, O., Shindler, K. S., Maguire, M. G., Wright, J. F., Volpe, N. J., McDonnell, J. W., Auricchio, A., High, K. A., & Bennett, J. 2008, "Safety and efficacy of gene transfer for Leber's congenital amaurosis", *N.Engl.J.Med.*, vol. 358, no. 21, pp. 2240-2248.

Makridou, P., Burnett, C., Landy, T., & Howard, K. 2003, "Hygromycin B-selected cell lines from GAL4-regulated pUAST constructs", *Genesis.*, vol. 36, no. 2, pp. 83-87.

Malvern Instruments Ltd. 2009, "Dynamic Light Scattering", *Malvern Instruments Ltd. web site* [online] <http://www.malvern.co.uk/LabEng/technology/dynamic_light_scattering/dynamic_light_scattering.htm>

Malvern Instruments Ltd. 2009b, "Zeta potential measurement using laser Doppler electrophoresis", *Malvern Instruments Ltd. web site* [online] <http://www.malvern.co.uk/LabEng/technology/zeta_potential/zeta_potential_LDE.htm>

Manoharan, M. 2002, "Oligonucleotide conjugates as potential antisense drugs with improved uptake, biodistribution, targeted delivery, and mechanism of action", *Antisense Nucleic Acid Drug Dev.*, vol. 12, no. 2, pp. 103-128.

Marshall, E. 2000, "Improving gene therapy's tool kit", *Science*, vol. 288, no. 5468, p. 953.

Matsui, H., Johnson, L. G., Randell, S. H., & Boucher, R. C. 1997, "Loss of binding and entry of liposome-DNA complexes decreases transfection efficiency in differentiated airway epithelial cells", *J.Biol.Chem.*, vol. 272, no. 2, pp. 1117-1126.

Matveev, S., Li, X., Everson, W., & Smart, E. J. 2001, "The role of caveolae and caveolin in vesicle-dependent and vesicle-independent trafficking", *Adv.Drug Deliv.Rev.*, vol. 49, no. 3, pp. 237-250.

Maxfield, F. R. & McGraw, T. E. 2004, "Endocytic recycling", *Nat.Rev.Mol.Cell Biol.*, vol. 5, no. 2, pp. 121-132.

McBride, J. L., Boudreau, R. L., Harper, S. Q., Staber, P. D., Monteys, A. M., Martins, I., Gilmore, B. L., Burstein, H., Peluso, R. W., Polisky, B., Carter, B. J., & Davidson, B. L. 2008, "Artificial miRNAs mitigate shRNA-mediated toxicity in the brain: implications for the therapeutic development of RNAi", *Proc.Natl.Acad.Sci.U.S.A*, vol. 105, no. 15, pp. 5868-5873.

McLachlan, G., Davidson, D. J., Stevenson, B. J., Dickinson, P., Davidson-Smith, H., Dorin, J. R., & Porteous, D. J. 1995, "Evaluation in vitro and in vivo of cationic liposome-expression construct complexes for cystic fibrosis gene therapy", *Gene Ther.*, vol. 2, no. 9, pp. 614-622.

Meier, O. & Greber, U. F. 2003, "Adenovirus endocytosis", *J.Gene Med.*, vol. 5, no. 6, pp. 451-462.

Melchior, F. & Gerace, L. 1995, "Mechanisms of nuclear protein import", *Curr.Opin.Cell Biol.*, vol. 7, no. 3, pp. 310-318.

Meyer, M. & Wagner, E. 2006, "Recent developments in the application of plasmid DNA-based vectors and small interfering RNA therapeutics for cancer", *Hum.Gene Ther.*, vol. 17, no. 11, pp. 1062-1076.

Minakuchi, Y., Takeshita, F., Kosaka, N., Sasaki, H., Yamamoto, Y., Kouno, M., Honma, K., Nagahara, S., Hanai, K., Sano, A., Kato, T., Terada, M., & Ochiya, T. 2004, "Atelocollagen-mediated synthetic small interfering RNA delivery for effective gene silencing in vitro and in vivo", *Nucleic Acids Res.*, vol. 32, no. 13, p. e109.

Mislick, K. A., Baldeschwieler, J. D., Kayyem, J. F., & Meade, T. J. 1995, "Transfection of folate-polylysine DNA complexes: evidence for lysosomal delivery", *Bioconjug.Chem.*, vol. 6, no. 5, pp. 512-515.

Monahan, P. E., Jooss, K., & Sands, M. S. 2002, "Safety of adeno-associated virus gene therapy vectors: a current evaluation", *Expert.Opin.Drug Saf*, vol. 1, no. 1, pp. 79-91.

Murphy D. B. 2002, *Fundamental of Light Microscopy and Electronic Imaging*, 1st edition, Wiley-Liss Inc., New York.

Mustapa, M. F., Bell, P. C., Hurley, C. A., Nicol, A., Guenin, E., Sarkar, S., Writer, M. J., Barker, S. E., Wong, J. B., Pilkington-Miksa, M. A., Papahadjopoulos-Sternberg, B., Shamlou, P. A., Hailes, H. C., Hart, S. L., Zicha, D., & Tabor, A. B. 2007, "Biophysical characterization of an integrin-targeted lipopolyplex gene delivery vector", *Biochemistry*, vol. 46, no. 45, pp. 12930-12944.

Nakase, I., Niwa, M., Takeuchi, T., Sonomura, K., Kawabata, N., Koike, Y., Takehashi, M., Tanaka, S., Ueda, K., Simpson, J. C., Jones, A. T., Sugiura, Y., & Futaki, S. 2004, "Cellular uptake of arginine-rich peptides: roles for macropinocytosis and actin rearrangement", *Mol.Ther.*, vol. 10, no. 6, pp. 1011-1022.

Napoli, C., Lemieux, C., & Jorgensen, R. 1990, "Introduction of a Chimeric Chalcone Synthase Gene into Petunia Results in Reversible Co-Suppression of Homologous Genes in trans", *Plant Cell*, vol. 2, no. 4, pp. 279-289.

Nelson, D. L. & Cox, M. M. 2004, *Lehninger Principles of Biochemistry*, 4th edition, W. H. Freeman & Co., New York.

Newman, C. M. & Bettinger, T. 2007, "Gene therapy progress and prospects: ultrasound for gene transfer", *Gene Ther.*, vol. 14, no. 6, pp. 465-475.

Nichols, B. 2003, "Caveosomes and endocytosis of lipid rafts", *J.Cell Sci.*, vol. 116, no. Pt 23, pp. 4707-4714.

Niculescu-Duvaz, D., Heyes, J., & Springer, C. J. 2003, "Structure-activity relationship in cationic lipid mediated gene transfection", *Curr.Med.Chem.*, vol. 10, no. 14, pp. 1233-1261.

Ogris, M., Carlisle, R. C., Bettinger, T., & Seymour, L. W. 2001, "Melittin enables efficient vesicular escape and enhanced nuclear access of nonviral gene delivery vectors", *J.Biol.Chem.*, vol. 276, no. 50, pp. 47550-47555.

Ogris, M., Steinlein, P., Kursa, M., Mechtler, K., Kircheis, R., & Wagner, E. 1998, "The size of DNA/transferrin-PEI complexes is an important factor for gene expression in cultured cells", *Gene Ther.*, vol. 5, no. 10, pp. 1425-1433.

Okamura, K., Hagen, J. W., Duan, H., Tyler, D. M. & Lai, E. C., 2007, “The mirtron pathway generates microRNA-class regulatory RNAs in Drosophila”, *Cell,* vol. 130, pp. 89-100.

Opko Health., 2007, “OPKO Health Initiates Phase 3 Trial of Bevasiranib for the Treatment of AMD”, *Opko Health web site* [online]

<http://investor.opko.com/releasedetail.cfm?ReleaseID=255940>

Opko Health., 2009, “OPKO Health Announces Update on Phase III Clinical Trial of Bevasiranib”, *Opko Health web site* [online] <http://investor.opko.com/releasedetail.cfm?ReleaseID=369294>

Paddison, P. J., Caudy, A. A., Bernstein, E., Hannon, G. J., & Conklin, D. S. 2002, "Short hairpin RNAs (shRNAs) induce sequence-specific silencing in mammalian cells", *Genes Dev.*, vol. 16, no. 8, pp. 948-958.

Park, T. G., Jeong, J. H., & Kim, S. W. 2006, "Current status of polymeric gene delivery systems", *Adv.Drug Deliv.Rev.*, vol. 58, no. 4, pp. 467-486.

Parton, R. G., Joggerst, B., & Simons, K. 1994, "Regulated internalization of caveolae", *J.Cell Biol.*, vol. 127, no. 5, pp. 1199-1215.

Patil, M. L., Zhang, M., Betigeri, S., Taratula, O., He, H., & Minko, T. 2008, "Surface-modified and internally cationic polyamidoamine dendrimers for efficient siRNA delivery", *Bioconjug.Chem.*, vol. 19, no. 7, pp. 1396-1403.

Pelkmans, L., Kartenbeck, J., & Helenius, A. 2001, "Caveolar endocytosis of simian virus 40 reveals a new two-step vesicular-transport pathway to the ER", *Nat.Cell Biol.*, vol. 3, no. 5, pp. 473-483.

Perales, J. C., Grossmann, G. A., Molas, M., Liu, G., Ferkol, T., Harpst, J., Oda, H., & Hanson, R. W. 1997, "Biochemical and functional characterization of DNA complexes capable of targeting genes to hepatocytes via the asialoglycoprotein receptor", *J.Biol.Chem.*, vol. 272, no. 11, pp. 7398-7407.

Pillai, R. S., Bhattacharyya, S. N., & Filipowicz, W. 2007, "Repression of protein synthesis by miRNAs: how many mechanisms?", *Trends Cell Biol.*, vol. 17, no. 3, pp. 118-126.

Preall, J. B., He, Z., Gorra, J. M., & Sontheimer, E. J. 2006, "Short interfering RNA strand selection is independent of dsRNA processing polarity during RNAi in Drosophila", *Curr.Biol.*, vol. 16, no. 5, pp. 530-535.

Ramsay, E. & Gumbleton, M. 2002, "Polylysine and polyornithine gene transfer complexes: a study of complex stability and cellular uptake as a basis for their differential in-vitro transfection efficiency", *J.Drug Target*, vol. 10, no. 1, pp. 1-9.

Ramsay, E., Hadgraft, J., Birchall, J., & Gumbleton, M. 2000, "Examination of the biophysical interaction between plasmid DNA and the polycations, polylysine and polyornithine, as a basis for their differential gene transfection in-vitro", *Int.J.Pharm.*, vol. 210, no. 1-2, pp. 97-107.

Rand, T. A., Petersen, S., Du, F., & Wang, X. 2005, "Argonaute2 cleaves the anti-guide

strand of siRNA during RISC activation", *Cell*, vol. 123, no. 4, pp. 621-629.

Read, M. L., Singh, S., Ahmed, Z., Stevenson, M., Briggs, S. S., Oupicky, D., Barrett, L. B., Spice, R., Kendall, M., Berry, M., Preece, J. A., Logan, A., & Seymour, L. W. 2005, "A versatile reducible polycation-based system for efficient delivery of a broad range of nucleic acids", *Nucleic Acids Res.*, vol. 33, no. 9, p. e86.

Reynolds, A., Leake, D., Boese, Q., Scaringe, S., Marshall, W. S., & Khvorova, A. 2004, "Rational siRNA design for RNA interference", *Nat.Biotechnol.*, vol. 22, no. 3, pp. 326-330.

Richard, J. P., Melikov, K., Vives, E., Ramos, C., Verbeure, B., Gait, M. J., Chernomordik, L. V., & Lebleu, B. 2003, "Cell-penetrating peptides. A reevaluation of the mechanism of cellular uptake", *J.Biol.Chem.*, vol. 278, no. 1, pp. 585-590.

Robbins, M., Judge, A., Ambegia, E., Choi, C., Yaworski, E., Palmer, L., McClintock, K., & MacLachlan, I. 2008, "Misinterpreting the therapeutic effects of siRNA caused by immune stimulation", *Hum.Gene Ther.*, vol. 19, no. 10, pp. 991-999.

Romano, N. & Macino, G. 1992, "Quelling: transient inactivation of gene expression in Neurospora crassa by transformation with homologous sequences", *Mol.Microbiol.*, vol. 6, no. 22, pp. 3343-3353.

Rosenberg, S. A., Aebersold, P., Cornetta, K., Kasid, A., Morgan, R. A., Moen, R., Karson, E. M., Lotze, M. T., Yang, J. C., Topalian, S. L., & . 1990, "Gene transfer into humans--immunotherapy of patients with advanced melanoma, using tumor-infiltrating lymphocytes modified by retroviral gene transduction", *N.Engl.J.Med.*, vol. 323, no. 9, pp. 570-578.

Ruby, J. G., Jan, C. H. & Bartel, D. P., 2007, “Intronic microRNA precursors that bypass Drosha processing”, *Nature,* vol. 448, pp. 83-6.

Saito, M., Mazda, O., Takahashi, K. A., Arai, Y., Kishida, T., Shin-Ya, M., Inoue, A., Tonomura, H., Sakao, K., Morihara, T., Imanishi, J., Kawata, M., & Kubo, T. 2007, "Sonoporation mediated transduction of pDNA/siRNA into joint synovium in vivo", *J.Orthop.Res.*, vol. 25, no. 10, pp. 1308-1316.

Sambrook, J. & Russell, D. W. 2001, *Molecular cloing: A laboratory manual*, Cold Spring Harbor Laboratory Press, Cold Spring Habour, New York.

Sazani, P. & Kole, R. 2003, "Therapeutic potential of antisense oligonucleotides as modulators of alternative splicing", *J.Clin.Invest*, vol. 112, no. 4, pp. 481-486.

Schaffer, D. V., Fidelman, N. A., Dan, N., & Lauffenburger, D. A. 2000, "Vector unpacking as a potential barrier for receptor-mediated polyplex gene delivery", *Biotechnol.Bioeng.*, vol. 67, no. 5, pp. 598-606.

Schaffer, D. V. & Lauffenburger, D. A. 1998, "Optimization of cell surface binding enhances efficiency and specificity of molecular conjugate gene delivery", *J.Biol.Chem.*, vol. 273, no. 43, pp. 28004-28009.

Scherer, L. J. & Rossi, J. J. 2003, "Approaches for the sequence-specific knockdown of mRNA", *Nat.Biotechnol.*, vol. 21, no. 12, pp. 1457-1465.

Schmid, S. L. 1997, "Clathrin-coated vesicle formation and protein sorting: an integrated process", *Annu.Rev.Biochem.*, vol. 66, pp. 511-548.

Selkirk, S. M. 2004, "Gene therapy in clinical medicine", *Postgrad.Med.J.*, vol. 80, no. 948, pp. 560-570.

Sen, G. L. & Blau, H. M. 2005, "Argonaute 2/RISC resides in sites of mammalian mRNA decay known as cytoplasmic bodies", *Nat.Cell Biol.*, vol. 7, no. 6, pp. 633-636.

Shapiro, H. M. 2003 *Practical Flow Cytometry*, 4th edition, John Wiley and Sons Inc., Hoboken, New Jersey.

Shim, M. S. & Kwon, Y. J. 2008, "Controlled delivery of plasmid DNA and siRNA to intracellular targets using ketalized polyethylenimine", *Biomacromolecules.*, vol. 9, no. 2, pp. 444-455.

Simoes, S., Slepushkin, V., Pires, P., Gaspar, R., de Lima, M. P., & Duzgunes, N. 1999, "Mechanisms of gene transfer mediated by lipoplexes associated with targeting ligands or pH-sensitive peptides", *Gene Ther.*, vol. 6, no. 11, pp. 1798-1807.

Singh, R., Tian, B., & Kostarelos, K. 2008, "Artificial envelopment of nonenveloped viruses: enhancing adenovirus tumor targeting in vivo", *FASEB J.*, vol. 22, no. 9, pp. 3389-3402.

Sioud, M. & Sorensen, D. R. 2003, "Cationic liposome-mediated delivery of siRNAs in adult mice", *Biochem.Biophys.Res.Commun.*, vol. 312, no. 4, pp. 1220-1225.

Smart, E. J., Graf, G. A., McNiven, M. A., Sessa, W. C., Engelman, J. A., Scherer, P. E., Okamoto, T., & Lisanti, M. P. 1999, "Caveolins, liquid-ordered domains, and signal transduction", *Mol.Cell Biol.*, vol. 19, no. 11, pp. 7289-7304.

Soutschek, J., Akinc, A., Bramlage, B., Charisse, K., Constien, R., Donoghue, M., Elbashir, S., Geick, A., Hadwiger, P., Harborth, J., John, M., Kesavan, V., Lavine, G., Pandey, R. K., Racie, T., Rajeev, K. G., Rohl, I., Toudjarska, I., Wang, G., Wuschko, S., Bumcrot, D., Koteliansky, V., Limmer, S., Manoharan, M., & Vornlocher, H. P. 2004, "Therapeutic silencing of an endogenous gene by systemic administration of modified siRNAs", *Nature*, vol. 432, no. 7014, pp. 173-178.

Stepanenko, O. V., Verkhusha, V. V., Kuznetsova, I. M., Uversky, V. N., & Turoverov, K. K. 2008, "Fluorescent proteins as biomarkers and biosensors: throwing color lights on

molecular and cellular processes", *Curr.Protein Pept.Sci.*, vol. 9, no. 4, pp. 338-369.

Sternberg, B., Hong, K., Zheng, W., & Papahadjopoulos, D. 1998, "Ultrastructural characterization of cationic liposome-DNA complexes showing enhanced stability in serum and high transfection activity in vivo", *Biochim.Biophys.Acta*, vol. 1375, no. 1-2, pp. 23-35.

Stoll, S. M., Sclimenti, C. R., Baba, E. J., Meuse, L., Kay, M. A., & Calos, M. P. 2001, "Epstein-Barr virus/human vector provides high-level, long-term expression of alpha1-antitrypsin in mice", *Mol.Ther.*, vol. 4, no. 2, pp. 122-129.

Sullenger, B. A. & Gilboa, E. 2002, "Emerging clinical applications of RNA", *Nature*, vol. 418, no. 6894, pp. 252-258.

Sundaram, S., Lee, L. K., & Roth, C. M. 2007, "Interplay of polyethyleneimine molecular weight and oligonucleotide backbone chemistry in the dynamics of antisense activity", *Nucleic Acids Res.*, vol. 35, no. 13, pp. 4396-4408.

Sundaram, S., Viriyayuthakorn, S., & Roth, C. M. 2005, "Oligonucleotide structure influences the interactions between cationic polymers and oligonucleotides", *Biomacromolecules.*, vol. 6, no. 6, pp. 2961-2968.

Suzuki, T., Nishida, K., Kakutani, K., Maeno, K., Yurube, T., Takada, T., Kurosaka, M., & Doita, M. 2009, "Sustained long-term RNA interference in nucleus pulposus cells in vivo mediated by unmodified small interfering RNA", *Eur.Spine J.*, vol. 18, no. 2, pp. 263-70.

Swanson, J. A. & Watts, C. 1995, "Macropinocytosis", *Trends Cell Biol.*, vol. 5, no. 11, pp. 424-428.

Takei, K. & Haucke, V. 2001, "Clathrin-mediated endocytosis: membrane factors pull the trigger", *Trends Cell Biol.*, vol. 11, no. 9, pp. 385-391.

Tang, M. X. & Szoka, F. C. 1997, "The influence of polymer structure on the interactions of cationic polymers with DNA and morphology of the resulting complexes", *Gene Ther.*, vol. 4, no. 8, pp. 823-832.

Thomas, C. E., Ehrhardt, A., & Kay, M. A. 2003, "Progress and problems with the use of viral vectors for gene therapy", *Nat.Rev.Genet.*, vol. 4, no. 5, pp. 346-358.

Thoren, P. E., Persson, D., Isakson, P., Goksor, M., Onfelt, A., & Norden, B. 2003, "Uptake of analogs of penetratin, Tat(48-60) and oligoarginine in live cells", *Biochem.Biophys.Res.Commun.*, vol. 307, no. 1, pp. 100-107.

Thornhill, S. I., Schambach, A., Howe, S. J., Ulaganathan, M., Grassman, E., Williams, D., Schiedlmeier, B., Sebire, N. J., Gaspar, H. B., Kinnon, C., Baum, C., & Thrasher, A. J. 2008, "Self-inactivating gammaretroviral vectors for gene therapy of X-linked severe combined immunodeficiency", *Mol.Ther.*, vol. 16, no. 3, pp. 590-598.

Tomari, Y., Matranga, C., Haley, B., Martinez, N., & Zamore, P. D. 2004, "A protein sensor for siRNA asymmetry", *Science*, vol. 306, no. 5700, pp. 1377-1380.

Toub, N., Malvy, C., Fattal, E., & Couvreur, P. 2006, "Innovative nanotechnologies for the delivery of oligonucleotides and siRNA", *Biomed.Pharmacother.*, vol. 60, no. 9, pp. 607-620.

Trehin, R. & Merkle, H. P. 2004, "Chances and pitfalls of cell penetrating peptides for cellular drug delivery", *Eur.J.Pharm.Biopharm.*, vol. 58, no. 2, pp. 209-223.

Tsien, R. Y. 1998, "The green fluorescent protein", *Annu.Rev.Biochem.*, vol. 67, pp. 509-544.

Uchida, H., Tanaka, T., Sasaki, K., Kato, K., Dehari, H., Ito, Y., Kobune, M., Miyagishi, M., Taira, K., Tahara, H., & Hamada, H. 2004, "Adenovirus-mediated transfer of siRNA against survivin induced apoptosis and attenuated tumor cell growth in vitro and in vivo", *Mol.Ther.*, vol. 10, no. 1, pp. 162-171.

Urban-Klein, B., Werth, S., Abuharbeid, S., Czubayko, F., & Aigner, A. 2005, "RNAi-mediated gene-targeting through systemic application of polyethylenimine (PEI)-complexed siRNA in vivo", *Gene Ther.*, vol. 12, no. 5, pp. 461-466.

Valencia-Sanchez, M. A., Liu, J., Hannon, G. J., & Parker, R. 2006, "Control of translation and mRNA degradation by miRNAs and siRNAs", *Genes Dev.*, vol. 20, no. 5, pp. 515-524.

Van Vliet, L. D., Chapman, M. R., Avenier, F., Kitson, C. Z., & Hollfelder, F. 2008, "Relating chemical and biological diversity space: a tunable system for efficient gene transfection", *Chembiochem.*, vol. 9, no. 12, pp. 1960-1967.

Verma, I. M. & Somia, N. 1997, "Gene therapy -- promises, problems and prospects", *Nature*, vol. 389, no. 6648, pp. 239-242.

Vermeulen, A., Behlen, L., Reynolds, A., Wolfson, A., Marshall, W. S., Karpilow, J., & Khvorova, A. 2005, "The contributions of dsRNA structure to Dicer specificity and efficiency", *RNA.*, vol. 11, no. 5, pp. 674-682.

Vickers, T. A., Koo, S., Bennett, C. F., Crooke, S. T., Dean, N. M., & Baker, B. F. 2003, "Efficient reduction of target RNAs by small interfering RNA and RNase H-dependent antisense agents. A comparative analysis", *J.Biol.Chem.*, vol. 278, no. 9, pp. 7108-7118.

Vives, E., Brodin, P., & Lebleu, B. 1997, "A truncated HIV-1 Tat protein basic domain rapidly translocates through the plasma membrane and accumulates in the cell nucleus", *J.Biol.Chem.*, vol. 272, no. 25, pp. 16010-16017.

von Harpe, A., Petersen, H., Li, Y., & Kissel, T. 2000, "Characterization of commercially available and synthesized polyethylenimines for gene delivery", *J.Control Release*, vol. 69, no. 2, pp. 309-322.

Wadia, J. S., Stan, R. V., & Dowdy, S. F. 2004, "Transducible TAT-HA fusogenic peptide enhances escape of TAT-fusion proteins after lipid raft macropinocytosis", *Nat.Med.*, vol. 10, no. 3, pp. 310-315.

Wagner, E., Plank, C., Zatloukal, K., Cotten, M., & Birnstiel, M. L. 1992, "Influenza virus hemagglutinin HA-2 N-terminal fusogenic peptides augment gene transfer by transferrin-polylysine-DNA complexes: toward a synthetic virus-like gene-transfer vehicle", *Proc.Natl.Acad.Sci.U.S.A*, vol. 89, no. 17, pp. 7934-7938.

Wang, C. Y. & Huang, L. 1987, "pH-sensitive immunoliposomes mediate target-cell-specific delivery and controlled expression of a foreign gene in mouse", *Proc.Natl.Acad.Sci.U.S.A*, vol. 84, no. 22, pp. 7851-7855.

Wells, D. J. 2004, "Gene therapy progress and prospects: electroporation and other physical methods", *Gene Ther.*, vol. 11, no. 18, pp. 1363-1369.

Weinberg, M. S. & Wood, M. J., 2009, "Short non-coding RNA biology and neurodegenerative disorders: novel disease targets and therapeutics', *Hum. Mol. Genet.,* vol. 18, pp. 27-39.

Whitehead, K. A., Langer, R., & Anderson, D. G. 2009, "Knocking down barriers: advances in siRNA delivery", *Nat.Rev.Drug Discov.*, vol. 8, no. 2, pp. 129-138.

Wienhues, U., Hosokawa, K., Hoveler, A., Siegmann, B., & Doerfler, W. 1987, "A novel method for transfection and expression of reconstituted DNA-protein complexes in eukaryotic cells", *DNA*, vol. 6, no. 1, pp. 81-89.

Williams, D. A. & Baum, C. 2003, "Medicine. Gene therapy--new challenges ahead", *Science*, vol. 302, no. 5644, pp. 400-401.

Wilusz, C. J. & Wilusz, J. 2004, "Bringing the role of mRNA decay in the control of gene expression into focus", *Trends Genet.*, vol. 20, no. 10, pp. 491-497.

Winkler, K. E. 2004, "Killing the messenger", *Nat.Rev.Drug Discov.*, vol. 3, no. 10, pp. 823-824.

Winter, J., Jung, S., Keller, S., Gregory, R. I. & Diederichs, S., 2009, “Many roads to maturity: microRNA biogenesis pathways and their regulation”, *Nat. Cell. Biol.,* vol. 11, pp. 228-34.

Wood, K.V. 1990, Firefly luciferase : A new tool for molecular biologists, *Promega Notes,* **28**, 1.

Wrobel, I. & Collins, D. 1995, "Fusion of cationic liposomes with mammalian cells occurs after endocytosis", *Biochim.Biophys.Acta*, vol. 1235, no. 2, pp. 296-304.

Wu, G. Y. & Wu, C. H. 1987, "Receptor-mediated in vitro gene transformation by a soluble DNA carrier system", *J.Biol.Chem.*, vol. 262, no. 10, pp. 4429-4432.

Xia, H., Mao, Q., Eliason, S. L., Harper, S. Q., Martins, I. H., Orr, H. T., Paulson, H. L., Yang, L., Kotin, R. M., & Davidson, B. L. 2004, "RNAi suppresses polyglutamine-induced neurodegeneration in a model of spinocerebellar ataxia", *Nat.Med.*, vol. 10, no. 8, pp. 816-820.

Xu, B., Wiehle, S., Roth, J. A., & Cristiano, R. J. 1998, "The contribution of poly-L-lysine, epidermal growth factor and streptavidin to EGF/PLL/DNA polyplex formation", *Gene Ther.*, vol. 5, no. 9, pp. 1235-1243.

Zamore, P. D., Tuschl, T., Sharp, P. A., & Bartel, D. P. 2000, "RNAi: double-stranded RNA directs the ATP-dependent cleavage of mRNA at 21 to 23 nucleotide intervals", *Cell*, vol. 101, no. 1, pp. 25-33.

Zauner, W., Kichler, A., Schmidt, W., Mechtler, K., & Wagner, E. 1997, "Glycerol and polylysine synergize in their ability to rupture vesicular membranes: a mechanism for increased transferrin-polylysine-mediated gene transfer", *Exp.Cell Res.*, vol. 232, no. 1, pp. 137-145.

Zeira, E., Manevitch, A., Khatchatouriants, A., Pappo, O., Hyam, E., Darash-Yahana, M., Tavor, E., Honigman, A., Lewis, A., & Galun, E. 2003, "Femtosecond infrared laser-an efficient and safe in vivo gene delivery system for prolonged expression", *Mol.Ther.*, vol. 8, no. 2, pp. 342-350.

Zenke, M., Steinlein, P., Wagner, E., Cotten, M., Beug, H., & Birnstiel, M. L. 1990, "Receptor-mediated endocytosis of transferrin-polycation conjugates: an efficient way to introduce DNA into hematopoietic cells", *Proc.Natl.Acad.Sci.U.S.A*, vol. 87, no. 10, pp. 3655-3659.

Zhang, G., Gao, X., Song, Y. K., Vollmer, R., Stolz, D. B., Gasiorowski, J. Z., Dean, D. A., & Liu, D. 2004, "Hydroporation as the mechanism of hydrodynamic delivery", *Gene Ther.*, vol. 11, no. 8, pp. 675-682.

Zhdanov, R. I., Podobed, O. V., & Vlassov, V. V. 2002, "Cationic lipid-DNA complexes-lipoplexes-for gene transfer and therapy", *Bioelectrochemistry.*, vol. 58, no. 1, pp. 53-64.

Zheng, J. N., Pei, D. S., Mao, L. J., Liu, X. Y., Mei, D. D., Zhang, B. F., Shi, Z., Wen, R. M., & Sun, X. Q. 2009, "Inhibition of renal cancer cell growth in vitro and in vivo with oncolytic adenovirus armed short hairpin RNA targeting Ki-67 encoding mRNA", *Cancer Gene Ther.*, vol. 16, no. 1, pp. 20-32.

Zuhorn, I. S., Bakowsky, U., Polushkin, E., Visser, W. H., Stuart, M. C., Engberts, J. B., & Hoekstra, D. 2005, "Nonbilayer phase of lipoplex-membrane mixture determines endosomal escape of genetic cargo and transfection efficiency", *Mol.Ther.*, vol. 11, no. 5, pp. 801-810.

Appendix I

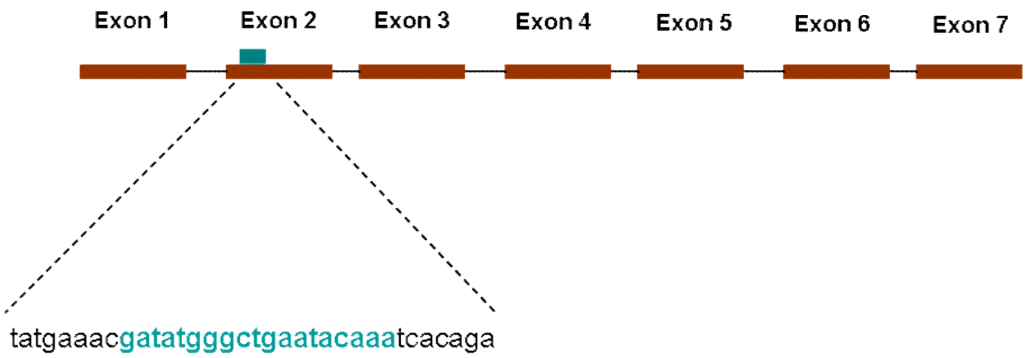

The sequence of the luciferase targeting siRNA purchased from Dharmacon is shown in blue.

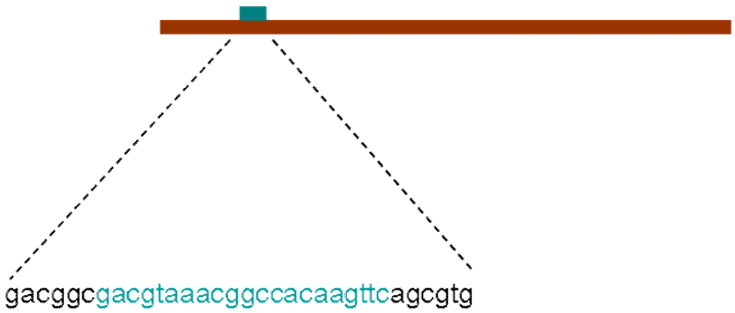

The sequence of the eGFP targeting siRNA purchased from Dharmacon is shown in blue.

Appendix I

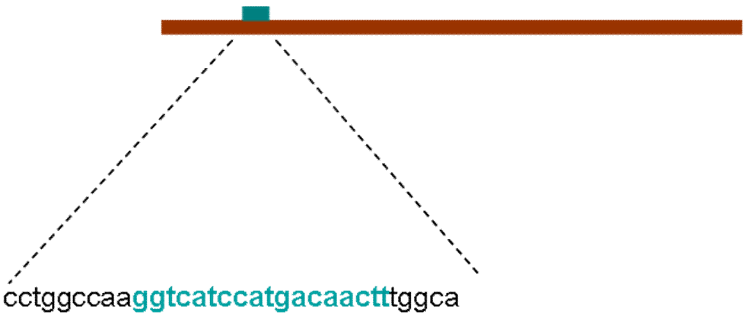

The sequence of the GAPDH targeting siRNA was provided by Ambion is shown in blue.

Appendix II

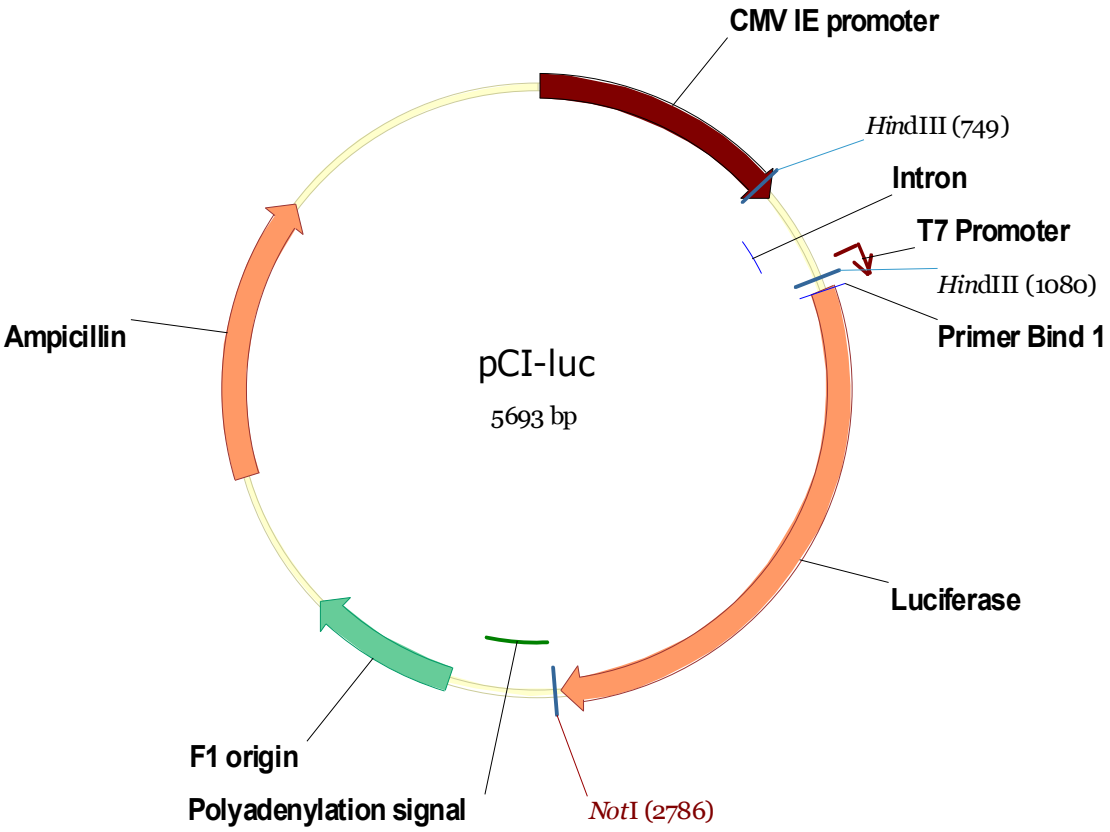
CMV IE promoter
HindIII (749)
Intron
T7 Promoter
HindIII (1080)
Primer Bind 1
Ampicillin
pCI-luc
5693 bp
Luciferase
F1 origin
Polyadenylation signal
NotI (2786)

Appendix II

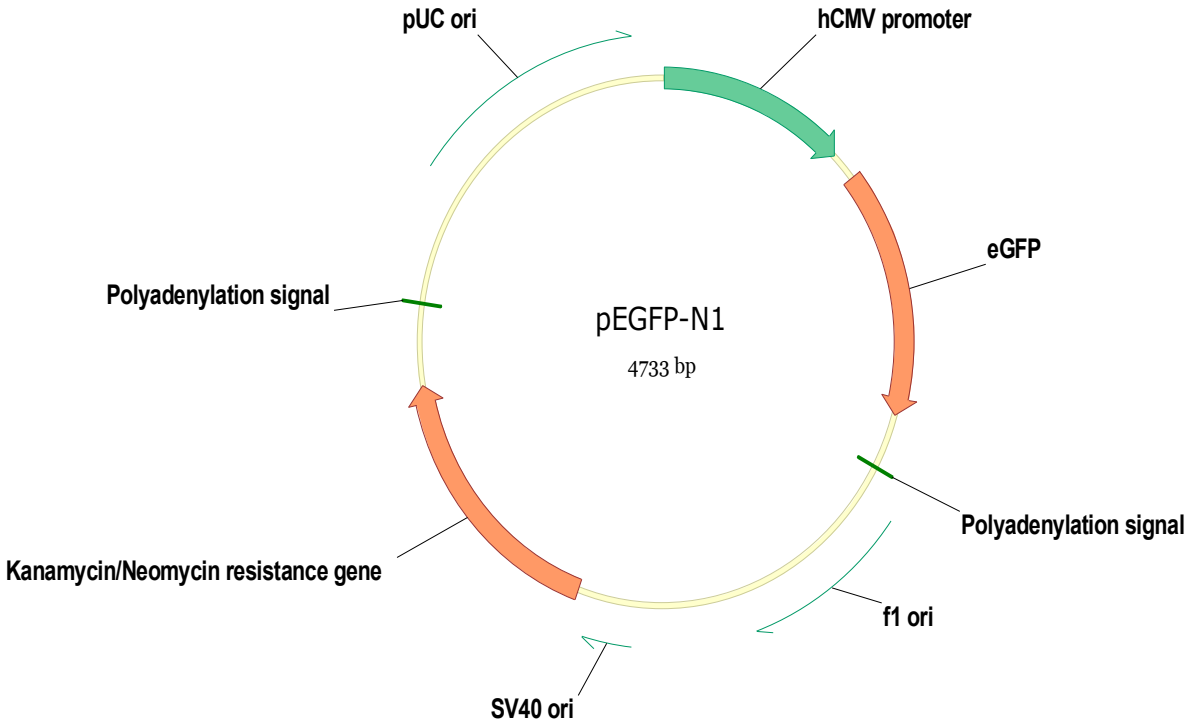
pUC ori
hCMV promoter
eGFP
Polyadenylation signal
pEGFP-N1
4733 bp
Polyadenylation signal
Kanamycin/Neomycin resistance gene
f1 ori
SV40 ori

Appendix III

GAPDH knockdown model for NIH 3T3 and HT1080

The GAPDH knockdown model can be used to investigate endogenous gene knockdown. In this model, the cells were seeded 24 hours prior to transfection. Having prepared the siRNA complexes with siRNA targeting GAPDH in Optimem, the cells were transfected and the GAPDH levels were analysed 48 hours post-transfection. The cells treated with irrelevant siRNA complexes could indicate the non-specific gene silencing although cell toxicity could also decrease GAPDH activity.

Figure I shows the results of the GAPDH knockdown on NIH 3T3 and HT1080 cells. The percentage of relative fluorescent unit (RFU) refers to the GAPDH activity normalised to the untreated cell control. The siRNA transfection complexes were formed using a commercial reagent, siLentfect, and siRNA targeting GAPDH (siGAPDH) or irrelevant siRNA (irr). The amount of the siLentfect and siRNA used per well in the 96 well plate were as indicated.

It was observed that the same complex formulation mediated different levels of gene silencing in different cell lines. As shown in **Figure IA**, 0.1µg siLentfect with 20 nM siGAPDH per well mediated around 80% GAPDH silencing in HT 1080 cells whereas the same complexes did not mediate any gene silencing in NIH 3T3 cells **(Figure IB)**. In fact, 0.4 µg siLentfect with 20nM siGAPDH per well was needed to mediate 60% of GAPDH knockdown in NIH 3T3 cells. This indicated that different cell types would have different optimal complex formations for gene silencing.

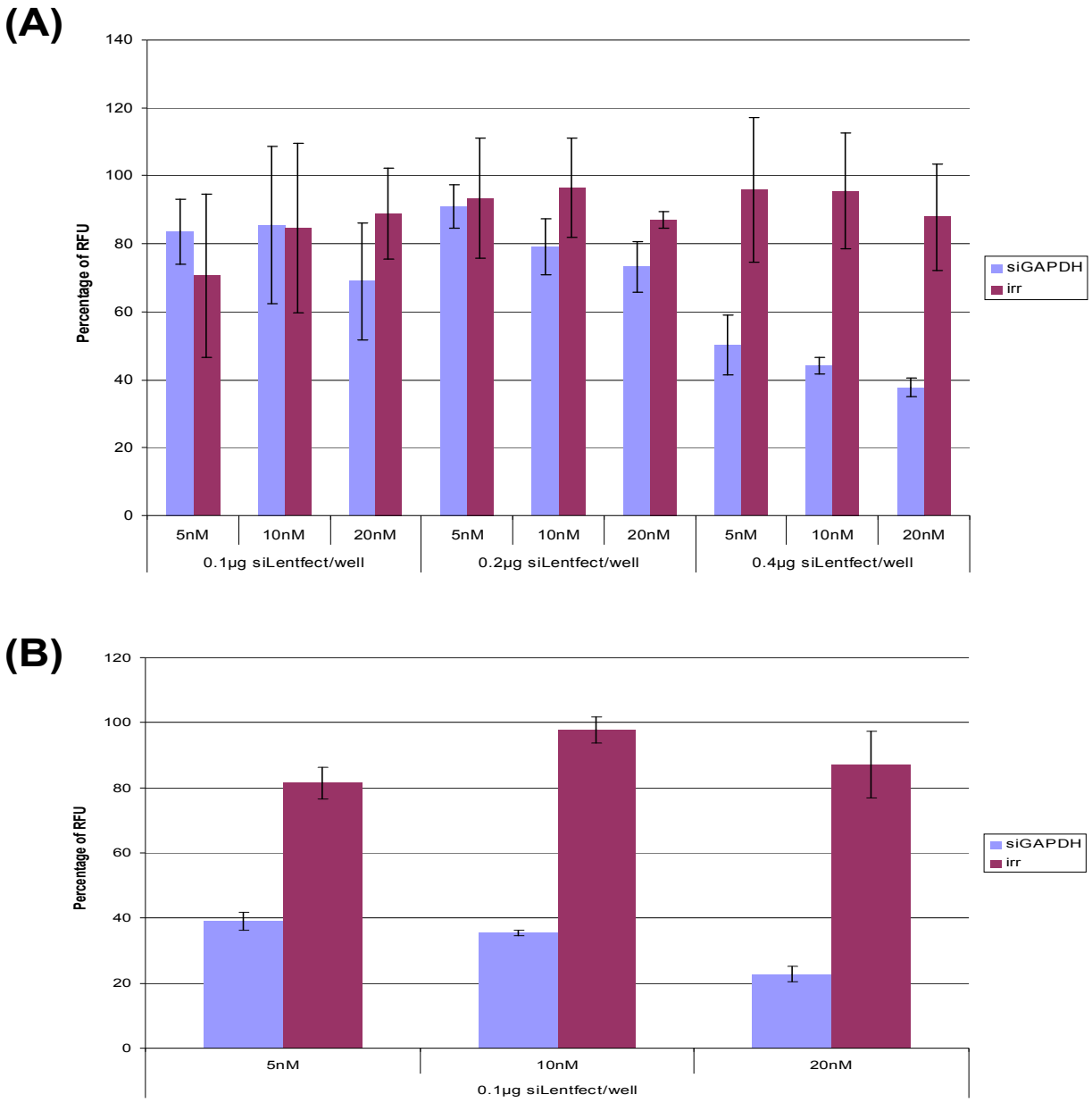

Figure I The GAPDH knockdown model. 5 × 10^4 cells were seeded 24 hours prior to transfection. siRNA transfection complexes were made by mixing siLecfect with siRNA for 30 minutes in Optimem. The complexes were then overlaid onto the cells for 24 hours. After removing the transfection complexes, full growth medium was added to the cells. The remaining GAPDH activity relative to the untreated control was analysed 2 days post-transfection. **(A)** remaining GAPDH activity within NIH 3T3 cells. **(B)** remaining GAPDH activity within HT1080 cells. siGAPDH refers to siRNA targeting GAPDH; irr refers to siRNA not targeting any mRNA in the cells. Percentage of RFU: the relative fluorescence unit (RFU) of the samples normalised with the RFU of the untreated control.

Appendix IV

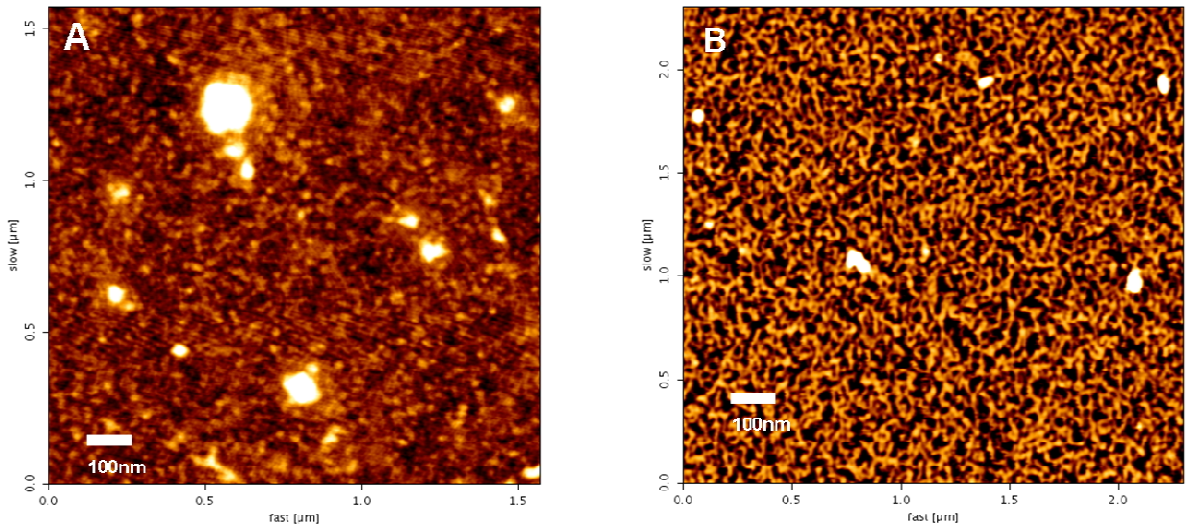

Atomic force micrographs of (A) B-PEI siRNA and (B) L-PEI siRNA complexes. 10 µg of siRNA was diluted to 25 µl in Ultrapure water and mixed with 25 µl PEIs in Ultrapure water at 20:1 N/P ratio at room temperature. The complexes were then diluted to 500 µl in Ultrapure water and transferred to a freshly cleaved mica slide. The polyplexes were allowed to adhere for 5 min, and were dried using a nitrogen gas flow. Samples were investigated within 2 h after preparation. AFM was performed on a JPK NanoWizard (JPK Instruments, Berlin, Germany). Silicon nitride tips attached to cantilevers of a length of 230 µm and a resonance frequency of about 160 kHz were used (NSC16 AlBS, Micromasch, Tallinn, Estonia). AFM was performed in tapping mode. The height images shown were recorded at a scan frequency of 1 Hz.

Appendix V

Appendix IV consists of four pages which showed the sequence of the arginine based peptide, the sizes of the arginine based peptide siRNA complexes, the gene silencing efficiency of the arginine based peptide siRNA complexes, localisation of siRNA mediated by the arginine based peptide complexes and plasmid delivery efficiency of the arginine based peptide.

The sequence of the arginine based peptide (RVG-9R)

YTIWMPENPRPGTPCDIFTNSRGKRASNGGGGRRRRRRRRR

Molecular weight = 4843

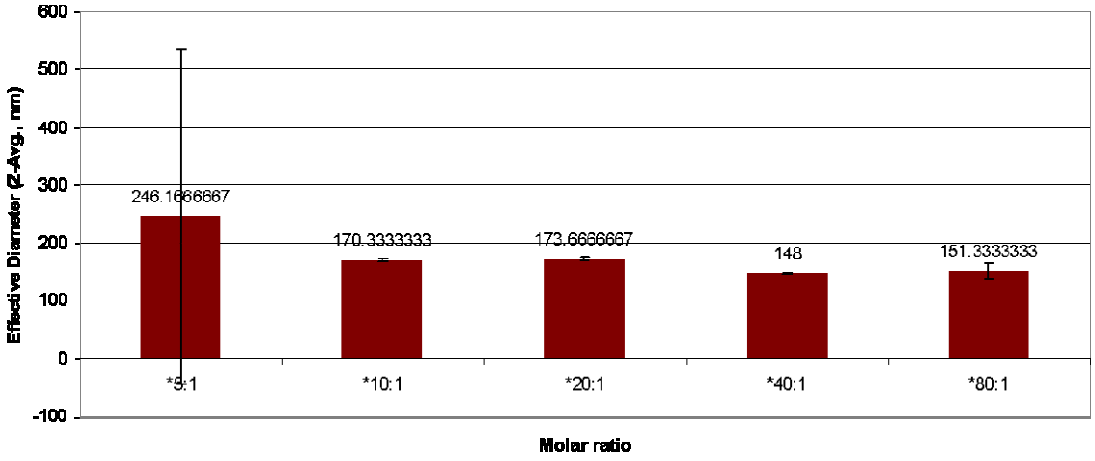

The effective diameter of the RVG-9R siRNA complexes. The RVG-9R peptides were mixed with siRNA in distilled water at different molar ratios for 60 minutes. The size of the complexes was then measured using Zetasizer Nano ZS. The formulations of the complexes are expressed as molar ratio ratio. A molar ratio 10:1 was reported to form siRNA complexes and mediated gene silencing (Kumar et al. 2007).

Appendix V

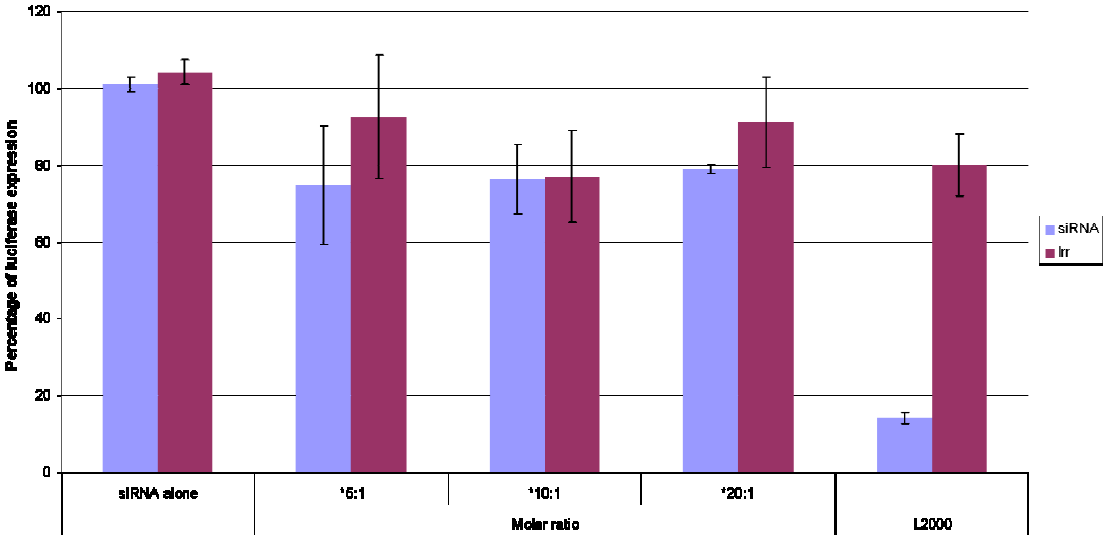

siRNA transfection efficiency mediated by the RVG-9R peptide siRNA complexes. The transfection procedures were performed according to Kumar et al. 2007. Briefly, Neuro 2a luciferase expressing cells were seeded 24 hours before transfection. The complexes were made by mixing the RVG-9R peptides with siRNA targeting luciferase (siLuc) in serum free DMEM at different molar ratio for 15 minutes at room temperature. Complexes with siRNA targeting eGFP (sieGFP) were used as a control to assess non-specific gene silencing mediated by the complexes. Following removal of full growth medium, complexes were overlaid onto the cells for 4 hours. After removing the transfection complexes, full growth medium was added to the cells. Luciferase activity in the cells was analysed 24 hours post-transfection to estimate the transfection efficiencies of the complexes. The formulations of the complexes are expressed as a molar ratio. A molar ratio 10:1 was reported to form siRNA complexes and mediated gene silencing (Kumar et al. 2007).

Appendix V

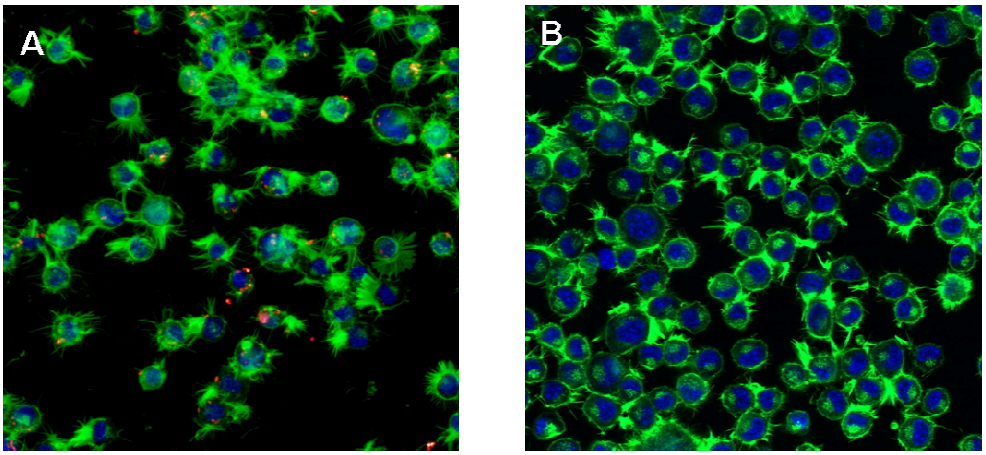

Localisation of siRNA following transfection. Neuro 2a cells were seeded 24 hours before transfection. The complexes were made by mixing the RVG-9R peptides with Cy 3 labelled siRNA (Red) for 15 minutes. Following removal of full growth medium, complexes were overlaid onto the cells for 4 hours. The cells were then washed and stained with phalloidin for the F-actin on the cell membrane (Green) and DAPI for the nucleus (Blue). **(A)** Cells exposed to the L2000/siRNA complex, **(B)** cells exposed to the RVG-9R/siRNA complex.

Appendix V

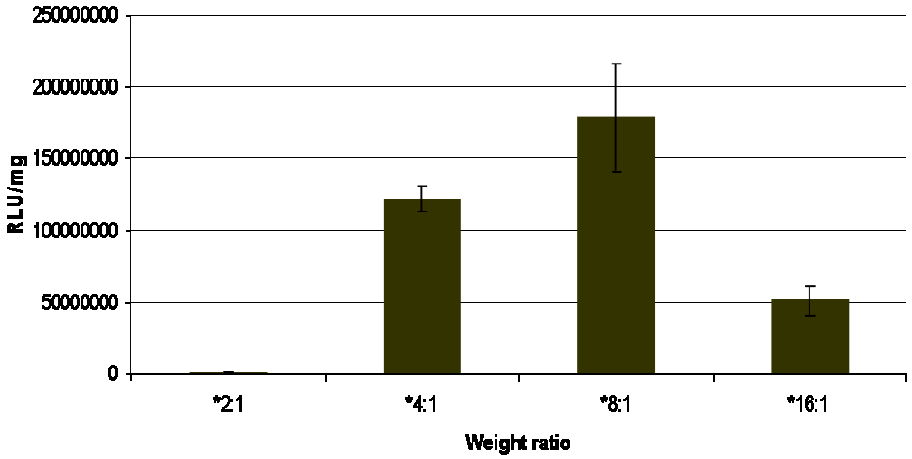

Plasmid transfection efficiency mediated by the RVG-9R/plasmid (pCI-Luc). To test if the RVG-9R can function as a nucleic acid delivery reagent, plasmid transfection was performed. Neuro 2a cells were seeded 24 hours before transfection. The complexes were made by mixing peptides with pCI-Luc in Optimem at different weight ratios for 30 minutes. Following removal of full growth medium, complexes were overlaid onto the cells for 4 hours. After removing the transfection complexes, full growth medium was added to the cells. Luciferase expression in the cells was analysed 24 hours post-transfection to estimate the transfection efficiencies of the complexes. The formulations of the complexes are expressed as a weight ratio.